CORA Cork Open Research Archive
Cartlann Taighde Oscailte Chorcaí

Title	The role of glucocorticoid-induced tumour necrosis factor receptor in developing mouse sympathetic neurons
Authors	McKelvey, Laura
Publication date	2013
Original Citation	McKelvey, L. 2013. The role of glucocorticoid-induced tumour necrosis factor receptor in developing mouse sympathetic neurons. PhD Thesis, University College Cork.
Type of publication	Doctoral thesis
Rights	© 2013, Laura McKelvey - http://creativecommons.org/licenses/by-nc-nd/3.0/
Download date	2026-11-07 15:06:24
Item downloaded from	https://hdl.handle.net/10468/1291



UCC
University College Cork, Ireland
Coláiste na hOllscoile Corcaigh

The role of Glucocorticoid-induced Tumour Necrosis Factor Receptor in developing mouse sympathetic neurons

By

Laura McKelvey

A thesis presented to

the National University of Ireland

in partial fulfilment of requirements for

the degree of Doctor of Philosophy in Neuroscience

Department of Anatomy and Neuroscience,

National University of Ireland Cork,

Ireland

Supervisor: Doctor Gerard O'Keeffe

Head of Department: Professor John Cryan

May 2013

For last year's words belong to last year's language

And next year's words await another voice.

And to make an end is to make a beginning.

T.S. Eliot

Declaration

All work presented in this thesis is original. I wish acknowledge the contribution of Dr. Aoife Nolan, Mr. Sean Crampton for their assistance with transfections and preparation for microarray analysis and Dr. Humberto Guterriez for analysis of microarray results.The work was carried out under the supervision of Dr. Gerard O'Keeffe between August 2010 and May 2013 in the Department of Anatomy and Neuroscience, University College, Cork, Ireland. This dissertation has not been submitted in whole or in part for any other degree, diploma or qualification at any other University.

_____

Laura McKelvey

May 2013

Publications arising from this work

Abstracts

L. Mckelvey, C. Riccardi, G.W. O'Keeffe. Characterisation of the molecular mechanisms mediating *GITR*-regulated axonal growth. Neuroscience Ireland 2011, NUI Maynooth, Ireland

Laura McKelvey, Humberto Gutierrez, Giuseppe Nocentini, Sean J. Crampton, Carlo R. Riccardi[3], Gerard W. O'Keeffe. The intracellular portion of GITR enhances NGF-promoted neurite growth through an inverse modulation of Erk and NF-κB signalling. Neuroscience Ireland 2012, RCSI Dublin, Ireland.

Papers

McKelvey L, Gutierrez H, Nocentini G, Crampton SJ, Davies AM, Riccardi CR, O'Keeffe G W (2012). The intracellular portion of GITR enhances NGF-promoted neurite growth through an inverse modulation of Erk and NF-kappaB signalling. Biol Open 1: 1016-1023.

McKelvey L, Shorten GD, O'Keeffe GW (2013). Nerve growth factor-mediated regulation of pain signalling and proposed new intervention strategies in clinical pain management. J Neurochem 124: 276-289.

Article

McKelvey L (2012). Feel the Pain. The Boolean: 59-62.

Table of Contents

1.0 **Abstract** 6

2.0 **Abbreviations** **7**

3.0 **Introduction** 12

3.1 **The autonomic nervous system** 12

3.2 **The sympathetic nervous system** 13

3.2.1 The organisation of the SNS 14

3.2.2 Activation of the SNS 15

3.3 **Sympathetic innervation of the lymphatic system** 16

3.3.1 Sympathetic regulation of the immune system 18

3.4 **The development of the SNS** 19

3.4.1 Stages of development of the SNS 20

3.4.2 Signalling throughout stages of SNS development 21

3.5 **NGF** 24

3.5.1 Discovery of NGF 25

3.5.2 Mechanism of action of NGF 26

3.5.3 TrkA 26

3.5.4 ERK1/2 signalling 28

3.5.5 ERK1/2 signalling in sympathetic axonal growth and target innervation 30

3.5.6 P75NTR 31

3.5.7 NF-κB 33

3.5.8 NF-κB and neurite growth 36

3.6 **GITR** 38

3.6.1 GITR in the immune system 38

3.6.2 GITR acts as a costimulatory molecule 39

3.6.3 GITR in the nervous system 40

3.6.4 GITR signalling 41

3.7 **Clinical importance of the correct development of the SNS** 42

3.7.1 HSAN IV 44
3.7.2 GITR and clinical applications 45
3.8 **Objectives of the present study** 46

4.0 **Materials and methods** 47
4.1 **Animal Husbandry** 47
4.2 **Tissue culture** 47
4.2.1 Superior cervical ganglia dissection 47
4.2.2 Tissue culture procedures 49
4.2.2.1 P1 SCG neuronal growth 50
4.2.2.2 P1 SCG neuronal survival in different concentrations of NGF 50
4.2.2.3 P1 SCG neuron growth response in different concentrations of NGF 51
4.2.2.4 P1 SCG neuron transfections 51
4.2.2.4.1 Plasmids 52
4.3 **Immunochemist**ry 54
4.3.1 Immunocytochemistry (ICC) 54
4.3.2 Immunohistochemistry (IHC) 56
4.3.3 Whole mount organ IHC 56
4.4 **Protein quantification** 57
4.4.1 Protein extraction from cells 57
4.4.2 Western blotting 57
4.5 **Analysis of mRNA expression** 58
4.5.1 RNA extraction 58
4.5.2 cDNA synthesis 59
4.5.3 Reverse transcriptase – polymerase chain reaction 59
4.5.4 Agarose gel electrophoresis 61
4.6 **Growth analysis** 61
4.7 **Statistics** 61

5.0 **Determination of the role of GITR in the growth of developing sympathetic neurons** 62

5.1 **Aims** 62

5.2 **Abstract** 63

5.3 **Introduction** 63

5.4 **Results** 65

5.4.1 GITR and GITRL are expressed by P1 mouse SCG neurons 65

5.4.2 Dose response of NGF effects on survival of P1 mouse SCG neurons 65

5.4.3 Dose response of NGF effects on the growth of P1 mouse SCG neurons 66

5.4.4 A GITRL antagonist reduces NGF-promoted axonal growth at an NGF concentration of 1ng/ml 66

5.4.5 A GITRL antagonist does not reduce NGF-promoted axonal growth at an NGF concentration of 4ng/ml 67

5.4.6 A GITRL antagonist does not reduce NGF-promoted axonal growth at an NGF concentration of 10ng/ml 68

5.4.7 Enhancement of axonal growth by GITRL-GITR signalling does not require the intracellular tail of GITRL 68

5.4.8 GITRδK does not affect axonal growth of P1 SCG neurons 69

5.4.9 GITRδZ does not affect axonal growth of P1 SCG neurons 70

5.4.10 Axonal growth of P1 mouse SCG neurons is mediated by a juxtamembrane region of GITR 70

5.4.11 *In Silico* analysis of the GPD of GITR 71

5.4.12 The CPRE (amino acids 8 to 11) site of the GPD of GITR does not mediate its growth promoting effects 72
5.4.13 Inactivating mutation of Tyr190 and Ser199 of the GPD of GITR does not inhibit axonal growth 72
5.4.14 Constitutive phosphorylation of Tyr190 and Ser199 of the GPD of GITR inhibits axonal growth 73
5.4.15 Summary of Chapter 5.0 73
5.5 Discussion 90

6.0 **Dual-regulation of Erk and NF-κB signalling by GITR in the regulation of axonal growth in developing sympathetic neurons** 96
6.1 **Aims** 96
6.2 **Abstract** 97
6.3 **Introduction** 97
6.4 **Results** 99
6.4.1 GITRL-GITR signalling does not affect phospho-TrkA in P1 mouse SCG neurons 96
6.4.2 GITRL-GITR signalling regulates NF-κB activity in P1 SCG neurons 100
6.4.3 GITRL-GITR signalling regulates NF-κB activity through the GPD of GITR in P1 SCG neurons 101
6.4.4 Inhibition of IKKβ prevents the effects of GITR inhibition on growth in P1 mouse SCG neurons 101
6.4.5 P1 SCG cells overexpressing both GITRL and p65 are larger than cells expressing p65 alone however NF-κB activity is comparable in these cells 102
6.4.6 GITR regulates ERK1/2 phosphorylation via the GPD in P1 SCG neurons 103
6.4.7 Putative phosphorylation sites of the GPD of GITR have no effect on phospho-p65 or phospho-ERK1/2 activity 104

6.4.8 Constitutive phosphorylation of residues at Thr190 and Ser199, (amino acids 12 and 21), sites of the GPD of GITR results in a reduction in TrkA expression 105

6.5 **Discussion** 135

7.0 **Heterogenous requirement for GITR in the regulation of peripheral target innervation of the sympathetic nervous system** 139

7.1 **Aims** 139

7.2 **Abstract** 140

7.3 **Introduction** 140

7.4 **Results** 142

7.4.1 TH is expressed by mouse SCG cells *in vivo* and *in vitro* 142

7.4.2 GITR is required for sympathetic NGF-target innervation of the heart and bladder of neonatal mice 143

7.4.3 Inhibition of GITRL-GITR signalling resulted in an upregulation of TNFα and IGF-R1 in P1 mouse SCG 144

7.5 Discussion 155

8.0 **Final Discussion** 160

9.0 **Bibliography** 165

10.0 **Acknowledgements** 192

1.0 Abstract

Hereditary sensory autonomic neuropathy IV (HSAN IV) is an autosomal recessive disorder characterised by inability to feel pain and anhidrosis and is a consequence of defective NGF/TrkA signalling and growth of sensory and sympathetic neurons. Glucocortiocoid-induced tumour necrosis factors receptor (GITR), a transmembrane protein, activated by its specific ligand, GITRL, is well known for its role in the regulation of innate and acquired immune system responses. Recently, GITR was found to be required for NGF-dependant and extracellular signal-related kinase 1/2 (ERK1/2)-induced neurite growth and target innervation in the developing sympathetic nervous system (SNS). Given this novel role of GITR, it is possible that strategies targeting GITR have potential therapeutic benefit in promoting neurite growth in autonomic neuropathies such as HSAN IV. Using P1 mouse SCG neurons as a model, in addition to various SCG cell treatments, knock down models and transfection methods, we investigated whether GITR increases the sensitivity of sympathetic neurons to NGF; the region of GITR required for the enhancement of NGF-promoted growth, the signalling pathways downstream of GITR and how extensively GITR is involved in regulating peripheral innervation of the SNS. Results indicate that the region responsible for the growth promoting effects of GITR lies in its juxtamembrane intracellular region (here termed the growth promoting domain (GPD)) of GITR. The GPD of GITR activates ERK1/2 and inhibits nuclear factor kappa B (NF-κB) in an inverse fashion to provide an optimal cellular growth environment for P1 SCG neurons. While deleting the GPD of GITR had no effect on TrkA expression, constitutive phosphorylation of specific sites in the GPD reduced TrkA expression indicating a possible role for GITR in increasing the sensitivity of SCG neurons to NGF by the regulation of these sites, TrkA expression and subsequent NGF/TrkA binding. GITR appears to be heterogeneously required for NGF-promoted target innervation of SCG neurons in some organs, implying additional factors are involved in extensive NGF-target innervation of the SNS. In conclusion, this study answers basic biological questions regarding the molecular mechanism behind the role of GITR in the development of the SNS, and provides a basis for future research if GITR modulation is to be developed as a strategy for promoting axonal growth.

2.0 Abbreviations

ACh	Acetylcholine
ACTH	Adrenocorticotropic hormone
AM	Adrenal medulla
ANOVA	Analysis of variance
ANS	Autonomic nervous system
APC	Antigen presenting cells
AR	Adrenergic receptors
BAFF	B cell activation factor
BAX	Bcl-2-associated X protein
BDNF	Brain-derived neurotrophic factor
BMP	Bone morphogenetic protein
C	Cervical
CCA	Common carotid artery
CIPA	Congenitol insensitivity to pain with anhidrosis
CN	Cranial nerve
CNS	Central nervous system
CNTF	Ciliary neurotrophic factor
CPT	Choline-phosphate cytidylyltransferase
CREB	Cyclic AMP responsive element-binding protein
CRH	Corticotrophin-releasing hormone
DC	Dendritic cells
DMEM	Dulbecco's modified eagle media
DRG	Dorsal root ganglia
DUSP	Dual specificity phosphatases

E	Embryonic
ECN	External carotid nerve
EGF	Epidermal growth factor
Elk-1	Ets-like gene 1
ERK	Extracellular signal-related kinase
FAP	Familial amyloid polyneuropathy
GDNF	Glial cell-derived neurotrophic factor
GIT	Gastrointestinal tract
GITR	Glucocorticoid-induced tumour necrosis factor receptor
GITRL	GITR Ligand
GRB2	Growth factor receptor bound 2
GDP	Guanosine diphosphate
GSK3b	Glycogen synthase kinases 3 beta
GTP	Guanosine triphosphate
H	Hour
HBSS	Hank's balanced salt solution
HEK 293	Human embryonic kidney cell line 293
HGF	Hepatocyte growth factor
HPA	Hypothalamic pituitary axis
HRP	Horseradish peroxidase
HSAN	Hereditary sensory autonomic neuropathies
ICA	Internal carotid artery
ICD	Intracellular domain
ICN	Internal carotid nerve
IFN-γ	Interferon-gamma
IKK	I kappa B kinase

IL-1	Interleukin-1
IMG	Inferior mesenteric ganglia
JNK	c-Jun N-terminal kinase
KO	Knock out
KSR	Kinase suppressor of Ras
L	Lumbar
MAP1B	Microtubule-associated protein 1B
MAPK	Mitogen-activated protein kinase
Min	Minute
MP1	MEK partner 1
NCC	Neural crest cell
NE	Norepinephrine
NFAT	Nuclear factor of activated T-cells
NF-κB	Nuclear factor kappa B
NGF	Nerve growth factor
NIK	NF-κB inducing kinase
NKCs	Natural Killer cells
NPY	Neuropeptide Y
NRIF	Neurotrophin receptor interacting factor
NRP-1	Neuropilin-1
NT-3	Neurotrophin-3
P	Postnatal
P75NTR	p75 Neurotrophic factor receptor
PI3K	Phosphatidyl inositol-3
PC	Phosphatidylcholine
PKA	Protein kinase A

PNS	Peripheral nervous system
RHD	Rel homology domain
RPE cells	Retinal pigment epithelial cells
RPS3	Ribosomal protein S3
RSK	Ribosomal protein S6 kinase
SC	Sympathetic chain
SCG	Superior cervical ganglia
SEM	Standard error of mean
Sema3A	Semamorphin-3A
SDF1	Stomal-cell derived factor 1
SG	Stellate ganglia
Shc	Src homology 2 domain containing
SMG	Submandibular gland/Superior mesenteric ganglia
SNS	Sympathetic nervous system
SOS	Son of sevenless
SRF	Serum response factor
SYK	Spleen tyrosine kinase
T	Thoracic
TAD	Transcriptional activating domain
TCR	T-cell antigen receptor
TH	Tyrosine hydroxylase
TNF	Tumour necrosis factor
TNFR1	TNF receptor 1
TNFRSF	Tumour necrosis factor receptor superfamily
TRADD	TNFR1-assocated death domain protein
TRAF	TNF-receptor associated factor

Treg cells	Regulatory T cells
TrkA	Tyrosine kinase A receptor
VCAM-1	Vascular adhesion molecule-1

3.0 Introduction

3.1 The autonomic nervous system

The autonomic nervous system (ANS) plays a pivotal role in a wide range of physiological functions including homeostasis, and dysfunction of the ANS leads to a variety of diseases (*Moberg, 2000*). The term 'autonomic' nervous system was coined by Langley in his 1898 paper in the *Journal of Physiology* when he stated: "I propose the term 'autonomic nervous system' for the sympathetic system and the allied nervous system of the cranial and sacral nerves and for the local nervous system of the gut" (*Langley, 1898*).

The ANS is a subdivision of the nervous system which can be grossly divided into two main divisions; the central nervous system (CNS) consisting of the brain and spinal cord and the peripheral nervous system (PNS). The PNS is made up of both sensory and motor systems, which carry information in both afferent and efferent projections to and from the CNS respectively. The motor division of the PNS is composed of the ANS and somatic nervous system. Collectively, the ANS consists of parasympathetic and sympathetic nervous systems of which afferent nerves convey impulses from sensory organs, muscles, the circulatory system and all organs of the body to the controlling centre of the hypothalamus in the brain and elicits autonomic reflex responses through efferent autonomic nerves. Autonomic efferent nerves subsequently elicit appropriate reactions of the heart, the vascular system, and organs of the body to variations in environment (eg. temperature), posture, food intake, stressful experiences and other changes to which an individual is exposed. Together, the parasympathetic and sympathetic nervous systems provide automatic regulation of smooth muscle, cardiac muscle and glands and is associated with the control of involuntary action (Figure 3.1) (*Martini, 2004*). The hypothalamus receives visceral sensory information (eg. blood pressure); spinal cord information (eg. body temperature); visual (eg. light/dark) and complex sensory information (eg. emotion and smell) via the nucleus of the solitary tract; brainstem reticular formation; retina; limbic and olfactory system respectively and subsequently controls digestion; body temperature, circadian rhythm, reproduction and feeding. The hypothalamus has two major outputs; endocrine signals to or through the pituitary gland and neural signals to the ANS. Ouput to the ANS

involves lateral hypothalamic projection to the lateral medulla (where the parasympathetic vagal nuclei and sympathetic cells that descend to the spinal cord lie), through which, the hypothalamus controls the ANS *(Martini, 2004).*

The parasympathetic or cranio-sacral division of the ANS consists of preganglionic fibres which originate in the brainstem and sacral segments of the spinal cord and synapse in ganglia close to or within the target organs. The parasympathetic system is responsible for a state known as 'rest and digest' as parasympathetic activation acts to reduce metabolic rate, decrease heart and blood pressure, increase salivary and digestive gland secretions, increase motility and blood flow in the gastrointestinal tract (GIT), and stimulate urination and defecation (*Martini, 2004*).

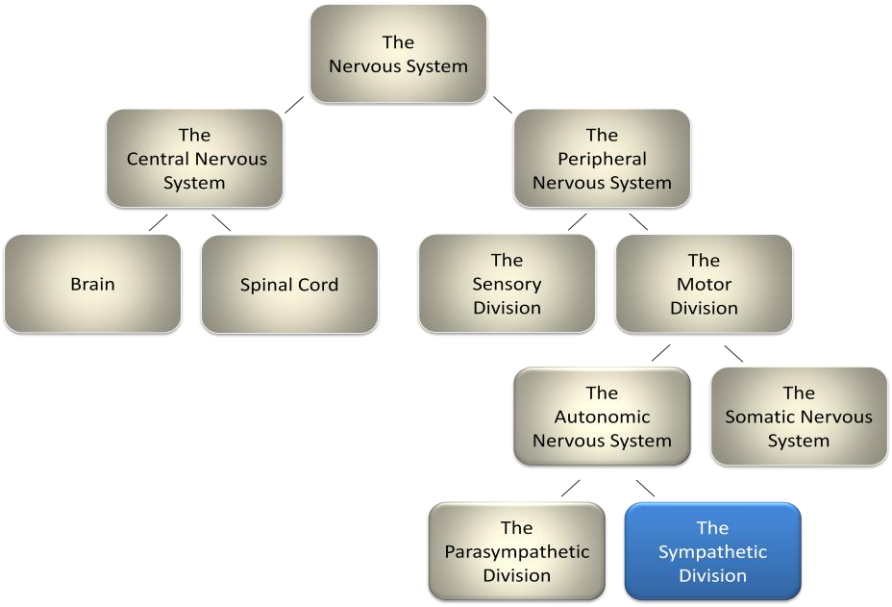


Figure 3.1: The nervous system

The nervous system is composed of two main divisions, the CNS and the PNS. The PNS is separated into sensory and motor divisions and the motor into the ANS and Somatic Nervous System. The ANS is composed of the parasympathetic and sympathetic nervous systems.

3.2 The sympathetic nervous system

The sympathetic nervous system (SNS) or the thoracolumbar division of the ANS consists of preganglionic fibres which emerge from the thoracic and superior lumbar segments of the spinal cord and synapse in ganglia near the spinal cord. The SNS

produces what is known as the ‘fight or flight’ response, which may involve heightened mental alertness, increased metabolic activity, increased heart rate and blood pressure, increased blood flow to skeletal muscle, increased respiratory rate, dilation of respiratory passageways, activation of sweat glands and temporary suspension of digestive and urinary functions (*Martini, 2004*).

3.2.1 The organisation of the SNS

The basic anatomical arrangement of the SNS consists of preganglionic neurons, prevertebral sympathetic ganglia, paravertebral sympathetic ganglia, the adrenal medulla and postganglionic neurons. Preganglionic neuron’s cells bodies lie in the the intermediolateral (IML) column of the gray matter of spinal cord segements T1 – L3 (T=Thoracic, L=Lumbar levels) and extend fibres to sympathetic ganglia where preganglionic and postganglionic neurons synapse. Unpaired prevertebral ganglia are located anterior to the vertebral column and include the celiac (CG), superior and inferior mesenteric (SMG and IMG) ganglia. Paired paravertebral ganglia are located parallel to the vertebral column and include the superior cervical (SCG), stellate (SG), thoracic, lumbar, saccral and coccygeal ganglia. The adrenal medulla (AM) is a modified ganglia located in the centre of the adrenal gland. Postganglionic neurons emerge from ganglia and innervate peripheral target organs (*Glebova and Ginty, 2005*) (Figure 3.2).

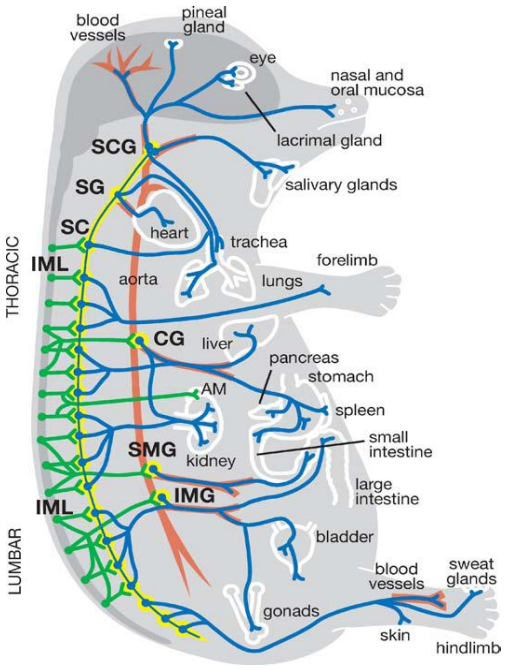


Figure 3.2: Schematic representation of the SNS anatomy in the mouse

Preganglionic sympathetic neurons (green) with cells bodies located in the IML column at thoracic and lumbar spinal cord segments synapse on postganglionic neurons (blue) in sympathetic ganglia. Paravertebral ganglia include the SCG, SG and sympathetic chain (SC) ganglia. Prevertebral ganglia include the CG, SMG and the IMG. Selected targets innervated by postganglionic neurons are shown. The AM receives preganglionic sympathetic innervation *(Glebova and Ginty 2005)*.

3.2.2 Activation of the SNS

The SNS is activated in response to a stimulus, such as in 'fight or flight' situations (*Goldstein, 1987*) resulting in subsequent release of neurotransmitters from postganglionic neurons which then activate receptors on peripheral target tissue (Figure 3.3). Neurotransmitters are specialized chemical substances that send messages from one nerve ending across synapses to other nerves. Examples of neurotransmitters include acetylcholine (ACh); epinephrine (adrenaline); norepinephrine (noradrenaline) (NE) and dopamine. Preganglionic sympathetic neurons release ACh, while most postganglionic sympathetic neurons release NE and therefore neurons are termed cholinergic and adrenergic neurons respectively (*Esler, et al., 1985*). Postganglionic sympathetic neurons subsequently activate

adrenergic receptors (ARs), including α1, α2, α3, β1 or β2 receptors on the peripheral target tissue (*Martini, 2004*).

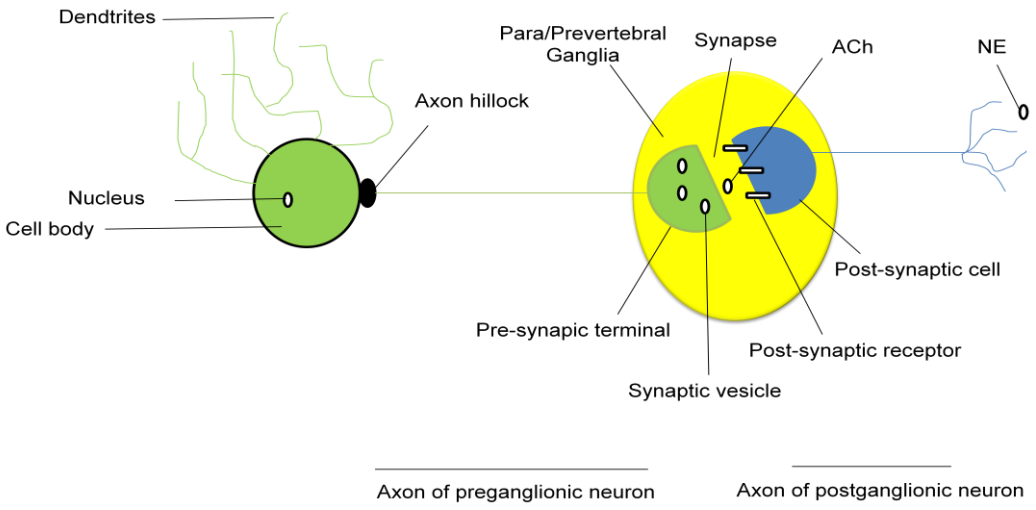


Figure 3.3: Activation and neurotransmitter release from sympathetic neurons

Preganglionic sympathetic neurons (green) synapse with the postganglionic neurons (blue) at para and prevertebral ganglia (yellow). Preganglionic neurons release neurotransmitter ACh from vesicles (white) of presynaptic terminal (green) at synapse with postsynaptic cell (blue) receptors of postganglionic neurons. Postganglionic neurons release NE from axon terminals to activate adrenergic receptors in peripheral targets cells.

3.3 Sympathetic innervation of the lymphatic system

The SNS is responsible for the innervation to all the organs of the lymphatic system including the thymus, spleen, lymph nodes and bone marrow (Figure 3.4) (*Felten, et al., 1985; Meltzer, et al., 1997; Panuncio, et al., 1999*). The lymphatic system works together with the integumentary, cardiovascular, respiratory, digestive and nervous systems to create a physiological immune system. The immune system enables the body to fight against infection and disease by two responses, the innate and adaptive immune responses (*Martini, 2004*).

The innate immune response functions in an antigen non-specific manner, by a variety of cells including monocytes, macrophages, dendritic cells (DCs), natural

killer cells (NKCs), basophils, eosinophils and granulocytes. The innate immune response is usually the body's first line of defence (*Martini, 2004*).

The adaptive immune response functions in an antigen-specific manner and does so by T and B lymphocyte cells. There are three types of lymphocyte cells; T (thymus dependant), B (bone marrow-derived and responsible for antibody-mediated immunity or humoral immunity) and NKCs. T cells can be divided into Cytotoxic or effector T cells (attack foreign bodies, involved in cell-mediated immunity or cellular immunity), Helper T cells (stimulate T and B cells) and Supressor T cells (inhibit T and B cells) and are also known as T regulatory cells (Treg). Following antigen presentation by antigen presenting cells (APCs) and costimulatory signals (eg. through CD28 receptor), effector T cells are triggered. The expansion of activated T cells is controlled by Treg cells including CD4+CD25+, CD8+CD25+, CD8+CD28- or CD4-CD8-CD3+ T-cells. There is interplay amongst effector T-cells, Treg cells and APCs and this determines the outcome of an immune response (*Beissert, et al., 2006; Sakaguchi, et al., 1995*). B cells can differentiate into plasma cells, responsible for the production and secretion of antibodies. NKCs are large granular lymphocytes which attack foreign cells, virus-infected cells and cancer cells. Through the adaptive immune response, the body develops a memory for a faster response following re-exposure (*Martini, 2004*).

The sympathetic input to the thymus originates from sympathetic chain ganglia extending from the SCG caudal to the T3 sympathetic ganglion (*Nance, et al., 1987*). Prevertebral sympathetic ganglia associated with the celiac-mesenteric plexus in addition to sympathetic postganglionic neurons that arise from the sympathetic chain ganglia of T1-T12 region of the thoracic spinal cord provide a major sympathetic input to the spleen (*Cano, et al., 2001; Nance and Burns, 1989*). There is less known regarding the specific origin of sympathetic innervation of lymph nodes however the origin is thought to reflect the specific regions of the body where the lymph nodes reside (*Nance and Sanders, 2007*). Similar to that of lymph nodes, neuroanatomical studies examining the origin of innervation of bone marrow is limited. This said femoral bone marrow innervation has been linked to thoracolumbar paravertebral sympathetic ganglia that receive input from T8-L1 spinal sympathetic preganglionic neurons (*Denes, et al., 2005*).

3.3.1 Sympathetic regulation of the immune system

The brain receives input from sensory neurons (e.g. dorsal root ganglia (DRG)) or immune stimuli (e.g. cytokines) (*Besedovsky and del Rey, 1992; Besedovsky and del Rey, 1996; Nance and Sanders, 2007*). Signals are transported to the brain via blood (*Banks and Kastin, 1991*) or cytokine receptors on the vagus nerve (*Watkins, et al., 1995*). In the case of an adaptive immune response, the brain communicates with the periphery by two pathways. The first pathway is via hypothalmic pituitary adrenal axis (HPA) and the second is via the SNS. The HPA regulation of immune function involves the release of corticotrophin releasing hormone (CRH) from the hypothalamus which stimulates the release of adrenocorticotropic hormone (ACTH) from the pituitary gland and subsequent release of corticosteroids from the adrenal cortex (*Webster, et al., 2002*). The SNS extends fibres to innervate organs of the immune system (*Meltzer, et al., 1997; Panuncio, et al., 1999*) by a vascular route (*Bellinger, et al., 2001*). The activation of the SNS stimulates the release of NE (*Esler, et al., 1985*) in addition to neuropeptide Y (NPY) (*Ruohonen, et al., 2009*) and opioids (*Hall, et al., 1998; Straub, 2004*) from sympathetic neurons. NE is released over the length of the sympathetic fibres (*Madden, et al., 1995; Shimizu, et al., 1994*) and binds to target immune cells, B and T lymphocytes, at their adrenergic receptor β2AR (*Kohm and Sanders, 2001*). Stimulation of the β2AR on an immune cell induces an increase in the intracellular level of cAMP, which activates protein kinase A (PKA) signalling cascade to regulate a variety of immune processes. Responses include leukocyte activation, cytokine production, and cell trafficking (*Cole, et al., 1999; Cole, et al., 1998; Kammer, 1988; Madden, et al., 1995; Ottaway and Husband, 1994; Sanders and Straub, 2002*).

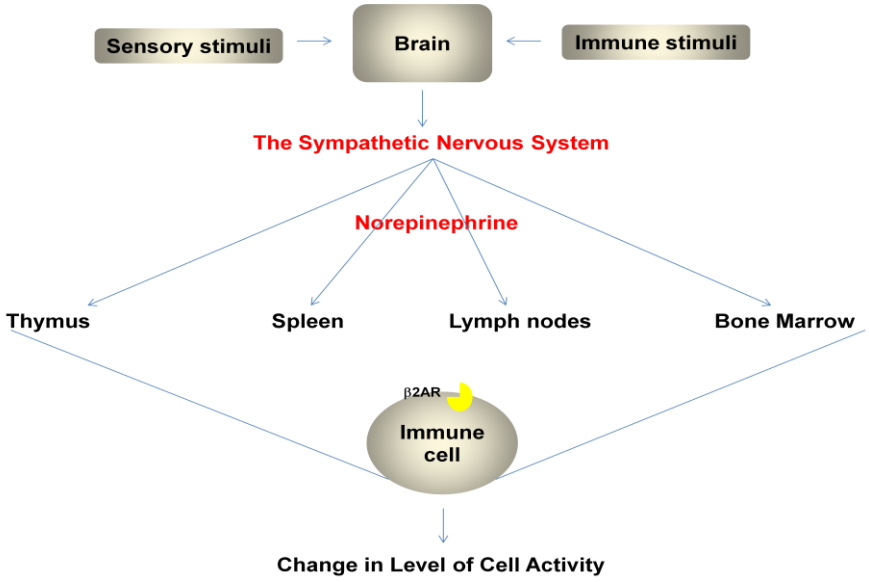


Figure 3.4: Sympathetic innervation of immune organs

All immune organs receive substantial sympathetic innervation from sympathetic postganglionic neurons. Input to the brain comes from sensory neurons (e.g. DRG) or immune stimuli (e.g. cytokines). The primary pathway for the neural regulation of immune function is provided by the SNS and its main neurotransmitter, NE. Activation of the SNS primarily inhibits the activity of cells associated with the innate immune system, while it either enhances or inhibits the activity of cells associated with the adaptive immune system. Via AR's, which are primarily of the β2AR subtype, NE is able to regulate the level of immune cell activity by initiating a change in the level of cellular activity, which often involves a change in the level of gene expression for cytokines and antibodies. Adapted from Nance and Sanders, 2007.

3.4 The development of the SNS

The correct development of sympathetic neurons is essential in order to establish an optimal functioning SNS. The SNS undergoes development between the gestation periods of E12-15 in rats (E=Embryonic day of gestation) *(Rubin 1985a; Rubin 1985b; Rubin 1985).* Sympathetic precursor cells first appear in the cervical region on E12 as a column along the dorsal aorta at all cervical levels *(Rubin 1985a).* Cells accumulate adjacent to cervical segments 1-5 (C1-5) forming a primitive SCG between days E12-14 *(Rubin 1985a).* Cells are scarce at more caudal cervical levels, forming a narrow region which is later filled with axons and form the cervical sympathetic trunk *(Rubin 1985a).* Enhanced proliferation occurs at the lowest cervical and upper thoracic levels that results in an accumulation of cells that form

the SCG and SG *(Rubin 1985a)*. With accumulation of cells and growth of the embryo, the cervical sympathetic trunk elongates *(Rubin 1985a)*. By E14, the SCG extends from C1-5, however, by E16, the SCG extends from C1-3 indicating these cells aggregate as opposed to disperse along the length of the cervical sympathetic trunk *(Rubin 1985a)*. Some cells of the SCG extend processes by E12. These cells extend long fibres that follow a linear course and resemble postganglionic axons, with most axons extending rostrally, and run along branches of the carotid artery and establish the internal and external carotid nerves. Postganglionic axons then grow toward peripheral regions along their arterial branches and subsequently along cranial nerves. For example, the postganglionic axon destined for the lacrimal gland emerges from the SCG along the internal carotid nerve, transfers to the facial nerve and follows a facial nerve branch to the orbit and innervates the lacrimal gland by E15 *(Rubin 1985a).* By E14, postganglionic cells possess a number of dendritic processes in addition to their axons. Dendrites can be differentiated from axons on E14 as they appear narrower, closer to the cell body, follow irregular trajectories and branch frequently *(Rubin 1985a).* Synaptic formations occur on soma and dendrites of ganglionic cells by E14 *(Rubin 1985c)*. There is subsequently an increase in the number of dendritic synapses by E15 and this number soon exceeds that of somatic contacts. At birth, most synaptic contacts are dendritic as opposed to somatic (85%) (*Rubin, 1985b; Rubin, 1985c*).

3.4.1 Stages of development of the SNS

The development of sympathetic neurons involves cell migration, ganglia formation, differentiation into sympathetic neurons, axonal extension and target innervation (*Glebova and Ginty, 2005*). Sympathetic neurons, like parasympathetic, arise from neural crest cells (NCCs), an embryonic progenitor cell population. NCCs arise from neural folds of the neural tube and migrate ventromedially through the rostral half of each somite. Once they pass through the somites, NCCs migrate further ventrally toward the dorsal aorta and form ganglia (*Erickson, et al., 1989; Rickmann, et al., 1985*). The dorsal aorta releases molecules such as BMP-4 and BMP-7, which induce the NCCs to differentiate into sympathetic neurons (*Reissmann, et al., 1996*) (*Schneider, et al., 1999*); *Anderson, et al., 1997*) and these neurons then project

axons to peripheral targets (*Rubin, 1985a*). The extension and growth of axons to and within their targets during development of the SNS is controlled by a variety of attractive and repulsive cues or signals.

3.4.2 Signalling throughout stages of SNS development

NCCs migrate from the dorsal aspect of the neural tube initially following a ventromedial pathway via the rostral half of each somite and give rise to sympathetic ganglia in chicken embryos (*Erickson, et al., 1989; Rickmann, et al., 1985*). Cells migrate via the rostral half of somites due to repulsive signals from the caudal half. The caudal half of each somite express both Semaphorin-3A (Sema3A) and Ephrin-B1 in mice, rat and chick (*Adams, et al., 1996; Eickholt, et al., 1999; Giger, et al., 1996; Koblar, et al., 2000; Krull, et al., 1997; Wang and Anderson, 1997*). Both Sema3A and Ephrin-B1 molecules are inhibitory to migrating NCCs which express their respective receptors neuropilin-1 and EphB3 in mouse and chicken embryos (*Kawakami, et al., 1996; Kawasaki, et al., 2002; Krull, et al., 1997*). In addition, the caudal half of each somite expresse F-spondin and chondroitin sulphate proteoglycans, which were also inhibitory to migrating NCCs in avian embryos (*Debby-Brafman, et al., 1999; Krull, 2001*). The migration of NCCs further ventrally toward the dorsal aorta involves Neuregulin signalling. Neuregulins are a family of four structurally related proteins, part of the epidermal growth factor (EGF) family of proteins whose effects are mediated by members of ErbB family of tyrosine kinases (trks) (*Falls, 2003*). NCCs express ErbB2 and ErbB3, and neuregulin-1 is expressed by newly formed somites, the mesenchyme surrounding the dorsal aorta and the dorsal neural tube in mice (*Britsch, et al., 1998*). The bone morphogenetic protein (BMP) family member ligands, BMP4 and BMP7, are produced by the dorsal aorta and are required for the expression of Neuregulin 1, in addition to the expression of stromal cell–derived factor–1 (SDF1, a chemokine, also called CXCL12), which in turn mediates progenitor cell migration (*Kim, et al., 2003b; Rio, et al., 1997*).

The SCG is formed from the first cells that migrate ventrally. These cells coalesce into a column between C1–C7. Many of these cells then migrate rostrally, separate from the SG and form the SCG between C1-C4 in mice and rats (*Nishino, et al., 1999; Rubin, 1985a*). The rostral migration of SCG precursors involves artemin,

a member of the glial derived neurotrophic factor (GDNF) family, which acts at its receptor complex, Ret and GDNF family receptor a3 (GFRa3), in mice (*Durbec, et al., 1996; Enomoto, et al., 2001; Honma, et al., 2002; Nishino, et al., 1999*). Artemin is expressed by blood vessels and is chemoattractive to developing sympathetic neurons in mice (*Honma, et al., 2002*). Artemin may play a role in the rostral or caudal migration of cells that lead to the segmentation of columns of cells into ganglia throughout the sympathetic chain.

BMP-4 and BMP-7 are expressed in the dorsal aorta of mammalian and avian species at critical times during sympathetic neuron differentiation (*Reissmann, et al., 1996*). These dorsal aorta-derived BMPs act on NCCs, that aggregate to form ganglia primordia, adjacent to the dorsal aorta, and induce the differentiation of these cells into sympathetic neurons in the chick embryo (*Schneider, et al., 1999*). BMPs elicit the expression of a network of transcription factors that, in turn, control autonomic neuron differentiation (Goridis and Rohrer, 2002). This network includes Mash1 and the paired transcription factors Phox2a and Phox2b. Phox2 proteins bind to the promoter of the subtype-specific noradrenergic marker genes for tyrosine hydroxylase (TH) (*Goridis and Rohrer, 2002*). Additional transcription factors involved in the specification of the noradrenergic phenotype of sympathetic neurons include HAND2 (previously known as dhand), cash1 and GATA-3 (*Anderson, et al., 1997*). Sympathetic ganglion neuron differentiation depends upon both canonical and non-canonical pathways of BMP-mediated signalling. Canonical BMP signalling regulates the transcription of HAND2 and Phox2a, while non-canonical involves the activation of PKA (*Liu, et al., 2005*).

Postganglionic sympathetic neurons begin to extend axons during the formation of ganglia at E12 (*Rubin, 1985a*). Hepatocyte growth factor (HGF), also known as scatter factor, as it was originally identified as a molecule that could trigger motility in a variety of epithelial cell types (*Birchmeier and Gherardi, 1998*), is produced by sympathetic neurons, and functions to enhance sympathetic neuronal survival, differentiation and proximal axonal growth (*Maina, et al., 1998*). HGF cooperates with NGF in postnatal neurons to promote arborisation of sympathetic neurons (*Yang, et al., 1998*) via both phosphoinositide-3 kinase (PI-3 kinase) and

mitogen activated protein kinase (MAP kinase)-dependent mechanisms (*Thompson, et al., 2004*).

Axon extension uses a vasculature route, in that axons travel to their targets by hitching a ride on arteries. Artemin (already discussed) is expressed in smooth muscles of blood vessels, and its receptor components Ret and GFR3A, mediate this projection of axons along arterial vasculature in mice (*Baloh, et al., 1998; Enomoto, et al., 2001*). Although known to be required for migration, axonal projections of sympathetic neuroblasts and proximal extension of postganglionic sympathetic axons, in artemin -/- mice studies, sympathetic innervation of peripheral targets still exist (*Enomoto, et al., 2001; Honma, et al., 2002*). This suggests there is another factor at play in the role of proximal axon extension of sympathetic neurons.

Neurotrophin 3 (NT-3), a member of the neurotrophin family, is expressed by blood vessels and can induce proximal sympathetic axon extension along arterial vasculature on route to innervate peripheral targets of mice (*ElShamy, et al., 1996; Kuruvilla, et al., 2004*). In NT-3 -/ - mice, sympathetic axons fail to enter the pineal gland and the external ear and infusion of exogenous NT-3 into the external ear restored the sympathetic innervation in mutant mice (*ElShamy, et al., 1996*). But similar to that of artemin -/- studies, in NT-3 -/- mice, most targets received at least some peripheral target innervation (*ElShamy, et al., 1996*). This suggests that there are other molecules that contribute to axon extension along blood vessels during development. A number of molecules have been implicated in distal extension and target innervation of developing sympathetic neurons, including GDNF (*Yan, et al., 2003*), vascular cell adhesion molecule-1 (VCAM-1), and a4-integrins (*Wingerd, et al., 2002*). Recently, Wnt5a derived from sympathetic neurons was found to be required for *in vivo* distal axon extension, arborisation and target innervation in mice via Ror tyrosine kinase receptors (*Ryu, et al., 2013*). While SEMA3A signalling through receptor neuropilin-1 (NRP1) was found to regulate target innervation of developing sympathetic neurons (of the heart and aorta) in mice (*Maden, et al., 2012*). In distal axons of primary sympathetic neurons CTβ2 (isoforms of CTP: phosphocholine cytidylyltransferase (CT)), a major contributor to phosphatidylcholine (PC) synthesis, promoted axon branching (*Strakova, et al., 2011*). However, the most well studied mediator of distal axon extension is nerve growth factor (NGF) (*Levi-Montalcini, 1987*).

3.5 NGF

NGF is the founding member of the neurotrophin family which is a family of structurally related, secreted proteins that are essential for the development and functioning of the nervous system (*Lewin and Barde, 1996*). The neurotrophin family consists of a number of closely related factors including brain-derived neurotrophic factor (BDNF) (*Leibrock, et al., 1989*); NT-3 (already described) (*Maisonpierre, et al., 1990*); neurotrophin 4/5 (NT-4/5) (*Berkemeier, et al., 1991; Hallbook, et al., 1991*) and the prototype NGF (*Levi-Montalcini, 1987*).

NGF is required for the survival of sympathetic neurons *in vivo* (*Angeletti and Levi-Montalcini, 1971; Crowley, et al., 1994; Levi-Montalcini and Booker, 1960*) and *in vitro* (*Deshmukh and Johnson, 1997; Greene, 1977; Martin, et al., 1988*). In addition, *in vitro* experiments demonstrate the axonal growth promoting effects on NGF in sympathetic neurons (*Atwal, et al., 2000; Campenot, 1994; Campenot, et al., 1994; Cohen, et al., 1954; Deckwerth, et al., 1996; Mains and Patterson, 1973*). As NGF is crucial for the survival of developing sensory and sympathetic neurons, this poses an obvious difficulty for the investigation of the role of NGF directly in promoting axonal growth of these neurons *in vivo*. This difficulty was overcome by Patel et al 2000, who studied DRG cells of NGF -/- Bax -/- and Bax -/- TrkA -/- mice (*Patel, et al., 2000*). Bax is a pro-apoptotic member of the Bcl-2 family required for programmed cell death in a number of tissues (*Korsmeyer, 1999*). The loss of DRG neurons in NGF -/- mice was prevented in NGF -/- Bax -/- mice. This method allowed for the study of NGF function in axonal growth independent of its function in survival. Using this method, Glebova and Ginty 2004, found that NGF is heterogeneously required for axonal growth and peripheral innervation of sympathetic targets of both paravertebral and prevertebral sympathetic ganglia *in vivo*. In addition, this study also highlights that target organs vary in their individual NGF requirements for sympathetic innervation. In NGF -/- Bax -/- mice, there is an absence of sympathetic innervation in the submaxillary salivary gland, the parotid gland and the iris, all targets of the SCG. Sympathetic innervation of the heart and lungs, targets of the SG is drastically decreased in the absence of NGF. However, the sympathetic innervation of the trachea, a target primarily of the SCG and secondarily of the SG, is only slightly reduced in the absence of NGF when compared to controls. The spleen, stomach and kidney receive sympathetic

innervation from the CG and thoracic chain ganglia; the innervation of these targets is reduced in NGF -/- mice but to a lesser extent than that of the targets of the SCG. A reduction in sympathetic innervation in the absence of NGF is also evident in the Gastro-intestinal tract (GIT), ureters, bladder and gonads, also targets of CG, in addition to SMG and IMG, thoracic and lumbsaccral ganglia (*Glebova and Ginty, 2004*). This study confirms that, in addition to its role in neuronal survival, NGF plays a key role in axonal growth of sympathetic axons and consequently in the establishment of normal patterns of innervation in particular peripheral targets *in vivo*. However, the partial innervation of many organs in the absence of NGF confirmed that successful sympathetic axonal growth into peripheral targets is likely to depend on a range of factors with overlapping roles.

3.5.1 Discovery of NGF

NGF was discovered in the 1950s by Rita Levi-Montalcini and Victor Hamburger through a series of experiments on chicken embryos through the grafting of mouse sarcoma into the body wall of a 3 day old chicken embryo which was fixed 3-5 days later. Both sensory and sympathetic fibres entered the neoplastic tissue, building a high density network of fibres that branched between tumour cells. Sensory and sympathetic ganglia were significantly larger in chicken embryos grafted with sarcoma tissue compared to controls. They hypothesised that the neoplastic cells released a soluble diffusible agent that altered the differentiation and growth of developing neurons. This agent was termed a tumour nerve promoting factor, a factor that is now well known as NGF (*Levi-Montalcini, 1987*). NGF was purified from snake venom and injected into 6-8 day old chicken embryos resulting in overgrowth of sensory and sympathetic ganglia, and profuse branching into viscera and veins. This effect was inhibited with the application of NGF antiserum. An *in vitro* bioassay indicated that the submandibular gland is a source of NGF. Following injection of antiserum of submandibular-sourced NGF, mouse paravertebral and prevertebral ganglia disappeared (*Levi-Montalcini, 1987; Levi-Montalcini and Hamburger, 1951*). From these early experiments, it became clear that NGF is important for the regulation of survival of the developing sensory and sympathetic neurons.

3.5.2 Mechanism of action of NGF

NGF is produced in the peripheral targets of NGF-dependant neurons, such as the heart, submandibular gland and the iris in rats (*Heumann, et al., 1984; Korsching and Thoenen, 1985*). Recently, mouse heart vascular smooth muscle cells were shown to secrete NGF, attracting axons toward their final cardiac target (*Nam, et al., 2013*).

NGF production begins with the arrival of the earliest axons (*Davies, et al., 1987*) and its production in target organs determines the density of innervation by the SNS (*Korsching and Thoenen, 1983*). Early studies examining the role of NGF lead to the development of the neurotrophic hypothesis (*Levi-Montalcini, 1987; Levi-Montalcini and Hamburger, 1951*) which states that neurons compete for limiting amounts of target-derived survival factors and those that obtain sufficient amounts gain a competitive advantage over others and survive, whereas those that fail to compete die (*Oppenheim, 1989*). Therefore neurons innervate their peripheral targets initially in excess numbers and those in excess are eliminated by cell death following innervation of the target tissue.

NGF mediates its actions by binding two receptors, tyrosine kinase A (TrkA) and p75 neurotrophic factor receptor (p75NTR), both transmembrane glycoproteins, of which TrkA is a high affinity receptor and p75NTR, a low affinity receptor for NGF (*Davies, et al., 1993; Kaplan and Miller, 1997*). Deppmann et al put forward a model for neuronal competition during development. NGF is required for the expression and upregulation of TrkA in SCG neurons as deprivation of NGF in these neurons resulted in a reduction in TrkA upregulation and subsequent TrkA signalling. NGF also upregulated fellow members of the neurotrophin family, BDNF and NT-4 which promoted SCG neuronal cell death by binding p75NTR at subsaturating levels of NGF. However cell death was suppressed by concentrations of NGF that activate TrkA therefore neurons with enhanced NGF-survival signalling could facilitate the removal of other neurons through p75NTR-dependent pro-apoptotic signalling (*Deppmann, et al., 2008*).

3.5.3 TrkA

TrkA is a member of the Trk gene family, which includes TrkB, the receptor for BDNF and NT-4, and TrkC, the receptor for NT-3. NT-3 also activates TrkA but

only does so at much higher concentrations than NGF (*Kaplan and Miller, 1997*). TrkA is known as the high affinity receptor for NGF (*Mahadeo, et al., 1994*). NGF is released from peripheral targets and acts directly on distal extending axons to promote local growth (*Campenot, 1994; Kuruvilla, et al., 2004*). Following NGF/TrkA binding at distal axons, NGF/TrkA is internalised by a process known as endocytosis which may be clathrin (a protein involved in the formation of vesicles) dependent or clathrin-independent (*Doherty and McMahon, 2009*). One type of clathrin-independent mechanism is macropinocytosis, which involves the formation of plasma membrane protrusions that eventually fuse together and engulf large volumes of membrane and extracellular fluid. Pincher, an NGF-upregulated GTPase, is involved in clathrin-independent internalization (*Shao, et al., 2002*). The internalised vesicle becomes a signalling endosome and is eventually degraded. A signalling endosome refers to an endosome containing active ligand-receptor complexes that associate with and activate components of downstream growth and survival signalling pathways as they traffic within axons and cell bodies (*Harrington and Ginty, 2013*). Members of the RAB family of GTPases are involved in the transformation of vesicle to a signalling endosome (*Zerial and McBride, 2001*). The signalling endosome is transported in a retrograde fashion which involves the directed, coordinated movement of proteins or vesicles from distal axons (*Harrington and Ginty, 2013*) towards the neuronal soma and dendrites (*Sharma, et al., 2010*). At the cell soma the signalling endosome mediates a number of processes including neuronal survival, growth, gene expression, and synaptogenic signalling events (*Harrington and Ginty, 2013; Pazyra-Murphy, et al., 2009; Sharma, et al., 2010*). A transcriptional response is required for axonal growth over long periods of time (*Bodmer, et al., 2011*). Transcription factors involved in axonal growth include cyclic AMP responsive element-binding protein (CREB) (*Lonze, et al., 2002; Wickramasinghe, et al., 2008*), serum response factor (SRF) (*Wickramasinghe, et al., 2008)* and nuclear factor of activated T-cells (NFAT) (*Graef, et al., 2003*).

TrkA activates PI3-kinase–Akt and extracellular related kinase (ERK) pathways and their downstream effectors including PI3K stimulation of Akt and ERK stimulation of MAP kinase cascades (*Huang and Reichardt, 2003*); *Kaplan and Miller, 2000; Sofroniew, et al., 2001*). TrkA activates these pathways via Ras (see

below) in rat sympathetic neurons as shown by the inhibition of survival in these neurons with a neutralising antibody to p21Ras (*Nobes and Tolkovsky, 1995*).

3.5.4 ERK1/2 signalling

TrkA activation has been shown to promote axonal growth via the ERK1/2 pathway. ERK1/2 is one of the many MAP kinase (MAPK) family signalling cascades. These cascades are regulated by phosphorylation (covalent binding of phosphate groups to an amino acid residue in a process catalysed by enzymes called kinases (*Johnson and Lapadat, 2002*). The MAPK family consists of a number of kinases which share similar homology, the founding member of which is ERK, a 42kDa proteins that phosphorylates at tyrosine residues (*Boulton, et al., 1991*). The MAPK family includes five branches: ERK1/2; c Jun N-terminal (JNK) 1, 2, 3; p38; ERK 3, 4, 5 and ERK 6, 7, 8 (*Bogoyevitch and Court, 2004*). Different MAPK branches respond to different stimuli for example ERK responds to trophic factors and p38 responds to UV radiation (*Chang and Karin, 2001*). The common feature amongst all branches is three serially linked kinases in each pathway, MAPKKK, MAPKK, MAPK (where K=kinase), which can be described as the general pathway.

ERK1/2 activation has been shown to regulate cell proliferation, differentiation, motility, survival and growth in a number of tissues (*Meloche and Pouyssegur, 2007; Pearson, et al., 2001; Roux and Blenis, 2004*). In the PNS, ERK1/2 signalling is required for axonal growth and target innervation of NGF-dependant sympathetic neurons (*O'Keeffe, et al., 2008*). Growth factors activate ERK1/2 by binding to their relevant tyrosine kinase receptors (*Blume-Jensen and Hunter, 2001*). The tyrosine kinase cytoplasmic domain of these receptors contains regions that are subject to phosphorylation and autophosphorylation which act as recognition and recruitment sites for signalling proteins such as growth factor receptor bound 2 (GRB2), an adapter protein that binds trks directly or via another adapter protein, Src homology 2 domain containing transforming protein (Shc) (*Pelicci, et al., 1992; Rojas, et al., 1996*). GRB2 associates with nucleotide exchange factor Son of sevenless (SOS), which through guanine exchange, enhances GDP release and GTP binding to membrane bound product of proto-oncogene c-Rat sarcoma viral oncogene homolog (Ras), converting Ras GTPase into an active form (*Li, et al., 1993*). Ras then interacts with a number of downstream effectors. In the

ERK1/2 cascade, Ras acts as an adapter to activate Raf murine sarcoma viral oncogene homolog (Raf) kinases, the first of the central 3 tier core signalling module of all MAPKs (MAPKKK, MAPKK (MKK/MEK) and MAPK), where Raf = MAP3K (*Jelinek, et al., 1996*). There are three Raf proteins, Raf-1, A-Raf and B-Raf (*Rapp, et al., 1983*). Raf can be phosphorylated by v-Akt murine thymoma viral oncogene homolog (Akt), p21-activated protein kinase (PAK) and Sarcoma viral oncogene (Src). The phosphorylation of Raf activates MEK1/2 (MAPKK) (*Zheng and Guan, 1993*) which activates ERK1/2 (MAPK) by phosphorylation which occurs at two ERK sites, i.e. dual phosphorylation is required for significant ERK activation (*Ferrell and Bhatt, 1997*). MAPK signal transduction is regulated by dual specificity phosphatases (DUSPs) which dephosphorylate both sites. DUSPs are also known as MAPK phosphatases (MKPs) (*Caunt, 2012*). ERK signal transduction is assisted by scaffold proteins which increase specificity and efficiency of ERK signalling and regulate ERK signalling and include kinase suppressor of Ras (KSR), MEK partner 1 (MP1) and similar expression to FGF genes (Sef) (*Omerovic and Prior, 2009*). Activated ERK regulates growth factor responses in the cytosol and translocates to the nucleus where it phosphorylates a number of transcription factors that regulate gene expression. Cytosol targets include members of the ERK pathway acting in a negative feedback loop such as SOS (*Dong, et al., 1996*) as well as ribosomal protein S6 kinases (RSK) which translocates to the nucleus and phosphorylates factors such as CREB (*Xing, et al., 1996*). Additional nuclear targets include ternary complex factors (TCFs) such as Ets-like gene 1 (Elk-1) (*Marais, et al., 1993*) and proto oncogene v-myc myelocytomatosis viral oncogene homolog (c-myc) (*Sears, et al., 2000*).

Several neurotrophic factor-regulated transcription factors — including CREB, SRF and NFAT, mentioned earlier, have been implicated in promoting axonal outgrowth *in vivo* (*Graef, et al., 2003; Lonze, et al., 2002; Wickramasinghe, et al., 2008*). Embryonic mice deficient in calcineurin-NFAT signalling display dramatic defects in sensory axonal outgrowth, however little or no defects in neuronal differentiation or survival were found (*Graef, et al., 2003*). CREB is required for survival and axon extension of sensory and sympathetic neurons demonstrated by impaired axonal growth and projections in cultured neurons from CREB null mice (*Lonze, et al., 2002*). SRF-mediated NGF signalling is required for

axonal growth, branching, and target innervation by embryonic DRG sensory neurons via MEK/ERK signalling shown by murine gene deletion studies of SRF. This resulted in defects in extension and arborization of peripheral axonal projections in the target field *in vivo* which was similar to the target innervation defects observed in mice lacking NGF (*Wickramasinghe, et al., 2008*).

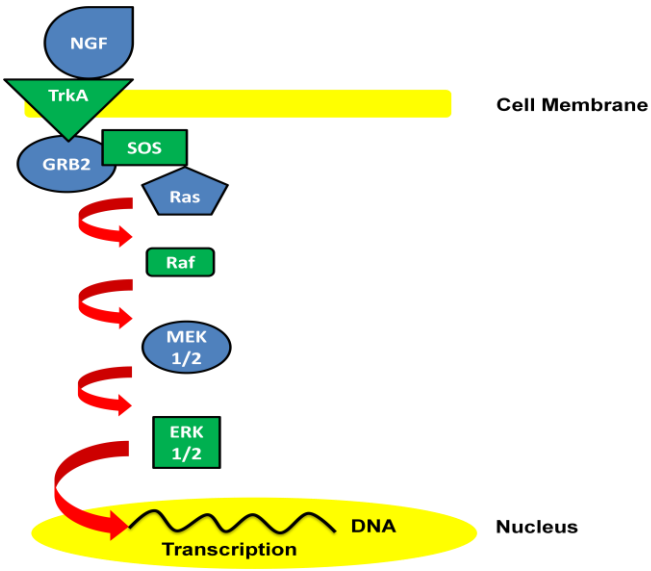


Figure 3.5: The MAPK signalling pathway

Ligand (eg. NGF) binds to its receptor (eg. TrkA) on the cell membrane which binds to docking proteins such as GRB2. GRB2 binds and activates SOS and subsequently Ras and MAP3K (eg. Raf) followed by MAP2Ks (MEK1/2) and lastly MAPKs (ERK1/2) resulting in transcription of target genes and changes in gene expression.

3.5.5 ERK1/2 signalling in sympathetic axonal growth and target innervation

MAPK was found to mediate neurite growth-enhancing actions of NGF in neonatal sympathetic neurons, as seen by pharmacological inhibition of MEK1 and MEK2 which blocked NGF-induced phosphorylation of ERK1/2 and resulted in a significant reduction of axonal growth in neonatal sympathetic neurons (*Thompson, et al., 2004*). Further support for MAPK in axonal growth comes from Goold et al which found that NGF/TrkA signalling via MAPK activated serine/threonine kinase glycogen synthase kinase 3beta (GSK3β) which phosphorylated microtubule-associated protein 1B (MAP1B) which regulated microtubule dynamics in growing axons and induced axonal growth (*Goold and Gordon-Weeks, 2005*). To assess the importance of MAPK activation in NGF-promoted axonal growth in neonatal

sympathetic neurons, O'Keeffe et al. studied the effect of U0126, a selective pharmacological blocker of MEK 1 and 2, the kinases that phosphorylate ERK1/2. This compound caused a substantial decrease in the size and complexity of the neurite arbors of neonatal mouse sympathetic neurons grown with NGF. NGF activation of MAPK signalling in the growth promotion of developing sympathetic neurons is facilitated by a member of the tumour necrosis factor (TNF) receptor superfamily (TNFRSF), namely glucocorticoid-induced tumour necrosis factor receptor (GITR). O'Keeffe et al showed that ERK1/2 activation was reduced in neonatal sympathetic neurons from GITR -/- mice (*O'Keeffe, et al., 2008*). More recently, Egr3, a transcriptional regulator whose expression is coupled to MAPK signalling (*Eldredge, et al., 2008; Li, et al., 2011*), has been implicated in NGF promotion of axonal growth via MAPK signalling. Using a method employed by Glebova and Ginty, Bax was eliminated and sympathetic neuron death was prevented (*Glebova and Ginty, 2004*) allowing for analysis of the effect of deleting Egr3 on target innervation. Mice with simultaneous loss of Bax and Egr3 had atrophic sympathetic neurons, dysautonomia (autonomic dysfunction) and sympathetic target tissue innervation abnormalities. Target tissue innervation was not effected uniformly, with some tissues showing severe sympathetic innervation abnormalities, while in other tissues no innervation abnormalities were observed. The conclusion was Egr3 is required for normal terminal axon extension, branching and target tissue innervation of sympathetic neurons following NGF induction of MAPK signalling (*Eldredge, et al., 2008; Li, et al., 2011*).

3.5.6 p75NTR

Like GITR, p75NTR is a member of the TNFRSF and binds all members of the neurotrophin family (*Frade and Barde, 1998; Rodriguez-Tebar, et al., 1990*). p75NTR consists of an extracellular, transmembrane and cytoplasmic domain, the latter of which contains a 'death' domain similar to other members of this family (*Liepinsh, et al., 1997*).

p75NTR is expressed by developing sympathetic neurons at low levels as they project along NT-3-expressing vasculature and other intermediate targets of sympathetic neurons, however these levels peak upon innervation of final target fields (*Verdi and Anderson, 1994; Wyatt and Davies, 1995*). At the stage of peak

expression of p75NTR, sympathetic neurons become less sensitive to NT-3 indicating that p75NTR is involved in the switch in neuron responsiveness from NT-3 to NGF (*Kuruvilla, et al., 2004*). The expression of p75NTR is dependent on NGF, demonstrated by the dramatic decrease in p75NTR expression in the absence of NGF in sympathetic neurons (*Kuruvilla, et al., 2004*).

p75NTR induces cell death and cell survival depending on the cellular context. p75NTR promotes cell death by apoptosis in a ligand-independent and dependant manner. Ligand-independent p75NTR-mediated cell apoptosis occurs in cell lines and neurons from DRG while ligand-dependant p75NTR-mediated cell death occurs in proprioceptive, sympathetic and oligodendrocytes neurons *in vitro*, and neurons of the developing retina, spinal cord, sympathetic ganglia and cholinergic basal forebrain nuclei *in vivo (Frade and Barde, 1998)*. Following ligand binding, the intracellular region of p75NTR interacts with NRIF to transduct the cell death signal as seen by a reduction in cell death of the developing retina of NRIF -/- mice to the same extent as in p75NTR -/- and NGF -/- mice (*Casademunt, et al., 1999*). In support of the Deppmann et al 2008 study mentioned above, p75NTR induced apopotic cell death in sympathetic neurons and therefore contributed to normal developmental elimination of neurons as seen by excess SCG neurons in p75NTR -/- mice during the apoptotic period (*Bamji, et al., 1998*). BDNF is synthesized by sympathetic neurons upon NGF exposure resulting in sympathetic neuron cell death (*Deppmann, et al., 2008*). BDNF binding to p75NTR in sympathetic neurons results in JNK activation, specifically, JNK3, which then causes a transcriptional up-regulation of the metalloprotease TACE/ADAM17 leading to receptor cleavage. The freed intracellular domain (ICD) prolongs the activation of JNK, ultimately resulting in apoptosis (*Kenchappa, et al., 2010*).

p75NTR promotes the survival of sensory and sympathetic neurons by increasing the neurons sensitivity to NGF as seen by a 2- to 3-fold decreased sensitivity to NGF in embryonic and postnatal DRG and SCG neurons from p75NTR deficient mice (*Lee, et al., 1994b*). p75NTR increases the binding affinity in addition to the internalisation of NGF and TrkA, demonstrated by kinetic analysis in which a 25-fold increase in rate of association between NGF and TrkA when TrkA is co-expressed with p75NTR compared to when TrkA is expressed alone in PC12 cell lines (*Mahadeo, et al., 1994*). The high affinity site formation between NGF and

TrkA has been attributed to the interaction between the transmembrane and cytoplasmic domains of TrkA and p75NTR where p75NTR alters the conformation of TrkA to generate high affinity NGF binding (*Esposito, et al., 2001*). Recently, the juxtamembrane ICD of p75NTR was found to be required to potentiate TrkA-mediated signalling (*Matusica, et al., 2013*). Furthermore, the ICD of p75NTR modulated the binding of NGF to TrkA by significantly increasing the amount of NGF bound to TrkA-expressing cells, with no change in the surface expression of either p75NTR or TrkA receptors (*Matusica, et al., 2013*). p75NTR-mediated activation of the transcription factor nuclear factor kappa B (NF-κB) plays a role in enhancing the survival response of developing sensory neurons to NGF. Antibodies that block binding of NGF to the p75NTR prevented NGF-induced NF-κB activation and reduced the NGF survival response in sensory neurons of embryonic mouse trigeminal ganglia (*Hamanoue, et al., 1999*).

In addition, p75NTR exhibits growth promoting effects in different neuronal populations. Decreased p75NTR expression by antisense oligonucleotides in media resulted in a reduction in the growth of chick embryonic sensory neurons (*Wright, et al., 1992*). p75NTR supports axonal growth of some sympathetic neurons as seen by lack of sympathetic innervation of the pineal gland and reduced or absent innervation of footpad sweat glands in p75NTR-/- mice (*Lee, et al., 1994a*).

3.5.7 NF-κB

NF-κB is a regulator of axonal growth in developing sympathetic neurons (*Gutierrez and Davies, 2011*), but is most well known for its role in the immune system. In the immune system, NF-κB regulates the expression of genes involved in innate and adaptive immune responses, inflammatory responses, cell survival and cell proliferation (*Hayden, et al., 2006; Liang, et al., 2004; Tergaonkar, 2006*).

NF-κB is a transcription factor consisting of homodimers or heterodimers of a family of five structurally related proteins: p65 (RelA); RelB; c-Rel; p50 and p52, of which the p50/p65 heterodimer is predominant in many cell types, including the nervous system (*Karin, 1999*). These protein subunits are related through an N-terminal, 300 amino acid, DNA binding/dimerization domain, called the Rel homology domain (RHD), through which they can form homodimers and heterodimers that bind to 9-10 base pair DNA sites, known as κB sites, in the

promoter and enhancer regions of genes, thereby modulating gene expression (*Chen, et al., 1998*). p65 (RelA), c-Rel and RelB contain C-terminal transcriptional activation domains (TADs), which enables them to activate target gene expression. In contrast, p50 and p52 do not contain C-terminal TADs; therefore, p50 and p52 repress transcription unless they are bound to a protein containing a TAD, such as RelA, c-Rel, RelB or Bcl-3 (a related transcriptional co-activator). Unlike the other NF-κB family members, p50 and p52 are derived from larger precursors, p105 and p100, respectively (*Chen and Greene, 2004; Hayden and Ghosh, 2004; Hoffmann, et al., 2006; Rothwarf and Karin, 1999*). A more recent study demonstrated that another essential subunit of NF-κB, ribosomal protein S3 (RPS3), cooperates with Rel dimers to achieve full binding and transcriptional activity. As an integral component, RPS3 plays a critical role in determining the DNA binding affinity and regulatory specificity of NF-κB (*Wan, et al., 2007*).

There are two signalling pathways leading to the activation of NF-κB known as the canonical or classical pathway (*Hayden and Ghosh, 2004*) and the non-canonical or alternative pathway (*Bonizzi and Karin, 2004*). The two types of NF-κB activation pathways differ in respect to the types of activating stimuli; the I kappa B kinase (IKK) components involved and the targeted NF-κB subunits. In both pathways, NF-κB is held in an inactive form in the cytosol by interaction with a member of the I kappa B (IκB) family of inhibitory proteins IκBα, IκBβ, IκBε, IκBγ, of which IκBα and IκBβ are the most abundant (*Hacker and Karin, 2006*). Upon stimulation by extracellular inducers, IκB kinase complex (IKK complex) consisting of catalytic kinase subunits IKKα and/or IKKβ and the regulatory non-enzymatic scaffold protein NEMO/IKKγ is phosphorylated (*Karin and Ben-Neriah, 2000*) which leads to ubiquitination and proteosome-mediated degradation of IκB or ubiquitination without proteosomal-mediated degradation, depending on the pathway (*Karin and Ben-Neriah, 2000*). This results in the liberation of the NF-κB subunit, which translocates to the nucleus, where they bind to κB sequences in the promoter and enhancer regions of responsive genes. NF-κB activation leads to the expression of the IkBα gene, which consequently sequesters NF-κB subunits and terminates transcriptional activity unless a persistent activation signal is present (*Baldwin, 1996; Chen, et al., 1998; Hacker and Karin, 2006; Karin, 1999; Perkins, 2007*).

In the canonical pathway (Figure 3.6), NF-κB proteins RelA, c-Rel, RelB and p50 are activated by IKKβ which phosphorylates IκB at serines 32 and 36 leading to subsequent ubiquitination and proteasome-mediated degradation of IκB, resulting in the translocation of the liberated NF-κB subunit to the nucleus where it binds to κB elements in the promoter and enhancer regions of responsive genes, resulting in gene induction or gene repression (*Bonizzi and Karin, 2004; Gilmore, 2006; Hayden and Ghosh, 2004; Karin, 1999; Scheidereit, 2006; Tergaonkar, 2006*).

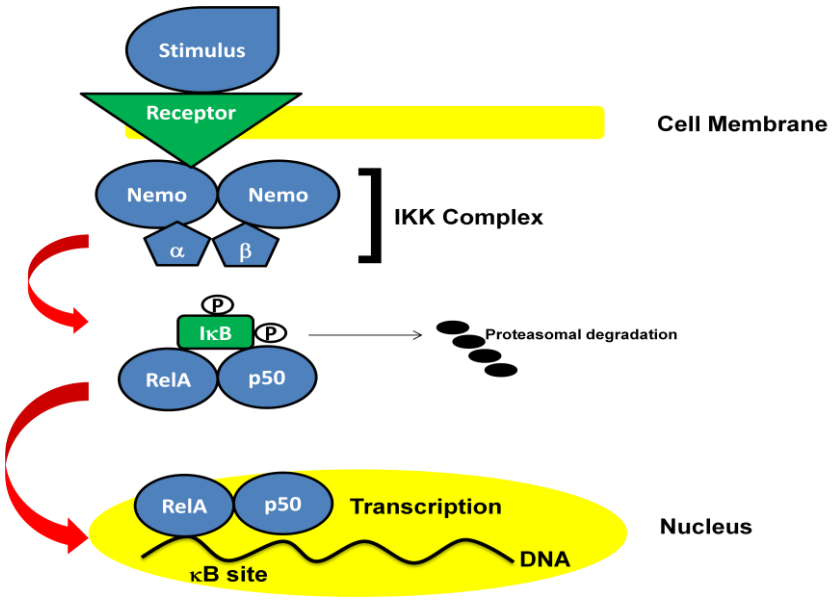


Figure 3.6: The canonical NF-κB pathway

Ligand-receptor binding leads to the recruitment and activation of an IKK complex comprising IKKα and IKKβ catalytic subunits and two molecules of NEMO/IKKγ. The IKK complex then phosphorylates IκB at serine 32 and 36, leading to the ubiquitination and proteosome-mediated degradation of IκB. NF-κB is then freed from IκB allowing for its translocation to the nucleus to activate target genes regulated by κB sites.

In the non-canonical pathway (Figure 3.7), NF-κB protein p100/RelB complex is activated by NF-κB inducing kinase (NIK)-mediated phosphorylation of IKKα, which (without requiring IKKβ or NEMO) phosphorylates p100 at tyrosine 42 (Tyr42) to trigger ubiquitination without proteasome-mediated degradation and processing of p100 (*Senftleben, et al., 2001; Xiao, et al., 2001*) leading to subsequent translocation of the liberated NF-κB to the nucleus where it binds to κB elements in the promoter and enhancer regions of responsive genes, resulting in gene induction or gene repression (*Bonizzi and Karin, 2004*).

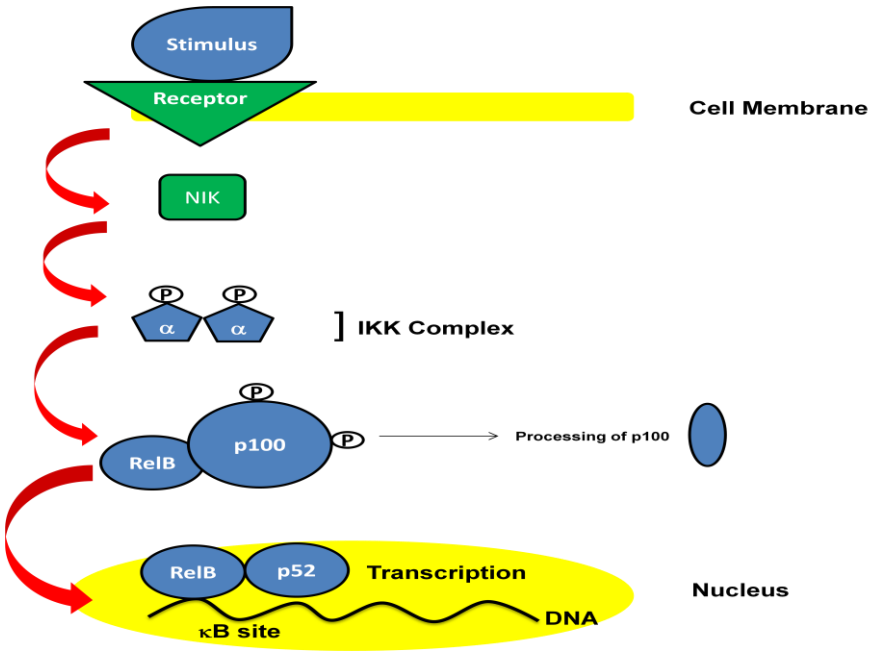


Figure 3.7: The non-canonical NF-κB pathway

Ligand-receptor binding leads to the activation of NIK, which phosphorylates and activates an IKK α complex which in turn phosphorylates p100 leading to the liberation of p52/RelB. This heterodimer subsequently translocates to the nucleus to activate target genes regulated by κB sites.

3.5.8 NF-κB and neurite growth

NF-κB signalling has been shown to regulate the axonal growth of developing sympathetic neurons (*Gutierrez, et al., 2008; Nolan, et al., 2011*). However, the first evidence of NF-κB signalling in the regulation of axonal growth came from studies on sensory neurons of the PNS. NF-κB is required for the promotion of growth in developing sensory neurons in mice (*Gallagher, et al., 2007; Gavalda, et al., 2009b; Gutierrez and Davies, 2011; Gutierrez, et al., 2005; Gutierrez, et al., 2008*). Developing sensory neurons require BDNF and ciliary neurotrophic factor (CNTF) for neurite growth *(Gavalda, et al., 2009b; Gallagher, et al., 2007).* However, the pathways used by these neurotrophins differ. BDNF/NF-κB signalling is required for neurite growth in embryonic sensory neurons, whereas NF-κB signalling in neurite growth is BDNF-independent in postnatal neurons *(Gavalda, et al., 2009b).* CTNF activation of NF-κB is found in postnatal sensory neurons *(Gallagher, et al., 2007),* where CTNF employs tyrosine phosphorylation of IκBα and involves spleen

tyrosine kinase (SYK) phosphorylation to promote sensory neurite growth *(Gallagher, 2007).* The developmental switch in pathway requirements for BDNF from embryonic to late embryonic and postnatal sensory neurons is interesting. In embryonic sensory neurons, BDNF activates NF-κB via tyrosine phosphorylation of IκBα by Src kinase. The promotion of neurite growth in E18 and P1 nodose neurons does not require BDNF to activate canonical NF-κB signalling via serine phosphorylation of IκBα, i.e. NF-κB signalling is BDNF-independent in these neurons (*Gutierrez, et al., 2005*). The reason behind this developmental switch in signalling requirements of these neurons is currently being investigated.

In developing sympathetic neurons of the PNS, NF-κB signalling has the opposite effect in that it is involved in the inhibition of axonal growth (*Gutierrez, et al., 2008*). Basal levels of NF-κB activity are present in sympathetic neurons from the SCG of neonatal mice (*Gutierrez, et al., 2008; Nolan, et al., 2011*). When this level of NF-κB activity is enhanced, there is a reduction in sympathetic neurite growth (*Gutierrez, et al., 2008*). The growth inhibitory effects of NF-κB in sympathetic neurons have been shown to be mediated through a canonical pathway in which activated IKKβ phosphorylates IκBα, leading to its ubiquitination and proteosome-mediated degradation, allowing the liberated p65/p50 dimer to translocate to the nucleus (*Gutierrez, et al., 2008*). A number of signals activate this pathway, including tumour necrosis factor α (TNFα) (*Gutierrez, et al., 2008*). Upon binding to TNF receptor-1 (TNFR1), TNFα recruits several adapter proteins such as TNFR1-associated death domain proteins (TRADDs); receptor interacting protein 1 (RIP1) and TNFR-associated factors (TRAFs 2 and 5) and the IKK complex (*Gutierrez and Davies, 2011*). p65, a known substrate of IKKβ (Sakurai et al, 1999), is phosphorylated at serine 536 following TNFα treatment resulting in elevated levels of phospho-S536-p65 which is required for the growth inhibitory effects of NF-κB activation in these neurons (*Gutierrez, et al., 2008*). More recently it has been shown that this basal level of NF-κB activity present in SCG neurons can be modified by other factors present in the SCG such as interleukin-1β (IL-1β) (*Nolan, et al., 2011*). Nolan et al found that exogenous IL-1β acts directly on the axons of developing sympathetic neurons to inhibit their growth via NF-κB signalling. Basal

levels of NF-κB do not negatively influence axonal growth in developing sympathetic neurons (*Gutierrez, et al., 2008*) and given that there are factors in these neurons that enhance NF-κB activity resulting in axonal growth inhibition such as IL-1β (IL-1β is synthesised in sympathetic ganglia neurons) (*Nolan, et al., 2011*), it is possible that there are also factors in these neurons that prevent the elevation of NF-κB activity and therefore prevent growth inhibition.

3.6 GITR

GITR (TNFRSF18), the 18th member of the TNFRSF, is a type I transmembrane protein, first identified in 1997 in T-cell hybridomas that were treated with dexamethasone, a synthetic member of the glucocorticoid class of steroid drugs that has anti-inflammatory and immunosuppressant properties (*Nocentini, et al., 1997*). GITR is activated by its specific ligand GITRL, a type II transmembrane protein (*Bossen, et al., 2006; Gurney, et al., 1999; Kim, et al., 2003a; Kwon, et al., 1999; Ronchetti, et al., 2004; Tone, et al., 2003; Yu, et al., 2003*). GITR and its specific ligand GITRL have recently been implicated in NGF-promoted growth and target innervation of developing sympathetic neurons (*O'Keeffe, et al., 2008*), however GITRL-GITR signalling is most well known for its role in the immune system where it is involved in regulating innate and acquired immune responses (*Krausz, et al., 2007; Nocentini and Riccardi, 2005*).

3.6.1 GITR in the immune system

GITR is expressed in a number of cells in the immune system. GITR is expressed at high levels in effector T cells, Treg cells and activated NKCs (*Cosmi, et al., 2003; Kanamaru, et al., 2004; Kim, et al., 2006; Kohm, et al., 2004; McHugh, et al., 2002; Ronchetti, et al., 2004; Scotto, et al., 2004; Stephens, et al., 2004; Uraushihara, et al., 2003; Zelenika, et al., 2002*); at medium levels in naïve effector T cells, NKCs, mast cells, eosinophils, basophils, activated B cells, activated monocytes/macrophages and activated DCs (*Cuzzocrea, et al., 2006; Hanabuchi, et al., 2006; Kanamaru, et al., 2004; Kim, et al., 2006; Kohm, et al., 2004; McHugh, et al., 2002; Nakae, et al., 2006; Ronchetti, et al., 2004; Santucci, et al., 2007; Shimizu, et al., 2002; Wang, et al., 2005*) and at low levels in B cells, monocytes/macrophages and osteoclasts (*Cuzzocrea, et al., 2006; Hanabuchi, et al.,*

2006; Santucci, et al., 2007; Shimizu, et al., 2002; Shin, et al., 2006). GITRL, the specific ligand for GITR, is expressed at high levels in activated DCs, activated monocytes/macrophages and endothelial cells (*Cardona, et al., 2006; Hanabuchi, et al., 2006; Nardelli, et al., 2006; Suvas, et al., 2005*), at medium levels in DCs, moncytes/macrophages, B cells and activated T cells (*Hanabuchi, et al., 2006; Kim, et al., 2003a; Kwon, et al., 1999; Shin, et al., 2003; Stephens, et al., 2004; Tone, et al., 2003; Yu, et al., 2003*) and at low levels in eosinophils and basophils (*Hanabuchi, et al., 2006*).

In non-lymphoid tissue, mouse GITR (mGITR) mRNA is expressed at high levels in lung, kidney and small intestine tissue and at low levels in liver, ovary, brain, testis, adipose tissue, muscle and heart tissue (*Krausz, et al., 2007*). In addition, GITR expression can be detected on osteoclast precursor cells, keratinocytes and retinal pigment epithelial (RPE) cells (*Kim, et al., 2004; Shin, et al., 2005; Wang, et al., 2005*). Human GITR (hGITR) is expressed in a similar pattern in lung, brain, kidney and liver tissue (*Gurney, et al., 1999; Kwon, et al., 1999*).

3.6.2 GITR acts as a costimulatory molecule

The activation of T cells depends on specific antigens and T-cell antigen receptors (TCRs) ligation on T cells or on recognition of antibody-coated target cells sensed by NKCs. The outcome of this recognition is determined by costimulatory molecules that provide signals that amplify, complement, and modulate signals from TCR or NKCs. Costimulation is described as a pathway of intercellular communication that depends on the expression of complementary glycoproteins on the surface of interacting cells (*Zhu, et al., 2011*).

GITR is a costimulating molecule (*Ronchetti, et al., 2004*). GITR costimulation increases activation and proliferation of TCR-triggered CD4+ and CD8+ T-cells (*Esparza and Arch, 2005a; Kanamaru, et al., 2004; Ronchetti, et al., 2004; Stephens, et al., 2004; Tone, et al., 2003*). The proliferation response of CD4+ and CD8+ peripheral T cell subpopulations was potentiated when a GITR costimulus was added to an anti-CD3 stimulus. In addition, the expression of the main activation-induced receptor (IL-2Rα) and production of IL-2 and IFNγ were increased more with a GITR costimulus than with anti-CD3 alone (*Ronchetti, et al.,*

2004). GITR also inhibits the suppressive function of CD4+/CD25+ Tregs cells. Agonist anti-GITR antibody reverses the suppressive effect of Treg cells (*McHugh, et al., 2002; Nocentini, et al., 1997; Shimizu, et al., 2002*). GITR can inhibit Treg activity directly (*Nocentini and Riccardi, 2005*) or indirectly by increasing T effector cell activation and increasing resistance to Tregs cells (*Shevach and Stephens, 2006*).

3.6.3 GITR in the nervous system

Recently, GITR and GITRL have been shown to be expressed in the developing mouse SCG (*O'Keeffe, et al., 2008*). Peak levels of GITR and GITRL mRNA can be detected in SCG neurons from E15-P1, shortly after the onset of naturally occurring neuronal death in these neurons, when sympathetic axons have begun to innervate and branch in their targets (*Glebova and Ginty, 2004; O'Keeffe, et al., 2008; Wright, et al., 1983; Wyatt, et al., 1997*). GITR and GITRL are expressed on all neuronal cells in the SCG and co-localise with β-III tubulin and TrkA in P0 SCG neurons (*O'Keeffe, et al., 2008*). To determine the role of GITRL-GITR in developing sympathetic neurons, GITRL-GITR signalling was inhibited in a number of ways including antisense knockdown of GITR, targeted deletion of GITR and blocking GITRL-GITR interaction using a decoy GITR-IgG, all of which reduced the ability of NGF to promote neurite growth from these neurons without affecting their survival (*O'Keeffe, et al., 2008*). These growth promoting effects of GITR were found only in the immediate postnatal stage of development (P1-3), indicating that GITR is required for the growth of sympathetic axons of neonatal SCG neurons (*O'Keeffe, et al., 2008*).

In terms of the mechanism of GITRL-GITR signalling in developing sympathetic neurons, GITR-IgG experiments suggest that GITRL-GITR signalling operates via an autocrine route. Blocking GITRL-GITR interaction at the level of individual neurons with function blocking GITR-IgG inhibits NGF-promoted neurite growth. In addition, the immunohistochemical staining pattern of GITRL *in vivo* is also consistent with autocrine GITRL-GITR signalling in sympathetic neurons. GITRL and GITR are clearly co-expressed in neurons of the SCG however GITRL immunoreactivity was undetectable in intermediate and distal SCG targets such as cranial arteries, nasal mucosa and iris (*O'Keeffe, et al., 2008*)

It is well established in the immune system that GITR acts as a costimulatory molecule to regulate effector T cell (*Esparza and Arch, 2005a; Kanamaru, et al., 2004; Ronchetti, et al., 2004; Stephens, et al., 2004; Tone, et al., 2003*) and Treg cell activity (*McHugh, et al., 2002; Nocentini, et al., 1997; Nocentini and Riccardi, 2005; Shevach and Stephens, 2006; Shimizu, et al., 2002*). To investigate whether GITR acted in a costimulatory fashion in SCG neurons as it does in T lymphocytes, SCG neurons were grown with the broad-spectrum, irreversible caspase inhibitor Boc-D-FMK to prevent the neurons from dying in the absence of NGF and treated with agonist GITRL-IgG. GITRL-IgG treatment had no effect on the smaller neurite arbors of these neurons in the absence of NGF suggesting GITR cannot promote growth of SCG neurons alone and works in a costimulatory manner with NGF (*O'Keeffe, et al., 2008*). In terms of the *in vivo* relevance of these findings, GITR signalling was found to be required for proper establishment of sympathetic innervation as seen by a reduction of sympathetic innervation in the iris and nasal muscosa (organs which normally receive dense sympathetic innervation) of GITR -/- mice compared to wild type litter mate controls (*O'Keeffe, et al., 2008*).

3.6.4 GITR signalling

TNF Receptor Associated Factors (TRAFs) are adapter proteins that transmit extracellular signals upon recruitment to the cytoplasmic domains of TNFRs, such as GITR, where they serve as foci for the induction of molecular events including NF-κB and MAPK activation (*Arch, et al., 1998; Dempsey, et al., 2003*). GITR binds and activates several TRAFs resulting in the activation or inhibition of NF-κB and MAPK pathways (*Esparza and Arch, 2005a; Gurney, et al., 1999; Kwon, et al., 1999*). TRAF 4 enhances NF-κB activation triggered by GITR (*Esparza and Arch, 2004*). When TRAF 4 was co-expressed with GITR and GITRL in a human embryonic kidney cell line (HEK 293 cells), receptor-induced NF-κB activation was significantly increased. Expression of TRAF 4 in the absence of GITR-induced signalling did not affect NF-κB activity, indicating that TRAF 4 is involved in GITR-triggered NF-κB signal transduction (*Esparza and Arch, 2004*). TRAF 2 inhibits NF-κB activation triggered by GITR. Transfection with an overexpression plasmid containing full length TRAF 2 significantly reduced NF-κB activation

triggered by GITR in HEK 293 cells *(Esparza and Arch, 2005b).* In the immune system GITR triggers the activation of MAPK signalling cascades including ERK, JNK and p38 (*Esparza and Arch, 2005a; Esparza, et al., 2006; Ronchetti, et al., 2004*). TRAF 5, triggered by GITR, activates NF-κB in addition to specific subsets of MAPKs including p38 and ERK. TRAF 5 deficiency results in diminished GITR-induced activation of NF-κB, p38 and ERK and enhances antigen-dependent T cell proliferation (*Esparza, et al., 2006*).

In developing sympathetic neurons, GITR also activates ERK signalling (*O'Keeffe, et al., 2008*). NGF-promoted ERK1/2 phosphorylation is almost eliminated in neurons from GITR -/- mice. Agonist GITRL-IgG enhances NGF-promoted ERK1/2 phosphorylation, however GITR induction of ERK1/2 did not occur in the absence of NGF. This effect of GITR signalling on NGF-promoted ERK activation in the nervous system mirrors the costimulatory role of GITR in the immune system, where GITR/CD3-stimulation promoted ERK1/2 activation in T cells (*Ronchetti, et al., 2004*).

3.7 Clinical importance of correct development of the SNS

As described earlier, sympathetic neurons innervate organs of the immune system including the thymus, spleen, lymph nodes and bone marrow (Figure 3.4) (*Felten, et al., 1985; Meltzer, et al., 1997; Panuncio, et al., 1999*). Sympathetic neurons release catecholamines that bind receptors of target immune B and T cells (*Kohm and Sanders, 2001*) and regulate a variety of immune processes including leukocyte activation, cytokine production, and cell trafficking (*Cole, et al., 1999; Cole, et al., 1998; Kammer, 1988; Madden, et al., 1995; Ottaway and Husband, 1994; Sanders and Straub, 2002*). The importance of the development of sympathetic neurons and their impact on immune system function is highlighted by an autonomic peripheral neuropathy called Hereditary Sensory Autonomic Neuropathy (HSAN) IV described below.

Autonomic peripheral neuropathies are one of four types of peripheral neuropathies which are characterised by trauma or disease to nerves of the PNS. Other peripheral neuropathies include mononeuropathies in which one nerve is affected (*Ghali, et al., 2012*); mononeuritis multiplex where one or more nerves are

affected and is associated with inflammatory conditions (*Makol and Grover, 2008*) and polyneuropathies (*Centner, et al., 2013; Lee, et al., 2013*) affecting multiple nerves in the body. Peripheral autonomic neuropathies affect neurons of the ANS and as a result can affect all systems of the body. Peripheral autonomic neuropathies can be acquired by disease such as diabetes (*Kamenov and Traykov, 2012*) or inherited such as in Familial amyloid polyneuropathy (FAP) (*Plante-Bordeneuve and Said, 2011*); Fabry disease (*Tuttolomondo, et al., 2013*); Porphyrias (*Trier, et al., 2013*) and Hereditary sensory autonomic neuropathies (HSANs). HSAN IV is one of five neuropathies of the HSAN spectrum. HSAN IV results from TrkA mutations and defective TrkA/NGF signalling affecting the development of sympathetic and sensory neurons of the PNS (*Rotthier, et al., 2012*) and therefore is the most relevant of the HSAN spectrum to the current topic however HSAN I, II, III and V will be discussed briefly.

HSAN I is an inherited autosomal dominant disease due to a mutation in the gene for Serine palmitoyltransferase, long chain base subunit 1 (SPTLC1) located on chromosome 9q22.1-22. The *SPTLC1* gene provides instructions for making a subunit of an enzyme called serine palmitoyltransferase (SPT) which is involved in making fats called sphingolipids. Sphingolipids are important components of cell membranes and play a role in many cell functions such as protein processing and transport. Onset of HSAN I is in the 2nd to 4th decade of life and symptoms include paresthesia, numbness, weakness, muscle wasting, and heel ulcers (*Axelrod and Gold-von Simson, 2007*). HSAN II is an inherited autosomal recessive disease, due to a mutation in the gene for WNK lysine deficient protein kinase 1 (WNK1) located on chromosome 12p13.33. The *WNK1* gene provides instructions for making multiple isoforms of the WNK1 protein. The different WNK1 isoforms are important in several functions in the body, including blood pressure regulation and pain sensation. Onset of HSAN II is in infancy and early years of life. Symptoms include absence of pain, thermal, touch, and pressure sensation. There is sensory loss and depressed deep tendon reflex (DTR) in some patients (*Axelrod and Gold-von Simson, 2007; Lafreniere, et al., 2004*). HSAN III, also known as familial dysautonomia, or Riley Day syndrome, is an inherited autosomal recessive disease, due to a mutation in the gene for inhibitor of kappa light polypeptide gene enhancer

in B-cells, kinase complex-associated protein (IKBKAP) located on chromosome 9q31. The *IKBKAP* gene provides instructions for making a protein called IKK complex-associated protein (IKAP) which is found in a variety of cells throughout the body, including brain cells and believed to play a role in transcription of proteins that affect cell cytoskeleton and movement, important in the development of cells. HSAN III has an onset in infancy and early years of life. Symptoms include absence or reduced pain and temperature sensation but normal touch sensation. Additional features include recurrent gastrointestinal upsets, little lacrimation, anhidrosis, no sensation of tongue, depressed or absent DTR, temperature fluctuations, recurrent fractures, osteomyelitis, gait difficulties, Charcot joints, ligamentous laxicity and scoliosis (*Axelrod and Gold-von Simson, 2007; Bar-On, et al., 2000*). HSAN V is an inherited autosomal recessive disease, due to a mutation in the gene for NGF located on chromosome 1p13. Symptoms include absence of pain; however normal touch, pressure and vibration sensation is present. Additional features include fractures, bone necrosis, osteochondritis and neuropathic joint destruction (*Minde, et al., 2004*).

3.7.1 HSAN IV

HSAN IV, also known as 'Congenital Insensitivity to Pain with Anhidrosis' (CIPA), 'Familial dysautonomia type II' or 'congenital sensory neuropathy with anhidrosis' is a rare autosomal recessive disorder (*Toscano and Andria, 2001*) first reported in 1963, when two siblings presented with an inability to feel pain and to sense temperature (*Swanson, 1963*). HSAN IV results from mutations in the gene for TrkA located on chromosome 1q21-22 (*Indo, et al., 1996*). Mutations occur in the extracellular (NGF binding) and intracellular (signal transduction) domains of TrkA (*Mardy, et al., 1999*). TrkA mutations have been reported in HSAN IV patients from different ethnic groups, including families of Ecuadorian and Japanese descent (*Mardy, et al., 1999*), Israeli-Bedouin Tribes (*Shatzky, et al., 2000*) and a patient of Spanish origin (*Sarasola, et al., 2011*). These mutations result in impairment of NGF binding to TrkA or of signal transduction following NGF binding. As a result, in this condition, subsets of sensory and sympathetic neurons do not develop normally. In

consequence, neuropathological findings include an absence of small unmyelinated fibres, a decrease in number of myelinated fibres in peripheral nerves, an absence of nociceptive innervation of the epidermis and diminished sympathetic innervation of eccrine sweat glands. These anatomical findings explain the physiological basis underlying the main symptoms of HSAN IV, pain insensitivity and inability to sweat (anhidrosis) in HSAN IV patients (*Langer, et al., 1981; Swanson, et al., 1965*). Additional clinical characteristics of HSAN IV, which illustrate the diverse roles of NGF/TrkA signalling in the PNS and CNS, are episodic fevers, self-mutilation and mental retardation. HSAN IV patients are prone to bone fractures and slow healing; joint dislocations and deformities; skin infections; impaired immune responses and renal failure (*Indo, et al., 1996*).

Reduced immune responses, including reduced T and B lymphocytes proliferation and cytokine (IL-2) production, and NKC activity in the spleen are associated with a decline in sympathetic innervation in the secondary lymphoid organs, spleen and lymph nodes in aged female rats (*ThyagaRajan, et al., 2011*). TrkA is expressed by many cells of the immune system including neutrophils, mast cells, and B and T lymphocytes (*Marshall, et al., 1990; Melamed, et al., 1996; Otten, et al., 1989*). Mutations in TrkA have also been found to result in defective lymphocyte signalling which may explain why HSAN IV patients have a greater incidence of infection than age matched controls. Specifically, B cells have defective TrkA phosphorylation and consequently display defects in cytoskeleton assembly and MAP kinase activation (*Melamed, et al., 2004*). One TrkA mutation (1926-ins-T) is associated with impaired neutrophil chemotaxis, which may contribute to the greater incidence of infection in patients with HSAN IV (*Beigelman, et al., 2009*).

3.7.2 GITR and clinical applications

In the immune system, GITR can enhance T cell activation and inhibition of Treg cells (*McHugh, et al., 2002; Shimizu, et al., 2002*). Thus, agonist anti-GITR treatment can potentially overcome tolerance to self- and tumor-antigens, making it an attractive target for development as a cancer immunotherapy. Agonist anti-GITR treatments have been found effective in enhancing T cell-mediated anti-tumor activity *in vivo*. Agonist anti-GITR monoclonal antibody, (DTA-1), induced the

regression of small established B16 melanoma tumors in mice (*Cohen, et al., 2010*). Recently, an agonist anti-human GITR mAb (TRX518) has been developed by Tolerex Inc. (now GITR Inc), and similar to anti-GITR, provides potent costimulation to human lymphocytes *in vitro*. A dose-escalation (route of administration: I.V.) phase I clinical trial for unresectable stage III or IV malignant Melanoma or other solid tumors is currently recruiting at Memorial Sloan-Kettering Cancer Center (New York, NY) using TRX518 (NCT01239134) (*Melero, et al., 2013*).

3.8 Objectives of the present study

In the PNS, GITR has recently been shown to be crucial for NGF-promoted growth of developing sympathetic neurons (*O'Keeffe, et al., 2008*). The discovery of this previously unknown signalling loop that is essential for the ability of NGF to promote axonal growth has revealed a new regulatory element in target field innervation in the developing SNS, however the exact mechanism by which GITR regulates NGF signalling is unknown. This study intends to answer basic biological questions regarding the molecular mechanism of GITR in the peripheral SNS in an early step toward identifying whether strategies targeting GITR have potential therapeutic benefit in promoting neurite growth. There are four sets of interrelated aims in this Thesis:

- To determine if GITR increases the sensitivity of sympathetic neurons to NGF.
- To identify the region of GITR required for the enhancement of NGF-promoted growth.
- To investigate the signalling pathways downstream of the GITR.
- To determine how extensively GITR is involved in regulating peripheral innervation in the sympathetic nervous system.

4.0 Materials and Methods

4.1 Animals husbandry

The animals sacrificed for tissue in the present studies were C57bl/6, CD-1 and SV-129 mice and were sourced from the Biological Unit in UCC and University of Perugia, Italy (Professor Carlo Ricarrdi). No animals underwent any surgical procedures for experimental purposes. All mice were treated humanely at all times under the "The Animals (Scientific Procedures) Act 1986".

4.2 Tissue Culture

All primary cell cultures were prepared from freshly dissected superior cervical ganglia (SCG) tissue from Postnatal day 1 and 2 (P1 & 2) mice and carried out in a sterile laminar Class II flow cabinet (Microflow: Biological Safety Cabinet) using aseptic techniques. Primary cell cultures were maintained in a humidified atmosphere containing 5% CO_2 at 37˚C.

4.2.1 Superior cervical ganglia dissection

Postganglionic sympathetic neurons of the SCG are an extensively used, experimentally tractable model for studying the molecular basis of axonal growth and target innervation in developing sympathetic neurons (*Gutierrez, et al., 2008; Nolan, et al., 2011; O'Keeffe, et al., 2008*). Mice aged P1 were used as peak levels of both GITR and ligand are expressed in the developing SCG on P1, shortly after the onset of naturally occurring neuronal death in the SCG, when sympathetic axons have begun to innervate and branch extensively in their targets (*O'Keeffe, et al., 2008*). P1 mice were sacrificed by decapitation using a sterile scissors and transferred to a 90mm Petri dish (Fannin Healthcare) containing ice-cold Hank's Balanced Salt Solution (HBSS) (with sodium bicarbonate and without phenol red, Ca2+ or Mg2+, Sigma) and kept on ice. Further dissections were carried out using a dissection microscope (Leica Wild M8) in a fume hood (Brassaire). Using the

dissecting microscope for accurate visualisation, heads were anchored anteriorly at the level of the nose using forceps, and the superior aspect of heads were transected using scissors and removed to expose the cerebral cortex. The cerebral cortex was then removed to expose the occipital bone and proximal vertebrae. Heads were then bisected in a saggital plane with scissors, using the centre of the occipital bone and vertebrae as a landmark and placed in a second Petri dish containing fresh HBSS. The medial/internal surface of the bisected head was orientated superiorly and proximal cervical vertebrae (levels C1-3) were carefully removed by cutting at superior and inferior intervertebral joints to expose the translucent SCG located at the bifurcation of the common carotid artery. The ganglion was carefully removed using forceps and placed in a third petri dish containing fresh HBSS. Using electrolytically sharpened tungsten needles, any attached extraneous tissue was removed from the SCG which were then transferred to a 15ml tube (Greiner Bio-One) containing fresh HBSS.

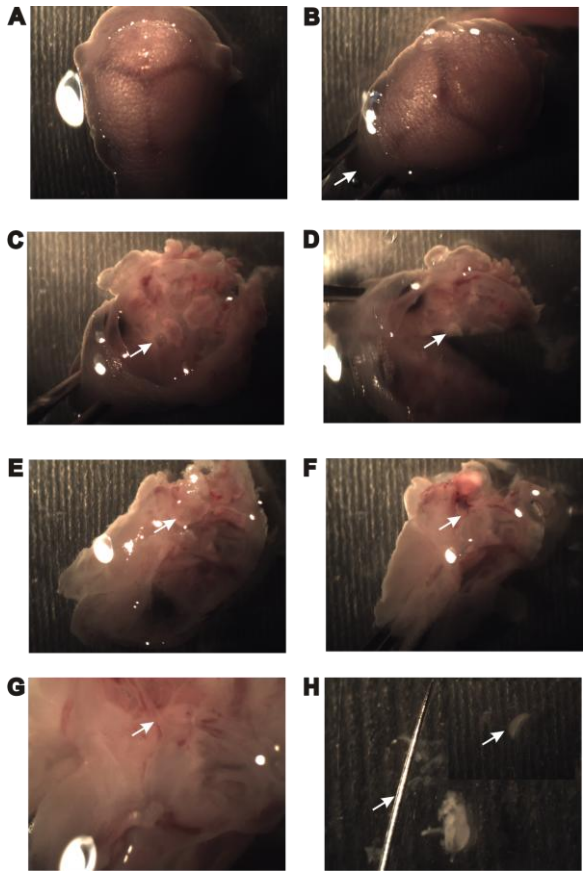


Figure 4.1: Superior cervical ganglia dissection procedure

Head is placed in a Petri dish containing fresh HBSS (A) and anchored using forceps (B). The superior aspect of the head is transected using scissors, lifted away and cortex is removed to expose the proximal cervical vertebrae (C). The head is bisected in a saggital plane by scissors using the centre of the vertebrae as a guide (D). Once bisected, the right and left sides of the head are placed in a fresh Petri dish where the internal or medial aspect of the head is facing superiorly (E). The proximal cervical vertebrae are removed to expose the underlying SCG located at the bifurcation of the common carotid artery (F, G). The SCG is removed using a forceps and placed into a Petri dish containing fresh HBSS. The SCG is cleaned of extraneous tissue using tungsten needles (H).

4.2.2 Tissue culture procedures

SCG were incubated in 1ml of trypsin (Sigma) for 20min at 37ºC. Cells were then washed X2 with 2mls F12 solution (1.06g F12 powder (Invitrogen); 10% Fetal calf serum (Sigma); 1% Penicillin/streptomycin solution (Sigma); made up to 100ml deionised H2O; filter sterilized, pH 7.2-7.4) to inhibit trypsin action. Ganglia were then washed X2 in growth media (Dulbecco's Modified Eagle Medium (DMEM:

Sigma); 1% penicillin/streptomycin; 1% glutamine (Sigma); 1% N2 (Invitrogen); 2% B27 (Invitrogen) and 10ng/ml NGF (R&D Systems)). SCG were then gently triturated 6-10 times using a sterile pipette tip in the second wash of growth media forming a single cell suspension.

4.2.2.1 P1 SCG neuronal growth

SCG cells were obtained and cell suspension prepared as described in 4.2.1 and 4.2.2. 5µl of cell suspension (cells in second wash of growth media) was transferred to a 90mm Petri dish (Fannin Healthcare) and cell density was assessed under a light microscope (Leica). Assessment of cell density helps to determine the volume of cell suspension required per well for growth analysis. Higher density (~50,000/well) of cells makes it more difficult to analyse cell growth and therefore a lower cell density (~50,000/well) is required for growth analysis than for survival transfection and immunocytochemistry experiments. An appropriate amount of cell suspension was added to the growth media. 80µl of cell solution in media was added to each well. Cells were grown overnight in sterile 4-well tissue culture 35.0/10mm (Greiner Bio-One) dishes in 37ºC. Plates were coated with polyornitine (500µg/ml, Sigma) and laminin (1mg/ml, (Sigma) diluted in 1ml of HBSS with phenol red and without Ca2+ or Mg2+ (Invitrogen) Sigma).

4.2.2.2 P1 SCG neuronal survival in different concentrations of NGF

SCG cells were obtained and cell suspension prepared as described in 4.2.1 and 4.2.2. Cells were plated at high density (~50,000/well) in growth media containing varying concentrations of NGF (10, 4, 1, 0.2, 0.04, 0.01 and 0 ng/ml). Cells were grown for 3, 24, 48 and 72h at 37°C. At the end of each time point, the number of surviving neurons was counted. At the end of time points 24, 48 and 72h, the number of surviving cells were counted and calculated as a percentage of the number of cells that survived at 3h.

4.2.2.3 P1 SCG neuron growth response in different concentrations of NGF

SCG cells were obtained and cell suspension prepared as described in 4.2.1 and 4.2.2. Cells were plated at low density (number of cells per well per dish was not counted, however it was ensured that neurons have enough room to extend processes) in growth media containing varying concentrations of NGF (10, 4, 1, 0.2, 0.04, 0.01 and 0 ng/ml) and Caspase III inhibitor (Boc-D-FMK) (4ug/ml; Calbiochem) to prevent cell death in cultures treated with low NGF concentrations. Cells were treated with recombinant mouse GITR ligand/TNFSF18 (1ug/ml; R&D Systems) (rmGITRL) and mouse GITR Ligand/TNFSF18 Antibody, Polyclonal rat IgG (5ug/ml; R&D Systems) (GITRL-IgG). rmGITRL has been found to costimulate mouse T cell proliferation in the presence of anti-CD3, while GITRL-IgG neutralises GITRL induced proliferation in mouse CD4+ T cells (*Tone, et al., 2003*). Cells were left to grow overnight on polyornitine and laminin coated 35mm dishes in 37°C. The next day cells were immunocytochemically stained for the neuronal marker β-III tubulin (Section 4.3), imaged using an inverted fluorescence microscope (Olympus IX70 Provis attached to an Olympus DP70 camera) and growth was determined using sholl analysis (*Gutierrez, et al., 2008*) (Section 4.6).

4.2.2.4 P1 SCG neuron transfections

All transfections were performed using a microporater (Neon, Invitrogen) (*Gutierrez, et al., 2008*). During transfection, a number of electrical pulses at a set voltage and duration were applied to the cells causing a transient reversible breakdown of the cellular membrane. This resulted in the formation of pores which can allow exogenous molecules, such as DNA, siRNA, antibodies, peptides or drugs to enter the cell. Equipment settings or parameters include: voltage (V), pulse width or duration (ms) and number of pulses applied.

SCG cells were obtained and cell suspension prepared as described in 4.2.1 and 4.2.2 with the following changes. SCG cells were dissociated in 1ml of trypsin for 20-23 min. Cells were then washed X2 with 2ml of transfection media (DMEM; 1% glutamine; 1% N2; 2% B27; 10ng/ml NGF) containing 10% Fetal calf serum to

inhibit trypsin action and then washed X2 in 2ml of PBS. Cells were gently triturated in resuspension buffer (Invitrogen) until dissociated. 12μl of resupension buffer was used per transfection. A red fluorescent plasmid (RFP) or an enhanced green fluorescent plasmid (EGFP) (0.5μg) was added to the cell suspension in order to identify transfected cells. To estimate the relative level of NF-κB activation, neurons were transfected with a plasmid expressing GFP under the control of an NF-κB promoter (*Gutierrez, et al., 2008*). The cell suspension was then equally divided into treatment groups and appropriate plasmids (1μg) were added to cell suspensions (Table 4.1). Following optimization, the most effective transfection parameters were determined to be 1100 volts, 30ms and 2 pulses. Once transfected at these parameters, cells were added to transfection media and grown overnight on polyornitine and laminin coated 35mm dishes in 37°C. The next day, cells were imaged using an inverted fluorescence microscope (Olympus IX70 Provis attached to an Olympus DP70 camera) and growth was determined using Sholl analysis (*Gutierrez, et al., 2008*) (Section 4.6). Images to obtain mean somal fluorescence intensity in cultures transfected with κB reporter was obtained using Zeiss Axioplan confocal microscope and mean somal intensity was determined using LSM510 software (*Gutierrez, et al., 2008*).

2.2.2.3.1 Plasmids

Plasmids were provided by Dr. Gutteriez, School of Biosciences, Cardiff University and Professor Riccardi from the Department of Clinical and Experimental Medicine, Pharmacology, University of Perugia, Italy.

All plasmids used were derived from pcDNA3.1 (Invitrogen) and included those expressing GITR, Antisense GITR, GITRδK, GITRδZ, GITRδW, GITRL, GITRLδW, GITRδ2, GITRδ4, GITRδ5, IκBα, Antisense GITR, IKKB dominant negative (DN) and p65.

Specific regions of the GITR cytoplasmic domain are missing in mutant plasmids GITRδK, GITRδZ and GITRδW. The intracellular region of GITRL is missing in mutant plasmid GITRLδW. Two putative phosphorylation sites were identified using

In silico analysis programs including DISPHOS; NetPhos 2.0; GPS Predictor software programs. Putative phosphorylation sites identified were Thr190 and Ser199 (amino acid 12 and 21). In addition, basic residues, Cys186-Glu189 (CPRE) (amino acids 8-11), conserved among the "GITR sub family" of receptors (CD27, OX40, 4-1BB) were identified (*Krausz, et al., 2007*). Mutant plasmids of GITR were then created in which insertions replaced these sites. In GITRδ2, Cys186-Glu189 (CPRE), (amino acids 8 to 11), were replaced with alanines. In GITRδ4, Thr190 and Ser199, (amino acid 12 and 21) were replaced with alanines. In GITRδ5, Thr190 and Ser199, (amino acid 12 and 21), were replaced with glutamic acid.
Plasmids were shipped on Whatman 3mm thickness paper and cut out. 50µl of 10mM Tris pH 7.6 was added, mixture was vortexed and left to re-hydrate for 5min. Following brief centrifugation, the supernatant liquid was used to transform competent bacteria.

Plasmids	**Sequences**
GITR (cytoplasmic region)	IWQLRRQHMCPRETQPFAEVQLSAEDA CSFQFPEEERGEQTEEKCHLGGRWP
GITRδK	IWQLRRQHMCPRETQPFAEVQLSAEDA CSFQFPEEERG
GITRδZ	IWQLRRQHMCPRETQPFAEVQLS
GITRδW	IW
GITRL	MEEMPLRESSPQRAERCKKSWLLCIVA LLLMLLCSLGTLIYTSLKPTAIESCMVK FELSSSKWHMTSPKPHCVNTTSDGKLK ILQSGTYLIYGQVIPVDKKYIKDNAPFVV QIYKKNDVLQTLMNDFQILPIGGVYELH AGDNIYLKFNSKDHIQKNNTYWGIILMP DLPFIS

GITRLδW	WLLCIVALLLMLLCSLGTLIYTSLKP TAIESCMVKFELSSSKWHMTSPKPHCV NTTSDGKLKILQSGTYLIYGQVIPVDKK YIKDNAPFVVQIYKKNDVLQTLMNDFQ ILPIGGVYELHAGDNIYLKFNSKDHIQKN NTYWGIILMPDLPFIS
GITRδ2	IWQLRRQHMAAAATQPFAEVQLSAEDA CSFQFPEEERGEQTEEKCHLGGRWP
GITRδ4	IWQLRRQHMCPREAQPFAEVQLAAEDA CSFQFPEEERGEQTEEKCHLGGRWP
GITRδ5	IWQLRRQHMCPREEQPFAEVQLEAEDA CSFQFPEEERGEQTEEKCHLGGRWP

Table 4.1 Plasmids and amino acid sequences used in transfection experiments

4.3 Immunochemistry

4.3.1 Immunocytochemistry (ICC)

SCG cells were cultured as described in 4.2.1 and 4.2.2. The following day, cells were fixed in 1ml ice cold methanol (VWR) per dish for growth cultures or 4% paraformaldehyde (PFA) per dish for transfection cultures for 10min, washed X3 with 1ml PBS and blocked with 1ml 5% Bovine Serum Albumin (BSA) (Sigma) in PBS for 1h at room temperature (RT) to block antibodies binding to non-specific sites. Cultures were incubated with desired primary antibody diluted in 1% BSA in PBS and left overnight at 4ºC. Primary antibodies used included those directed against: Tyrosine hydroxylase (TH); Tyrosine kinase A (TrkA); phospho-TrkA; Glucocorticoid-induced tumour necrosis factor receptor (GITR); GITR Ligand (GITRL); β-III tubulin; phospho-ERK1/2; and phospho-pSer536-p65 (phospho-p65 subunit of NF-κB) (Table 4.2). The following day, the primary antibody was

removed and cultures were washed X3 in 1ml PBS and incubated with the appropriate secondary antibody diluted in 1% BSA in PBS for 2h at RT (Table 2.3). Cultures were washed for 5min with DAPI (Sigma) in PBS (1:5000 dilution) for nuclear staining before final washes X2 of PBS. Photomicrographs were taken on an Olympus 1X70 Provis Inverted Fluoresence Microscope attached to an Olympus DP70 camera and Zeiss Axioplan confocal microscope. Sholl analysis was performed on β-III tubulin stained neurons (*Gutierrez, et al., 2008*) (Section 4.6).

Name	Labels	Raised in	Working dilution	Supplier
β-III tubulin	Post-mitotic neurons	Mouse	1:200	Promega
TH	Sympathetic neurons	Rabbit	1:100	Millipore
TrkA	Tyrosine kinase A	Rabbit	1:200	Millipore
p-TrkA	Phosphorylated TrkA	Rabbit	1:50	Millipore
GITR	Glucocorticoid-tumour necrosis factor receptor (GITR)	Goat	1:100	Santa cruz
GITRL	GITR Ligand	Goat	1:100	Santa cruz
Phospho-ERK1/2	Phosphorylated ERK1/2	Rabbit	1:100	Cell signalling
Phospho-pSer536-p65	Phosphorylated p65 (subunit of NF-κB) on residue Serine 536	Rabbit	1:50	Cell signalling

Table 4.2 Primary antibodies used in immunocytochemistry experiments

Antibody type	Reactivity	Host	Working dilution	Supplier
Alexa fluor 488	Mouse	Goat	1:500	Invitrogen
Alexa fluor 594	Goat	Donkey	1:500	Invitrogen
Alexa fluor 488	Rabbit	Goat	1:500	Invitrogen
Alexa fluor 594	Rabbit	Goat	1:500	Invitrogen

Table 4.3 Secondary antibodies used in immunocytochemistry experiments

4.3.2 Immunohistochemistry (IHC)

P1 pups were decapitated and the heads were placed in 4% paraformaldehyde for 24h. They were then rinsed in PBS before being cryoprotected in a 30% sucrose solution until tissue sinks. Samples were then equilibrated in 1:1 sucrose : OCT for 2h at 4°C before freezing in OCT. Whole heads were transversely sectioned at a thickness of 15µm and each section was placed on a superfrost plus slide (Thermo Scientific). Sections were permeablized in 1% Triton X-100 before blocking with 5% goat serum for 1h at RT. Sections were then stained for TH overnight (Table 4.2) before visualisation with appropriate secondary antibody (Table 4.3).

4.3.3 Whole mount organ IHC

Whole mount DAB-TH immunohistochemistry was performed on sympathetic target organs including trachea, heart, stomach, small intestines, ureter and bladder. Following decapitation, organs were dissected from P1 SV-129 GITR+/+ and GITR-/- mice and fixed overnight in 4% PFA. The next day organs were dehydrated in 50% methanol and 80% for 1h each. Endogenous peroxidise activity in organs was quenched by placing organs in 80% methanol /20% Dimethyl Sulfoxide (Sigma) /3% Hydrogen peroxide (H2O2) (Merck) overnight at 4ºC. The next day the organs were rehydrated in 50% methanol, 30% methanol and PBS for 1h each at RT. Organs were incubated in blocking solution containing 4% BSA and 1%Triton X (Sigma) in PBS overnight at 4°C. The next day, the organs were incubated with rabbit anti-TH primary antibody (Millipore; 1:250 in 4% BSA in 1% Triton X/PBS) and left on a

rocker for 72h at 4°C. Organs were then washed X3 in 1% Triton X-100/PBS for 2h followed by incubation with secondary antibody anti-rabbit TH horseradish peroxidise (HRP) IgG (Promega; 1:300 in 4% BSA in 1% Triton X/PBS) and left on a rocker overnight at 4ºC. The next day, organs were washed X3 in 1% Triton X-100/PBS for 2h followed by incubation in Diaminobenzidine (DAB) (Sigma: 0.5mg/ml) and placed on a rocker overnight at 4ºC. The following day, organs were fixed in 4% PFA for 1h at RT and then rinsed in PBS and dehydrated in 50% and 80% for 2h each and 100% methanol overnight. The next day, organs were cleared in benzyl benzoate/benzyl alcohol (Sigma; 2:1) for 1h at RT. The organs were then imaged using a dissecting microscope (Olympus SZX7). A modified line incept method was used to analyse axonal branching and density (*Mayhew, 1991*).

4.4 Protein quantification

4.4.1 Protein extraction from cells

P1 SCG cells from SV-129 GITR+/+ and GITR-/- mice were cultured in a 96-well plate (Corning Incorporated). 200µl of a high density cell solution (as described in section 4.2.2), was pipetted into each well and incubated at 37°C overnight. Wild type cells were treated with GITRL-IgG (1ug) for 1h. Medium was carefully removed and 100µl of RIPA buffer (50mM Tris-HCl; 150mM NaCl; 2mM EDTA; 0.5% Na-Deoxycholate; 0.1% SDS and 1% Triton X), 10µl of phenylmethylsulfonyl fluoride (PMSF), 10µl sodium orthovanadate and 10µl sodium fluoride was added to lyse the cells. The plate was incubated on ice for 1h and the bottom of each well was scratched with a pipette tip to detach any remaining adhering cells. This RIPA buffer containing the protein was then transferred into individually labelled 0.5ml eppendorf tubes (Sarstedt) and stored at -20°C.

4.4.2 Western blotting

A 5% sodium dodecyl sulphate (SDS)–polyacrylamide electrophoresis stacking gel cast above a 10% resolving gel was used to separate proteins for Western blotting.

Samples were prepared by adding a chosen concentration of protein (~20mg) to an equal volume of sample buffer (0.25M Tris-HCl pH 6.8; 8% SDS; 30% Glycerol; 0.02% Bromophenol Blue) and boiled for 5 min to denature the protein. 15µl of each sample was loaded into the gel alongside 3-5µl of molecular weight protein standards (Bio-Rad). Electrophoresis was initiated by applying 150V for 60 min to the running apparatus (Bio-Rad) containing Tris-glycine running buffer with SDS (Sigma). Electrophoretic transfer to the membrane was carried out at 100V for 60 min using a Mini Trans-Blot Electrophoretic Transfer Cell (Bio-Rad, CA-USA) while immersed in transfer buffer (5.85g Tris-base; 2.93g glycine and 50ml methanol in 1L distilled water). After transfer, the membrane was incubated in a 5% BSA blocking solution for 60 min on a rocker (~55 oscillations/min) at RT and then washed briefly in PBS with 1% TWEEN (Fisher Scientific). The primary antibodies used were mouse antiserum to β-III-tubulin (1mg/ml, Promega: 1:10,000), rabbit anti-phospho-S536-p65 (1:1000; Cell Signalling); rabbit anti-phospho IKK (1:1000; Cell Signalling) and rabbit anti-phospho ERK1/2 (1:1000; Cell Signalling). The membrane was incubated in one of these overnight at 4°C. The blot underwent 6 washes in PBS containing 0.05% Tween (PBS-T: 6 X 5 min) before detection with the relevant peroxidase-linked secondary antibodies (Promega) and ECL-plus (Amersham).

4.5 Analysis of mRNA expression

4.5.1 RNA extraction

SCG were dissected from P1 SV-129 GITR+/+ and GITR-/- mice and placed in a tube containing ice-cold HBSS. The tube was centrifuged at 500 rpm for 2 min, the supernatant was discarded and the tissue pellet stored immediately at -80˚C until required. Total RNA was extracted using the RNeasy kit (Qiagen) according to the manufacturer's instructions. 700µl of RLT buffer + 0.7µl β-mercaptoethanol (Sigma) was added to 20mg of tissue in a 1.5ml eppendorf (Sarstedt). A needle (Sterican®) and syringe (BD Plastipak™) were used to break up tissue and the tube was centrifuged for 3min @ full speed using an eppendorf 5415C centrifuge. The supernatant was transferred to another tube where an equal volume of 70% ethanol

(J.T. Baker) was added. This mixture was placed in a spin cup and spun for 15s @ 10,000rpm. Flow through was discarded. DNA was digested using an RNase-Free DNase Set (Qiagen). The membrane of the spin cup was washed X2 in RPE buffer and spun @ 10,000rpm. Flow through was discarded. RNA was eluted in 50µl of nuclease-free water (Ambion) by spinning it for 1 min @ 10,000 rpm. RNA concentration was maximized by passing elute through the membrane a second time. RNA concentration in ng/µl was determined by using a Spectrophotometer (ND1000; NanoDrop Technologies, Inc).

4.5.2 cDNA synthesis

cDNA synthesis was performed using an ImProm-II Reverse Transcription System (Promega). A volume of sample that contained 1µg of RNA was determined and an RNA mix was made up using this volume, together with 0.5µl oligo dTs, 0.5µl random primers and nuclease-free water to make up a total volume of 11.5µl. A negative control was also prepared for each sample. The tubes were placed at 65°C for 5min in a PCR machine (Bio-Rad MJ Mini™ Personal Thermal Cycler). A mastermix containing 5X buffer (4µl), $MgCl_2$ (2µl), dNTPs (1µl: 10mM) and RNase inhibitor (0.5µl) was made up and 7.5µl was added to each tube followed by 1µl Reverse Transcriptase (RT) enzyme. Negative controls received 1µl nuclease-free water instead of RT. Tubes were placed at 37°C for 90min before dropping to 4°C. cDNA was stored at 4°C for 1-2 days and subsequently used in Reverse Transcriptase-Polymerase Chain Reaction (RT-PCR).

4.5.3 Reverse transcriptase – polymerase chain reaction

RT-PCR was carried out using a GoTaq Flexi DNA Polymerase system (Promega). 20.75µl of mastermix containing 5µl 5X PCR buffer, 1.5mM $MgCl_2$ (IL-1α primer only requires 0.5mM), 1.25mM PCR dNTPs and 10.25µl nuclease-free water was added to each tube. 2µl of cDNA, 2µl of desired sense and anti-sense primer and 0.25µl Taq polymerase were also added. A negative control containing negative RT

cDNA was also prepared for each primer. RT-PCR was carried out using mouse SCG tissue from P1 GITR+/+ and GITR-/- SV129 mice. Primer sequences and predicted product size is presented in table 4.4 and PCR primer programs used in table 4.5.

Target mRNA	Forward primer (5'-3' direction)	Reverse primer (5'-3 direction)	Size (bp)
GAPDH	TGGCACAGTCAAGGCTGAGA	CTTCTGAGTGGCAGTGATGG	388
IL-1α	GGCTCACTTCATGAGAACTGC	TGAACTCCTGCTTGACGATCC	289
IL-1RI	AGATGGAAGGACCTATGATG	TGCAGCATCTGACGACAGGA	641
IL-1RII	GGCAAGGAATACAACATCAC	TGGTTGTCAGTCGGTAGCTT	530
TNF	AGAACTCCAGGCGGTGTCTGT	CCTTGTCCCTTGAAGAGAACC	367
TNFRI	CCCAGGACTCAGGTACTGCCGT	CAGAGTGGGGTTGAAGCCGG	244
TNFRII	GATGAGAAATCCCAGGATGCAGTAGG	TGCTACAGACGTTCACGATGCAGG	264
IGF-1	GGACCAGAGACCCTTTGCGGG	GGCTGCTTTTGTAGGCTTCAGTGG	210
IGF-1R1	ACTGACCTCATGCGCATGTGCTGG	CTCGTTCTTGCGGCCCCCGTTCAT	345
TrkA	TCAACAAATGTGGACGGAGA	GTGGTGAACACAGGCATCAC	197

Table 4.4 List of RT-PCR primer sequences and predicted product size

Target mRNA	Denaturation	Annealing	Extension	Cycles (#)
GAPDH	95°C x 30s	55°C x 30s	72°C x 60s	25
IL-1α	95°C x 30s	55°C x 30s	72°C x 60s	32
IL-1R1	95°C x 40s	54°C x 40s	72°C x 30s	30
IL-1R2	95°C x30s	55°C x 30s	72°C x 60s	30
TNFα	95°C x 30s	55°C x 30s	72°C x 60s	32
TNFR1	95°C x 40s	54°C x 40s	72°C x 30s	30
TNFR2	95°C x 60s	59°C x 60s	72°C x 60s	30
IGF-1	94°C x 60s	58°C x 45s	72°C x 60s	42
IGF-1R1	94°C x 60s	60°C x 45s	72°C x 60s	40
TrkA	95°C x 40s	58°C x 60s	72°C x 60s	40

Table 4.5 Semi-quantitative RT-PCR conditions for primers

4.5.4 Agarose gel electrophoresis

PCR products were run on a 1.5% agarose gel. Gels were made using 1.5g agarose (Sigma) and 100ml 1X TAE buffer and dissolved by heating in a microwave (GoldStar Multiwave Oven). Safeview™, to label the DNA, was added to molten gel and poured into the gel tray to set for 30min. The gel tray was then lowered into the gel rig (Peqlab biotechnologie GmbH) and immersed in 1X TAE. 100bp ladder (7µl; New England Biolabs) and 10µl of each sample were loaded and gel was run at 100V for 1-1.5h on a Bio-Rad Power Pac 200. The gel was imaged with a UV transluminator with UVI Pro software and the gel was safely disposed of according to lab safety protocols.

4.6 Growth analysis

Each culture was performed at least three times (n=3) with 30-50 images per group taken using Olympus 1X70 Provis Inverted Fluoresence Microscope attached to an Olympus DP70 camera. All images were saved as jpegs and appropriate scale bars were added using Photoshop. Growth was determined by length of neurites and number of branches using Sholl analysis. Sholl analysis provides a graphic illustration of neurite length and branching with distance from the cell body (*Gutierrez, et al., 2008*).

4.7 Statistics

Statistical analysis was performed using the computer-based statistical package GraphPad Prism (GraphPad, US). Two-tailed unpaired Student's t-test was used to compare the mean of two groups as appropriate. Experiments comparing multiple groups were analysed using a one-way ANOVA with Tukey's post hoc test. Data are expressed as mean ± standard error of the mean (SEM) and deemed significant when $P < 0.05$.

5.0 Determination of the role of GITR in the growth of developing sympathetic neurons

5.1 Aims

- To confirm the expression of GITR and GITRL in P1 SCG neurons using immunocytochemistry
- To investigate the sensitivity of developing sympathetic neurons to NGF in response to GITR activation.
- To determine the region of GITR required for the growth promoting effects of GITRL-GITR signalling

5.2 Abstract

NGF is the prototypic neurotrophin required for the survival and growth of neurons of the developing PNS. The action of NGF is mediated through receptors TrkA and p75NTR. Recently, GITR of the TNFRSF has been identified as a receptor crucial for NGF-promoted axon extension and target innervation of NGF-dependant sympathetic neurons of the developing PNS. However, the precise regions of GITR responsible for mediating this effect are unknown. We aimed to explore this further using plasmids expressing mutant forms of the GITR receptor. To do this, neurons isolated from the SCG of P1 C57 mice, were transfected with mutant forms of GITR by microporation and axonal growth of these neurons was determined using Sholl analysis. Results indicated that GITRL-GITR signalling requires the extracellular region of GITRL and the juxtamembrane intracellular region of GITR. Using point-specific mutants of potential important residues identified by *In Silico* analysis, we found in addition that constitutive phosphorylation of Tyr190 and Ser199 sites (amino acids 12 and 21) of the identified growth promoting domain (GPD) of the intracellular GITR resulted in the inhibition of NGF-promoted growth of neonatal sympathetic neurons. In conclusion, this study shows that the growth promoting effects of GITR are mediated by a growth-promoting domain located at the juxtamembrane region of the intracellular region of GITR, in which sites Tyr 190 and Ser 199, appear to play a role in the regulating axonal growth of developing sympathetic neurons.

5.3 Introduction

The growth of axons to and within their targets during development of the PNS is controlled by a variety of extrinsic and intrinsic signals (*Glebova and Ginty, 2005; Harrington and Ginty, 2013; Honma, et al., 2002; Markus, et al., 2002; Thompson, et al., 2004*). One of the key regulators of axonal growth in the PNS is NGF. In the PNS, postganglionic sympathetic neurons require a constant supply of target-derived NGF, in order to survive, and maintain their connections (*Glebova and Ginty, 2004; Harrington and Ginty, 2013; Levi-Montalcini and Angeletti, 1968*). Within the target regions innervated by these neurons, NGF acts locally on axon terminals to promote

their growth, branching and refinement of connections (*Campenot, et al., 1994; Edwards, et al., 1989*). NGF elicits its effects by binding two receptors; the p75NTR of the TNFRSF and TrkA of the family of Trk receptors (*Reichardt, 2006*). p75NTR increases the specificity and binding affinity of TrkA to NGF in the promotion of neuronal survival and growth (*Chao and Hempstead, 1995*).

GITR is a transmembrane protein that is activated by its specific ligand, GITRL (*Bossen, et al., 2006; Gurney, et al., 1999; Kim, et al., 2003a; Kwon, et al., 1999; Ronchetti, et al., 2004; Tone, et al., 2003; Yu, et al., 2003*). Like the p75NTR, GITR is a member of the TNFRSF, however unlike p75NTR, GITR does not contain a death domain. Upon activation, GITR recruits TRAF molecules, which bind to the intracellular region or the TRAF binding site of GITR causing subsequent activation of intracellular pathways to elicit functional responses (*Esparza and Arch, 2004; Esparza, et al., 2006; Ronchetti, et al., 2004; Zhou, et al., 2008*). In the immune system GITR functions as a costimulatory molecule and is involved in the regulation of innate and acquired immune responses (*Krausz, et al., 2007; Nocentini and Riccardi, 2005*). GITR activation amplifies the activation and proliferation of T cell antigen receptor (TCR)-triggered T cells (CD4+ and CD8+) (*Esparza and Arch, 2005a; Kanamaru, et al., 2004; Ronchetti, et al., 2004; Stephens, et al., 2004; Tone, et al., 2003*).

Recent data also describes new roles for GITR during nervous system development (O'Keeffe et al. 2008). Interestingly, GITR was found to act in a costimulatory manner in the enhancement of NGF-promoted axon growth and target innervation of neonatal sympathetic neurons (*O'Keeffe, et al., 2008*). Furthermore, GITRL-GITR signalling was found to exert its growth promoting effects during the immediate postnatal stages of development (P1-3) and operates via an apparent autocrine route as both GITRL and GITR were found to be expressed on the neuronal soma both *in vitro* and *in vivo* rather than being expressed on the neurites or in distal targets (*O'Keeffe, et al., 2008*).

The mechanism through which GITRL-GITR facilitates NGF-promoted axon growth was shown to centre on a GITR-mediated facilitation of NGF-promoted ERK-activation (*O'Keeffe, et al., 2008*). Enhanced axonal growth and branching produced by agonist GITRL-IgG treatment in P1 SCG neurons is completely

abolished when neurons are treated with ERK1/2 blocker U0126 demonstrating that the enhanced ERK1/2 activation brought about by stimulating GITR (with GITRL-IgG) is responsible for the increase in NGF-promoted axonal growth. However the precise region of the GITR receptor that regulates this effect is unknown. In this chapter we sought to determine the region of GITR required for its enhancement of NGF-promoted growth and to determine if GITR activation increased sympathetic neuron's sensitivity to NGF.

5.4 Results

5.4.1 GITR and GITRL are expressed by P1 mouse SCG neurons.

In order to confirm the expression of GITR and GITRL in neonatal mouse sympathetic neurons, immuncytochemical staining for GITR and GITRL was performed. The SCG were removed from P1 C57 mice, dissociated, and plated in a defined media containing 10ng/ml NGF and grown overnight at 37°C. The following day, cells were fixed and immunocytochemically stained for GITR (Figure 5.1 A) and GITRL (Figure 5.1B). Both GITR and GITRL were located in the extranuclear region consistent with transmembrane proteins (*Nocentini, et al., 1997*), (confirmed by co-staining with nuclear stain DAPI) of neuronal cells (confirmed by co-localisation with neuronal stain β-III tubulin) (*O'Keeffe, et al., 2008*) of the SCG.

5.4.2 Dose response of NGF effects on survival of P1 mouse SCG neurons.

NGF is required for the survival of developing sympathetic neurons (*Levi-Montalcini, 1987*). The p75NTR increases the sensitivity of developing neurons to NGF as part of the TrkA/p75NTR high affinity receptor complex that mediates the pro-survival effects that NGF exerts on these neurons (*Chao and Hempstead, 1995*). As GITR is a member of the same family as p75NTR and promotes the growth and target innervation of NGF-dependant neurons (*O'Keeffe, et al., 2008*), it is possible that GITR may also increase the sensitivity of SCG neurons to NGF in a similar fashion to p75NTR. Before we examined this, a baseline for the NGF requirements of P1 SCG for survival and growth was first established. P1 SCG neurons were grown in a defined media containing different concentrations of NGF (0.01, 0.04,

0.2, 1, 4 and 10ng/ml) and grown for 24, 48 and 72h at 37°C. The effect on survival was examined by counting the numbers of neurons surviving at each time point (24, 48 and 72h) and calculated as a percentage of number of neurons that survived at 3h. A significant increase in survival (***$P \leq 0.001$, **$P \leq 0.01$) was evident in cells grown in 4-10ng/ml NGF after 24h (Figure 5.2 A), 48h (Figure 5.2 B) and 72h (Figure 5.2 C) compared to untreated controls.

5.4.3 Dose response of NGF effects on the growth of P1 mouse SCG neurons.

Similar to 5.4.2, where a baseline of NGF requirements for P1 SCG neurons survival was established, we performed a similar experiment to determine the effects of varying concentrations of NGF on axonal growth. To prevent cell death, a cell-permeable, irreversible, broad-spectrum caspase inhibitor III from Calbiochem was added to the medium. P1 SCG neurons were grown in a defined media containing 0.01, 0.04, 0.2, 1, 4 and 10ng/ml NGF overnight at 37°C followed by growth assessment using Sholl analysis. There was a significant increase in neurite length in neurons treated with 0.2, 1, 4 and 10ng/ml compared with untreated controls (***$P \leq 0.001$, *$P \leq 0.05$) (Figure 5.3 A, C, D). In addition, there was a significant increase in neurite branching in neurons treated with 0.2, 1, 4 and 10ng/ml compared to untreated controls (***$P \leq 0.001$, *$P \leq 0.05$) (Figure 5.3 B, C, D).

5.4.4 A GITRL antagonist reduces NGF-promoted axonal growth at an NGF concentration of 1ng/ml and 4ng/ml.

Baseline growth experiments (5.4.3) identified 4-10ng/ml NGF as concentrations that induce a significant increase in sympathetic neuronal growth. Previously, the p75NTR was found to increase neuron's sensitivity to NGF at low (2.5ng/ml) and not high (10ng/ml) concentrations of NGF (*Lee, et al., 1994b*). Given that GITR is from the same super family, it may function similarly and affect a neuron's sensitivity to NGF at different concentrations of NGF. For this reason, we next examined the effect of GITRL-GITR signalling on the sensitivity of neurons to NGF grown in 1ng/ml. P1 SCG cells were treated with two commercially available

compounds; agonist recombinant GITRL (rmGITRL) (1μg/ml) or antagonist GITRL-IgG (5μg/ml) and grown overnight in a defined media containing 1ng/ml NGF at 37°C. The following day, cells were fixed and immunocytochemically stained for the neuronal marker β-III tubulin. The extent of growth of neurons was determined using Sholl analysis. Agonist rmGITRL treatment of neurons grown in 1ng/ml NGF had no effect on length of neurites (Figure 5.4 A), branching (Figure 5.4 B) or Sholl profiles (Figure 5.4.C) of these neurons. Representative line drawings represent these results (Figure 5.4 D). Antagonist GITRL-IgG treatment of neurons grown in 1ng/ml NGF had no effect on length of neurites (Figure 5.4 A), however antagonist GITRL-IgG treatment did result in a significant reduction in branching (**$P \leq 0.01$) recovered with combination treatment with Agonist rmGITRL (Figure 5.4 B), in addition to a reduction in Sholl profiles, reflected in representative line drawings of neurons grown in 1ng/ml NGF (Figure 5.4 C, D).

5.4.5 A GITRL antagonist does not reduce NGF-promoted axonal growth at an NGF concentration of 4ng/ml.

In continuing to investigate whether GITRL-GITR signalling affects a neuron's sensitivity to NGF using different concentrations of NGF, we next examined the effect of GITRL-GITR signalling on the growth of neurons in 4ng/ml NGF. P1 SCG cells were treated with agonist rmGITRL (1μg/ml) or antagonist GITRL-IgG (5μg/ml) and grown overnight in a defined media containing 4ng/ml NGF at 37°C. The following day, cells were fixed and immunocytochemically stained for the neuronal marker β-III tubulin. The extent of growth of neurons was determined using Sholl analysis. Treatment of neurons with agonist rmGITRL, grown in 4ng/ml NGF had no effect on length of neurites (Figure 5.5 A) or branching (Figure 5.5 B), reflected in Sholl profiles (Figure 5.5 C) and representative line drawings of treated neurons (Figure 5.5 D). Similarly, antagonist GITRL-IgG treatment of neurons grown in 4ng/ml NGF had no effect on neurite length (Figure 5.5 A) or branching (Figure 5.5 B). Sholl profiles (Figure 5.5 C) and representative line drawings of treated neurons (Figure 5.5 D) display no change in growth compared to control-treated neurons grown in 4ng/ml NGF.

5.4.6 A GITRL antagonist does not reduce NGF-promoted axonal growth at an NGF concentration of 10ng/ml.

To further examine if GITRL-GITR signalling affects sympathetic neuron's sensitivity to NGF, P1 SCG cells were treated with agonist rmGITRL (1µg/ml) or antagonist GITRL-IgG (5µg/ml) and grown overnight in a defined media containing 10ng/ml NGF at 37°C. The following day, cells were fixed and immunocytochemically stained for the neuronal marker β-III tubulin. The extent of growth of neurons was determined using Sholl analysis. Treatment with agonist rmGITRL had no effect on neurite length (Figure 5.6 A), branching (Figure 5.6 B) or Sholl profiles of neurons (Figure 5.6 C) in media containing 10ng/ml NGF. These results are reflected in representative line drawings of neurons treated with rmGITRL and grown in 10ng/ml NGF (Figure 5.6 D). Neurons treated with antagonist GITRL-IgG and grown in 10ng/ml NGF also showed no change in neurite growth (Figure 5.6 A), branching (Figure 5.6 B) or Sholl profile (Figure 5.6 C) when compared with control treated neurons. This is clear by line drawings from photomicrographs taken of these treated neurons (Figure 5.6 D).

5.4.7 Enhancement of axonal growth by GITRL-GITR signalling does not require the intracellular tail of GITRL.

We next examined the regions of GITR or GITRL that are required for the growth promoting effects of GITRL-GITR signalling. Firstly, we transfected P1 SCG neurons with overexpression vectors for GITRL and antisense GITR following which neurons were grown in media containing 10ng/ml NGF. This concentration of NGF (10ng/ml) has been used previously in similar experiments that examined the effect of GITRL-GITR signalling on the growth of neonatal sympathetic neurons (*O'Keeffe, et al., 2008*). Overexpression of GITRL resulted in a significant increase in neurite length (**$P \leq 0.01$) (Figure 5.7 A). This result is reflected in the Sholl profile of neurons where GITRL is over expressed (Figure 5.7 B) and in line drawings of GITRL-transfected neurons (Figure 5.7 C). When cells were transfected with a plasmid expressing antisense GITR, there was a significant decrease in neurite length (**$P \leq 0.01$) (Figure 5.7 A), where the reduction in the complexity of neurons transfected with antisense GITR is seen by the Sholl profiles of these

neurons (Figure 5.7 B) and representative line drawings of neurons (Figure 5.7 C) compared to controls. In the immune system GITRL-GITR signalling can occur in a "forward" manner whereby the signalling is mediated downstream of GITR following ligand binding, but it can also be 'reversed'. This means that signalling is via the intracellular tail of GITR ligand and not the receptor (*Bae, et al., 2008*). To investigate if this is the case in the developing SCG neurons, an expression vector overexpressing a mutated version of GITRL (GITRLδW), in which the intracellular tail of GITRL was deleted (a kind gift from Prof. Carlo Riccardi, University of Perugia, Italy) was transfected into P1 SCG neurons which were then grown overnight in a defined media containing 10ng/ml NGF and the effect on axonal growth was examined. There was no decrease in the growth of GITRLδW-transfected neurons compared to controls (i.e. cells transfected with empty plasmid) (where length of neurites from cells transfected with control versus GITRLδW = 1295 ± 189μm versus 1568 ± 168μm) demonstrated by the Sholl profile (Figure 5.7 D) and representative line drawings of transfected neurons (Figure 5.7 E). This result indicates that the intracellular region of GITRL is not responsible for the growth promoting effects of GITRL-GITR signalling in P1 SCG neurons.

5.4.8 GITRδK does not affect axonal growth of P1 SCG neurons.

GITR is a type I transmembrane protein consisting of intracellular, transmembrane and extracellular regions (*Nocentini, et al., 1997*). Result 5.4.7 indicates that GITRL-GITR activates intracellular signalling via GITR and not GITRL. Plasmids expressing mutated GITR proteins with specific deletions in the intracellular region of GITR, designation GITRδK, GITRδZ, and GITRδW, were used to identify the growth promoting domain (GPD) of GITR (plasmids were a kind gift from Prof. Carlo Riccardi, University of Perugia, Italy).

P1 SCG neurons were transfected with a plasmid expressing GITRδK which expresses a GITR protein lacking the sequence EQTEEKCHLGGRWP from the intracellular region (Figure 5.8 A), together with a GFP expression plasmid (to visualise transfected neurons) and grown overnight in a defined media containing

10ng/ml NGF at 37°C. Neurons transfected with GITRδK displayed no change in neurite length (Figure 5.8B) or branching (Figure 5.8C) compared with their control-transfected counterparts. These results are reflected in the Sholl profile (Figure 5.8 D) and line drawings (Figure 5.8 E) of transfected neurons compared with controls. This result indicates that the GPD of GITR is not located at the EQTEEKCHLGGRWP region of the intracellular portion of GITR.

5.4.9 GITRδZ does not affect neurite length of P1 SCG neurons.

In continuing to investigate the region of GITR responsible for its growth promotion effects, P1 SCG neurons were transfected with a plasmid expressing GITRδZ which expresses a GITR protein lacking the sequence AEDACSFQFPEEERGEQTEEKCHLGGRWP from the intracellular region (Figure 5.9 A). GITRδZ-transfected neurons displayed no change in neurite length (Figure 5.9 B) compared with controls. However that was a significant difference in branching compared with controls ($P < 0.05$). This result is reflected in the Sholl profile (Figure 5.9 D) and line drawings (Figure 5.9 E) of transfected neurons compared to controls. As high significant differences are not reported in both length and branching in trasnfected neurons compared to controls, this result indicates that the GPD of GITR is not located at the AEDACSFQFPEEERGEQTEEKCHLGGRWP region of the intracellular portion of GITR.

5.4.10 Axonal growth of P1 mouse SCG neurons is mediated by a juxtamembrane region of GITR.

To further investigate the region of GITR responsible for its growth promotion effects in sympathetic neurons, P1 SCG neurons were transfected with a plasmid expressing GITRδW that expresses a GITR protein in which the juxtamembrane region of GITR; QLRRQHMCPRETQPFAEVQLSAEDACSFQFPEEERGEQTEEKCHLGGRWP has been deleted (Figure 5.10 A) and the effect on growth of neurons was examined.

GITRδW-transfected cells displayed a significant reduction in neurite length (***$P \leq$ 0.001) (Figure 5.10 B) and branching (***$P \leq$ 0.001) compared to controls (Figure 5.10 C). The reduction in the growth of sympathetic neurons as a consequence of GITRδW transfection is demonstrated by the Sholl profile (Figure 5.10 D) and line drawings (Figure 5.10 E) of transfected neurons compared with controls. This result indicates that a juxtamembrane region, hereafter referred to as the GPD, of the intracellular domain of GITR is responsible for mediating the growth-promoting effects of GITRL-GITR signalling in developing SCG neurons.

5.4.11 *In Silico* analysis of the GPD of GITR.

Using *In Silico* analysis, a collaborating laboratory lead by Professor Carlo Riccardi, identified potential phosphorylation sites in the GPD of GITR. *In Silico* analysis software programs included DISPHOS; NetPhos 2.0 and GPS Predictor programs. The putative phosphorylation sites identified were Tyr190 and Ser199 (amino acid 12 and 21 of the GPD) (Figure 5.11 B). In addition, there are basic residues Cys186-Glu189 (CPRE) (amino acids 8-11) present in the GPD (Figure 5.11 B) that are conserved among the "GITR sub family" of receptors (CD27, OX40, 4-1BB) and are potentially involved in mediating protein-protein interactions (*Krausz, et al., 2007*). Also, this sequence of residues is located next to a tyrosine residue (Tyr190) and as such may promote the recruitment of specific kinase enzymes for the phosphorylation of that residue. GITR expression plasmids were then created in which the potential phosphorylation sites and conserved basic residues of the “GITR sub family” were mutated (a kind gift from Prof. Carlo Riccardi, University of Perugia, Italy). Figure 5.11 C depicts the GITR proteins with mutations of the putative phosphorylation sites and conserved basic residues in the GPD of GITR. In GITRδ2, Cys186-Glu189 (CPRE), (amino acids 8 to 11), of the GPD were replaced with alanines which may act to inhibit the mediation of protein-protein interactions and / or the recruitment of specific kinases to Tyr190 and therefore inhibit phosphorylation at this residue. In GITRδ4, Tyr190 and Ser199, (amino acid 12 and 21 of the GPD), were replaced with alanines which should act to inhibit phosphorylation at these sites. In GITRδ5, Tyr190 and Ser199, (amino acid 12 and

21 of the GPD), were replaced with glutamic acid which should act to cause constitutive phosphorylation at these sites.

5.4.12 The CPRE (amino acids 8 to 11) site of the GPD of GITR does not mediate its growth promoting effects.

P1 SCG neurons were transfected with GITRδ2 (mutant in which Cys186-Glu189, CPRE (amino acids 8 to 11) of the GPD were replaced with alanines which should inhibit the mediation of protein-protein interactions and / or the recruitment of specific kinases to Tyr190 and therefore inhibit phosphorylation at this residue) (Figure 5.12 A) were grown overnight in a defined media containing 10ng/ml NGF at 37°C and the effect on axonal growth was examined. Transfected cells exhibited no change in neurite length (Figure 5.12 B) or branching (Figure 5.12 C) compared to controls. This result is reflected in the Sholl profile (Figure 5.12 D) and line drawings (Figure 5.12 E) of transfected neurons. This result indicates that the inhibition of protein-protein interactions at these residues and / or the recruitment of specific kinases to Tyr190 and therefore the inhibition of phosphorylation at this residue of the GPD do not regulate GITRL-GITR promoted growth of P1 SCG neurons.

5.4.13 Inactivating mutation of Tyr190 and Ser199 of the GPD of GITR does not inhibit axonal growth.

P1 SCG neurons transfected with GITRδ4 (mutant in which Tyr190 and Ser199, (amino acid 12 and 21) of the GPD were replaced with alanines which should inhibit phosphorylation at these sites) (Figure 5.13 A) were grown overnight in a defined media containing 10ng/ml NGF at 37°C and the effect on axonal growth was examined. Transfected cells displayed no change in neurite length (Figure 5.13 B) or branching (Figure 5.13 C) compared to controls which is reflected in the Sholl profile (Figure 5.13 D) and line drawings (Figure 5.13 E) of transfected neurons. This result indicates that inhibition of phosphorylation at Tyr190 and Ser199, (amino acids 12 and 21) sites of the GPD of GITR has no effect on the growth promoting role of GITRL-GITR signalling in P1 SCG neurons.

5.4.14 Constitutive phosphorylation of Tyr190 and Ser199 of the GPD of GITR inhibits axonal growth.

P1 SCG neurons transfected with GITRδ5 (mutant in which Tyr190 and Ser199, (amino acid 12 and 21) of the GPD were replaced with glutamic acid causing sites to be constitutively phosphorylated) (Figure 5.14 A) were grown overnight in a defined media containing 10ng/ml NGF at 37°C and the effect on growth examined. Interestingly, there was a significant reduction in neurite length ($*P \leq 0.05$) (Figure 5.14 B) and branching ($**P \leq 0.01$) compared to controls (Figure 5.14 C). The reduction in growth of these neurons is reflected in the Sholl profile (Figure 5.14 D) and line drawings (Figure 5.14 E) of transfected neurons. This result indicates that continuous phosphorylation at Tyr190 and Ser199 (amino acids 12 and 21) sites of the GPD of GITR has a growth inhibitory effect on P1 SCG neurons.

5.4.15 Summary of Chapter 5.0.

Schema in Figure 5.15 illustrates a summary of chapter 5.0 results. In developing sympathetic neurons, GITRL activates GITR via the extracellular tail of GITR . This causes subsequent activation of GITR, of which the intracellular region is responsible for the growth promoting effects of GITR. Specifically, the juxtamembrane region of cytoplasmic GITR is responsible for these growth promoting effects and has been termed the GPD of GITR. Constitutive phosphorylation at sites Tyr190 and Ser199, (amino acids 12 and 21) of the GPD results in the inhibition of growth in P1 SCG neurons suggesting these sites are involved in the regulation of GITRL-GITR signalling in the promotion of growth of developing NGF-dependant sympathetic neurons of the PNS.

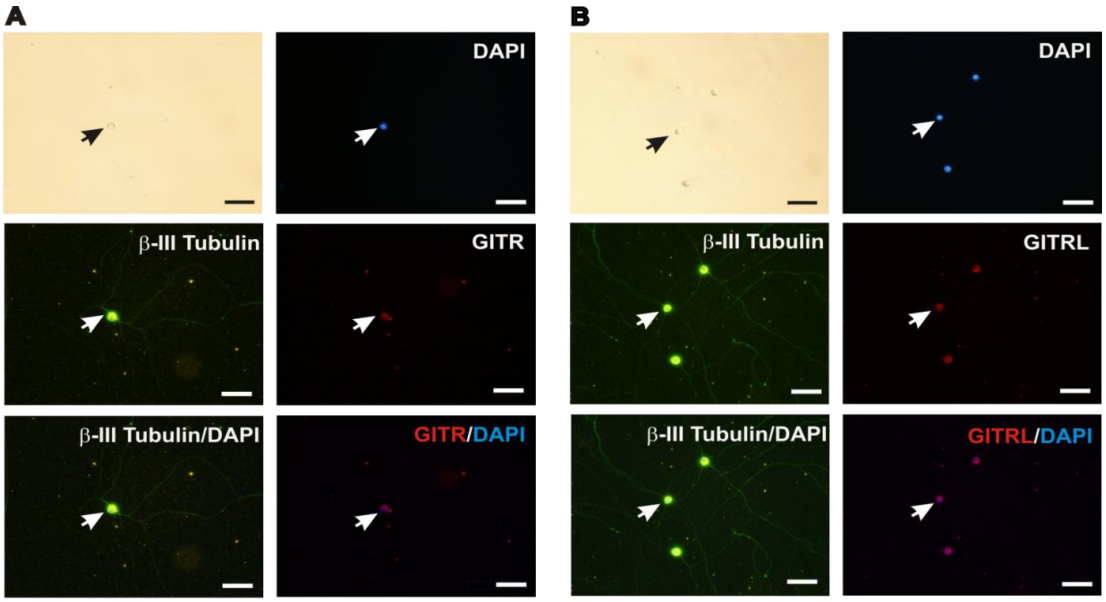


Figure 5.1: Expression of GITR and GITRL by P1 neonatal sympathetic neurons. P1 SCG neurons were grown for 24h in 10ng/NGF. Brightfield images (Top left corner of A and B) identify sympathetic neurons. Cells were fixed and immunocytochemically stained for (A) GITR (red) or (B) GITRL (red) together with β-III tubulin (green) and counterstained with DAPI (blue). Scale bar 50μm.

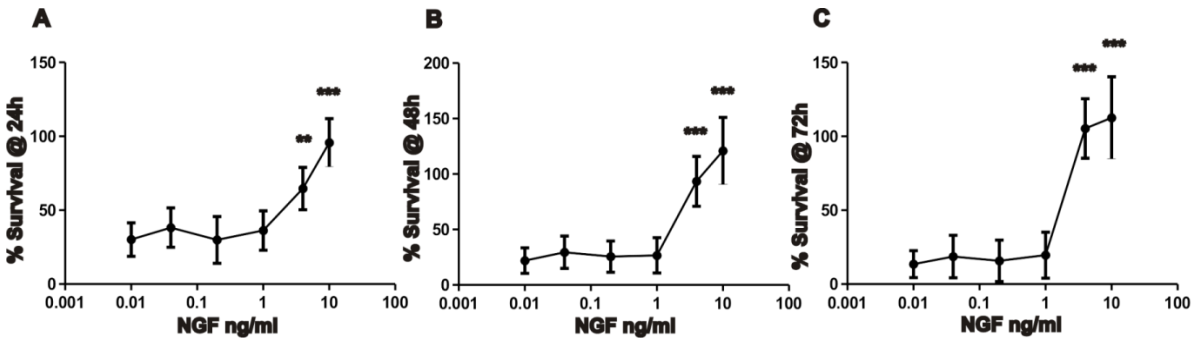


Figure 5.2: Dose response of the effect of NGF on the survival of P1 mouse SCG neurons after varying times in culture. P1 SCG neurons were grown in media containing 0.01, 0.04, 0.2, 1, 4 and 10ng/ml NGF for (A) 24h, (B) 48h and (C) 72h at 37°C. Control cultures were also grown in the absence of NGF. The survival of neurons at time points 24, 48 and 72h was calculated as a percentage of neurons that survived at 3h. Statistical comparisons: ** $P \leq 0.01$, *** $P \leq 0.001$ compared to controls was found using one way ANOVA and post hoc Tukey's test.

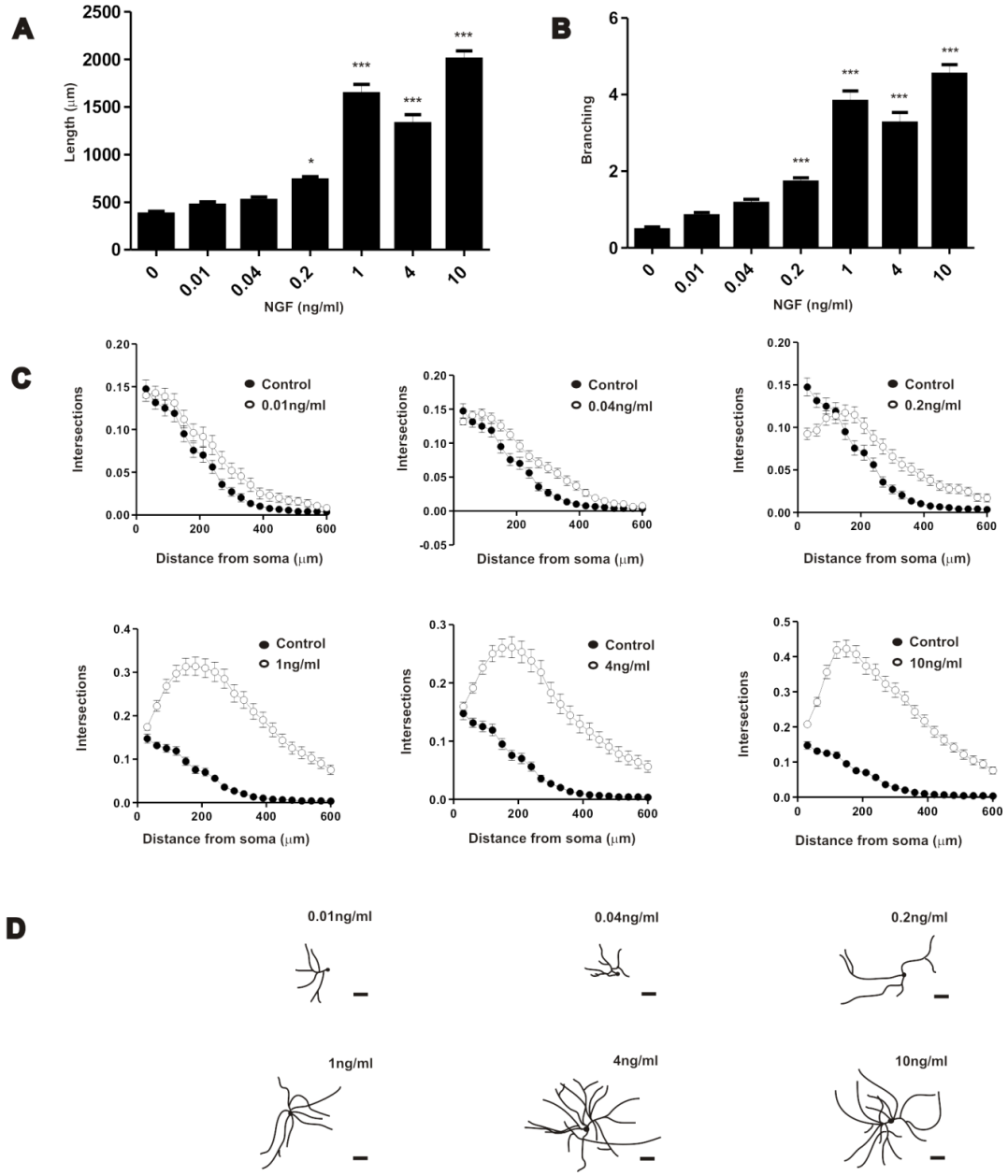

A
Length (μm)
2500
2000
1500
1000
500
0
*
***
***
***
0
0.01
0.04
0.2
1
4
10
NGF (ng/ml)
B
Branching
6
4
2
0
***
***
***
0
0.01
0.04
0.2
1
4
10
NGF (ng/ml)
C
Intersections
Control
0.01ng/ml
0.04ng/ml
0.2ng/ml
1ng/ml
4ng/ml
10ng/ml
Distance from soma (μm)
D
0.01ng/ml
0.04ng/ml
0.2ng/ml
1ng/ml
4ng/ml
10ng/ml

Figure 5.3: Dose response of the effect of NGF on the growth of P1 mouse SCG neurons after varying times in culture. P1 SCG neurons were grown in media containing 0.01, 0.04, 0.2, 1, 4 and 10ng/ml NGF for 24h at 37°C. Control cultures were also grown in the absence of NGF. Axonal growth was analysed using Sholl analysis. (A, B) Graphical representations of, (A) total neurite length and (B) total neurite branching in P1 SCG neurons grown in varying doses of NGF. (C) Sholl profiles of neurons grown in varying doses of NGF. (D) Representative photomicrographs of P1 SCG neurons grown in varying doses of NGF. Means ± standard error of 100-150 neurons per condition shown. Statistical comparisons: $*P \leq 0.05$, $*** P \leq 0.001$ compared to controls was found using one way ANOVA and post hoc Tukey's test. Scale bar = 50μm.

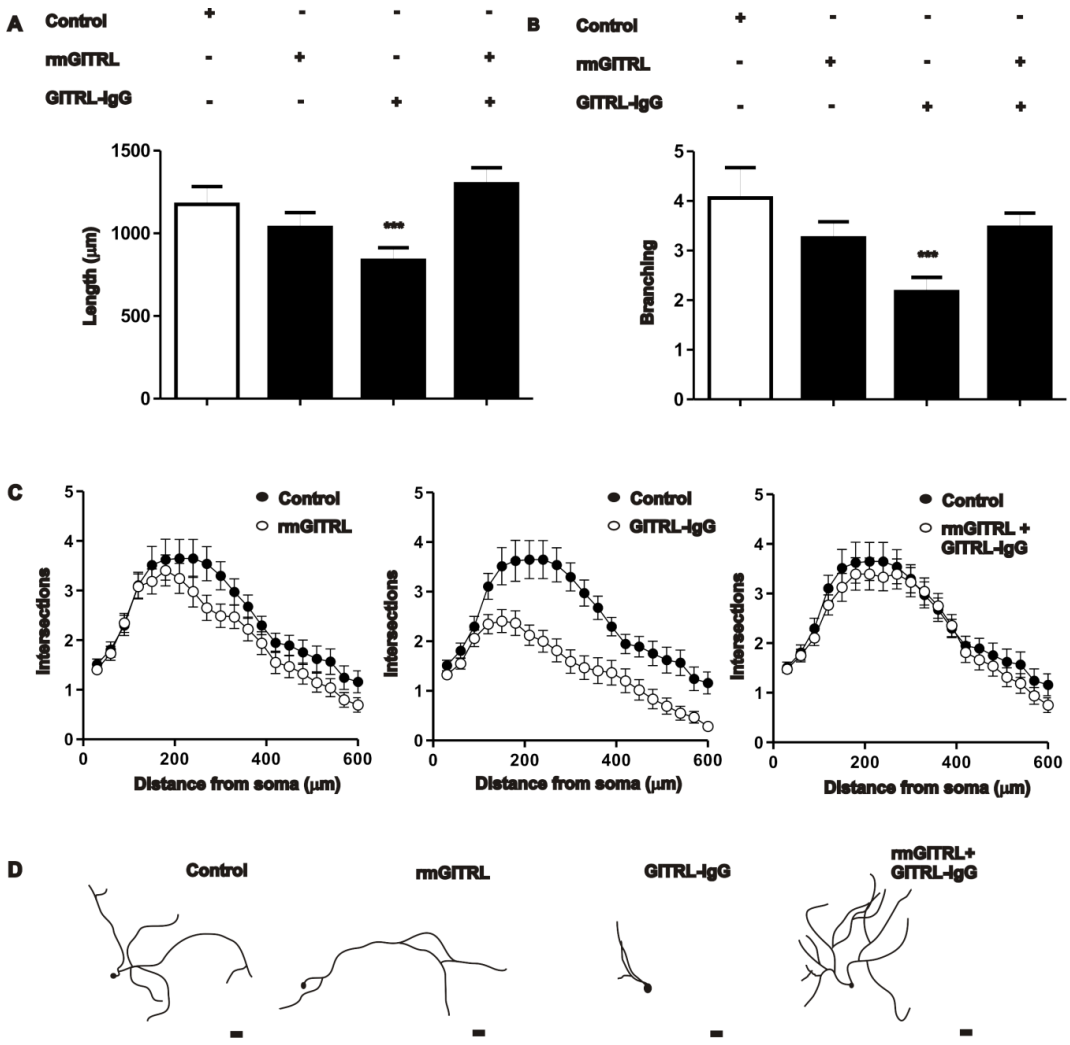


Figure 5.4: Axonal growth of P1 SCG neurons grown in 1ng/ml of NGF is significantly reduced following treatment with GITRL-IgG. P1 SCG neurons were treated with rmGITRL (1mg) or GITRL-IgG (5mg) and grown overnight in 1ng/ml NGF at 37°C. Control cultures were also grown in which only NGF was present. Axonal growth was analysed using Sholl analysis. (A, B) Graphical representations of, (A) total neurite length and (B) total neurite branching in P1 SCG neurons treated with rmGITRL or GITRL-IgG and grown overnight in 1ng/ml NGF. (C) Sholl profiles of neurons treated with rmGITRL or GITRL-IgG and grown overnight in 1ng/ml NGF. (D) Representative line drawings of P1 SCG neurons treated with rmGITRL or GITRL-IgG and grown overnight in 1ng/ml NGF. Means ± standard errors of 40-90 neurons per condition are shown. Statistical comparisons: *** $P < 0.001$ compared to controls was found using one way ANOVA and post hoc Tukey's test. Scale bar = 50µm.

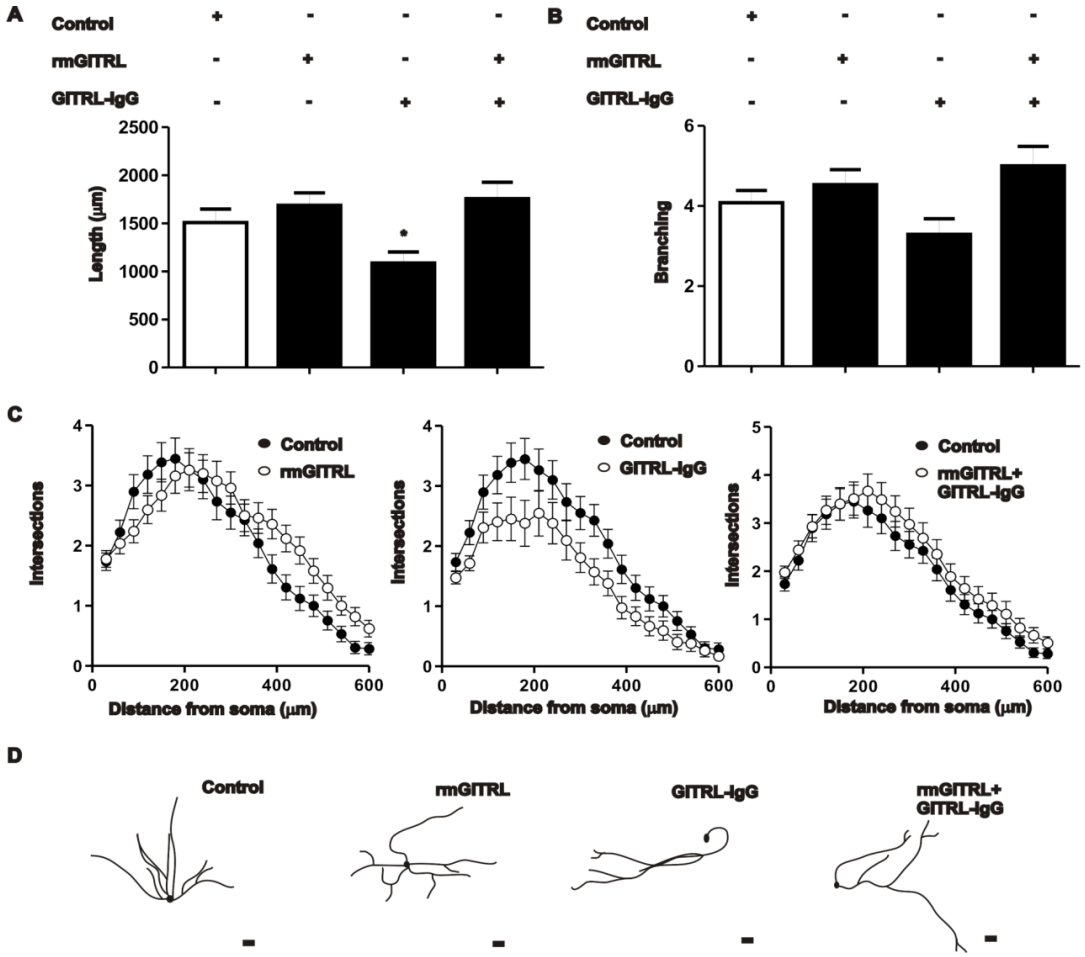


Figure 5.5: Axonal length of P1 mouse SCG neurons grown in 4ng/ml of NGF was reduced following treatment with GITRL-IgG but not rmGITRL. P1 SCG neurons were treated with rmGITRL (1µg) or GITRL-IgG (5µg) and grown overnight in 4ng/ml NGF in 37°C. Control cultures containing 4ng/ml NGF were also grown. Axonal growth was analysed using Sholl analysis. (A, B) Graphical representations of, (A) total neurite length and (B) total neurite branching of P1 SCG neurons treated with rmGITRL or GITRL-IgG and grown overnight in 4ng/ml NGF. (C) Sholl profiles of neurons treated with rmGITRL or GITRL-IgG and grown overnight in 4ng/ml NGF. (D) Representative line drawings of P1 SCG neurons treated with rmGITRL or GITRL-IgG and grown overnight in 4ng/ml NGF. Means ± standard errors of 40-90 neurons per condition is shown. Statistical comparisons: * $P < 0.05$ compared to controls was found using one way ANOVA and post hoc Tukey's test. Scale bar = 50µm.

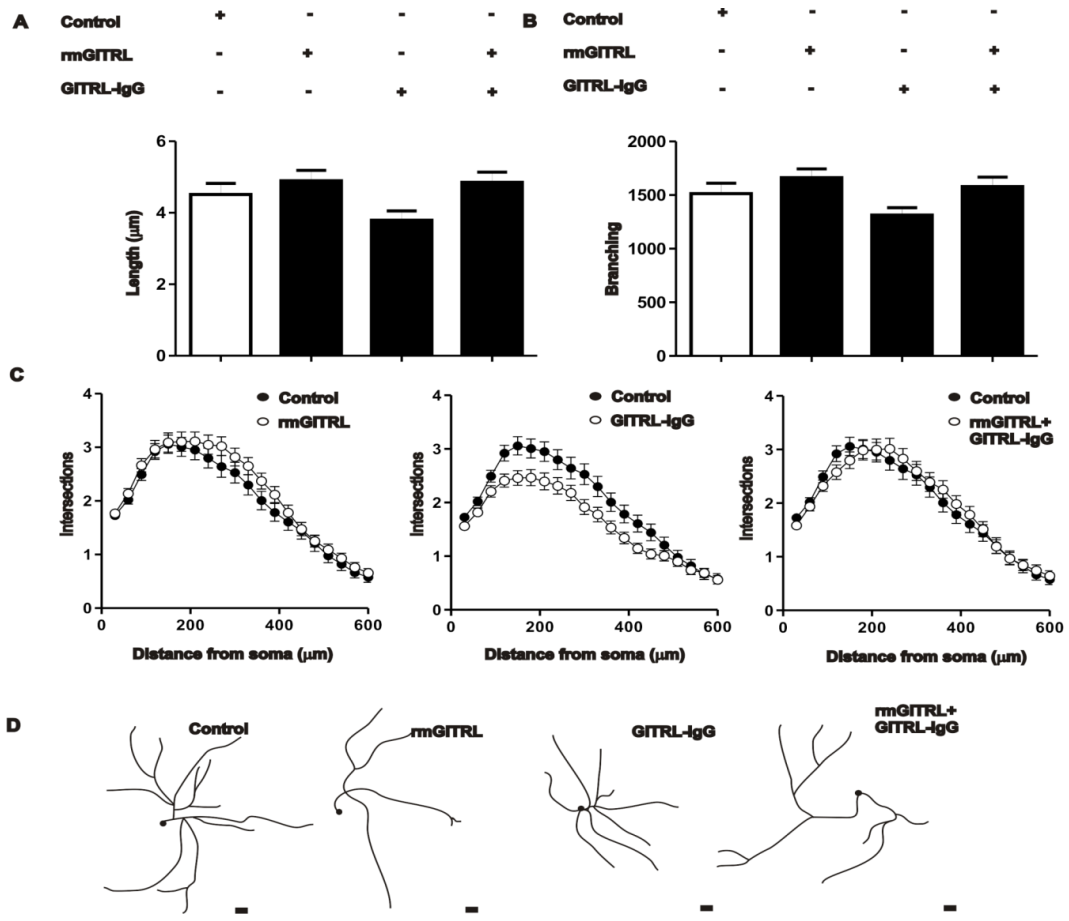


Figure 5.6: Axonal growth of P1 mouse SCG neurons grown in 10ng/ml of NGF was not affected following treatment with rmGITRL or GITRL-IgG. P1 SCG neurons were treated with rmGITRL (1µg) or GITRL-IgG (5µg) and grown overnight in 10ng/ml NGF in 37°C. Control cultures containing 10ng/ml NGF were also grown. Axonal growth was analysed using Sholl analysis. (A, B) Graphical representations of, (A) total neurite length and (B) total neurite branching of P1 SCG neurons treated with rmGITRL or GITRL-IgG and grown overnight in 10ng/ml NGF. (C) Sholl profiles of neurons treated with rmGITRL or GITRL-IgG and grown overnight in 10ng/ml NGF. (D) Representative line drawings of P1 SCG neurons treated with rmGITRL or GITRL-IgG and grown overnight in 10ng/ml NGF. Means ± standard errors of 40-90 neurons per condition are shown. Statistical comparisons: No significant differences compared to controls were found using one way ANOVA and post hoc Tukey's test. Scale bar = 50µm.

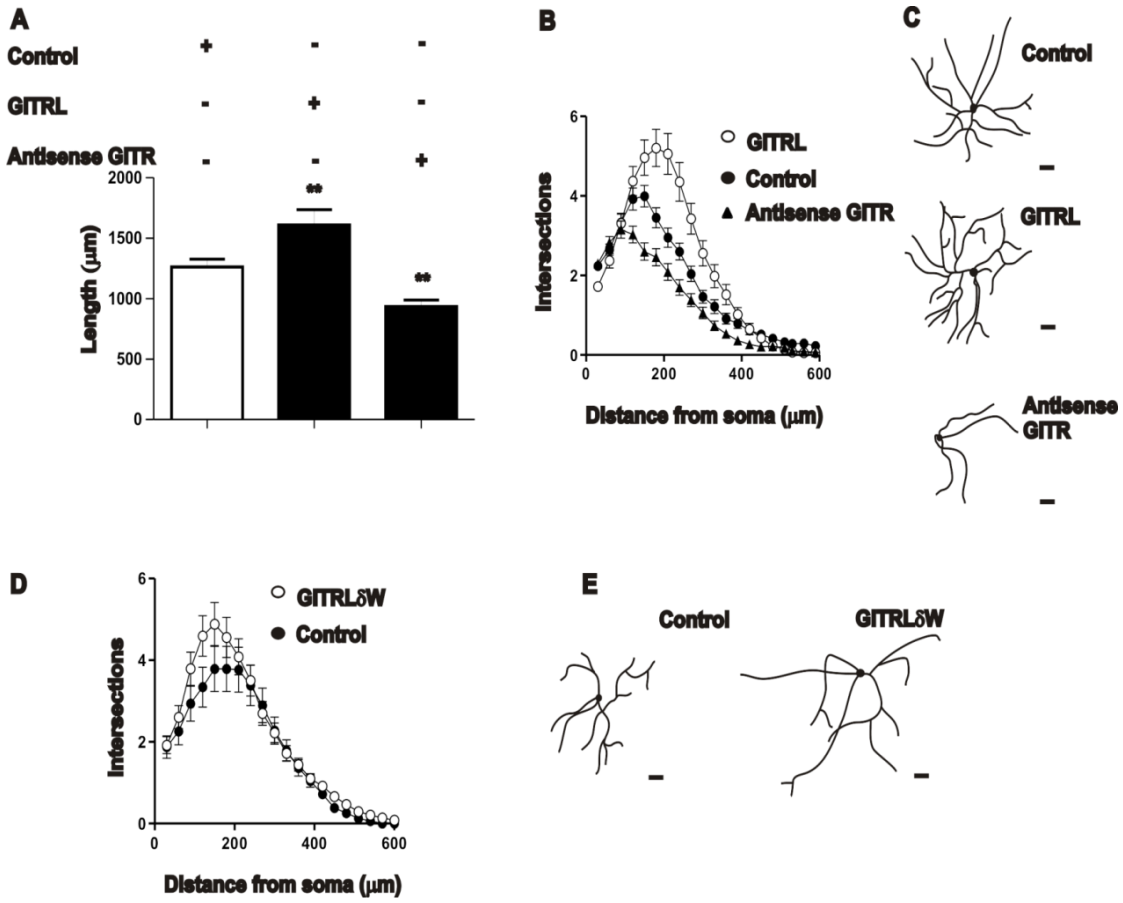


Figure 5.7: GITRL-GITR signalling may promote axonal growth via ligand-receptor binding at the extracellular domain of GITRL. P1 SCG neurons were transfected with a GFP plasmid (to visualise transfected neurites) together with GITRL (to promote GITRL-GITR signalling), antisense GITR (to inhibit GITRL-GITR signalling) and GITRLδW (in which in the intracellular portion of GITRL is missing) and grown overnight in 10ng/ml NGF at 37°C. Control cultures were also grown in which P1 SCG neurons were transfected with control or empty plasmid. Axonal growth was analysed using Sholl analysis. (A) Graphical representation of total neurite length of P1 SCG neurons transfected with GITRL and antisense GITR. (B) Sholl profiles of neurons transfected with GITRL or antisense GITR and grown overnight in 10ng/ml NGF. (C) Representative line drawings of P1 SCG neurons transfected with GITRL or antisense GITR and grown overnight in 10ng/ml NGF. (E) Sholl profile of neurons transfected with GITRLδW and grown overnight in 10ng/ml NGF. (D) Representative line drawings of P1 SCG neurons transfected with GITRLδW and grown overnight in 10ng/ml NGF. Length of neurites from cells transfected with control versus GITRLδW = 1295 ± 189mm versus 1568 ± 168mm. Means ± standard errors of 40-90 neurons per condition are shown. Statistical comparisons: $^{**}P \leq 0.01$ compared to controls was found using one way ANOVA and post hoc Tukey's test for multiple comparisons. Scale bar = 50μm.

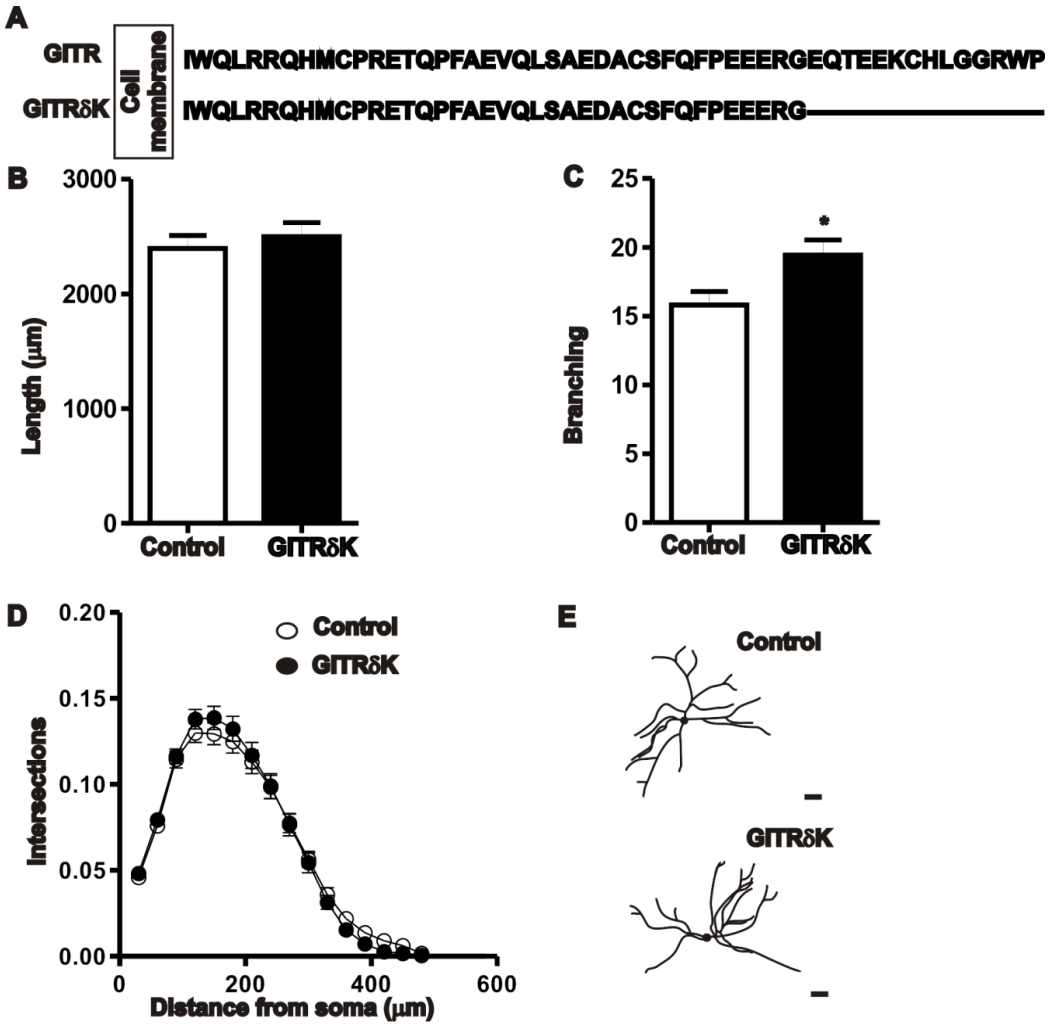


Figure 5.8: The EQTEEKCHLGGRWP region of GITR does not mediate its growth promoting effects. P1 SCG neurons were transfected with a GFP plasmid (to visualise transfected neurites) together with GITRδK (in which the portion of the cytoplasmic region of GITR, EQTEEKCHLGGRWP, was missing) and grown overnight in 10ng/ml NGF at 37°C. Control cultures were also grown in which P1 SCG neurons were transfected with control or empty plasmid. Axonal growth was analysed using Sholl analysis. (A) Primary structure of intracellular tail of GITR and portion deleted in GITRδK mutant. Graphical representations of, (B) total neurite length and (C) total neurite branching of P1 SCG neurons transfected with GITRδK and grown overnight in 10ng/ml NGF. (D) Sholl profile of neurons transfected with GITRδK and grown overnight in 10ng/ml NGF. (E) Representative line drawings of P1 SCG neurons transfected with GITRδK and grown overnight in 10ng/ml NGF. Means ± standard errors of >150 neurons per condition are shown. Statistical comparisons: $*P \leq 0.05$ compared to controls was found using an unpaired student t-test. Scale bar = 50μm.

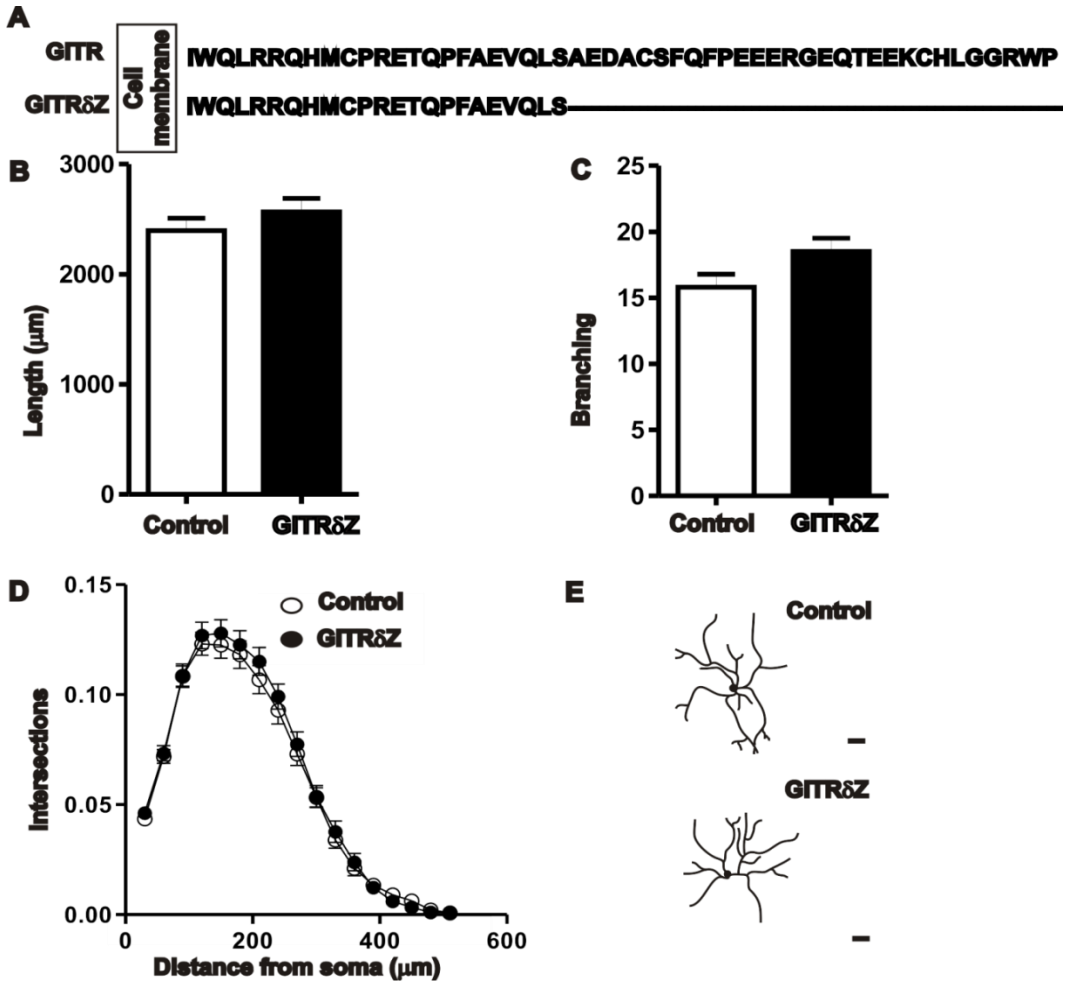


Figure 5.9: The AEDACSFQFPEEERGEQTEEKCHLGGRWP of GITR region of GITR does not mediate its growth promoting effects. P1 SCG neurons were transfected with a GFP plasmid (to visualise transfected neurites) together with GITRδZ (in which the portion of the cytoplasmic region of GITR, AEDACSFQFPEEERGEQTEEKCHLGGRWP, was missing) and grown overnight in 10ng/ml NGF at 37°C. Control cultures were also grown in which P1 SCG neurons were transfected with control or empty plasmid. Axonal growth was analysed using Sholl analysis. (A) Primary structure of intracellular tail of GITR and portion deleted in GITRδZ mutant. Graphical representations of, (B) total neurite length and (C) total neurite branching of P1 SCG neurons transfected with GITRδZ and grown overnight in 10ng/ml NGF. (D) Sholl profile of neurons transfected with GITRδZ and grown overnight in 10ng/ml NGF. (E) Representative line drawings of P1 SCG neurons transfected with GITRδZ and grown overnight in 10ng/ml NGF**.** Means ± standard errors of >150 neurons per condition are shown. Statistical comparisons: No significant differences compared to controls were found using an unpaired student t-test. Scale bar = 50μm.

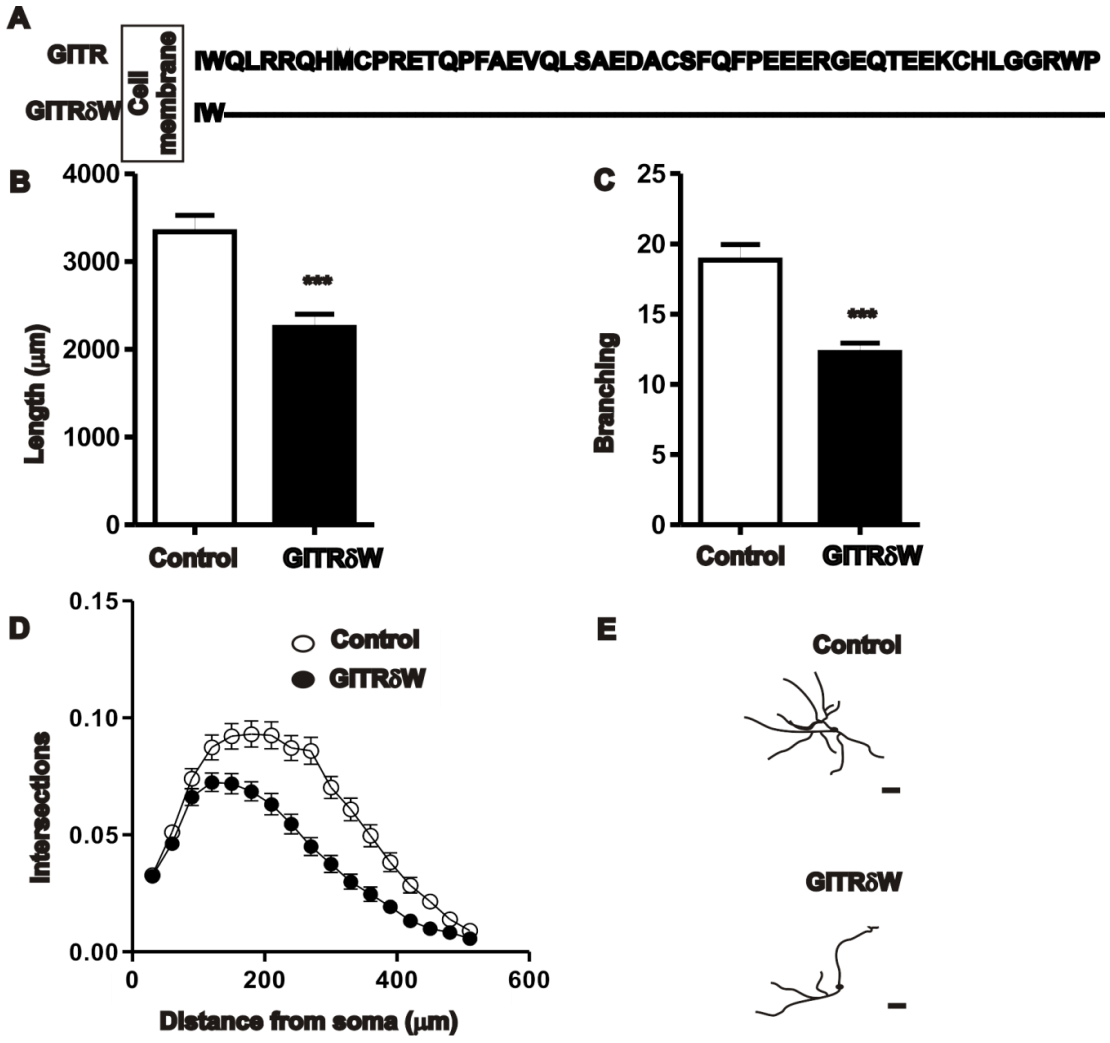


Figure 5.10: The growth promoting effects of GITR signalling require the juxtamembrane region of GITR. P1 SCG neurons were transfected with a GFP plasmid (to visualise transfected neurites) together with GITRδW (in which the portion of the cytoplasmic region of GITR, QLRRQHMCPRETQPFAEVQLSAEDACSFQFPEEERGEQTEEKCHLGGRWP is missing) and grown overnight in 10ng/ml NGF at 37°C. Control cultures were also grown in which P1 SCG neurons were transfected with control or empty plasmid. Axonal growth was analysed using Sholl analysis. (A) Primary structure of intracellular tail of GITR and portion deleted in GITRδW mutant. Graphical representations of, (B) total neurite length and (C) total neurite branching of P1 SCG neurons transfected with GITRδW and grown overnight in 10ng/ml NGF. (D) Sholl profile of neurons transfected with GITRδW and grown overnight in 10ng/ml NGF. (E) Representative line drawings of P1 SCG neurons transfected with GITRδW and grown overnight in 10ng/ml NGF. Means ± standard errors of >150 neurons per condition are shown. Statistical comparisons: ***$P \leq 0.001$ compared to controls was found using an using unpaired student t-test. Scale bar = 50μm.

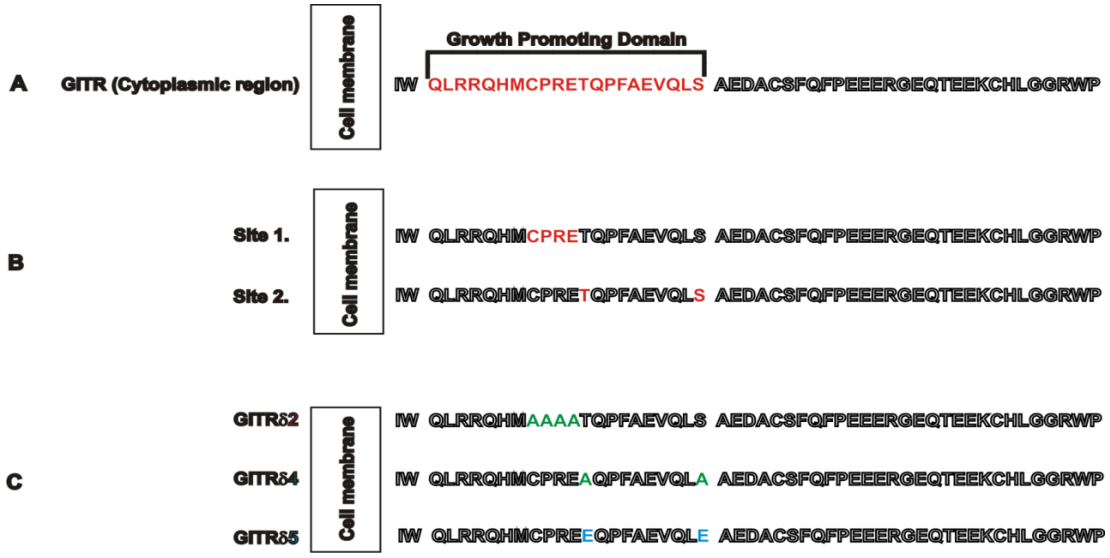


Figure 5.11: The growth promoting domain of GITR is located in the juxtamembrane region of the intracellular portion of GITR. (A) Schema showing the Growth promoting domain (GPD) of transmembrane GITR, located in the juxtamembrane region of the intracellular portion of GITR. (B) Site 1 consists of basic residues present in the GPD that are conserved among the "GITR sub family" of receptors (including CD27, OX40, 4-1BB). These sites are potentially involved in mediating protein-protein interactions and / or the recruitment of specific kinases to Tyr190. (B) Site 2 consisting of Tyr190 and Ser199 (amino acid 12 and 21 of the GPD) were identified as putative phosphorylation sites using *In Silico* analysis by DISPHOS; NetPhos 2.0 and GPS Predictor software programs. (C) Schema describing mutants of basic residues and the putative phosphorylation sites in the GPD of GITR. In GITRδ2, Cys186-Glu189 (CPRE), (amino acids 8 to 11), of the GPD were replaced with alanines. In GITRδ4, Tyr190 and Ser199, (amino acid 12 and 21 of the GPD), were replaced with alanines. In GITRδ5, Tyr190 and Ser199, (amino acid 12 and 21 of the GPD), were replaced with glutamic acid.

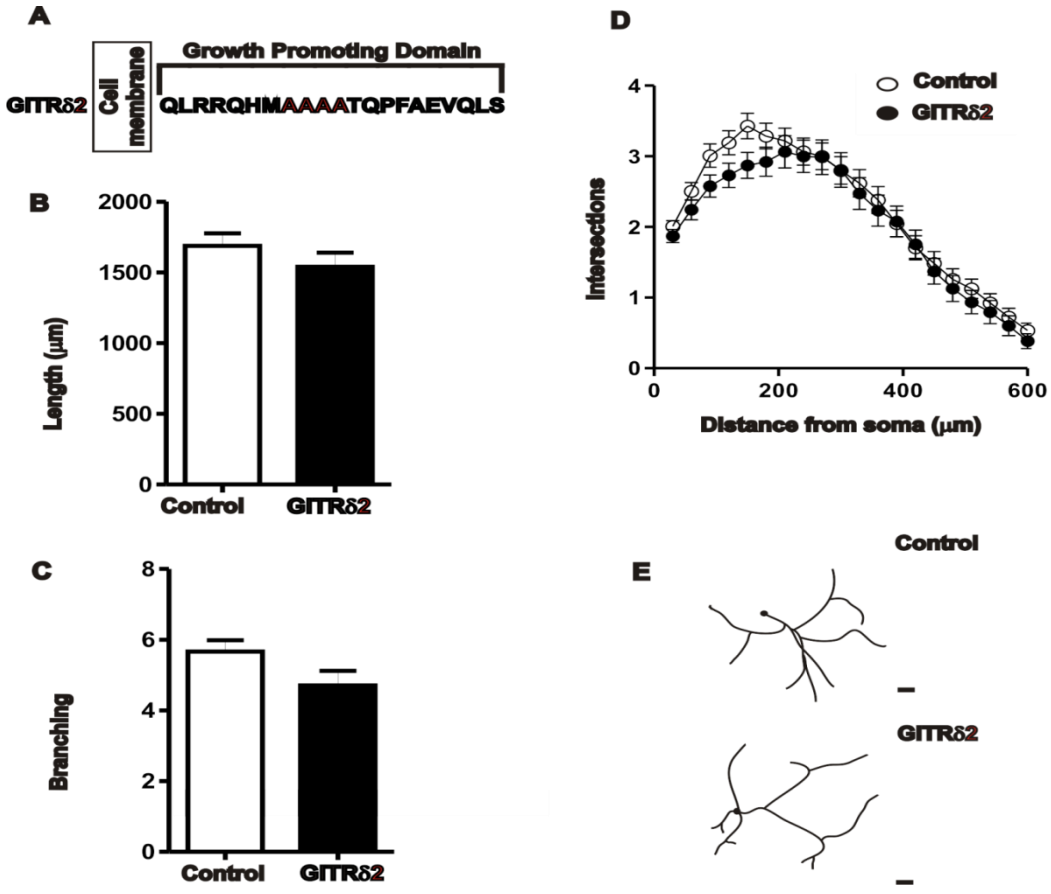


Figure 5.12: The growth promoting effects of GITR signalling are not mediated by the CPRE (amino acids 8 to 11) site of the GPD of GITR. P1 SCG neurons were transfected with a GFP plasmid (to visualise transfected neurites) together with GITRδ2 (mutant in which Cys186-Glu189, CPRE (amino acids 8 to 11) of the GPD were replaced with alanines) and grown overnight in 10ng/ml NGF at 37°C. Control cultures were also grown in which P1 SCG neurons were transfected with control or empty plasmid. Axonal growth was analysed using Sholl analysis. (A) Primary structure of GPD of GITR in which a portion is replaced in GITRδ2 mutant. Graphical representations of, (B) total neurite length and (C) total neurite branching of P1 SCG neurons transfected with GITRδ2 and grown overnight in 10ng/ml NGF. (D) Sholl profile of neurons transfected with GITRδ2 and grown overnight in 10ng/ml NGF. (E) Representative line drawings of P1 SCG neurons transfected with GITRδ2 and grown overnight in 10ng/ml NGF. Means ± standard errors of >150 neurons per condition are shown. Statistical comparisons: No significance difference compared to controls was found using an unpaired student t-test. Scale bar = 50µm.

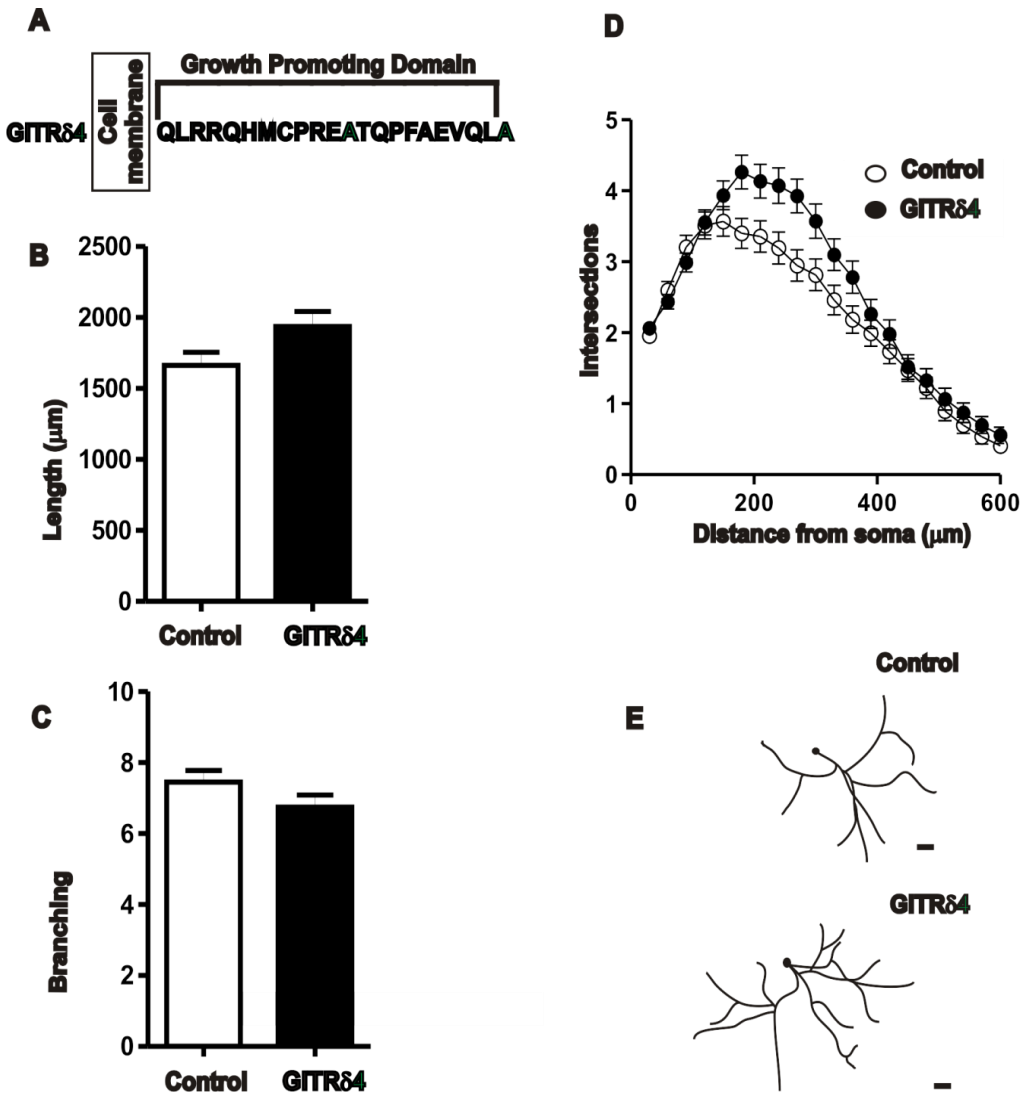


Figure 5.13: The growth promoting effects of GITR signalling are not affected by the inhibition of phosphorylation at Tyr190 and Ser199, (amino acids 12 and 21), sites of the GPD of GITR. P1 SCG neurons were transfected with a GFP plasmid (to visualise transfected neurites) together with GITRδ4 (mutant in which Tyr190 and Ser199, (amino acid 12 and 21) of the GPD were replaced with alanines) and grown overnight in 10ng/ml NGF at 37°C. Control cultures were also grown in which P1 SCG neurons were transfected with control or empty plasmid. Axonal growth was analysed using Sholl analysis. (A) Primary structure of GPD of GITR in which a portion is replaced in GITRδ4 mutant. Graphical representations of, (B) total neurite length and (C) total neurite branching of P1 SCG neurons transfected with GITRδ4 and grown overnight in 10ng/ml NGF. (D) Sholl profile of neurons transfected with GITRδ4 and grown overnight in 10ng/ml NGF. (E) Representative line drawings of P1 SCG neurons transfected with GITRδ4 and grown overnight in 10ng/ml NGF. Means ± standard errors of >150 neurons per condition are shown. Statistical comparisons: No significance difference compared to controls was found using an unpaired student t-test. Scale bar = 50µm.

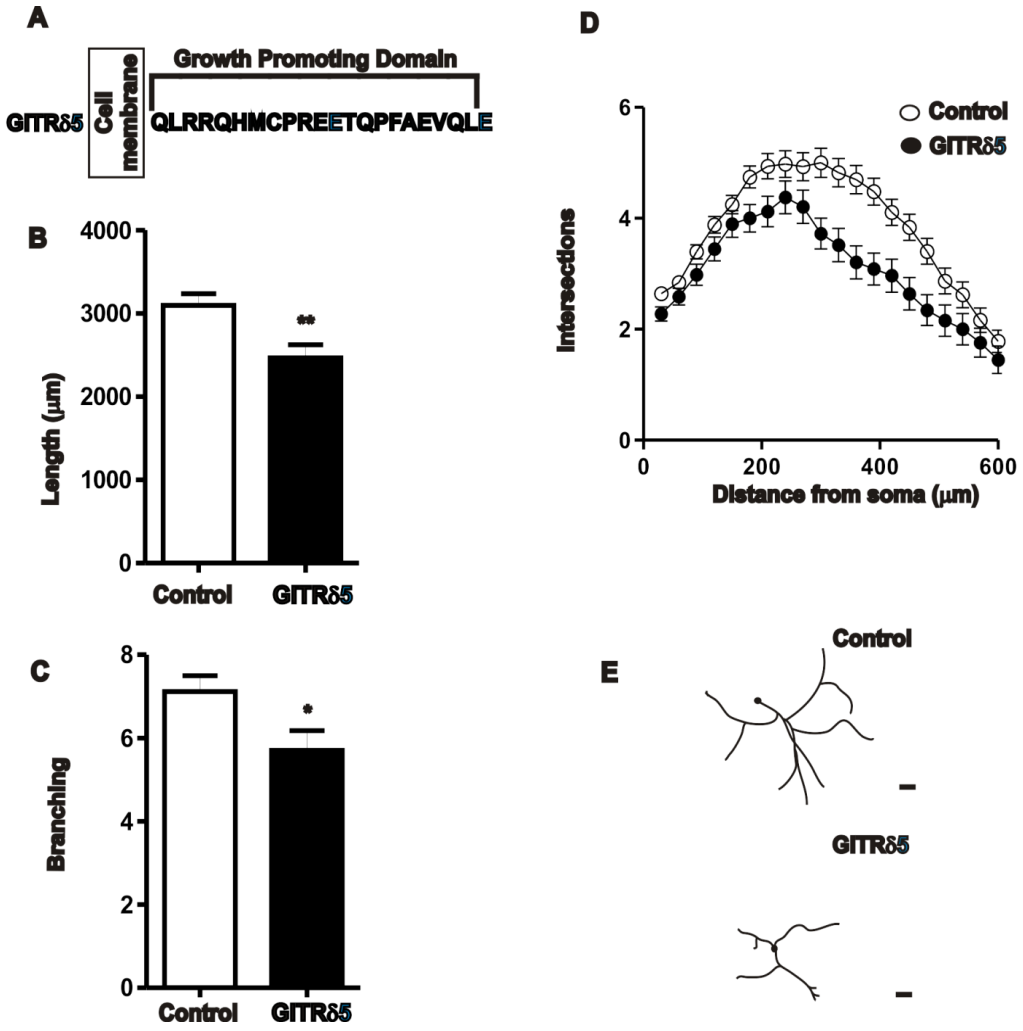


Figure 5.14: Constitutive phosphorylation of residues at Tyr190 and Ser199, (amino acids 12 and 21), sites of the GPD of GITR inhibits axonal growth. P1 SCG neurons were transfected with a GFP plasmid (to visualise transfected neurites) together with GITRδ5 (mutant in which Tyr190 and Ser199, (amino acid 12 and 21) of the GPD were replaced with glutamic acid) and grown overnight in 10ng/ml NGF at 37°C. Control cultures were also grown in which P1 SCG neurons were transfected with control or empty plasmid. Axonal growth was analysed using Sholl analysis. (A) Primary structure of GPD of GITR in which a portion is replaced in GITRδ5 mutant. Graphical representations of, (B) total neurite length and (C) total neurite branching of P1 SCG neurons transfected with GITRδ5 and grown overnight in 10ng/ml NGF. (D) Sholl profile of neurons transfected with GITRδ5 and grown overnight in 10ng/ml NGF. (E) Representative line drawings of P1 SCG neurons transfected with GITRδ5 and grown overnight in 10ng/ml NGF. Means ± standard errors of >150 neurons per condition are shown. Statistical comparisons: $^{**}P \leq 0.01$ and $^{*}P \leq 0.05$ compared to controls was found using an unpaired student t-test. Scale bar = 50μm.

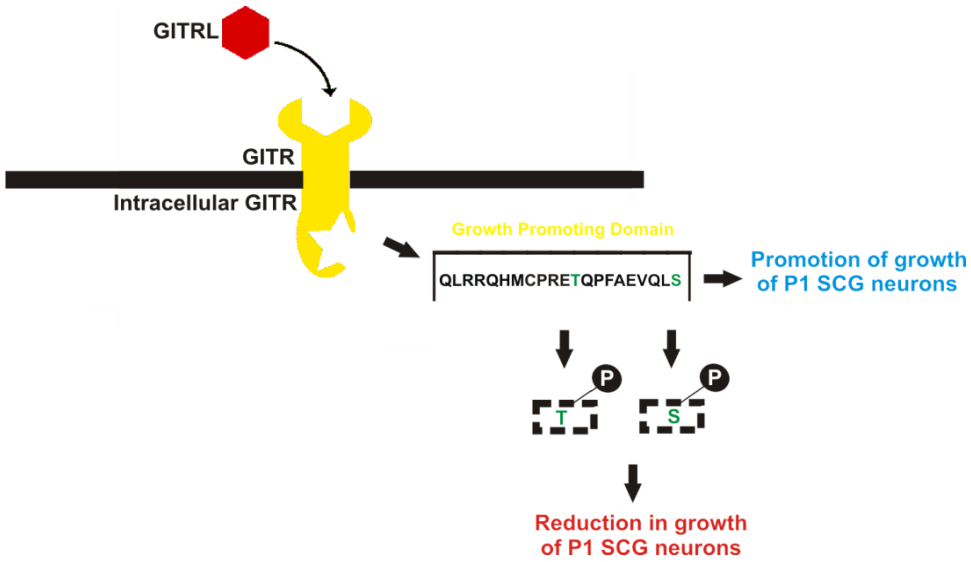


Figure 5.15: Schematic model showing GITRL-GITR binding and subsequent events during axonal growth in P1 mouse SCG neurons. This schematic model shows the proposed subsequent events following GITRL-GITR binding in P1 SCG neurons. GITRL-GITR binding stimulates the GPD of GITR, located in the intracellular region of GITR. The growth promoting region of GITR is involved in the promotion of axonal growth of P1 SCG neurons in the presence of NGF. However, when residues Tyr190 and Ser199, (amino acid 12 and 21) sites of the GPD of the intracellular region of GITR are constitutively phosphorylated, there is a reduction in axonal growth in P1 SCG neurons.

5.5 Discussion

GITR is the 18th member of the TNFRSF and is well known for its role in the immune system in which it regulates innate and acquired immune response responses (*Barao, 2012; Nocentini, et al., 1997; Ronchetti, et al., 2004*). In the developing PNS the role of GITR is just beginning to be elucidated. GITR appears to function in a costimulatory manner with NGF to promote the growth of developing sympathetic neurons of the PNS (*O'Keeffe, et al., 2008*), however the way in which GITR promotes the growth of sympathetic neurons and the region responsible for the growth promoting effects of GITR was not yet fully known. Thus the aim of this chapter was to investigate whether GITRL-GITR signalling increased sympathetic neurons sensitivity to NGF thereby facilitating NGF-promotion of growth in these neurons and to identify the region of GITR responsible for its growth promoting effects in developing sympathetic neurons of the PNS.

We hypothesised that GITR, being a relative of the p75NTR, may increase a neuron's sensitivity to a given concentration of NGF. p75NTR is a member of the TNFRSF and increases the sensitivity of sensory and sympathetic neurons to NGF (*Lee, et al., 1994b*). This is shown by decreased sensitivity for embryonic DRG and postnatal SCG neurons to NGF in p75NTR deficient compared to wild type mice. There is a significant reduction in the % survival of postnatal SCG neurons from p75NTR deficient mice in a range of NGF concentrations compared with controls. The EC50 required for the survival of neurons was greater in p75NTR-deficient SCG neurons (150 pg/ml/0.15ng/ml) than for wild-type neurons (50 pg/ml/0.05ng/ml) ($P \leq 0.05$, t-test) (*Lee, et al., 1994b*). GITR is a member of the same family as p75NTR and therefore it is possible that GITRL-GITR signalling increases the sensitivity of sympathetic neurons to NGF, thereby facilitating NGF-promotion of growth. To address this possibility, we first examined the % survival of P1 SCG neurons in a range of NGF concentrations after 1, 2 and 3 days as a baseline experiment. There was a dose response to NGF for the survival of neurons over the three days. This is in agreement with similar early studies on P1-3 rat sympathetic neurons derived from the SCG which demonstrated that in the absence of NGF, neurons do not survive past day one. When treated with a concentration of 0.5-1ng/ml NGF, P1-3 rat sympathetic neurons survived for up to 4 days. With an increase in NGF

concentration, there is an increase in cell survival but this effect reached saturation at 0.5µg/ml. The lowest NGF concentration, capable of sustaining neuronal survival for 3-4 weeks was found to be 10ng/ml (*Chun and Patterson, 1977*). This is the concentration of NGF used in the subsequent neuronal cultures in this study. Lockhart et al report findings that also reflect a similar dose response effect of NGF, although at lower dosages to the current study. Following testing 0; 0.5; 5; 50ng/ml, they reported that 5ng/ml was saturating for the survival of sympathetic neurons. However it must be noted that the form of NGF used in this study was a non-recombinant form of NGF and as such would be less active that the form of NGF used in the current study (*Lockhart, et al., 1997*).

GITR promotes growth but not the survival of postnatal sympathetic neurons (*O'Keeffe, et al., 2008*) and therefore to investigate whether GITR affects the sensitivity of neurons to NGF, we examined the effect GITRL-GITR signalling on the growth of developing sympathetic neurons in a range of NGF concentrations. Growth of non-treated developing sympathetic neurons was dose responsive where growth increased with higher NGF concentrations (Figure 5.3). This result is in agreement with Chun and Patterson who also found a dose response in which neuronal growth increased with concentrations of NGF from 0.05-.5µg/ml (*Chun and Patterson, 1977*). Following on from these baseline experiments, we looked at the effect of stimulation or inhibition of GITRL-GITR signalling by treating neurons with agonist rmGITRL and antagonist GITRL-IgG antibodies grown in media containing 1, 4 and 10ng/ml NGF. Only cells grown in 1ng/ml NGF demonstrated a response to antagonist GITRL-IgG, in which there was a reduction in branching in treated P1 SCG neurons (**$P \leq 0.001$) (Figure 5.4 B). Neurons displayed no response to treatment with agonist rmGITRL at any concentration of NGF (Result 5.4, 5.5, 5.6). These results indicate that GITRL-GITR signalling may affect the sensitivity of SCG neurons to NGF at low levels of NGF as neutralising GITRL-GITR signalling in SCG neurons treated with 1ng/ml NGF and not 10ng/ml reduced the branching of these neurons. p75NTR increases a neuron's sensitivity to TrkA in the presence of 1ngml of NGF (*Horton, et al., 1997*) and does so via modulating NGF/TrkA binding (*Barker and Shooter, 1994*). Binding of NGF to TrkA is reduced by disrupting NGF/p75NTR binding in PC12 cells by an anti-p75NTR antibody or by excess BDNF (*Barker and Shooter, 1994*) while p75NTR accelerates TrkA

mediated signalling (*Canossa, et al., 1996*). Recently, the intracellular domain of p75NTR (p75ICD) was shown to interact with TrkA and modulate the binding of NGF to TrkA, significantly increasing the amount of NGF bound to TrkA-expressing cells (*Matusica, et al., 2013*). Given that GITR is from the same super family, it may function similarly and the present results may indicate that GITR increases the sensitivity of these neurons to TrkA at low (1ngml) NGF concentrations (i.e. 1ng/ml). Repeating the above experiment on SCG cells from GITR-deficient mice in place of GITRL antibody treatments in a range of NGF concentrations would provide a more sensitive approach to investigating the effect of GITRL-GITR signalling on P1 SCG neurons to NGF.

In the immune system, "reverse" signalling through GITRL has been shown to occur in plasmacytoid DCs (pDCs) whereby GITRL-GITR signalling activates an intracellular signalling pathway, namely the NF-□B pathway, via GITRL and not through the GITR receptor (*Grohmann, et al., 2007*). To investigate if reverse GITRL-GITR signalling occurs in sympathetic neurons, P1 SCG neurons were transfected with a plasmid expressing GITRL□W (in which the intracellular region of GITRL is missing). Transfected cells were unaffected in terms of growth (Figure 5.7 E, F) suggesting one interpretation that GITRL-GITR signalling is not reversed and activation of intracellular pathways is through the receptor, GITR and not GITRL. To further investigate the presence of reverse signalling, staining for ligand (GITRL) and receptors (GITR) by immunocytochemistry and immunohistochemistry in the sympathetic cell bodies, postganglionic fibres and targets could be performed. Kisiswa et al 2013 found that tyrosine hydoxylase–positive sympathetic fibers of SCG target tissues (submandibular salivary gland, nasal turbinate tissue and iris), were clearly labeled by anti-TNFα (Ligand), but were not labeled by anti-TNFR1 (receptor) suggesting the possibility that TNFR1 might act as a reverse-signaling ligand for TNFα. To examine the possibility that GITR reverse signaling might influence the growth of sympathetic axons, one of the methods employed by Kisiswa et al could be used. Kisiswa et al cultured P0 SCG neurons with NGF to sustain their survival with and without a divalent TNFR1 divalent TNFR1-Fc chimera (in which the extracellular domains of two TNFR1 molecules are linked to the Fc part of a human IgG1 antibody), shown to be a potent reverse-signaling ligand for TNFα, and grew cells for 24h. Sholl analysis revealed that the TNFR1-Fc chimera treated

neurons had significantly greater neurite length number of branch points and Sholl profiles that those grown with NGF alone. This result indicated that TNFa reverse signaling promotes sympathetic axon growth.

The region of intracellular GITR responsible for the activation of intracellular pathways resulting in growth promoting effects in developing sympathetic neurons is not known. P1 SCG neurons were transfected with plasmids containing mutant versions of the intracellular region of GITR (GITRδK, GITRδZ and GITRδW). Cells transfected with GITRδW displayed a significant reduction in neurite length (***$P \leq 0.001$) (Figure 5.10 B) and branching (***$P \leq 0.001$) (Figure 5.10 B, C) compared with controls. This was not seen in cells transfected with GITRδZ (Figure 5.9 B, C). Cells transfected with GITRδK demonstrated an increase in branching (*$P \leq 0.05$). This is interesting and indicates that this region may be involved in the regulation of GITR promotion of growth as when it is deleted growth in terms of branching is enhanced. However, given the strength of significance in the reduction in length and branching (***$P \leq 0.001$) in cells transfected with GITRδW, results indicate that the region of GITR involved in NGF-promotion of developing sympathetic neuronal growth is located in the juxtamembrane region of the cytoplasmic or intracellular region of GITR (Figure 5.10 A), now termed the GPD of GITR. GITR, like other TNFRSF members, is a type I transmembrane protein consisting of a cytoplasmic, a transmembrane and an extracellular domain. Murine and human GITR genes comprise 5 exons (*Nocentini, et al., 2000*). The first 3 exons encode the extracellular domain; exon 4 encodes a small part of the extracellular domain, the transmembrane domain and part of the cytoplasmic domain while exon 5 encodes the cytoplasmic domain. mGITR is located on chromosome 4 and hGITR on chromosome 1 (*Gondek, et al., 2005; Nocentini, et al., 2000*). The cytoplasmic domain of mGITR and hGITR is respectively 52 and 53 amino acid residues long, and shows a high degree of homology, in addition to function, with the cytoplasmic domains of OX40, 4-1BB and CD27 which lead to the definition of a new sub family of the TNFRSF (*Nocentini, et al., 2000*). The homology covers two domains, domain 1, the sequence next to the –COOH terminus of the transmembrane region, and domain 2, close to the –COOH terminus of the proteins. GITR binds TRAF proteins, including TRAF 1, 2, 3 and 5, in order to activate subsequent intracellular pathways (*Cohen, et al.,*

2010; Esparza and Arch, 2005a; Gurney, et al., 1999; Hauer, et al., 2005; Kwon, et al., 1999; Schaer, et al., 2012). The TRAF binding site of members of the TNFRSF is located in domain 2 (*Park, et al., 1999*), and is located outside the region of the GPD. The intracellular region and TRAF binding site of GITR outside the GPD was disrupted in cells transfected with GITRδK and GITRδZ in chapter 5.0 and these cells grew normally (Figure 5.8 and 5.9). This suggests that GITRL-GITR signalling in developing sympathetic neurons is TRAF independent. Perhaps different adapter molecules are involved in the GITRL-GITR signal transduction in sympathetic neurons. In NK cells of the immune system, differential regulation of the NK cell receptor 2B4 is mediated by different adaptor molecules in mice and humans (*Lanier, 2005*). In addition, differences in murine and human GITRL oligomerics (e.g., primarily dimers in mouse vs. trimers and superclusters in human) (*Nocentini, et al., 2012*) may contribute to different responses by the receptor-bearing cells.

Basic residues conserved amongst the GITR sub family, possibly involved in protein-protein interactions were identified by Krausz et al and putative phosphorylation sites in the GPD of GITR were identified by *In Silico* analysis. Cys186-Glu189 (CPRE), (amino acids 8 to 11) are basic residues present in the GPD that are conserved among the "GITR sub family" of receptors (CD27, OX40, 4-1BB) (*Krausz, et al., 2007*) and are potentially involved in mediating protein-protein interactions and / or the recruitment of specific kinases to Tyr190 and therefore possibly inhibit phosphorylation at this residue. The putative phosphorylation sites identified are Tyr190 and Ser199 (amino acid 12 and 21 of the GPD) (Figure 5.11). Mutant plasmids of conserved residues and putative phosphorylation sites were created and transfected into P1 SCG neurons (Figure 5.11, 5.12, 5.13, 5.14). Interestingly, only cells transfected with mutant GITRδ5, in which Tyr190 and Ser199 (amino acid 12 and 21 of the GPD) was replaced with glutamic acid, acting to constitutively phosphorylate these sites, showed a response. P1 SCG cells transfected with GITRδ5 displayed a significant decrease in neurite length (**$P \leq 0.01$) (Figure 5.14 B) and branching (*$P \leq 0.05$) (Figure 5.14 C) compared to controls. Phosphorylation at these sites negatively influence the growth of these neurons suggesting (i) these residues maybe responsible for the regulation of GITR-promoted growth of NGF-dependant neurons and (ii) another molecule / pathway

must be involved to allow for the growth promotion effects of GITR. As discussed earlier, the juxtamembrane region of p75NTR was recently found to be necessary for p75NTR to enhance TrkA mediated growth of sympathetic neurons (*Matusica, et al., 2013*). Perhaps the juxtamembrane of GITR may be necessary for GITR-mediated growth by enhancement of TrkA and thus provide an alternate route to the TRAF dependant pathway in GITR signalling in NGF-dependant developing sympathetic neurons. These possibilities will be explored in chapter 6.0.

Results from chapter 5.0 offer a greater depth of understanding of the mechanism of GITRL-GITR signalling in NGF-dependant sympathetic neurons of the developing PNS. In short, we have learned GITRL-GITR binding and activation is possible via the extracellular region of GITRL, however additional experiements to eliminate reverse signalling through GITRL needs to be investigated. The region and possible phosphorylation sites of GITR responsible for regulating the growth promoting effects of GITRL-GITR signalling exists in the juxtamembrane region of the receptor. The next step will be to further elucidate the intracellular pathways involved in GITRL-GITR signalling in the promotion of growth of developing NGF-dependant sympathetic neurons of the PNS.

6.0 Dual-regulation of ERK and NF-κB signalling by GITR in the regulation of axonal growth in developing sympathetic neurons.

6.1 Aims

- To investigate the effect of GITRL-GITR signalling on phospho-TrkA.
- To examine the effect of GITRL-GITR signalling on NF-κB activity.
- To examine the effect of the GPD of GITR on ERK1/2 activity.
- To examine the effect of the GPD of GITR on TrkA phosphorylation.
- Investigate whether putative phosphorylation sites of the GPD are involved in GITRL-GITR regulation of NF-κB, ERK1/2 and TrkA phosphorylation.

6.2 Abstract

GITR is essential for NGF-dependant neurite growth in neonatal sympathetic neurons. However the signalling pathways downstream of GITR involved in the growth of these neurons are largely unknown. In the immune system, GITR regulates both NF-κB and MAPK pathways. In the PNS, GITR is required for the activation of ERK1/2 of the MAPK pathway, which is necessary for NGF-promoted neurite growth of developing sympathetic neurons. In chapter 5.0 of this thesis, the region of GITR responsible for its growth promoting effects was found to be located in the juxtamembrane region of intracellular GITR and this region has been termed the growth promoting domain (GPD). Here we investigate the effect of GITRL-GITR signalling and the contribution of the GPD of GITR, on NF-κB, ERK1/2 and TrkA activity. SCG neurons from P1 mice were transfected with plasmids expressing GITRL, IKKβDN and mutated forms of GITR (GITRδK, GITRδZ, GITRδW) and the effect on NF-κB, ERK1/2 and TrkA signalling was examined. Activation of GITRL-GITR signalling inhibited NF-κB and promoted the activation of ERK1/2 signalling while inhibition of GITRL-GITR signalling increased NF-κB dependant gene transcription and decreased ERK1/2 activation resulting in a reduction in neurite growth. In addition, SCG cells transfected with a GITR mutant in which phosphorylation of sites Thr190 and Ser199 (amino acid 12 and 21 of the GPD) were replaced with glutamic acid, resulted in a reduction of TrkA activity. These findings indicate that while TrkA is negatively affected by constitutive phosphorylation of specific GPD sites, GITRL-GITR signalling regulates the growth of NGF-dependant neonatal sympathetic neurons of the PNS via an inverse modulation of NF-κB and ERK1/2 signalling providing an optimal growth environment for developing sympathetic neurons.

6.3 Introduction

GITR is a type 1 transmembrane protein and member of the TNFRSF. Although well characterised in the immune system for its role in innate and acquired immune responses (*Krausz, et al., 2007*), GITR also has an important role in the development of the PNS in which it facilitates NGF-promoted growth of neonatal sympathetic neurons in a costimulatory manner (*O'Keeffe, et al., 2008*).

The exact mechanism by which GITR promotes NGF-dependant growth of sympathetic neurons is largely unknown. GITR has previously been shown to facilitate NGF-induced activation of ERK1/2 in the promotion of sympathetic neuronal growth, as there was a significant reduction in NGF-induced ERK1/2 activation in sympathetic neurons of GITR-/- mice (*O'Keeffe, et al., 2008*). In addition, the growth promoting effects of enhanced GITR signalling in NGF-dependant sympathetic neurons is achieved by facilitating NGF-induced ERK1/2 phosphorylation, as a reduction in GITRL-GITR promoted growth was abolished when enhanced ERK1/2 phosphorylation was blocked with known MEK inhibitor U0126 (*O'Keeffe, et al., 2008*). In the immune system, GITR potentiates the proliferative response of CD8+ and CD4+ T lymphocyte subpopulations when added with an anti-CD3 stimulus. This costimulation of GITR with anti-CD3 enhanced anti-CD3-induced ERK1/2 phosphorylation (*Ronchetti, et al., 2004*). This was demonstrated by higher levels of phosphorylated ERK1/2 following stimulation with anti-CD3 plus anti-GITR when compared with anti-CD3 alone. The increase in MAPK levels was observed in GITR+/+ but not in GITR–/– cells. The mechanism by which GITR facilitates ERK1/2 activation following costimulation with NGF or anti-CD3 is as yet unknown. As a member of TNFRSF, GITR may act in the same way as its fellow TNFRSF member p75NTR and promote NGF-dependant growth of neurons by interacting with the NGF receptor, TrkA and potentiate binding of NGF to TrkA, leading to increased neurite outgrowth in sympathetic neurons as a result of enhanced ERK1/2 signalling (*Matusica, et al., 2013*) .

In recent years, NF-κB has been identified as a key regulator of sympathetic axonal growth (*Gutierrez and Davies, 2011; Gutierrez, et al., 2008; Nolan, et al., 2011*). Basal levels of NF-κB activity are found in neonatal sympathetic neurons (*Gutierrez, et al., 2008; Nolan, et al., 2011*) and when this activity is enhanced by transfecting cells with plasmids expressing IKKβ, p65, p65/p50, or by treatment with TNFα, this results in a significant inhibition in neonatal SCG neurite growth (*Gutierrez, et al., 2008*). This growth inhibitory effect of NF-κB appears to be mediated via phosphorylation of p65 at serine 536 (*Gutierrez, et al., 2008*). Subsequently it was shown that there are factors present in SCG neurons and targets, such as IL-1β, that can enhance NF-κB activity resulting in the inhibition of neurite growth of these neurons (*Nolan, et al., 2011*). Data collected on NF-κB in

developing sympathetic neurons to date suggests phospho-S536-p65 must be elevated above a certain threshold before it exerts a growth inhibitory effect. It is possible that GITR signalling is required to inhibit NF-κB to "allow" axonal growth to occur. GITR has previously been shown to inhibit NF-κB signalling via binding TRAF 2. HEK 293 cells transfected with a plasmid overexpressing TRAF 2 resulted in the inhibition of NF-κB activity (*Esparza and Arch, 2005b*). Given the research to date, it is plausible that GITR facilitates NGF-promoted growth via promoting NGF/TrkA binding and ERK1/2 signalling in developing sympathetic neurons while dampening down the growth inhibitory effects of NF-κB allowing for an optimal environment for axonal growth in these neurons. In this chapter, we aim to explore this possibility in P1 SCG neurons by activating or inhibiting GITRL-GITR activity using treatments, knock out models and transfection methods and examine the effects on TrkA, ERK1/2 and NF-κB signalling.

6.4 Results

6.4.1 GITRL-GITR signalling does not affect phospho-TrkA in P1 mouse SCG neurons.

p75NTR is a member of the same family as GITR (TNFRSF) and has previously been shown to enhance sympathetic neuron's sensitivity to NGF at low (< 10ng/ml NGF) but not high (10ng/ml NGF) concentrations of NGF (*Lee, et al., 1994b*). Recently, p75NTR has been found to increase sympathetic neurons sensitivity to NGF by interacting with and potentiating binding of NGF to TrkA-expressing cells leading to increased neurite outgrowth in sympathetic neurons (*Matusica, et al., 2013*). In chapter 5.0, inhibition of GITRL-GITR by antagonist GITRL-IgG resulted in a decrease in neurite branching in P1 SCG cells grown in 1ng/ml NGF but did not affect branching in cells grown in 4 or 10ng/ml NGF indicating that GITR may enhance sympathetic neurons sensitivity to NGF at <10ng/ml concentrations. To investigate if GITRL-GITR signalling affects TrkA signalling in neurons grown in 1ng/ml NGF, P1 SCG neurons were treated with antagonist GITRL-IgG and grown overnight in media containing 1ng/ml NGF and the effect on the expression of phospho-TrkA was examined. Treatment of neurons with antagonist GITRL-IgG had no effect on phospho-TrkA levels of neurons as demonstrated by Figure 6.1 B in

which the levels of mean fluorescence of phospho-TrkA were not different to controls. This result is reflected in photomicrographs of phospho-TrkA in neurons (Figure 6.1 A). This result indicates that GITRL-GITR signalling may affect the growth of SCG neurons at low subsaturating levels of NGF. However, inhibition of GITRL-GITR signalling by antagonist GITRL-IgG appears to have no effect on phospho-TrkA signalling in these neurons grown in media containing 1ng/ml NGF.

6.4.2 GITRL-GITR signalling regulates NF-κB activity in P1 SCG neurons.

GITR is known to activate or inhibit NF-κB activity depending on the cellular context (*Esparza and Arch, 2004; Esparza, et al., 2006*), and NF-κB has been implicated as a key regulator of axonal growth (*Gutierrez and Davies, 2011; Gutierrez, et al., 2008*). However the effect of GITRL-GITR signalling on NF-κB activity in P1 SCG neurons has, to our knowledge, not been investigated. Overexpression of GITRL (Figure 6.2 A) and treatment with agonist GITRL-IgG (Figure 6.1 B) induced a reduction in NF-κB activity as seen by a reduction in κB-reporter signal (Figure 6.2 A), phospho-IKK and phospho-p65 (Figure 6.2 B). Overexpression of GITRL caused a reduction (**$P \leq 0.01$) in NF-κB activity to the same extent as cells transfected with a mutated dominant negative IκBα (containing serine to alanine substitutions at residues 32 and 36, known to inhibit NF-κB transcriptional activity (*Roff, et al., 1996*) (Figure 6.3 A). Conversely, when GITR is blocked using a function blocking antibody (GITR-IgG)(1ug/ml), there was a significant increase in NF-κB activity (**$P \leq 0.01$) (Figure 6.3 C). In addition, the expression of phospho-IKK and phospho-p65 was increased in GITR-/- SCG tissue compared to controls (Figure 6.3 D). To investigate the role of the GPD of GITR in the regulation of NF-κB activity, cells were transfected with a mutant plasmid GITRδW (in which the juxtamembrane region/GPD of GITR is missing) which resulted in an increase in NF-κB activity (**$P \leq 0.01$) (Figure 6.3 B). Together these results suggest GITRL-GITR signalling regulates NF-κB activity in mouse P1 SCG neurons.

6.4.3 GITRL-GITR signalling regulates NF-κB activity through the GPD of GITR in P1 SCG neurons.

To investigate whether GITRL-GITR signalling regulates NF-κB activity specifically through the GPD domain of GITR, P1 SCG cells were transfected with 3 mutant plasmids of the intracellular region of GITR and the effect on nuclear NF-κB activity, as assessed by levels of nuclear pSer536p65, was examined. Mutant plasmids included GITRδK, GITRδZ and GITRδW. There was no change in NF-κB activity in cells transfected with GITRδK (in which the portion of the cytoplasmic region of GITR, EQTEEKCHLGGRWP, was missing) compared to non-transfected cells and control-transfected cells (Figure 6.4 B) which is reflected in photomicrographs of GITRδK-transfected and control-transfected cells (Figure 6.4 A). Similarly, cells transfected with GITRδZ (in which the portion of the cytoplasmic region of GITR, AEDACSFQFPEEERGEQTEEKCHLGGRWP, was missing) displayed no change in nuclear NF-κB activity compared to non-transfected and control-transfected cells (Figure 6.5 B). This result is also reflected in photomicrographs of GITRδZ-transfected and control-transfected neurons (Figure 6.5 A). However there was a significant increase in NF-κB activity in cells transfected with GITRδW (in which the GPD is missing) when compared to controls (***$P \leq 0.001$) and non-transfected cells (***$P \leq 0.001$) (Figure 6.6 C). The difference in nuclear NF-κB activity in GITRδW-transfected cells compared to control-transfected cells can be seen in photomicrographs (Figure 6.6 A) and at a higher magnification (Figure 6.6 B). Collectively, these results suggest that GITRL-GITR signalling regulates NF-κB activity via the GPD of GITR.

6.4.4 Inhibition of IKKβ prevents the effects of GITR inhibition on growth in P1 mouse SCG neurons.

To determine if preventing enhanced NF-κB activation could reverse the decrease in neurite growth following GITR inhibition, cells were co-transfected with plasmids expressing antisense GITR or GITRδW (to inhibit GITRL-GITR signalling and induce a reduction in neurite growth) along with a K44A IKKβ dominant negative

(DN) plasmid (used because IKKβ is responsible for the growth inhibitory effects of NF-κB in P1 SCG neurons (*Gutierrez, et al., 2008*)) and the effect on growth was determined. Cells transfected with antisense GITR or GITRδW displayed the expected significant reduction in neurite length (** $P \leq 0.01$) / (*** $P \leq 0.001$) (Figure 6.7 A and 6.8 A) and branching (** $P \leq 0.001$) / (*** $P \leq 0.001$) (Figure 6.7 B and 6.8 B). However when antisense GITR or GITRδW was co-transfected with IKKβDN, cells displayed neurite length (Figure 6.7 A and 6.8 A) and branching (Figure 6.7 B and 6.8 B) comparable to control-transfected neurons. Growth profiles (Figure 6.7 C and 6.8 C) and representative line drawings (Figure 6.7 D and 6.8 D) of transfected neurons reflect these results. These results indicate that blocking NF-κB prevents the reduction in growth resulting from the inhibition of GITRL-GITR signalling and that the IKKβ-dependant NF-κB activity is responsible for the inhibition of neurite growth resulting from endogenous GITR inhibition.

6.4.5 P1 SCG cells overexpressing both GITRL and p65 demonstrate greater growth than cells expressing p65 alone however NF-κB activity is comparable in these cells.

P1 SCG cells transfected with plasmids overexpressing GITRL and p65 together exhibited significantly greater neurite length (*** $P \leq 0.001$) (Figure 6.9 A) and branching (*** $P \leq 0.001$) (Figure 6.9 B) compared to neurite length and branching in cells transfected with p65 alone. Cells transfected with GITRL alone displayed greater length (*** $P \leq 0.001$) (Figure 6.9 A) and branching (** $P \leq 0.01$) (Figure 6.9 B) compared to cells transfected with p65 and GITRL. Cells transfected with GITRL and p65 together displayed no difference in neurite length (Figure 6.9 A) or branching (Figure 6.9 B) when compared with control-transfected neurons. This is reflected in Sholl profiles (Figure 6.9 C) and representative line drawings (Figure 6.9 D) of transfected neurons. Interestingly, when nuclear NF-κB activity was assessed, by pSer536-p65 nuclear staining, cells transfected with both GITRL and p65 together displayed significantly increased NF-κB activity (*** $P \leq 0.001$) compared to controls (Figure 6.10 B) to the same extent as those cells expressing p65 alone (*** $P < 0.001$) (Figure 6.10 B) (Figure 6.17 C). Given that the extent of growth in

transfected neurons does not correlate with extent of NF-κB activity in these neurons, these results suggest GITR is initiating a second signal that opposes NF-κB activity therby leading to NGF-promoted growth in these neurons.

6.4.6 GITR regulates ERK1/2 phosphorylation via the GPD in P1 SCG neurons.

The results in 6.4.5 suggest that GITR is initiating a second signal that opposes NF-κB activity leading to NGF-promoted growth in these neurons. GITR has been previously reported to facilitate NGF-induced ERK1/2 activation in the promotion of SCG neuronal growth (*O'Keeffe, et al., 2008*) and therefore ERK1/2 is a potential second signal. There is a reduction in phospho-ERK1/2 in cultured SCG neurons from GITR-/- compared to GITR+/+ mice (Figure 6.14 A). In addition, cells transfected with GITRδW (plasmid in which the GPD of GITR is missing) displayed a significant reduction in phospho-ERK1/2 levels (*** $P \leq 0.001$) (Figure 6.17 B) compared with non-transfected and control-transfected neurons. This result is represented by photomicrographs of GITRδW and control-transfected neurons (Figure 6.17 A). This reduction in levels of phospho-ERK1/2 compared to non-transfected and control-transfected neurons was not observed in cells transfected with GITRδK (Figure 6.15 B) illustrated by photomicrographs of GITRδK-transfected and control-transfected neurons (Figure 6.15 A) or in cells transfected with GITRδZ (Figure 6.16 B) reflected in photomicrograph images of GITRδZ-transfected and control-transfected neurons (Figure 6.16 A) (GITRδK and GITRδZ are plasmids in which regions of the cytoplasmic domain outside the GPD are missing (Figure 5.8 and Figure 5.9). These results indicate that the regulation of ERK1/2 by GITR is via the GPD of GITR. Indeed cells transfected with GITRL and p65 displayed a greater level of phospho-ERK1/2 activity compared to cells transfected with p65 alone (*** $P \leq 0.001$) (Figure 6.18 D) and the same level of phospho-ERK1/2 as controls (Figure 6.18 A and D). When this is related to the effects on neurite length (Figure 6.9 A) (Figure 6.18 B) and branching (Figure 6.9 B), it is clear that the extent of NGF-promoted growth was related to the level of phospho-ERK1/2 in these neurons which can in turn be modulated by altering NF-κB activity (Figure 6.19).

6.4.7 Putative phosphorylation sites of the GPD of GITR have no effect on phospho-p65 or phospho-ERK1/2 activity.

The GPD of GITR regulates both phospho-p65 and phospho-ERK1/2 in neonatal sympathetic neurons (Figure 6.6 and 6.17). However the region of the GPD responsible for the inhibition/activation of these signalling pathways is unknown in neonatal sympathetic neurons. *In Silico* analysis identified putative phosphorylation sites in the GPD of GITR located at Thr190 and Ser199 (amino acid 12 and 21) of the GPD. In addition, there are basic residues, Cys186-Glu189 (CPRE) (amino acids 8-11), present in the GPD that are conserved among the "GITR sub family" of receptors (CD27, OX40, 4-1BB) (*Krausz, et al., 2007*) and are potentially involved in mediating protein-protein interactions. Mutant plasmids were then created in which insertions replaced putative phosphorylation sites and conserved basic residues. Figure 5.11 C in chapter 5.0 illustrates schema describing mutants of putative phosphorylation sites and conserved basic residues of the GPD of GITR. In mutant GITRδ2, Cys186-Glu189 (CPRE), (amino acids 8 to 11), of the GPD were replaced with alanines which should inhibit the mediation of protein-protein interactions and / or the recruitment of specific kinases to Tyr190 and therefore inhibit phosphorylation at this residue. In mutant GITRδ4, Thr190 and Ser199, (amino acid 12 and 21 of the GPD), were replaced with alanines which should act to inhibit phosphorylation at these sites and in mutant GITRδ5, Thr190 and Ser199, (amino acid 12 and 21 of the GPD), were replaced with glutamic acid which should act to promote constitutive phosphorylation at these sites. P1 SCG cells were transfected with GITRδ2, GITRδ4 and GITRδ5 mutant plasmids and displayed no change in phospho-p65 levels compared to non transfected and control transfected neurons (Figure 6.11 B, Figure 6. 12 B and Figure 6.13 B). These results are represented by photomicrographs of transfected and control-transfected neurons (Figure 6.11 A, Figure 6.12 A and Figure 6.13 A). Similarly phospho-ERK1/2 levels in P1 SCG neurons were unchanged following transfection with GITRδ2, GITRδ4 and GITRδ5 mutant plasmids when compared to non-transfected and control-transfected neurons (Figure 6.20 B, Figure 6.21 B and Figure 6.22 B). Again, these results are reflected in photomicrographs of mutant-transfected and control-transfected neurons (Figure 6.20 A, Figure 6.21 A and Figure 6.22 A). These

combined results indicate that GITRL-GITR regulation of NF-κB and ERK does not involve the putative phosphorylation sites identified by *In Silico* analysis or the conserved basic residues of the GITR 'sub family' of receptors located in the GPD of GITR.

6.4.8 Constitutive phosphorylation of residues at Thr190 and Ser199, (amino acids 12 and 21 sites of the GPD) of GITR results in a reduction in TrkA expression.

In chapter 5.0, we showed that constitutive phosphorylation at sites Thr190 and Ser199, (amino acids 12 and 21), sites of the GPD of GITR resulted in a significant reduction in growth of P1 SCG neurons (Figure 5.14). Given that phosphorylation at these sites had no effect on levels of phospho-p65 and phospho-ERK1/2 (Result 6.4.7), we next investigated the effect of these sites on the levels of phospho-TrkA and TrkA. As already described, the TNFRSF member p75NTR increases sympathetic neurons sensitivity to NGF by interacting with and and potentiating binding of NGF to TrkA expressing cells leading to increased neurite outgrowth in sympathetic neurons (*Matusica, et al., 2013*). P1 SCG neurons were transfected with plasmids GITRδW and GITRδ5 (transfection with both plasmids results in a reduction in growth in P1 SCG neurons) and the effect on the levels of both phospho-TrkA and TrkA was examined. TrkA is expressed in P1 SCG neurons as shown in Figure 6.24 and levels of TrkA (Figure 6.25 A and B) but not phospho-TrkA (Figure 6.23 A and B) are significantly reduced in P1 SCG neurons transfected with the GITRδ5 plasmid (** $P \leq 0.01$) compared to non-transfected and control-transfected neurons (Figure 6.24 B). However, TrkA levels are not significantly reduced in GITRδW transfected cells (Figure 6.25 B). These results are reflected in photomicrograph images of GITRδ5 and GITRδW-transfected and control-transfected neurons (Figure 6.25 A).

Taken together these results indicate that GITRL-GITR signalling inhibits NF-Kb signalling and potentiates ERK1/2 signalling which is essential for NGF-promoted neurite growth. In addition, phosphorylation of specific GPD residues negatively regulates P1 SCG TrkA expression and neuronal growth, in a manner independent of NF-κB and ERK signalling.

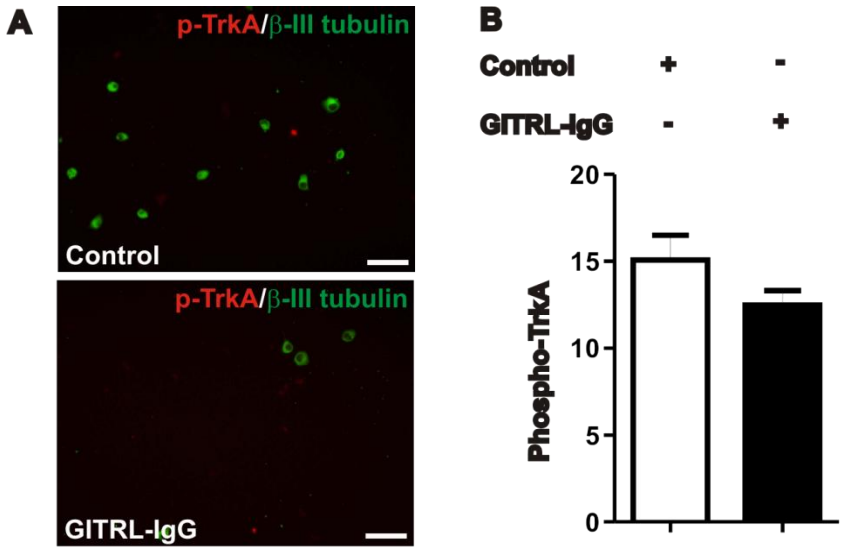


Figure 6.1: GITRL-GITR signalling does not affect the phosphorylation of TrkA in P1 mouse SCG neurons. P1 SCG cells were grown overnight in 1ng/ml NGF at 37°C in the presence or absence of antagonist GITRL-IgG (5µg/ml). The following day, cultures were fixed and immunocytochemically stained for phospho-TrkA and analysis of mean fluorescence was performed. (A) Photomicrographs of control and GITRL-IgG treated P1 SCG dissociated cultures labelled for phospho-TrkA (red) and counterstained with β-III tubulin (green). (B) Graphical representation of levels of phospho-TrkA in control and GITRL-IgG treated P1 SCG neurons. Means ± standard errors of 40-90 neurons per condition are shown. Statistical comparisons: No significant differences compared with control were found using an unpaired student t-test. Scale bar = 50µm.

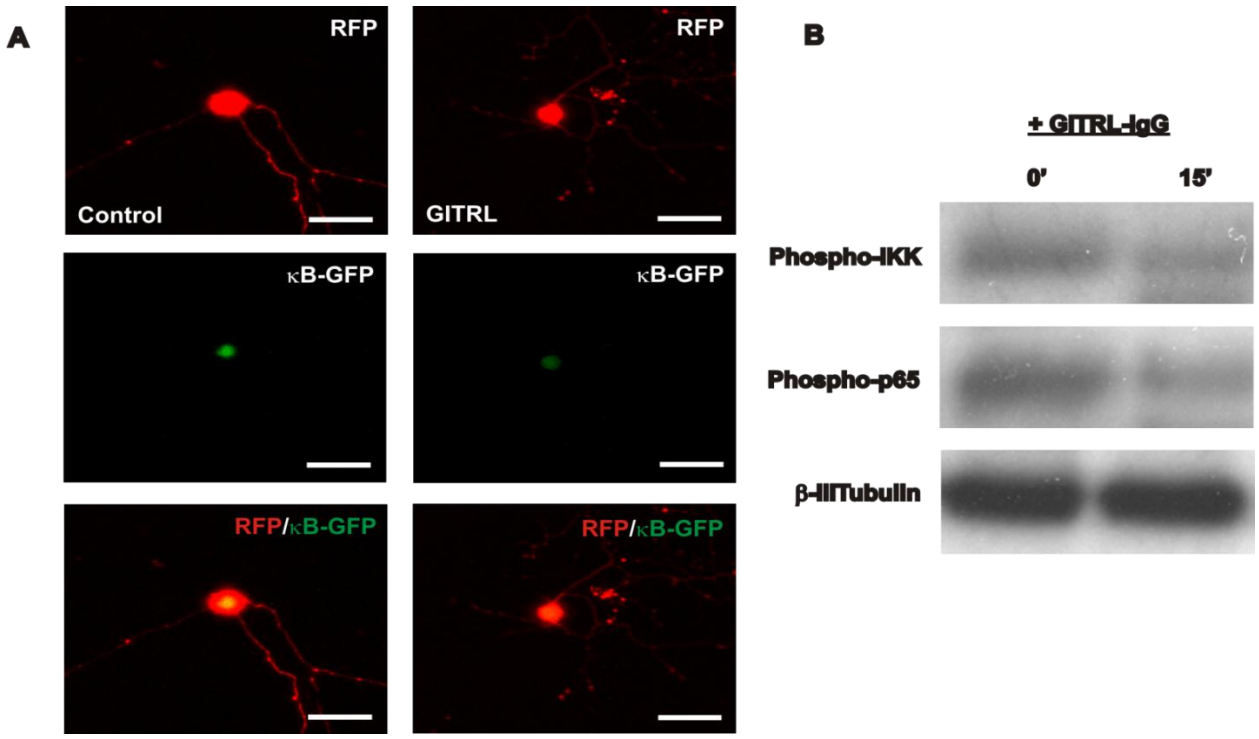


Figure 6.2: Overexpression of GITRL inhibits NF-κB activity in P1 mouse SCG neurons. P1 SCG neurons were transfected with a RFP plasmid (to visualise transfected neurites) together with GITRL (to promote GITRL-GITR signalling) and κB-GFP reporter (to measure NF-κB dependant transcriptional activity) and grown overnight in 10ng/ml NGF at 37°C. Control cultures were also grown in which P1 SCG neurons were transfected with control or empty plasmid. (A) Photomicrographs of P1 SCG neurons transfected with control, GITRL and κB-GFP reporter plasmids and grown overnight in 10ng/ml NGF. Scale bar = 50μm. (B) Representative Western blots showing levels of phospho-IKK, phospho-Ser536-p65 and β-III Tubulin in protein extracts of P1 mouse SCG neurons 24h after treatment with agonist GITRL-IgG (1μg/ml) for 0 and 15 min (0'= untreated neurons).

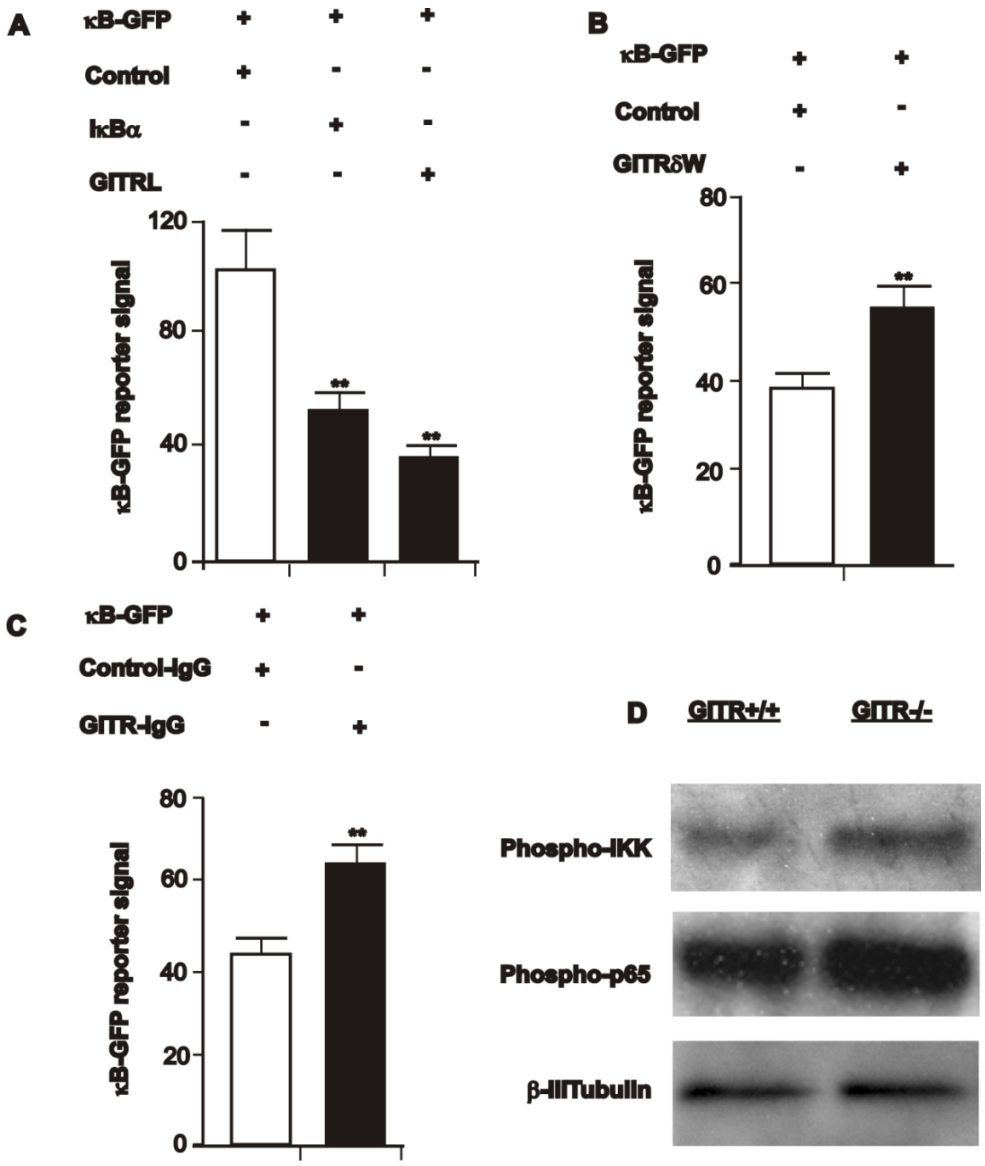


Figure 6.3: GITRL-GITR signalling regulates NF-κB-dependant transcriptional activity in P1 mouse SCG neurons. P1 SCG neurons were transfected with a RFP and κB-GFP reporter plasmids, together with a control, IκBα, GITRL, or GITRδW expression plasmids or alternatively, neurons were treated with GITR-IgG (1μg/ml) (function blocking antibody) and grown overnight in 10ng/ml NGF at 37°C. (A) Graphical representation of NF-κB-dependant transcriptional activity in IκBα and GITRL transfected neurons and (B) GITRδW transfected neurons compared to control transfected neurons. (C) Graphical representation of NF-κB dependant-transcriptional activity in GITR-IgG treated neurons compared to controls. All data were obtained 24h after transfection and analysis of mean nuclear fluorescence intensity was performed. Means ± SEM of 50-90 neurons per condition shown. Statistical analysis: $^{**}P \leq 0.01$ compared with control, using unpaired student t-test and one way ANOVA and post-hoc Tukey's. (D) Representative Western blots showing phospho-IKK, phospho-Ser536-p65 and β-III Tubulin in GITR+/+ and GITR-/- P1 mouse SCG neurons grown for 18h in 10ng/ml NGF.

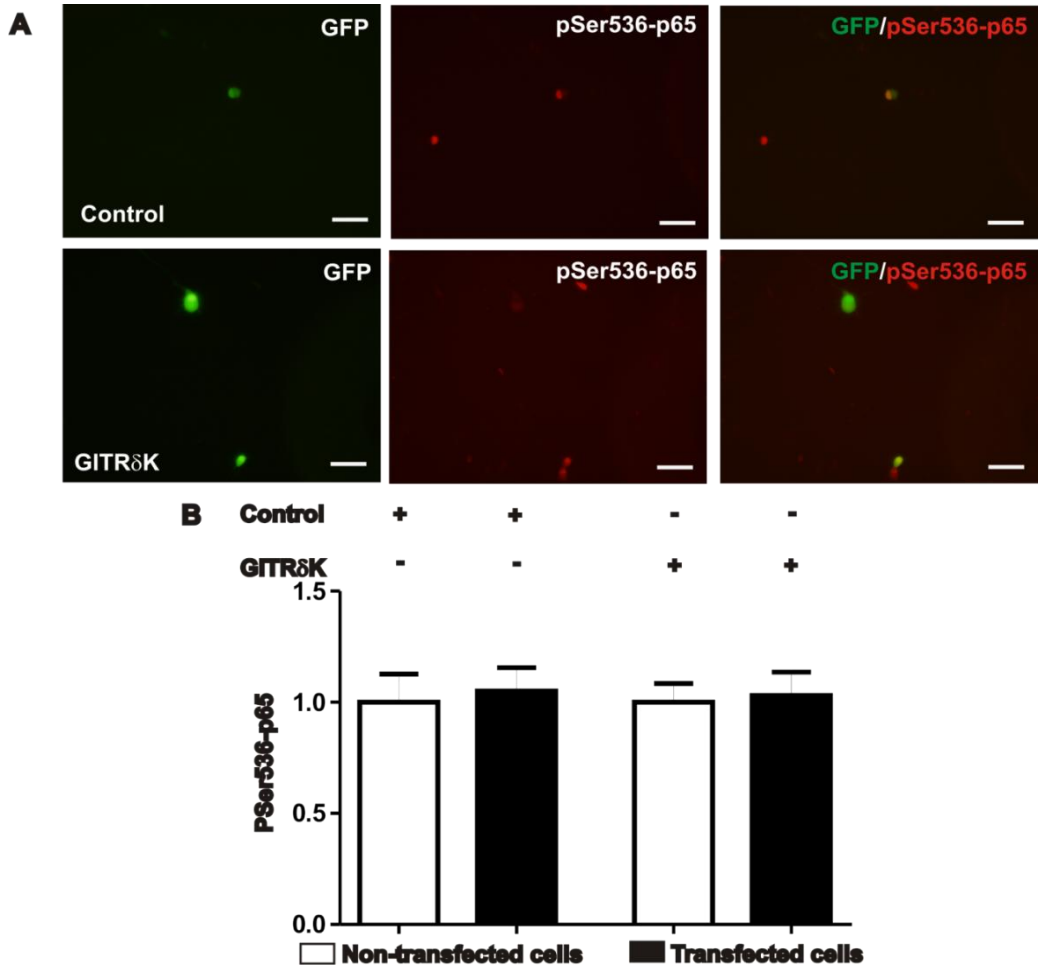


Figure 6.4: GITRL-GITR signalling does not regulate NF-κB activity in P1 mouse SCG neurons via the cytoplasmic region EQTEEKCHLGGRWP of GITR. P1 SCG neurons were transfected with a GFP plasmid (to visualise transfected neurons) together with GITRδK expression plasmid and grown overnight in 10ng/ml NGF at 37°C. Control cultures were also grown in which P1 SCG neurons were transfected with control or empty plasmid. The following day, cultures were fixed and immunocytochemically stained for pSer536-p65 (phospho NF-κB) and analysis of mean nuclear fluorescence was performed. (A) Photomicrographs of control and GITRδK-transfected dissociated cultures of P1 SCG neurons labelled for phospho-NF-κB (red) (B) Graphical representations of relevant differences in nuclear levels of phospho-NF-κB in GITRδK transfected, non-transfected and control-transfected P1 SCG neurons. Means ± standard errors of 40-90 neurons per condition are shown. Statistical comparisons compared with control: No significant differences were found using an unpaired student t-test. Scale bar = 50μm.

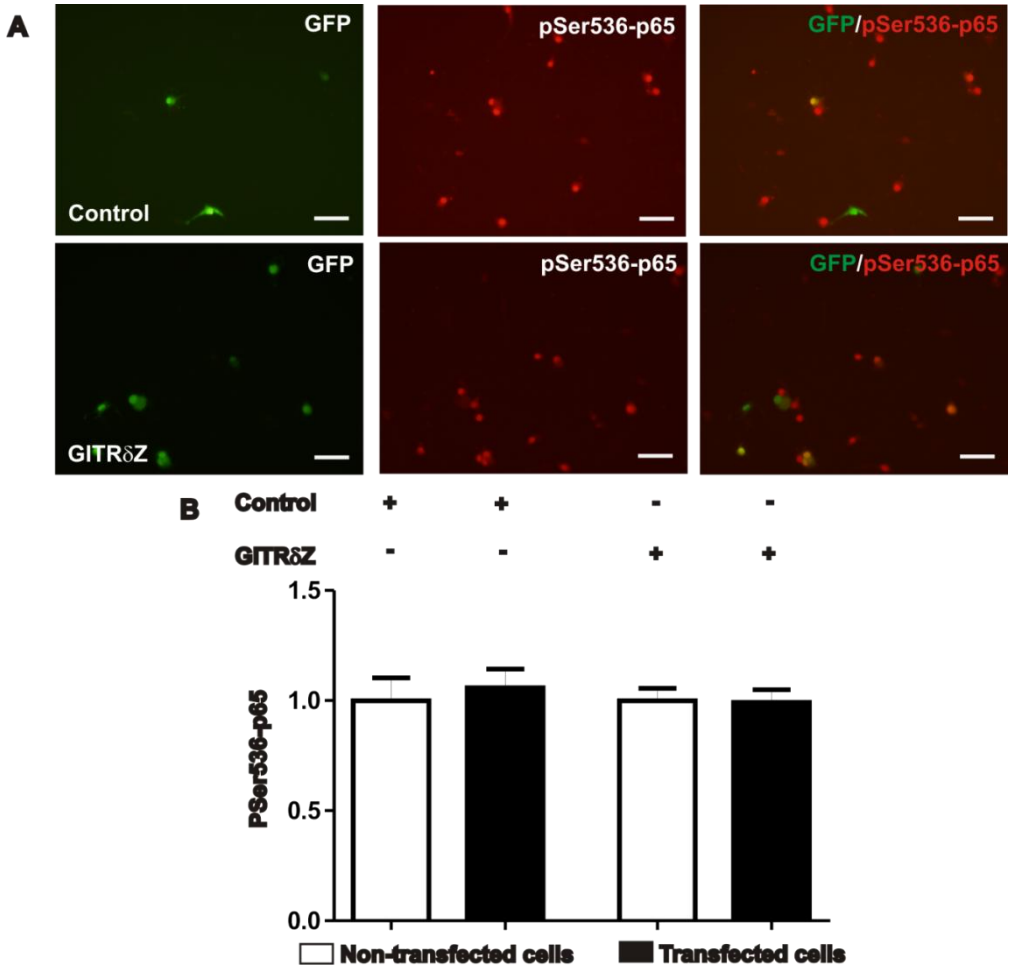


Figure 6.5: GITRL-GITR signalling does not regulate NF-κB in P1 mouse SCG neurons via the cytoplasmic region AEDACSFQFPEEERGEQTEEKCHLGGRWP of GITR. P1 SCG neurons were transfected with a GFP plasmid (to visualise transfected neurons) together with GITRδZ plasmid and grown overnight in 10ng/ml NGF at 37°C. Control cultures were also grown in which P1 SCG neurons were transfected with control or empty plasmid. The following day, cultures were fixed and immunocytochemically stained for pSer536-p65 (phospho-NF-κB) and analysis of mean nuclear fluorescence was performed. (A) Photomicrographs of control and GITRδZ-transfected dissociated cultures of P1 SCG neurons labelled for phospho-NF-κB (red). (B) Graphical representations of relevant differences in nuclear levels of phospho-NF-κB in GITRδZ-transfected, non-transfected and control-transfected P1 SCG neurons. Means ± standard errors of 40-90 neurons per condition are shown. Statistical comparisons compared with control: No significant differences were found using an unpaired student t-test. Scale bar = 50μm.

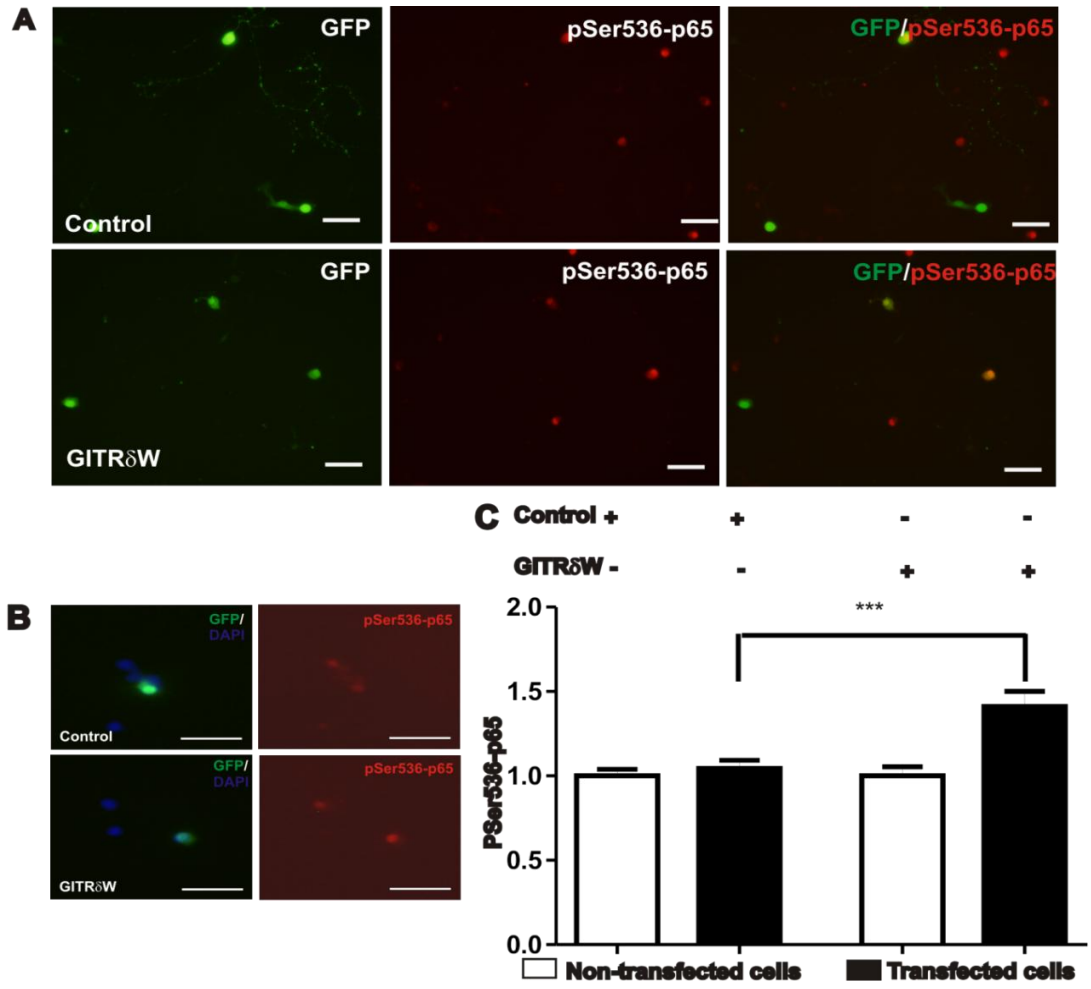


Figure 6.6: GITRL-GITR signalling regulates NF-κB in P1 mouse SCG neurons via the growth promoting domain of GITR. P1 SCG neurons were transfected with a GFP plasmid together with a control or GITRδW (in which the GPD of GITR, was missing) plasmid and grown overnight in 10ng/ml NGF at 37°C. The following day, cultures were fixed and immunocytochemically stained for pSer536-p65 (phospho-NF-κB) and analysis of mean nuclear fluorescence was performed. (A) Photomicrographs of control and GITRδW-transfected dissociated cultures of P1 SCG neurons labelled for phospho-NF-κB (red). (B) Photomicrographs of control and GITRδW-transfected dissociated cultures of P1 SCG neurons labelled for nuclear stain DAPI (purple) and phospho-NF-κB (red). (C) Graphical representations of relevant differences in nuclear levels of phospho-NF-κB in GITRδW-transfected, non-transfected and control-transfected P1 SCG neurons. Means ± standard errors of 40-90 neurons per condition are shown. Statistical comparisons compared with control: ***$P \leq 0.001$ using an unpaired student-test. Scale bar = 50μm.

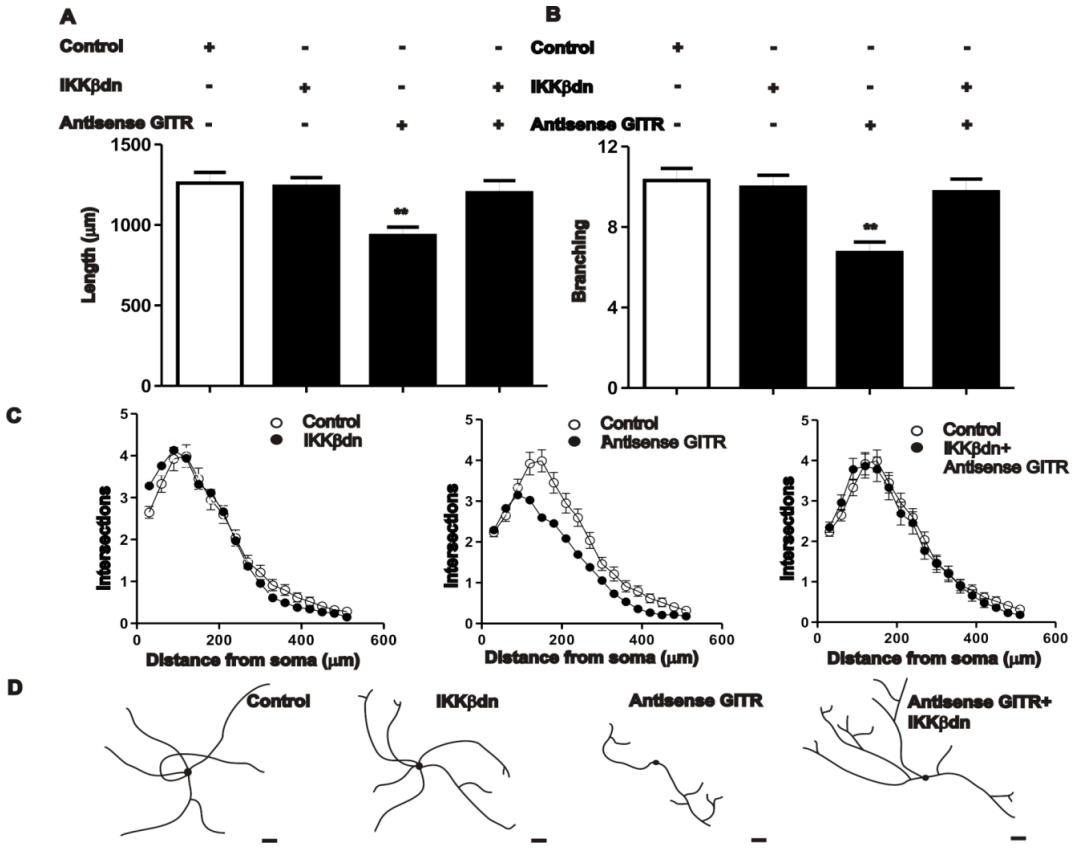


Figure 6.7: Dominant negative IKKβ (IKKβdn) prevents the growth inhibitory effects of antisense GITR on axonal growth. P1 SCG neurons were transfected with a GFP plasmid together with IKKβdn and/or antisense GITR (to inhibit GITRL-GITR signalling and growth promotion in P1 SCG neurons) and grown overnight in 10ng/ml NGF at 37°C. Control cultures were also grown in which P1 SCG neurons were transfected with control plasmid. Axonal growth was analysed using Sholl analysis. (A, B) Graphical representations of, (A) total neurite length and (B) total neurite branching in P1 SCG neurons transfected with either IKKβdn or antisense GITR or a combination of both and grown overnight in 10ng/ml NGF. (C) Sholl profiles of neurons transfected with either IKKβdn or antisense GITR or a combination of both and grown overnight in 10ng/ml NGF. (E) Representative line drawings of P1 SCG neurons transfected with IKKβdn, antisense GITR and both and grown overnight in 10ng/ml NGF. Means ± standard errors of >150 neurons per condition are shown. Statistical comparisons compared with control: $^{**}P \leq 0.01$ using one way ANOVA and post hoc Tukey's test. Scale bar = 50μm.

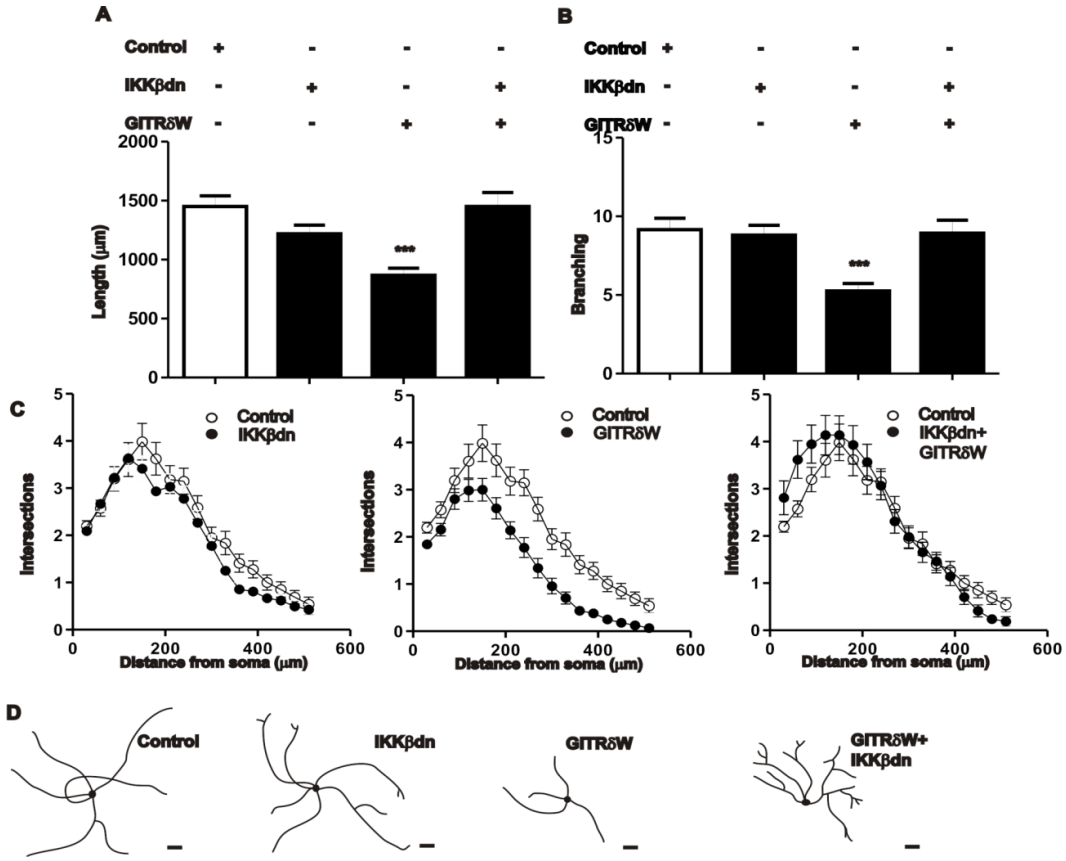


Figure 6.8: IKKβdn prevents the growth inhibitory effects of GITRδW on axonal growth in P1 mouse SCG neurons. P1 SCG neurons were transfected with a GFP plasmid together with either IKKβdn or GITRδW (lacking the GPD) and grown overnight in 10ng/ml NGF at 37°C. Control cultures were also grown in which P1 SCG neurons were transfected with control or empty plasmid. Axonal growth was analysed using Sholl analysis. (A, B) Graphical representations of, (A) total neurite length and (B) total neurite branching in P1 SCG neurons transfected with IKKβdn, GITRδW and both and grown overnight in 10ng/ml NGF. (C) Sholl profiles of neurons transfected with either IKKβdn or GITRδW or a combination of both and grown overnight in 10ng/ml NGF. (E) Representative line drawings of P1 SCG neurons transfected with either IKKβdn or GITRδW or a combination of both and grown overnight in 10ng/ml NGF. Means ± standard errors of >150 neurons per condition are shown. Statistical comparisons compared with control: *** $P \leq 0.001$ using one way ANOVA and post hoc Tukey's test. Scale bar = 50μm.

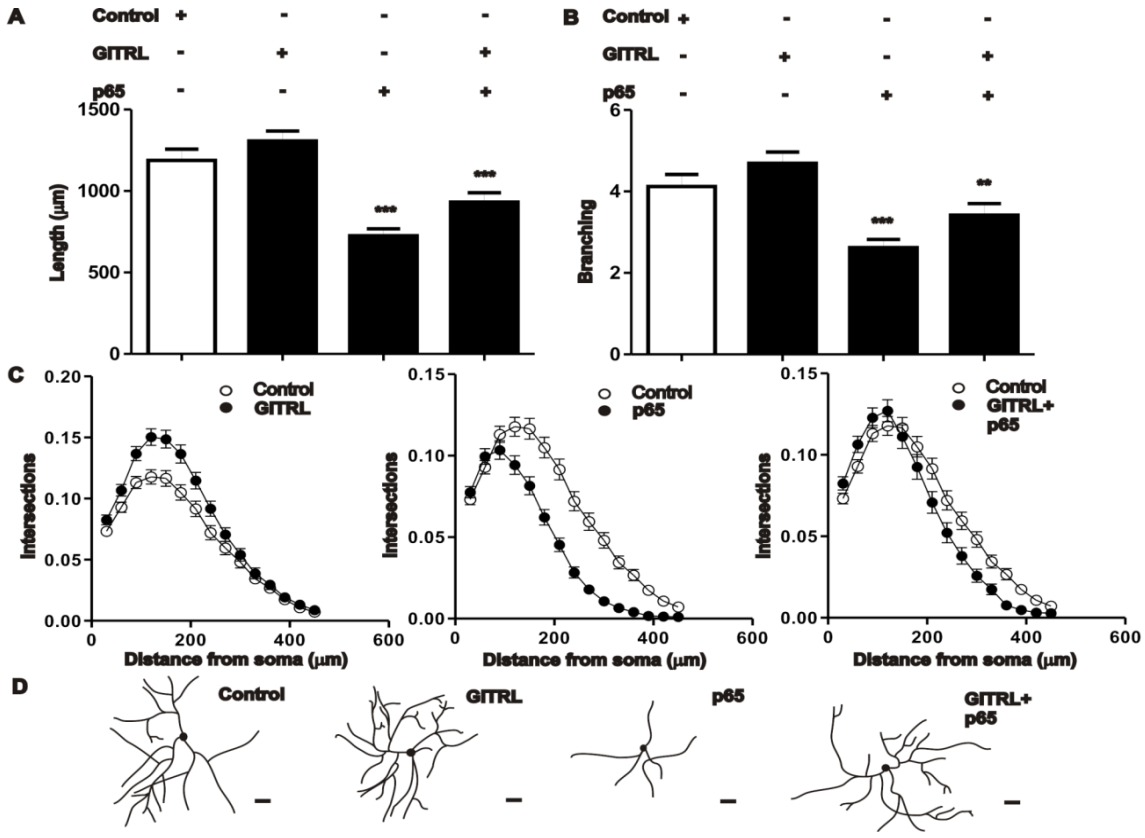
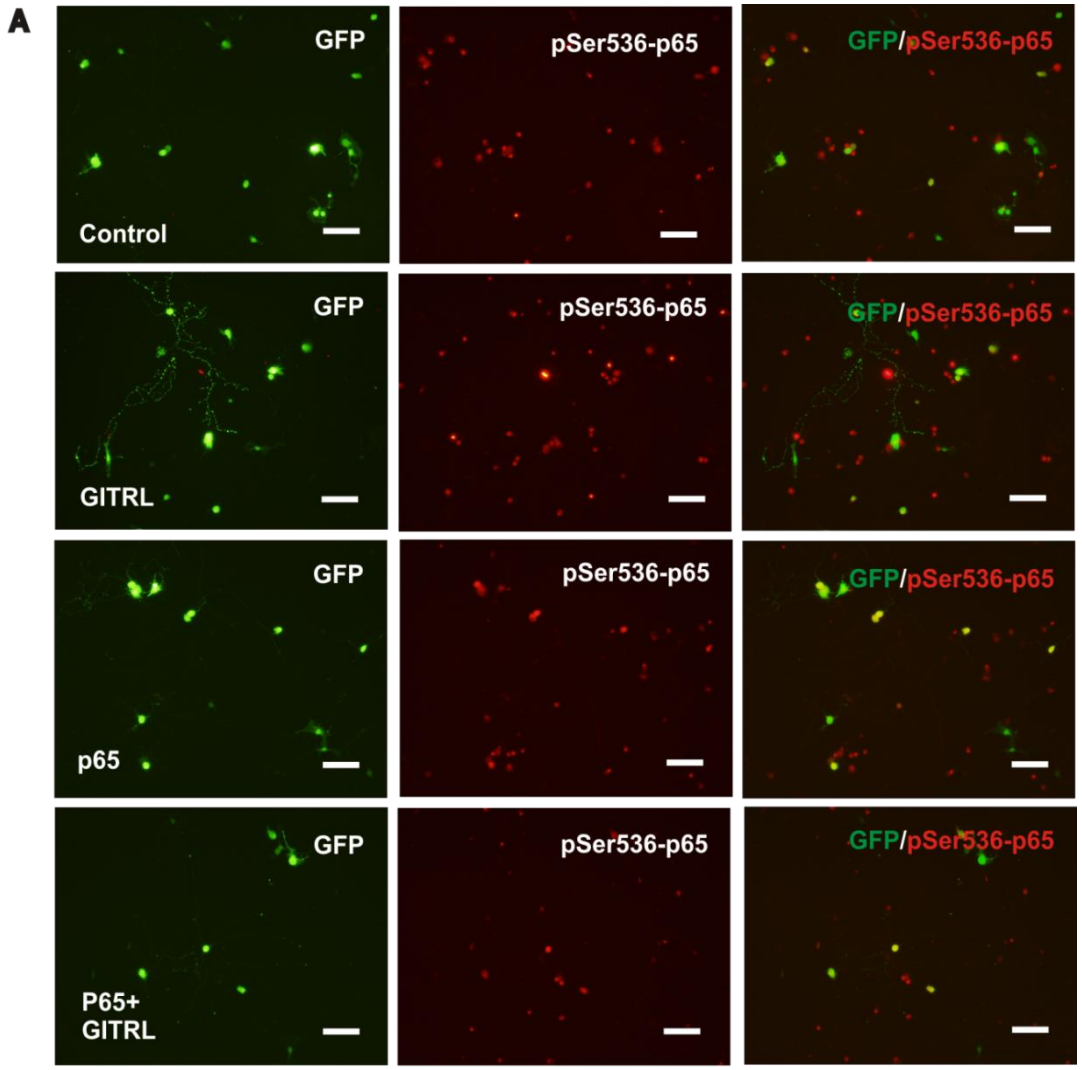


Figure 6.9: P1 mouse SCG neurons expressing GITRL and p65 demonstrate greater growth compared to those expressing p65 alone and demonstrate reduced growth than those expressing GITRL alone. P1 SCG neurons were transfected with a GFP plasmid (to visualise transfected neurites) together with either GITRL overexpression plasmid or p65 overexpression plasmid or combination of both and grown overnight in 10ng/ml NGF at 37°C. Control cultures were also grown in which P1 SCG neurons were transfected with control or empty plasmid. Axonal growth was analysed using Sholl analysis. (A, B) Graphical representations of, (A) total neurite length and (B) total neurite branching in P1 SCG neurons transfected with either GITRL or p65 or a combination of both and grown overnight in 10ng/ml NGF. (C) Sholl profiles of neurons transfected with either GITRL or p65 or a combination of both and grown overnight in 10ng/ml NGF. (D) Representative line drawings of P1 SCG neurons transfected with GITRL, p65 and both and grown overnight in 10ng/ml NGF. Means ± standard errors of >150 neurons per condition are shown. Statistical comparisons: Statistical comparisons compared with control: *** $P \leq 0.001$; ** $P \leq 0.01$ using one way ANOVA and post hoc Tukey's test. Scale bar = 50μm.


A
GFP
pSer536-p65
GFP/pSer536-p65
Control
GITRL
p65
P65+
GITRL

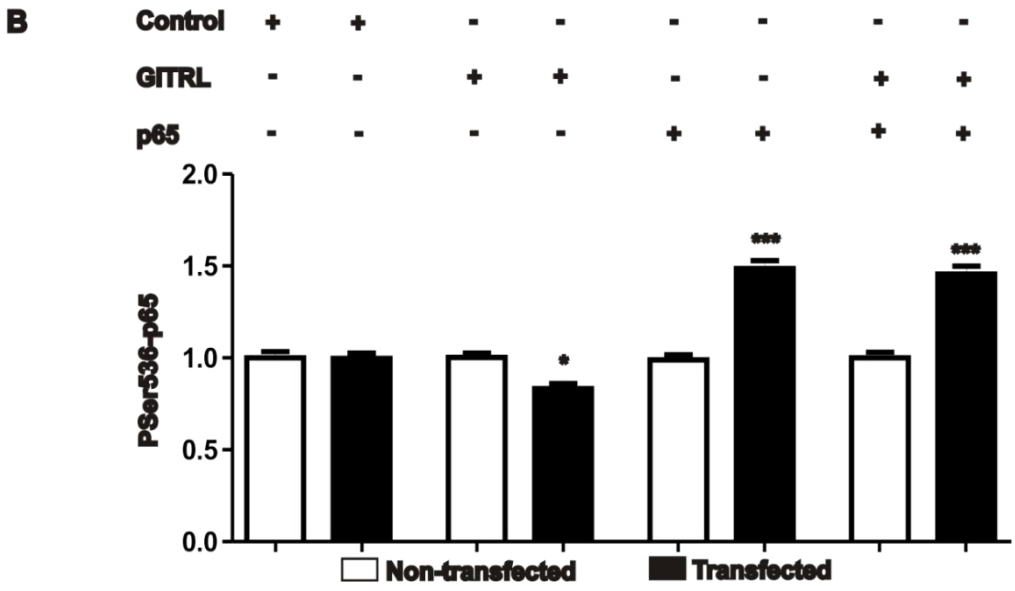

B
Control
GITRL
p65
PSer536-p65
2.0
1.5
1.0
0.5
0.0
***
*
Non-transfected
Transfected

Figure 6.10: P1 mouse SCG neurons expressing GITRL and p65 display the same level of NF-κB activity as those expressing p65 alone. P1 SCG neurons were transfected with a GFP plasmid together with either a control, GITRL and/or p65 expression plasmids and grown overnight in 10ng/ml NGF at 37°C. The following day, cultures were fixed and immunocytochemically stained for pSer536-p65 (phospho-NF-κB) and analysis of mean nuclear fluorescence was performed. (A) Photomicrographs of control GITRL, p65 and a combination of both GITRL and p65 transfected dissociated cultures of P1 SCG neurons labelled for phospho-NF-κB (red). (B) Graphical representations of relevant differences in nuclear levels of phospho-NF-κB in control, GITRL, p65 and a combination of both GITRL and p65 transfected and non-transfected P1 SCG neurons. Means ± standard errors of >150 neurons per condition are shown. Statistical comparisons compared with control: *** $P \leq 0.001$ using one way ANOVA and post hoc Tukey's test. Scale bar = 50μm.

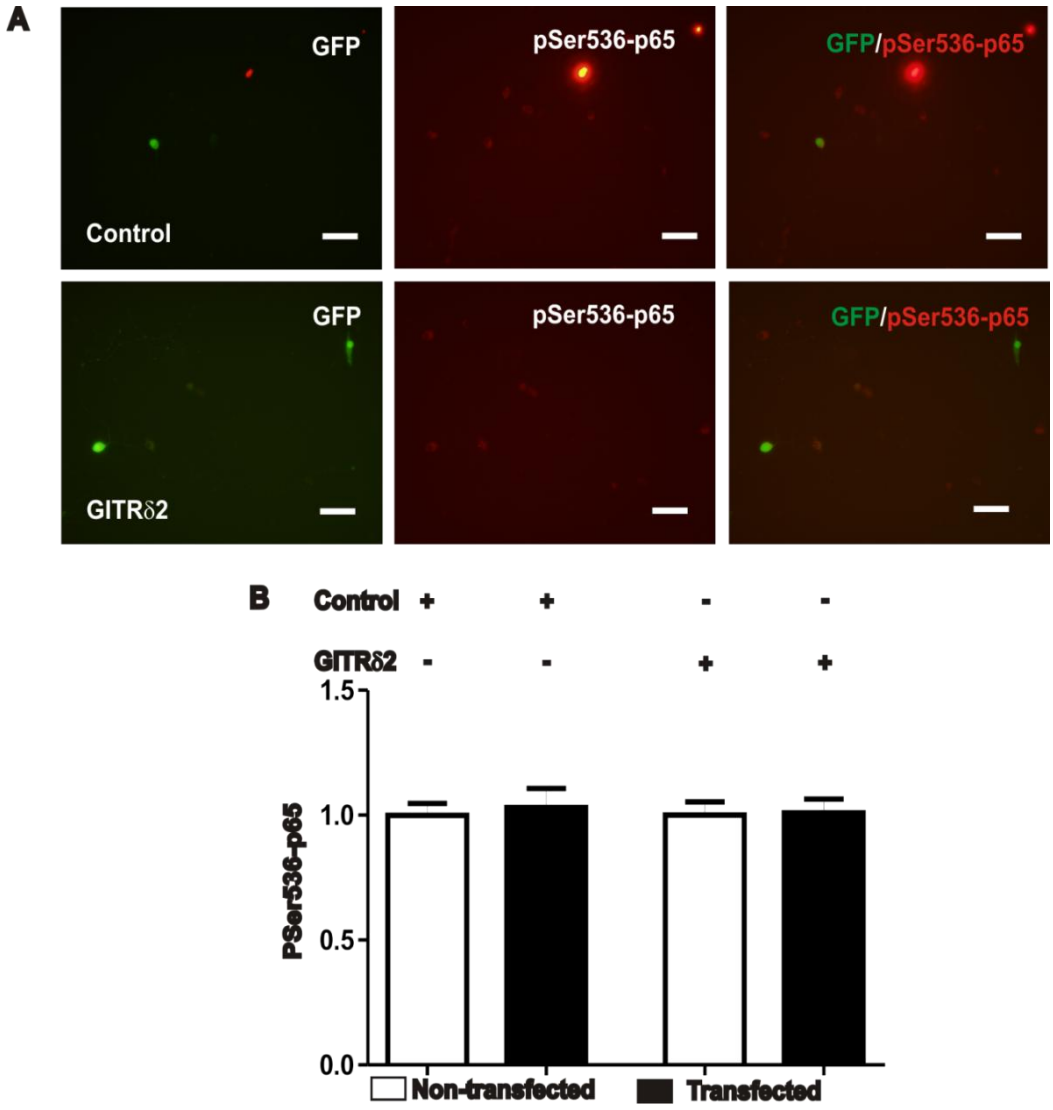


Figure 6.11: NF-κB activity is not affected by the inhibition of phosphorylation at CPRE (amino acids 8 to 11 sites of the GPD) of GITR. P1 SCG neurons were transfected with a GFP plasmid (to visualise transfected neurites) together with GITRδ2 (mutant in which Cys186-Glu189, CPRE (amino acids 8 to 11 of the GPD) were replaced with alanines) and grown overnight in 10ng/ml NGF at 37°C. Control cultures were also grown in which P1 SCG neurons were transfected with control or empty plasmid. The following day, cultures were fixed and immunocytochemically stained for pSer536-p65 (phospho-NF-κB) and analysis of mean nuclear fluorescence was performed. (A) Photomicrographs of control and GITRδ2-transfected dissociated cultures of P1 SCG neurons labelled for phospho-NF-κB (red). (B) Graphical representations of relevant differences in nuclear levels of phospho-NF-κB in control and GITRδ2-transfected and non-transfected P1 SCG neurons. Means ± standard errors of >150 neurons per condition are shown. Statistical comparisons compared with control: No significant differences were found using an unpaired student t-test. Scale bar = 50μm.

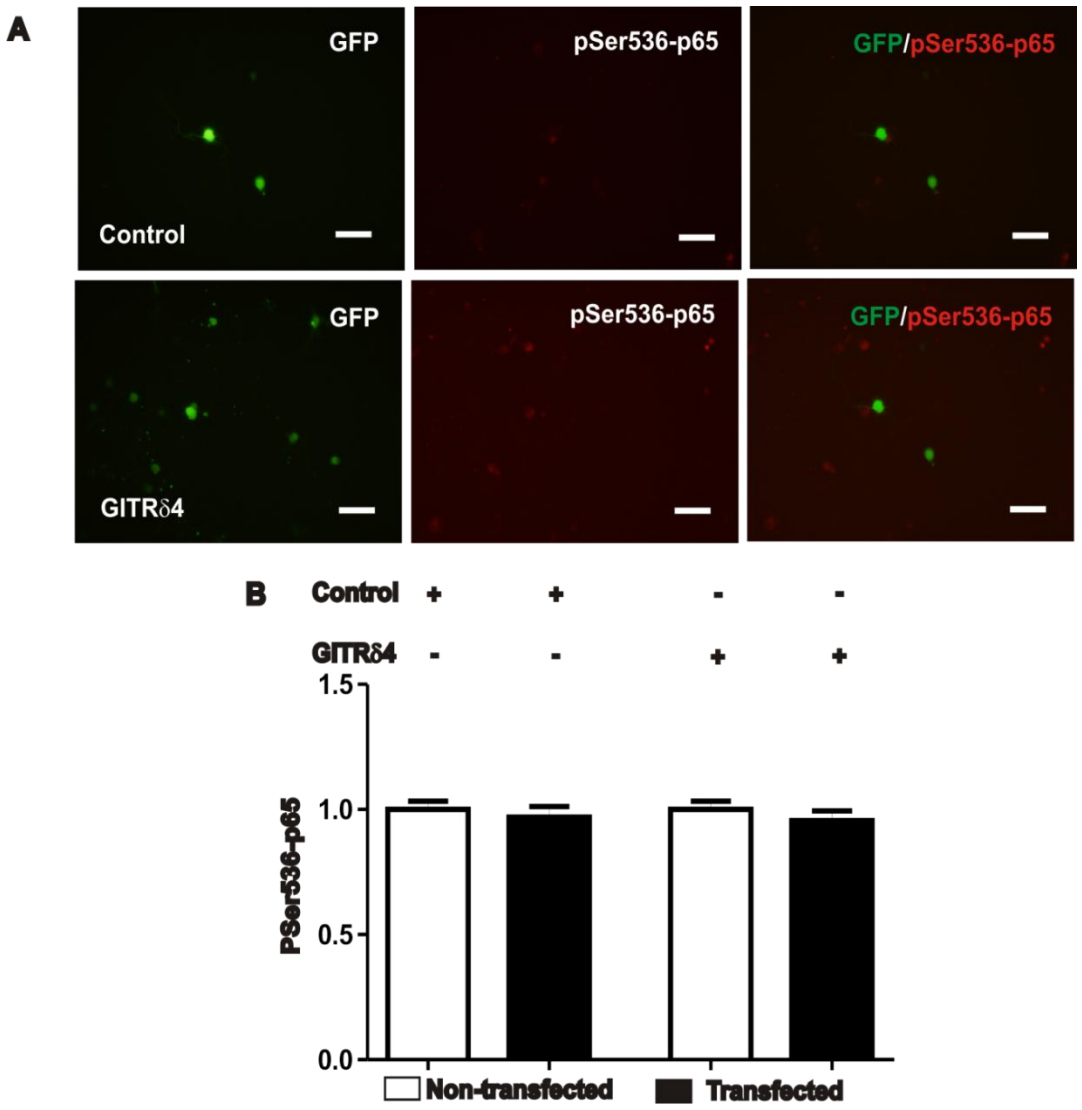


Figure 6.12: NF-κB activity is not affected by the inhibition of phosphorylation at Thr190 and Ser199 (amino acids 12 and 21 sites of the GPD) of GITR. P1 SCG neurons were transfected with a GFP plasmid (to visualise transfected neurites) together with GITRδ4 (mutant in which Thr190 and Ser199, (amino acid 12 and 21 of the GPD) were replaced with alanines) and grown overnight in 10ng/ml NGF at 37°C. Control cultures were also grown in which P1 SCG neurons were transfected with control or empty plasmid. The following day, cultures were fixed and immunocytochemically stained for pSer536-p65 (phospho-NF-κB) and analysis of mean nuclear fluorescence was performed. (A) Photomicrographs of control and GITRδ4-transfected dissociated cultures of P1 SCG neurons labelled for phospho-NF-κB (red). (B) Graphical representations of relevant differences in nuclear levels of phospho-NF-κB in control and GITRδ4-transfected and non-transfected P1 SCG neurons. Means ± standard errors of >150 neurons per condition are shown. Statistical comparisons compared with control: No significant differences were found using an unpaired student t-test. Scale bar = 50μm.

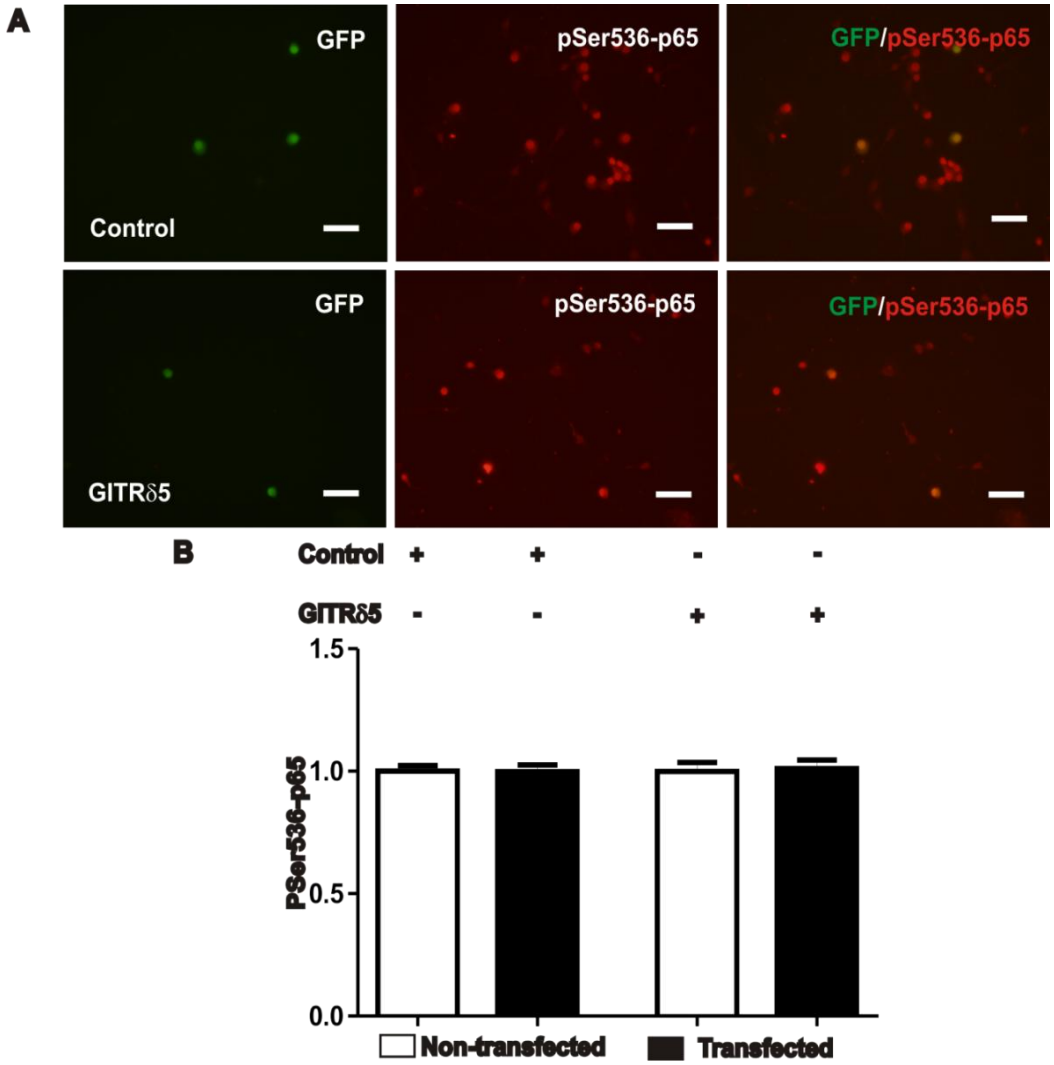


Figure 6.13: NF-κB activity is not affected by the phosphorylation of residues at Thr190 and Ser199 (amino acids 12 and 21 sites of the GPD) of GITR. P1 SCG neurons were transfected with a GFP plasmid (to visualise transfected neurites) together with GITRδ5 (mutant in which Thr190 and Ser199, (amino acid 12 and 21 of the GPD) were replaced with glutamic acid) and grown overnight in 10ng/ml NGF at 37°C. Control cultures were also grown in which P1 SCG neurons were transfected with control or empty plasmid. The following day, cultures were fixed and immunocytochemically stained for pSer536-p65 (phospho-NF-κB) and analysis of mean nuclear fluorescence was performed. (A) Photomicrographs of control and GITRδ5-transfected dissociated cultures of P1 SCG neurons labelled for phospho-NF-κB (red). (B) Graphical representations of relevant differences in nuclear levels of phospho-NF-κB in control and GITRδ5-transfected and non-transfected P1 SCG neurons. Means ± standard errors of >150 neurons per condition are shown. Statistical comparisons compared with control: No significant differences were found using an unpaired student t-test. Scale bar = 50µm.

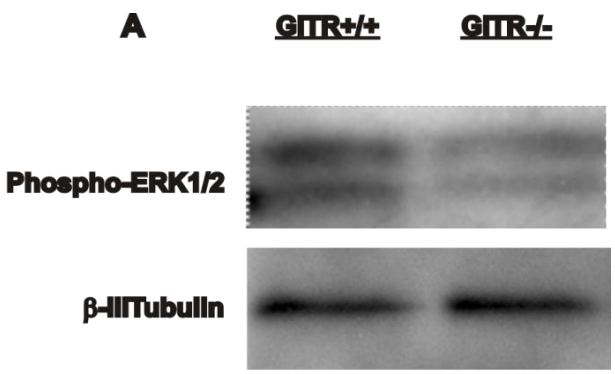


Figure 6.14: GITRL-GITR signalling regulates ERK1/2 activity in P1 mouse SCG neurons. (A) Representative Western blots showing levels of phospho-ERK1/2 and β-III Tubulin in protein extracts of GITR+/+ and GITR-/- P1 mouse SCG neurons grown for 18h in 10ng/ml NGF.

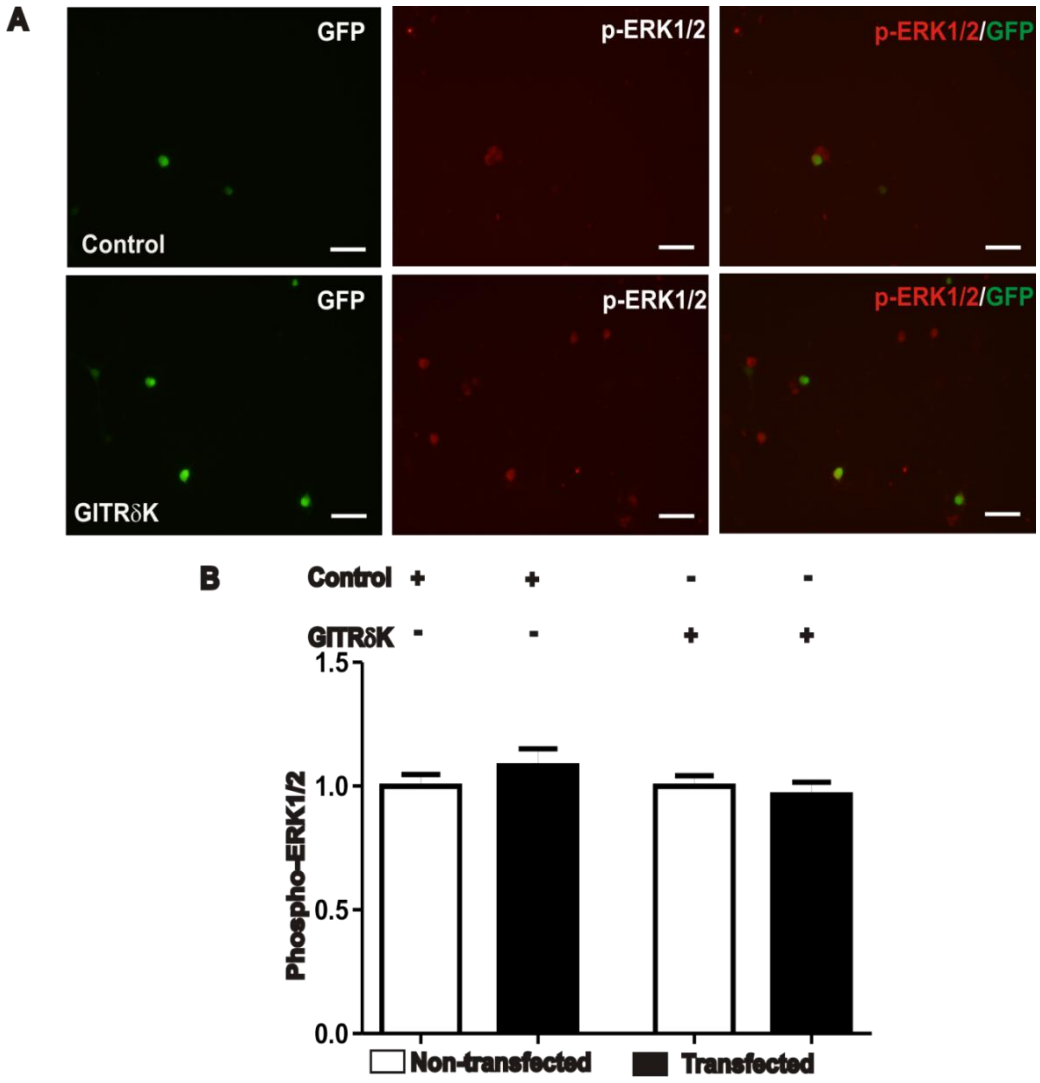


Figure 6.15: GITRL-GITR signalling does not regulate ERK1/2 phosphorylation in P1 mouse SCG neurons via the cytoplasmic region EQTEEKCHLGGRWP of GITR. P1 SCG neurons were transfected with a GFP plasmid (to visualise transfected neurites) together with GITRδK (in which the portion of the cytoplasmic region of GITR, EQTEEKCHLGGRWP, was missing) and grown overnight in 10ng/ml NGF at 37°C. Control cultures were also grown in which P1 SCG neurons were transfected with control or empty plasmid. The following day, cultures were fixed and immunocytochemically stained for phospho-ERK1/2 and analysis of mean fluorescence was performed. (A) Photomicrographs of control and GITRδK-transfected dissociated cultures of P1 SCG neurons labelled for phospho-ERK1/2 (red). (B) Graphical representations of relevant differences in levels of phospho-ERK1/2 in control and GITRδK-transfected and non-transfected P1 SCG neurons. Means ± standard errors of >150 neurons per condition are shown. Statistical comparisons compared with control: No significant differences were found using an unpaired student t-test. Scale bar = 50µm.

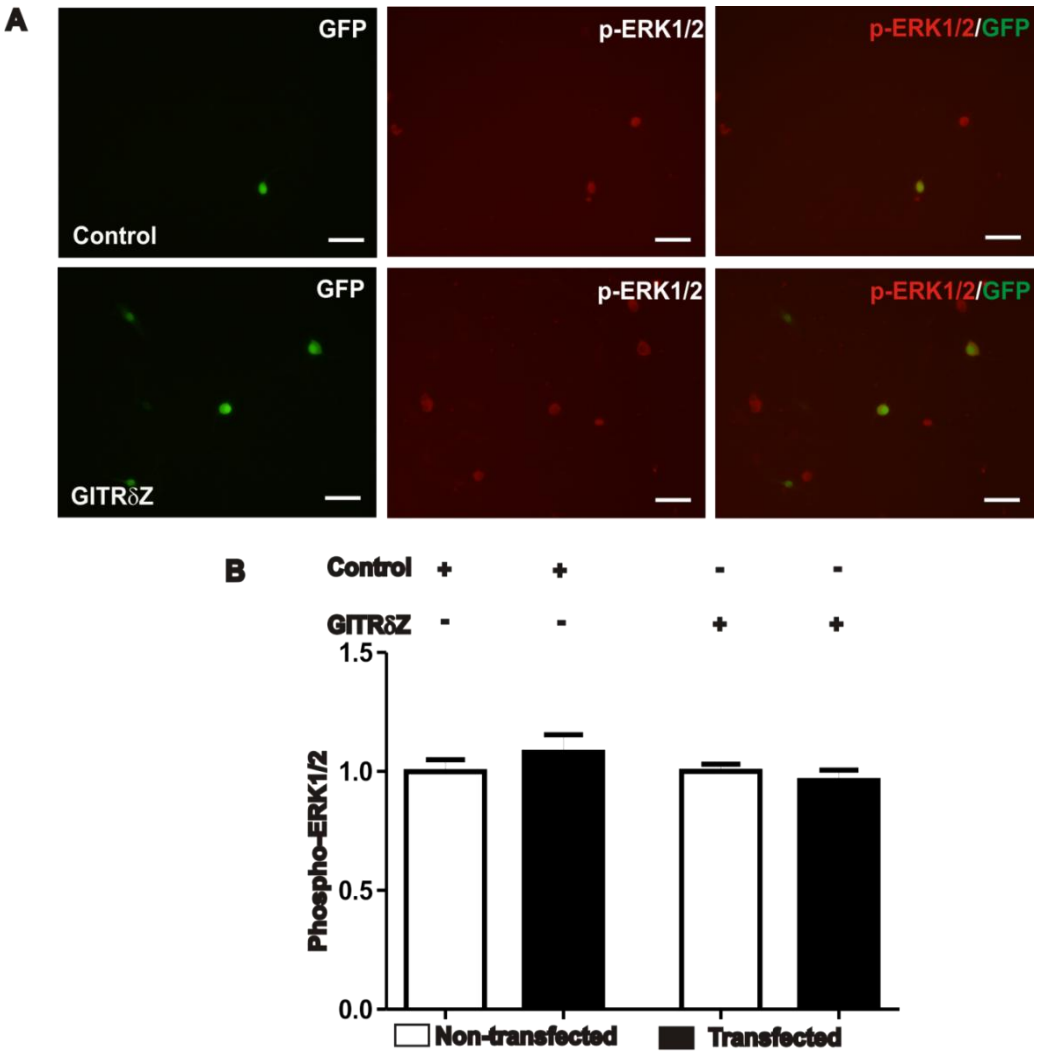


Figure 6.16: GITRL-GITR signalling does not regulate ERK1/2 phosphorylation in P1 mouse SCG neurons via the cytoplasmic region AEDACSFQFPEEERGEQTEEKCHLGGRWP of GITR. P1 SCG neurons were transfected with a GFP plasmid (to visualise transfected neurites) together with GITRδZ (in which the portion of the cytoplasmic region of GITR, AEDACSFQFPEEERGEQTEEKCHLGGRWP, was missing) and grown overnight in 10ng/ml NGF at 37°C. Control cultures were also grown in which P1 SCG neurons were transfected with control or empty plasmid. The following day, cultures were fixed and immunocytochemically stained for phospho-ERK1/2 and analysis of mean fluorescence was performed (A) Photomicrographs of control and GITRδZ-transfected dissociated cultures of P1 SCG neurons labelled for phospho-ERK1/2 (red). (B) Graphical representations of relevant differences in levels of phospho-ERK1/2 in control and GITRδZ-transfected and non-transfected P1 SCG neurons. Means ± standard errors of >150 neurons per condition are shown. Statistical comparisons compared with control: No significant differences were found using an unpaired student t-test. Scale bar = 50µm.

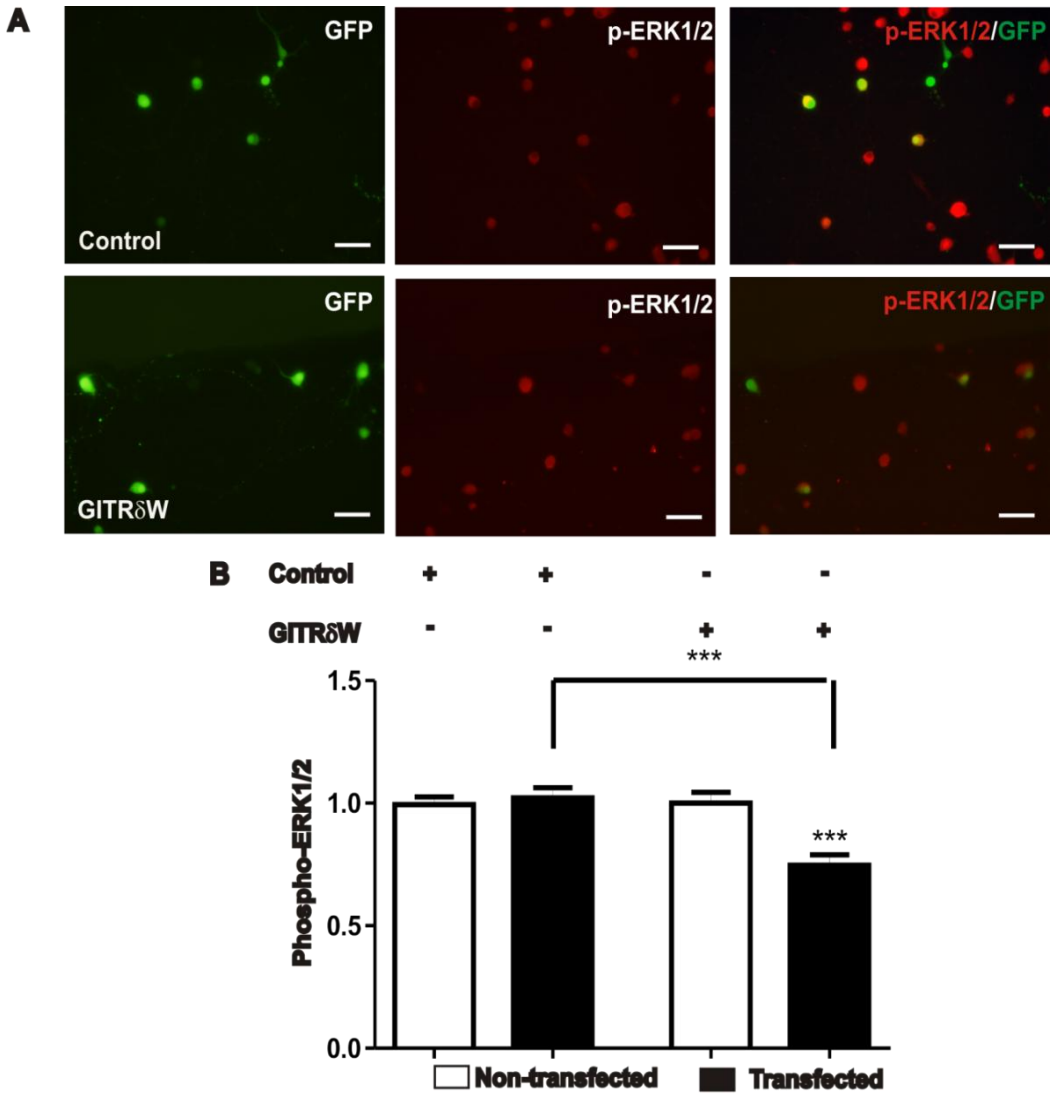


Figure 6.17: GITRL-GITR signalling regulates ERK1/2 phosphorylation in P1 mouse SCG neurons via the growth promoting domain of GITR. P1 SCG neurons were transfected with a GFP plasmid (to visualise transfected neurites) together with GITRδW (in which the GPD of GITR, was missing) and grown overnight in 10ng/ml NGF at 37°C. Control cultures were also grown in which P1 SCG neurons were transfected with control or empty plasmid. The following day, cultures were fixed and immunocytochemically stained for phospho-ERK1/2 and analysis of mean fluorescence was performed. (A) Photomicrographs of control and GITRδW-transfected dissociated cultures of P1 SCG neurons labelled for phospho-ERK1/2 (red). (B) Graphical representations of relevant differences in levels of phospho-ERK1/2 in control and GITRδW-transfected and non-transfected P1 SCG neurons. Means ± standard errors of >150 neurons per condition are shown. Statistical comparisons compared with control: ***$P \leq 0.001$ using an unpaired student t-test. Scale bar = 50µm.

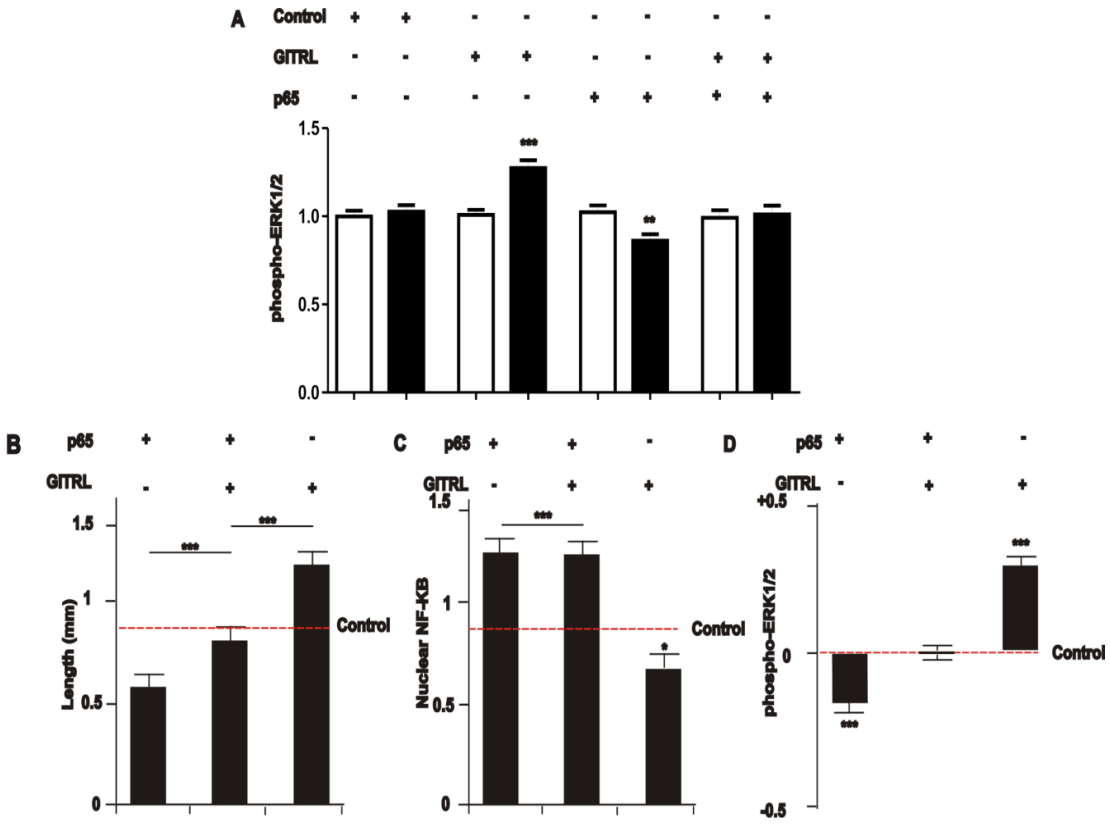


Figure 6.18: GITRL-GITR signalling regulates ERK1/2 phosphorylation in P1 mouse SCG neurons via the growth promoting domain of GITR. P1 SCG neurons were transfected with a GFP plasmid (to visualise transfected neurites) together with GITRδW (in which the GPD of GITR, was missing) and grown overnight in 10ng/ml NGF at 37°C. Control cultures were also grown in which P1 SCG neurons were transfected with control or empty plasmid. The following day, cultures were fixed and immunocytochemically stained for phospho-ERK1/2 and analysis of mean fluorescence was performed. (A) Photomicrographs of control and GITRδW-transfected dissociated cultures of P1 SCG neurons labelled for phospho-ERK1/2 (red). (B) Graphical representations of relevant differences in levels of phospho-ERK1/2 in control and GITRδW-transfected and non-transfected P1 SCG neurons. Means ± standard errors of >150 neurons per condition are shown. Statistical comparisons compared with control: ***$P \leq 0.001$ using an unpaired student t-test. Scale bar = 50µm.

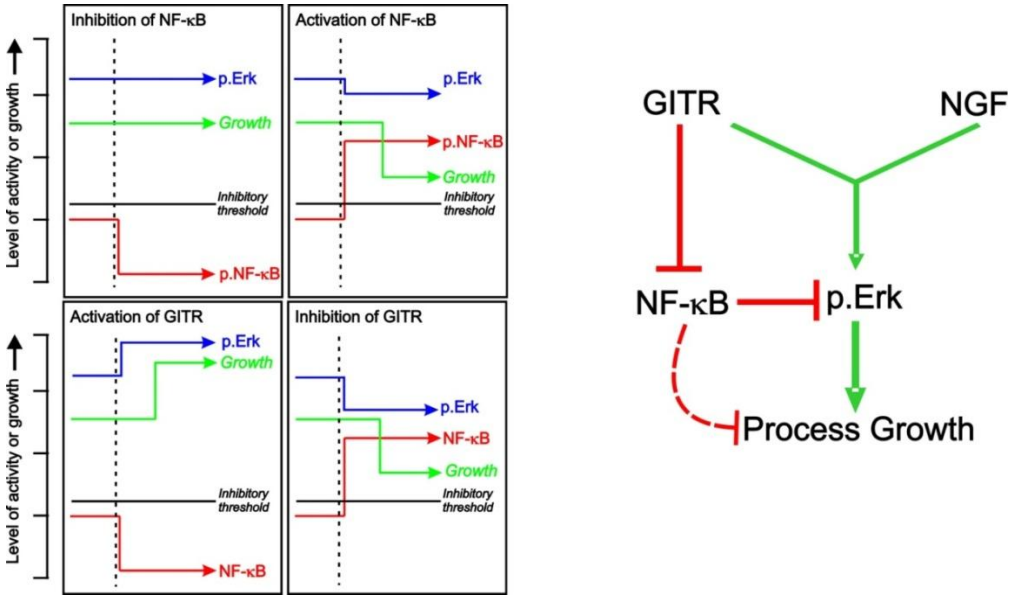


Figure 6.19: Schematic model showing proposed mechanism underlying the role of GITR in the promotion of axonal growth. In P1 mouse SCG neurons receiving an adequate supply of NGF, ERK1/2 signalling is enhanced and NF-κB signalling is inhibited, thus potentially providing an optimal cellular environment for axonal growth.

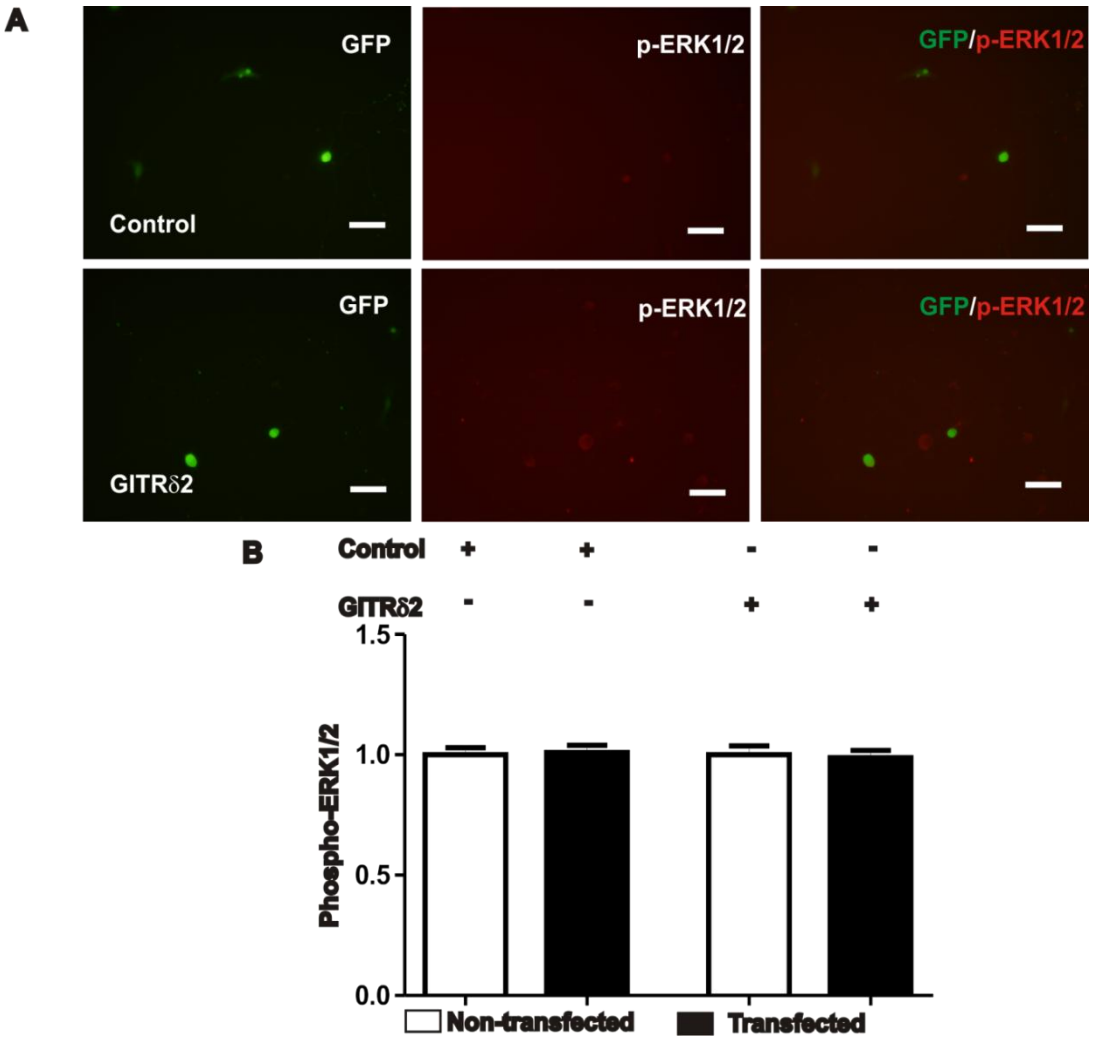


Figure 6.20: Phospho-ERK1/2 levels in P1 mouse SCG neurons are not affected by the inhibition of phosphorylation at CPRE (amino acids 8 to 11 sites of the GPD) of GITR. P1 SCG neurons were transfected with a GFP plasmid (to visualise transfected neurites) together with GITRδ2 (mutant in which Cys186-Glu189, CPRE (amino acids 8 to 11 of the GPD) were replaced with alanines) and grown overnight in 10ng/ml NGF at 37°C. Control cultures were also grown in which P1 SCG neurons were transfected with control or empty plasmid. The following day, cultures were fixed and immunocytochemically stained for phospho-ERK1/2 and analysis of mean fluorescence was performed. (A) Photomicrographs of control and GITRδ2-transfected dissociated cultures of P1 SCG neurons labelled for phospho-ERK1/2 (red). (B) Graphical representations of relevant differences in levels of phospho-ERK1/2 in control and GITRδ2-transfected and non-transfected P1 SCG neurons. Means ± standard errors of >150 neurons per condition are shown. Statistical comparisons compared with control: No significant differences were found using an unpaired student t-test. Scale bar = 50µm.

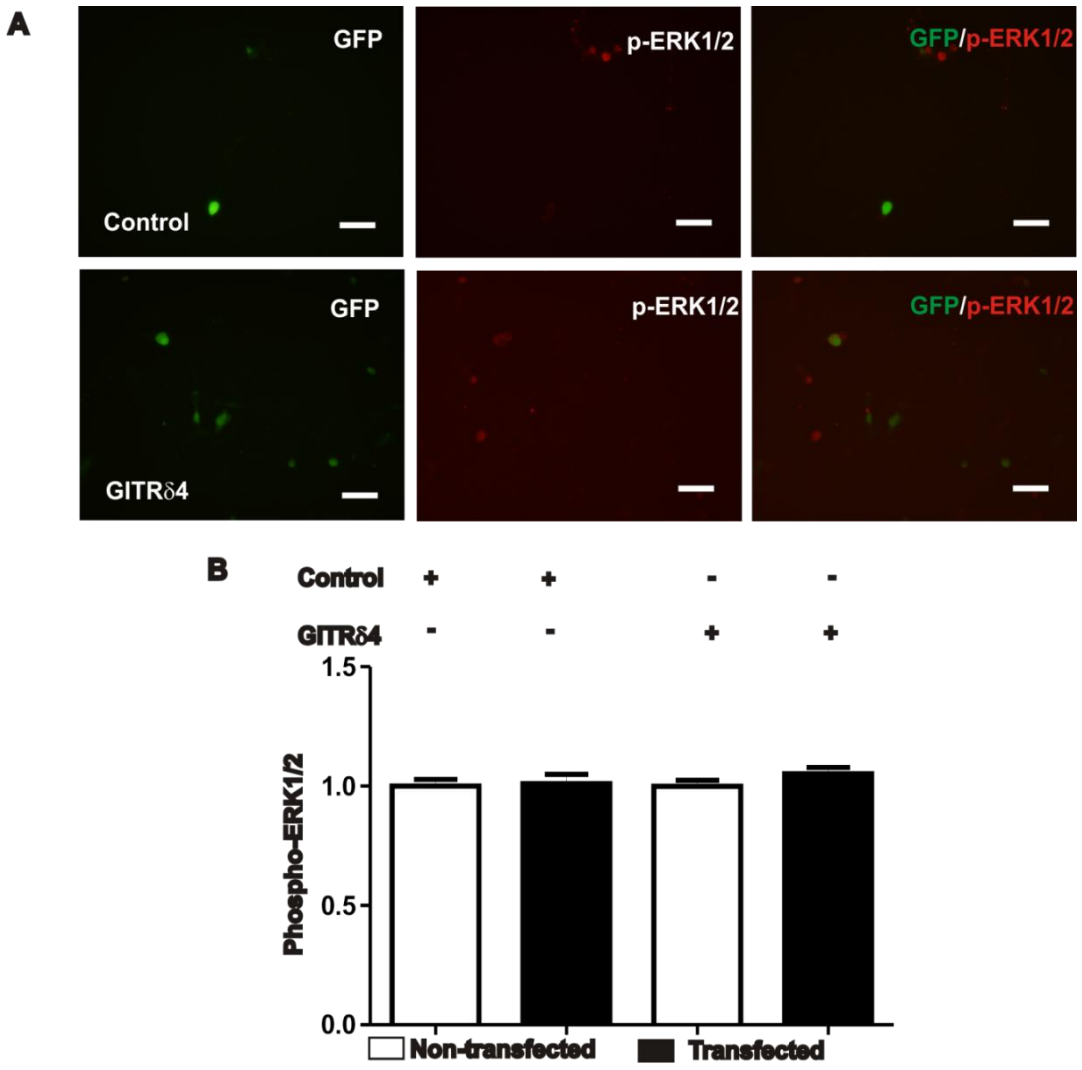


Figure 6.21: Phospho-ERK1/2 levels in P1 mouse SCG neurons is not affected by the inhibition of phosphorylation at Thr190 and Ser199 (amino acids 12 and 21 sites of the GPD) of GITR. P1 SCG neurons were transfected with a GFP plasmid (to visualise transfected neurites) together with GITRδ4 (mutant in which Thr190 and Ser199, (amino acid 12 and 21 of the GPD) were replaced with alanines) and grown overnight in 10ng/ml NGF at 37°C. Control cultures were also grown in which P1 SCG neurons were transfected with control or empty plasmid. The following day, cultures were fixed and immunocytochemically stained for phospho-ERK1/2 and analysis of mean fluorescence was performed. Control cultures were also grown in which P1 SCG neurons were transfected with control or empty plasmid. (A) Photomicrographs of control and GITRδ4-transfected dissociated cultures of P1 SCG neurons labelled for phospho-ERK1/2 (red). (B) Graphical representations of relevant differences in levels of phospho-ERK1/2 in control and GITRδ4-transfected and non-transfected P1 SCG neurons. Means ± standard errors of >150 neurons per condition are shown. Statistical comparisons compared with control: No significant differences were found using an unpaired student t-test. Scale bar = 50µm.

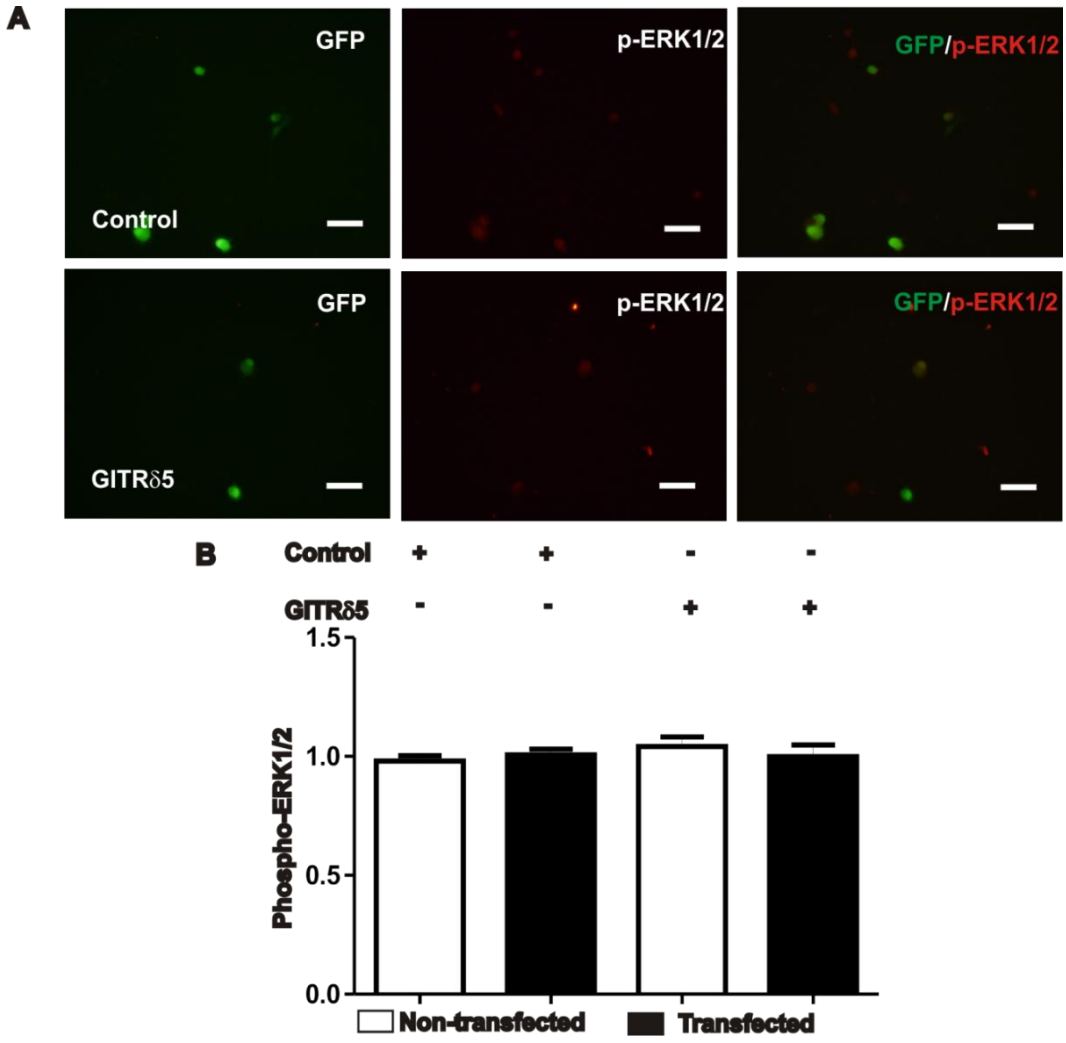


Figure 6.22: Phospho-ERK1/2 levels in P1 mouse SCG neurons is not affected by the phosphorylation of residues at Thr190 and Ser199 (amino acids 12 and 21 sites of the GPD) of GITR. P1 SCG neurons were transfected with a GFP plasmid (to visualise transfected neurites) together with GITRδ5 (mutant in which Thr190 and Ser199, (amino acid 12 and 21 of the GPD) were replaced with glutamic acid) and grown overnight in 10ng/ml NGF at 37°C. Control cultures were also grown in which P1 SCG neurons were transfected with control or empty plasmid. The following day, cultures were fixed and immunocytochemically stained for phospho-ERK1/2 and analysis of mean fluorescence was performed. (A) Photomicrographs of control and GITRδ5-transfected dissociated cultures of P1 SCG neurons labelled for phospho-ERK1/2 (red). (B) Graphical representations of relevant differences in levels of phospho-ERK1/2 in control and GITRδ5-transfected and non-transfected P1 SCG neurons. Means ± standard errors of >150 neurons per condition are shown. Statistical comparisons compared with control: No significant differences were found using an unpaired student t-test. Scale bar=50µm.

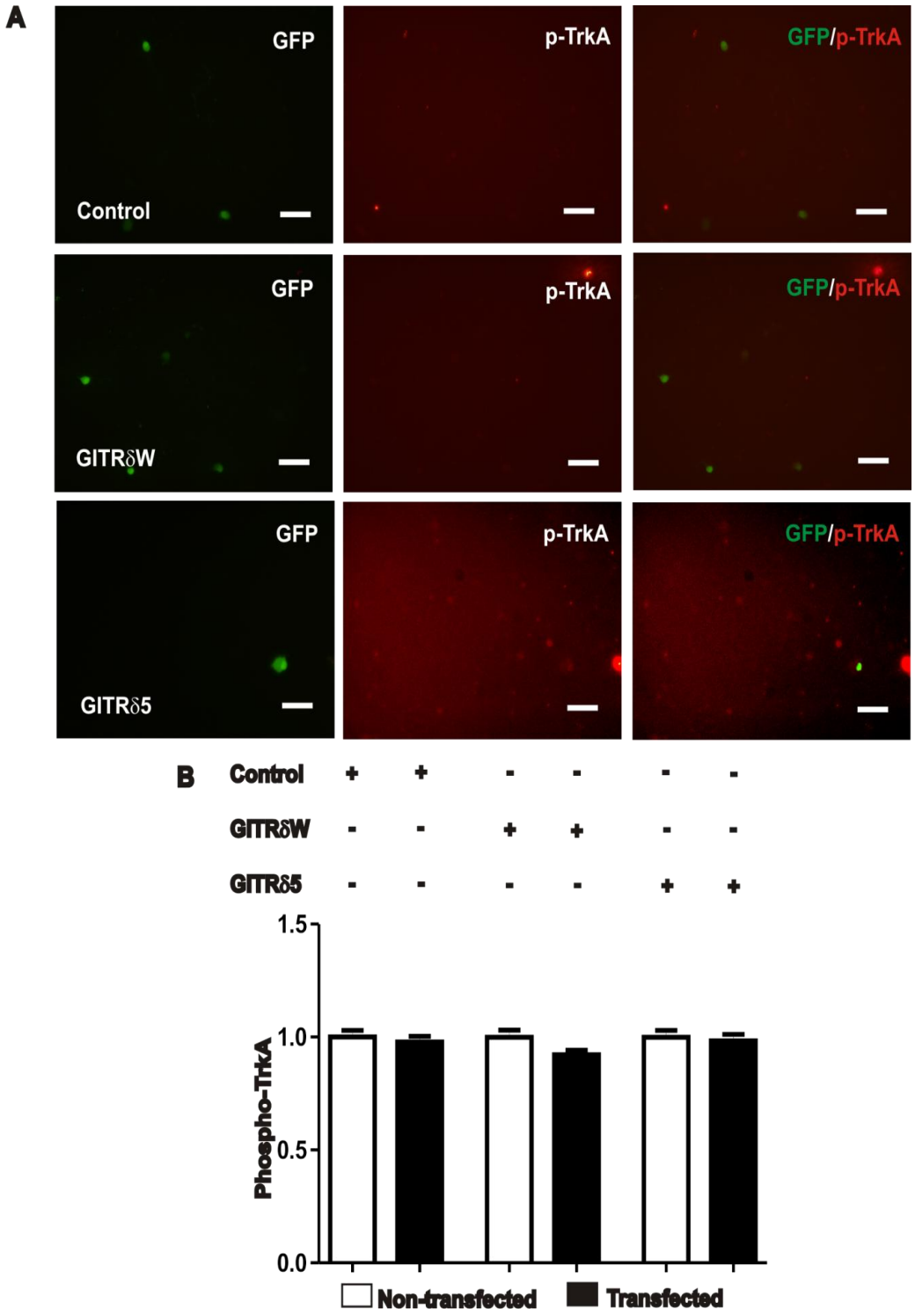

A
GFP
p-TrkA
GFP/p-TrkA
Control
GFP
p-TrkA
GFP/p-TrkA
GITRδW
GFP
p-TrkA
GFP/p-TrkA
GITRδ5
B
Control + + - - - -
GITRδW - - + + - -
GITRδ5 - - - - + +
Phospho-TrkA
1.5
1.0
0.5
0.0
Non-transfected
Transfected

Figure 6.23: The levels of phospho-TrkA in P1 mouse SCG neurons are not affected by the constitutive phosphorylation of residues Thr190 and Ser199 (amino acids 12 and 21 sites of the GPD) of GITR. P1 SCG neurons were transfected with a GFP plasmid together with GITRδW or GITRδ5 (mutant in which Thr190 and Ser199, (amino acid 12 and 21 of the GPD) were replaced with glutamic acid) and grown overnight in 10ng/ml NGF at 37°C. Control cultures were also grown in which P1 SCG neurons were transfected with control or empty plasmid. The following day, cultures were fixed and immunocytochemically stained for phospho-TrkA and analysis of mean fluorescence was performed. (A) Photomicrographs of control, GITRδW and GITRδ5-transfected dissociated cultures of P1 SCG neurons labelled for phospho-TrkA (red). (B) Graphical representations of relevant differences in levels of phospho-TrkA in control, GITRδW and GITRδ5-transfected and non-transfected P1 SCG neurons. Means ± standard errors of >150 neurons per condition are shown. Statistical comparisons compared with control: No significant differences were found using an unpaired student t-test. Scale bar = 50μm.

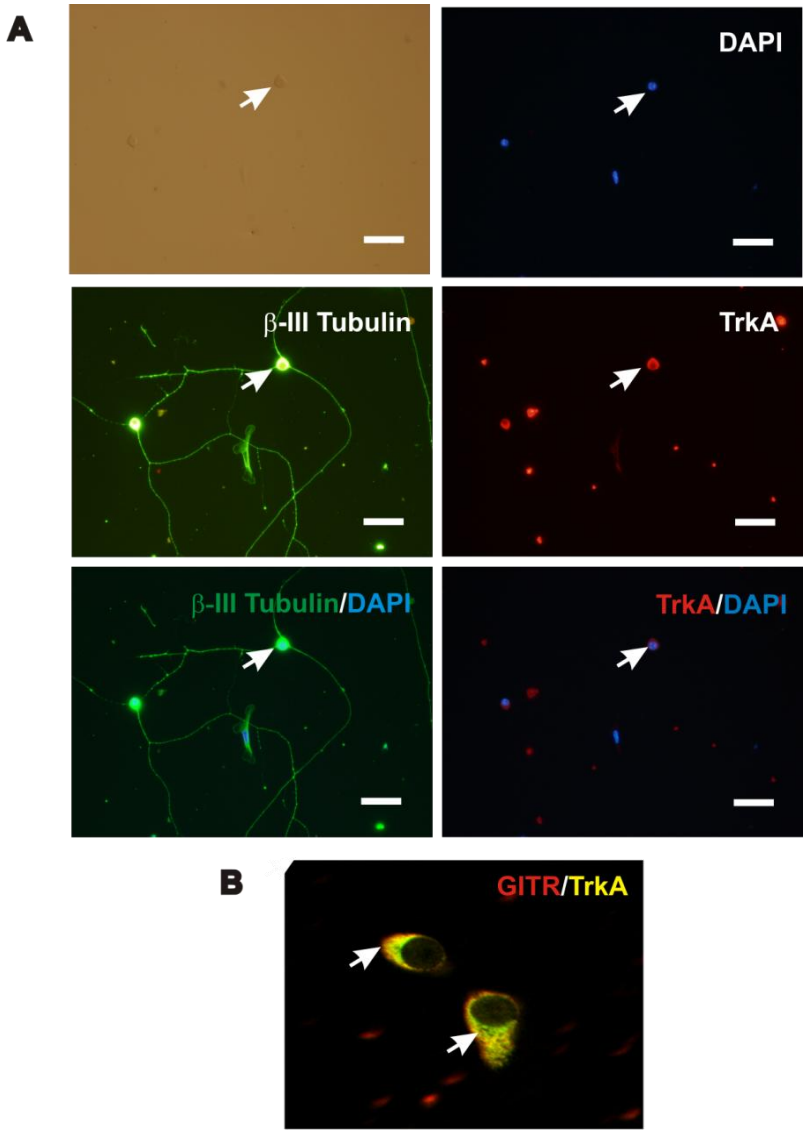


Figure 6.24: Expression of TrkA and GITR by P1 neonatal SCG neurons. P1 SCG neurons were grown for 24h in 10ng/ml NGF. Cells were identified using Brightfield imaging (Upper left corner). Cells were fixed and immunocytochemically stained for TrkA and GITR. (A) TrkA (red) together with β-III Tubulin (green) and counterstained with DAPI (blue) staining in P1 SCG neurons grown for 24h in 10ng/ml NGF. Scale bar 50µm. (B) GITR (red) and TrkA (green) staining in a 2µm confocal optical slice through two P1 SCG neurons, grown for 24h in 10ng/ml NGF. Scale bar = 2µm.

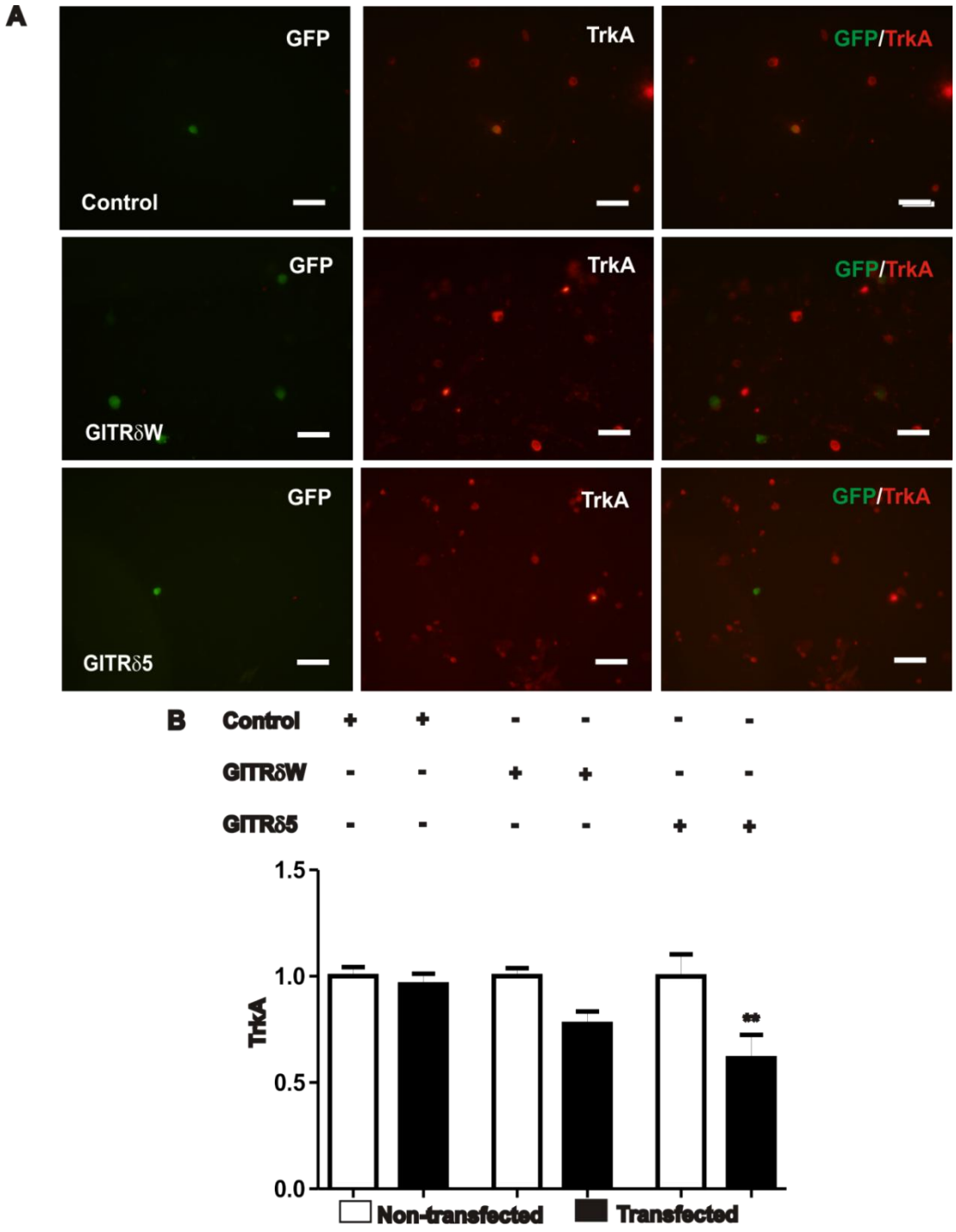

A
GFP
TrkA
GFP/TrkA
Control
GFP
TrkA
GFP/TrkA
GITRδW
GFP
TrkA
GFP/TrkA
GITRδ5
B
Control + + - - - -
GITRδW - - + + - -
GITRδ5 - - - - + +
TrkA
1.5
1.0
0.5
0.0
**
Non-transfected
Transfected

Figure 6.25: TrkA expression in P1 mouse SCG neurons is reduced by constitutive phosphorylation of residues at Thr190 and Ser199 (amino acids 12 and 21 of the GPD) of GITR. P1 SCG neurons were transfected with a GFP plasmid (to visualise transfected neurites) together with GITRδW (in which the GPD of GITR, was missing) or GITRδ5 (mutant in which Thr190 and Ser199, (amino acid 12 and 21 of the GPD) were replaced with glutamic acid) and grown overnight in 10ng/ml NGF at 37°C. Control cultures were also grown in which P1 SCG neurons were transfected with control or empty plasmid. The following day, cultures were fixed and immunocytochemically stained for TrkA and analysis of mean fluorescence was performed. (A) Photomicrographs of control, GITRδW and GITRδ5-transfected dissociated cultures of P1 SCG neurons labelled for TrkA (red). (B) Graphical representations of relevant differences in levels of TrkA in control, GITRδW and GITRδ5-transfected and non-transfected P1 SCG neurons. Means ± standard errors of >150 neurons per condition are shown. Statistical comparisons: $^{**}P \leq 0.01$ using one way ANOVA and post hoc Tukey's test. Scale bar = 50µm.

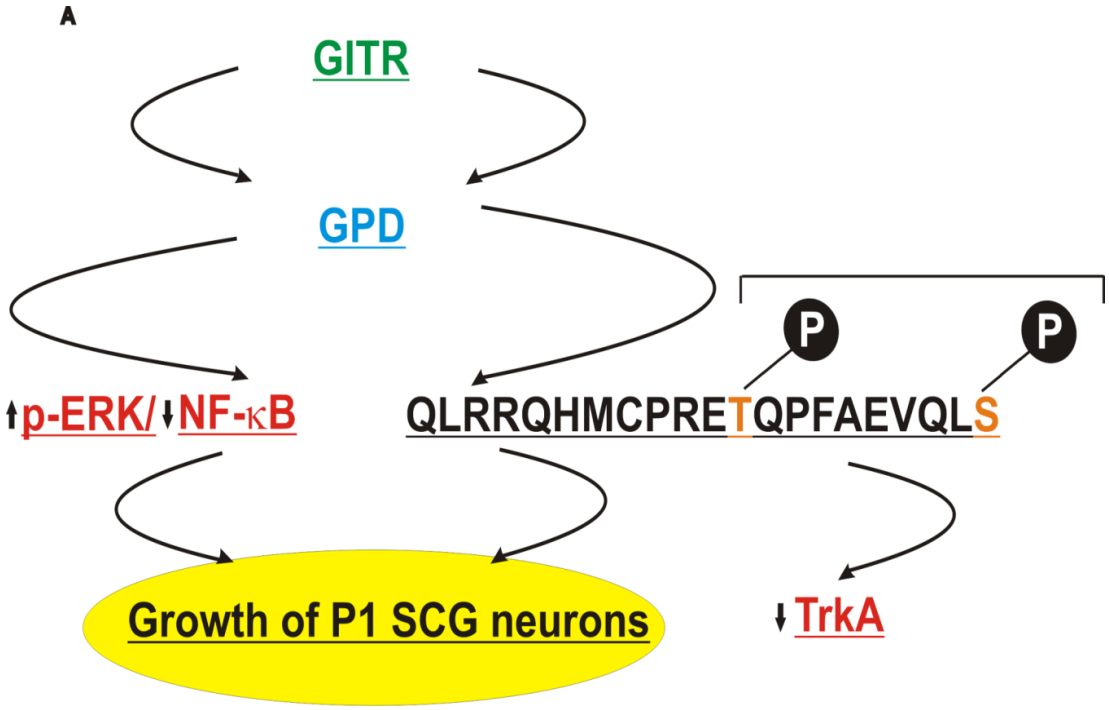


Figure 6.26: Summary: Schema showing proposed dual mechanism underlying the role of GITR in the promotion of axonal growth. (A) In the presence of NGF, the GPD of GITR regulates axonal neurite growth of sympathetic neurons. GITR exhibits and a reciprocal modulation of ERK1/2 and NF-κB signalling where ERK1/2 signalling is enhanced and NF-κB signalling is inhibited, providing an optimal cellular environment for axonal growth. Constitutive phosphorylation of specific GPD sites inhibit TrkA signalling, possibly acting as regulatory mechanism in GITRL-GITR promotion of NGF-mediated growth in developing sympathetic neurons.

6.5 Discussion

NGF, essential for the growth of developing sympathetic neurons, mediates its action through receptors TrkA of the Trk family and p75NTR of the TNFRSF (*Harrington and Ginty, 2013*). Recently, it was discovered that p75NTR interacts with TrkA and potentiates NGF / TrkA binding to enhance axonal growth of postnatal sympathetic neurons (*Matusica, et al., 2013*). GITR, the 18th member of the TNFRSF, is a transmembrane glycoprotein present in many cells of the body and is activated by its specific ligand GITRL (*Krausz, et al., 2007; Nocentini, et al., 1997*). GITRL-GITR signalling is well known for its role in the immune system, where it regulates innate and acquired immune system responses through the activation and inhibition of intracellular pathways including NF-κB and MAPK (*Esparza and Arch, 2004; Esparza and Arch, 2005b; Esparza, et al., 2006; Ronchetti, et al., 2004*). More recently, GITRL-GITR signalling was discovered to play a role in the development of the PNS where it is required for NGF-promotion of sympathetic neurite growth through activation of ERK1/2 of the MAPK pathway (*O'Keeffe, et al., 2008*).

In chapter 5.0, the region of GITR responsible for its growth promoting effects in developing sympathetic neurons was identified and is located in the juxtamembrane region of the intracellular GITR. To further establish the molecular mechanisms behind GITR in promoting the growth of developing sympathetic neurons, this chapter aimed to examine the effect of the GPD of GITR on intracellular signalling pathways, including NF-κB and ERK1/2.

The enhancement of basal levels of NF-κB, by factors such as TNFα, causes a reduction in neuronal growth in developing sympathetic neurons (*Gutierrez, et al., 2008; Nolan, et al., 2011*). NF-κB-mediated reduction in sympathetic neuronal growth is mediated through the canonical pathway in which activated IKKβ phosphorylates IκBα, leading to its ubiquitination and proteosome-mediated degradation, allowing the liberated p65/p50 dimer to translocate to the nucleus (*Gutierrez, et al., 2008*). Here, GITR and its specific ligand GITRL were found to be expressed in sympathetic neurons and stimulation or inhibition of GITRL-GITR signalling inhibited or activated NF-κB activity respectively. GITR inhibited NF-κB

allowing for normal sympathetic neurite growth which was demonstrated by alternative experiments where the reduction of neurite growth due to the inhibition of GITR was prevented when NF-κB activity was inhibited. GITR inhibition of NF-κB activity has been previously shown in the immune system (*Esparza and Arch, 2005b; Hauer, et al., 2005*). In general, members of the TNFRSF such as GITR require TRAF molecules to activate or inhibit intracellular signalling pathways (*Esparza and Arch, 2004; Esparza and Arch, 2005b; Hauer, et al., 2005*). GITR inhibition of NF-κB has been previously shown to involve the engagement of TRAF 2 (*Esparza and Arch, 2005b*) and TRAF 3 (*Hauer, et al., 2005*). In this chapter, GITR inhibition of NF-κB activity was mediated through the GPD of GITR. This was demonstrated by a significant increase in NF-κB nuclear activity in cells transfected with a mutant plasmid in which the GPD of GITR was missing. However, GITR/TRAF binding sites are located outside the GPD of GITR (*Krausz, et al., 2007*). There was no effect on neurite growth or NF-κB activity in cells transfected with mutant plasmids containing deletions of regions outside the GPD (GITRδK and GITRδZ plasmids) in this chapter. Deletions in these regions should have disrupted the TRAF binding sites of GITR. Therefore this suggests that GITR-inhibition of NF-κB in sympathetic neurons is TRAF-independent. The GPD is located in domain 1 of cytoplasmic GITR and TRAF binding sites are located in domain 2 (*Krausz, et al., 2007*). Working on the basis that GITR inhibits NF-κB activity through domain 1 (the GPD), which does not contain the TRAF binding motif, perhaps it is possible that domain 1 modulates TRAF function indirectly (*Krausz, et al., 2007*). GITR does not bind TRAF 4 directly however it does activate NF-κB signalling via TRAF 4. Esparza et al suggest that GITR activates NF-κB signalling by modulating TRAF 4 activity by an adapter protein (*Esparza and Arch, 2005b*). Indeed another member of the TNFRSF, CD40, has previously been found to activate NF-κB via a TRAF-independent mechanism. NF-κB was activated in HEK293 cells transfected with CD40 mutants (in which TRAF binding was impaired) *(Leo et al., 1999).* Instead CD40 binds an adapter protein, MyD88, and indirectly mediates NF-κB and ERK signalling pathways in these cells. Given that GITRL-GITR signalling regulates both NF-κB and ERK signalling and this regulation appears to originate outside the TRAF-binding domain of GITR, it is

possible that GITR recruits an adapter protein to indirectly activate or inhibit these pathways. Further work to elucidate the full mechanism of GITR-mediated inhibition of NF-κB activity is required. One way may be to scan for known adapter proteins used by TNFRSF (eg. MyD88) and examine the effect of transfection of GITRδW on adapter proteins expression and subsequently, NF-κB and ERK signalling by IHC, as used in the current study.

SCG cells transfected with GITRL and p65 together were larger than those transfected with p65 alone, however levels of nuclear NF-κB activity was the same in cells expressing GITRL with p65 and p65 alone. This suggested that GITR is engaging a second signal that opposes NF-κB growth-inhibitory effects allowing for NGF-promoted neurite growth. GITR has previously been shown to enhance ERK1/2 phosphorylation in cells of the immune system and the PNS (*O'Keeffe, et al., 2008; Ronchetti, et al., 2004*). In the SNS, GITR enhances NGF-activation of ERK1/2 resulting in neurite growth (*O'Keeffe, et al., 2008*). Here, we show GITR enhances ERK1/2 activation through the GPD of GITR. Interestingly, cells expressing GITRL and p65 had significantly higher and lower levels of phospho-ERK1/2 respectively compared to controls while cells transfected with GITRL and p65 together had the same level of phospho-ERK1/2 as to controls. Once related to effects on neurite growth, it was clear that the extent of NGF-promoted neurite growth was related to the level of phospho-ERK1/2 which can in turn be modulated by NF-κB signalling i.e. GITRL-GITR signalling exerted a reciprocal modulation of ERK1/2 and NF-κB signalling which is essential for NGF promoted neurite growth.

GITR reciprocally modulates ERK1/2 and NF-κB signalling for the promotion of neurite growth through the GPD of GITR. Putative phosphorylation sites in the GPD of GITR were identified by *In Silico* analysis as having the potential to activate or inhibit downstream pathways of GITR. However, cells transfected with mutant plasmids in which these sites were disrupted had no effect on NF-κB or ERK1/2 signalling in sympathetic neurons. This indicates that these pathways are regulated by other unidentified sites in the GPD of GITR. Interestingly, cells transfected with a mutant plasmid in which two sites, Thr190 and Ser199, (amino acid 12 and 21 of the GPD) were constitutively phosphorylated resulted in a significant decrease in TrkA and not phospho-TrkA expression in neurons. Why

TrkA and not phospho-TrkA is affected in these transfected cells is not yet known. Perhaps this is due to timing. If we consider p75NTR as a model for GITR, the intracellular region of p75NTR induces a conformational change in TrkA prior to NGF binding (*Esposito, et al., 2001; Matusica, et al., 2013*) and this may be the case here. Cells transfected with the GITRδW mutant exhibited a trend toward a decrease in TrkA expression in these neurons but this was not significant (Figure 6.25 B). Therefore from these results it cannot be concluded that removal of the GPD of GITR and constitutive phosphorylation and at the said sites reduced TrkA levels and subsequently neurite growth in these neurons. Constitutive phosphorylation mutation of Fas-associated death domain (FADD), an adaptor molecule for the TNFRSF and a distant relative of GITR, causes defective but not inhibition or absence of T cell proliferation (*Osborn, et al., 2007*). Constitutive phosphorylation mutation in the GPD of GITR results in defective neurite growth or growth inhibition. Given that constitutive phosphorylation at Thr190 and Ser199 reduced levels of TrkA, the high affinity receptor for NGF, regulation of phosphorylation at these sites of the GPD of GITR is important. Phosphorylation is regulated by phosphatases; such as dual specificity phosphatases (DUSPs) in the MAPK signal transduction pathway in which DUSPs dysphosphorylate both ERK 1 and 2 sites (*Finch, et al., 2012*). However, to our knowledge there are no known phosphatases or any other molecule that regulate the phosphorylation of Thr190 and Ser199 of the GPD of GITR in sympathetic neurons.

In summary, this chapter builds on chapter 5.0 which identified the growth promoting region of GITR for NGF-promoted neurite growth in sympathetic neurons. This chapter reveals that GITR promotes neurite growth through the GPD regulation of NF-κB and ERK1/2 signalling pathway where GITR facilitates an inverse regulation of these pathways to provide an optimal growth environment for sympathetic neurons. Lastly, expression of NGF receptor TrkA is regulated by specific residues in the GPD and appears to have a growth inhibitory effect on the sympathetic neurons which may signify an unknown regulatory region of GITR whose function remains to be explored.

7.0 Heterogenous requirement for GITR in the regulation of peripheral target innervation of the sympathetic nervous system

7.1 Aims

- To determine the extent to which GITRL-GITR signalling regulates peripheral target innervation of the sympathetic nervous system
- To investigate the changes in gene expression as a consequence of GITR signalling

7.2 Abstract

There is a heterogenous requirement for NGF, whereby NGF is required in a non-uniform manner, and NGF requirement differs depending on the target organ, in the promotion of growth and target innervation of sympathetic neurons of the PNS. GITR is crucial for NGF-promotion of growth and target innervation in the sympathetic nervous system. However this role of GITR has only been examined to date in postganglionic neurons of the SCG and their peripheral targets, namely the nasal mucosa and iris, of neonatal mice. To investigate the extent of the requirement for GITR in the regulation of NGF-promoted target innervation by other sympathetic neurons in the PNS, we examined neurite density and branching from P1 GITR-/- mice using whole mount immunohistochemistry for tyrosine hydroxylase (TH) as a way to identify sympathetic nerve terminals. These analyses revealed that there is a heterogenous requirement for GITR in the regulation of sympathetic innervation, GITR is required for NGF-promoted target innervation of the heart and bladder, but is not required for the normal innervation of the stomach, small intestine, trachea and urethra of P1 mice. In addition, we found that the expression of mRNAs encoding the pro-inflammatory cytokine TNFα and insulin growth factor 1 receptor (IGF-1R1) were upregulated in the SCG of GITR-/- mice compared to wildtype mice, possibly providing a link between GITR, inflammation and sympathetic neurite growth, in addition to identifying new molecules potentially involved in the regulation of neonatal neurite growth.

7.3 Introduction

NGF is required for the survival of sympathetic neurons *in vivo* (*Angeletti and Levi-Montalcini, 1971; Crowley, et al., 1994; Levi-Montalcini and Booker, 1960*) and *in vitro* (*Deshmukh and Johnson, 1997; Greene, 1977; Martin, et al., 1988*). Past *in vitro* experiments have demonstrated the axonal growth promoting effects of NGF in sympathetic neurons (*Atwal, et al., 2000; Cohen, et al., 1954; Deckwerth, et al., 1996; Glebova and Ginty, 2004; Mains and Patterson, 1973*). However the NGF requirement of sympathetic neurons for survival impeded efforts to examine the requirement for NGF in the promotion of axonal growth independent of its role in

survival *in vivo*. To circumvent the dramatic loss of sympathetic neurons seen in the NGF-/- mouse (*Crowley, et al., 1994*), Glebova and Ginty used concurrent elimination of pro-apoptotic family member, Bax, along with NGF, which allowed neurons to survive in the absence of NGF which then allowed them to investigate the effects of NGF deletion specifically on axonal growth. When the density of sympathetic innervation was examined in a variety of peripheral targets, it was found that sympathetic target innervation was absent in salivary glands and the eye; reduced in the heart and lungs; diminished in the spleen, stomach, small intestine, kidney, bladder and gonads, and unaffected in the trachea of neonatal Bax-/- NGF-/- mice (*Glebova and Ginty, 2004*). Collectively, and somewhat surprisingly, these results showed for the first time that there is a heterogenous requirement for NGF in the promotion of sympathetic neuron target innervation, despite its universal requirement for sympathetic neuronal survival, suggesting that other factors may be important for regulating target innervations.

Since 2004, additional factors have been shown to play a role in mediating axonal growth and target innervation of sympathetic neurons. NRP1, a receptor for guidance cues of the class 3 semaphorin (SEMA) family, have been shown to be expressed in sympathetic neurons and is involved in establishing normal target innervation of the heart and aorta in postnatal mice (*Maden, et al., 2012*). Wnt5a signalling, via the Ror receptor tyrosine kinase, derived from sympathetic neurons, and is required for target innervation *in vivo*. Deletion of Wnt5a results in sympathetic fibre extension and target field arborization deficits (*Ryu, et al., 2013*). Similarly, Egr3 is a NGF-induced transcriptional regulator, that is expressed within sympathetic neurons and is required for normal target innervations, as shown by target tissue abnormalities in mice with sympathetic neuron-restricted Egr3 ablation (*Quach, et al., 2013*).

It was previously shown that GITR and its ligand GITRL are co-expressed in neonatal sympathetic neurons and are required for *in vivo* growth and target innervation of mouse neonatal sympathetic neurons (*O'Keeffe, et al., 2008*). GITRL-GITR signalling promotes the growth and target innervation of sympathetic neurons only in the presence of NGF, i.e. GITR acts as a costimulatory molecule to NGF in axonal growth and target innervation of sympathetic neurons (*O'Keeffe, et al., 2008*).

A role for GITRL-GITR signalling in NGF-promoted target innervation of sympathetic neurons has only been established in the nasal mucosa and the iris (*O'Keeffe, et al., 2008*). It is not yet known if the requirements of sympathetic neurons for GITRL-GITR signalling in mediating peripheral target innervation vary to the same extent as NGF (*Glebova and Ginty, 2004*).

GITR is a relatively novel regulator of sympathetic neurite growth and changes in gene expression as a consequence of GITR signalling and how these changes affect neuronal growth is currently unknown. A number of factors inhibit neurite growth and include TNFα (*Gutierrez, et al., 2008; Neumann, et al., 2002*), LIGHT (*Gavalda, et al., 2009a*) and RANKL (*Gutierrez, et al., 2013*). Treatment with TNFα results in a significant inhibition of sympathetic neurite growth from neonatal mouse SCG neurons (*Gutierrez, et al., 2008*). The growth inhibitory effects induced by TNFα are comparable to the growth inhibitory effects resulting from inhibition of GITRL-GITR signalling in neonatal mouse SCG neurons (Chapter 5.0 and 6.0). In this study we investigated the extent to which GITRL-GITR signalling is required for peripheral target innervation by symapthetic neurons *in vivo*. To do this, we used whole mount immunohistochemistry for TH on organs isolated from GITR-/- and GITR+/+ mice to identify sympathetic axons present in these targets. In addition, using results from microarray studies performed in the lab, we also examined the expression of a number of mRNAs in SCG of GITR-/- and GITR+/+ mice using qualitative RT-PCR.

7.4 Results

7.4.1 TH is expressed by mouse SCG cells *in vivo* and *in vitro*

In order to confirm *in vivo* expression of sympathetic neuronal marker TH in mouse SCG, P1 mice heads were fixed, transversely cryosectioned at a thickness of 15μm, and immunohistochemically stained for TH. Photomicrographs of TH-stained transverse section identifies the right and left SCG (white arrow) (Figure 7.1 A) located in close proximity to the common carotid artery (red arrow) (Figure 7.1 A). To confirm *in vitro* expression of TH, P1 SCG were removed, dissociated, plated in a defined media containing 10ng/ml NGF and grown overnight in 37°C. The

following day, cells were fixed and immunocytochemically stained for nuclear marker DAPI, neuronal marker β-III tubulin and sympathetic neuronal marker TH (Figure 7.2 A). These results confirm TH expression in whole SCGs and dissociated cells from the SCG of P1 mice (Figure 7.1 A and 7.2 A).

7.4.2 GITR is required for sympathetic NGF-target innervation of the heart and bladder of neonatal mice

Previously it was found that organs of the peripheral nervous system have differential NGF requirements for target innervation (*Glebova and Ginty, 2004*). Since GITR is required for NGF-promoted growth of sympathetic neurons and target innervation of the nasal mucosa and iris, we investigated the extent of GITR requirement for target innervation in other peripheral target organs of the SNS. The extent of neurite density and branching was determined in the trachea, heart, stomach, small intestine, ureter and bladder of P1 GITR-/- mice using whole-mount DAB-TH immunostaining. Hearts from GITR-/- mice displayed a significant reduction in branching (** $P<0.01$) (Figure 7.4 C) but there was no reduction in neurite density (Figure 7.4 B) compared to heart from GITR+/+ mice. These results are reflected in whole mount images of the heart from GITR+/+ and GITR-/- mice (Figure 7.4 A). In addition, there was a significant reduction in sympathetic neurite density (** $P<0.01$) (Figure 7.8 B) and branching (* $P<0.05$) (Figure 7.8 C) in the bladder from P1 GITR-/- compared to GITR+/+ mice or controls. This reduction in both neurite density and branching is reflected in whole mount images of the bladder from GITR+/+ and GITR-/- mice (Figure 7.8 A). However, sympathetic neurite density or branching, in the trachea, stomach, small intestine and ureter was unaffected in GITR-/- mice compared to controls (Figure 7.3 B, C; Figure 7.5 B, C; Figure 7.6 B, C and 7.7 B, C). These results are represented by whole mount images of the trachea, stomach, small intestine and ureter from GITR +/+ and GITR-/- mice (Figure 7.3 A; Figure 7.5 A; Figure 7.6 A and 7.7 A). For a full table to compare target innervation of the trachea, heart, stomach, small intestine, ureters and bladder from GITR+/+ and GITR-/- mice, see table 7.1.

7.4.3 Inhibition of GITRL-GITR signalling resulted in an upregulation of TNFα and IGF-1R in P1 mouse SCG

Neonatal SCG neurons treated with TNFα display a significant reduction in neurite growth (*Gutierrez, et al., 2008*). Microarray studies performed on SCG tissue that was treated with 10ng/ml TNFα identified genes upregulated by treatment including IGF-1 and IGF-1R. Given that cells treated with TNFα exhibit similar growth inhibitory effects as cells in which GITRL-GITR signalling is inhibited (*Gutierrez, et al., 2008; O'Keeffe, et al., 2008*), it is plausible that the same genes are affected by TNFα treatment and GITRL-GITR inhibition. On this basis, we investigated changes, if any, in the expression of these genes in GITR-/- mice compared to GITR+/+ mice. Qualitative RT-PCR was performed on RNA extracted from neonatal GITR-/- and GITR+/+ SCG and expression of IGF-1, IGF-1R mRNAs was determined (Figure 7.9 A). In addition, the expression of cytokines IL-1α, TNF-α and receptors IL-1R1, IL1R2, TNFR1, TNFR2 mRNAs was also examined, as cytokines have growth inhibitory effects in sympathetic neurons (*Nolan, et al., 2011*) (Figure 7.9 B). In chapter 5.0 and 6.0, constitutive phosphorylation of specific residues on the GITR GPD resulted in both a reduction in neurite growth and TrkA expression in P1 SCG neurons (Figure 5.14 and Figure 6.24) and therefore the expression of TrkA Mrna was also examined in P1 GITR-/- mice (Figure 7.9.C). RT-PCR analysis revealed a qualitative upregulation of IGF-1R and TNFα mRNAs in P1 SCG from GITR-/- mice compared to controls (Figure 7.9 A and B).

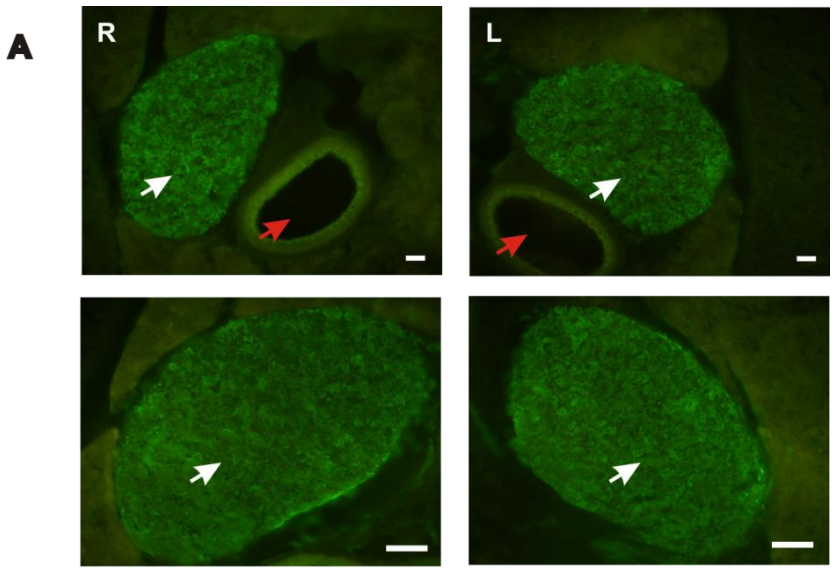


Figure 7.1: Expression of TH in the P1 neonatal SCG. P1 mice heads were fixed, cryoprotected and transversely cryosectioned at a thickness of 15µm. Sections were then stained for (A) TH (white arrow) located next to common carotid artery (red arrow). Photomicrographs display (R) right and (L) left SCG. Scale bar 50µm.

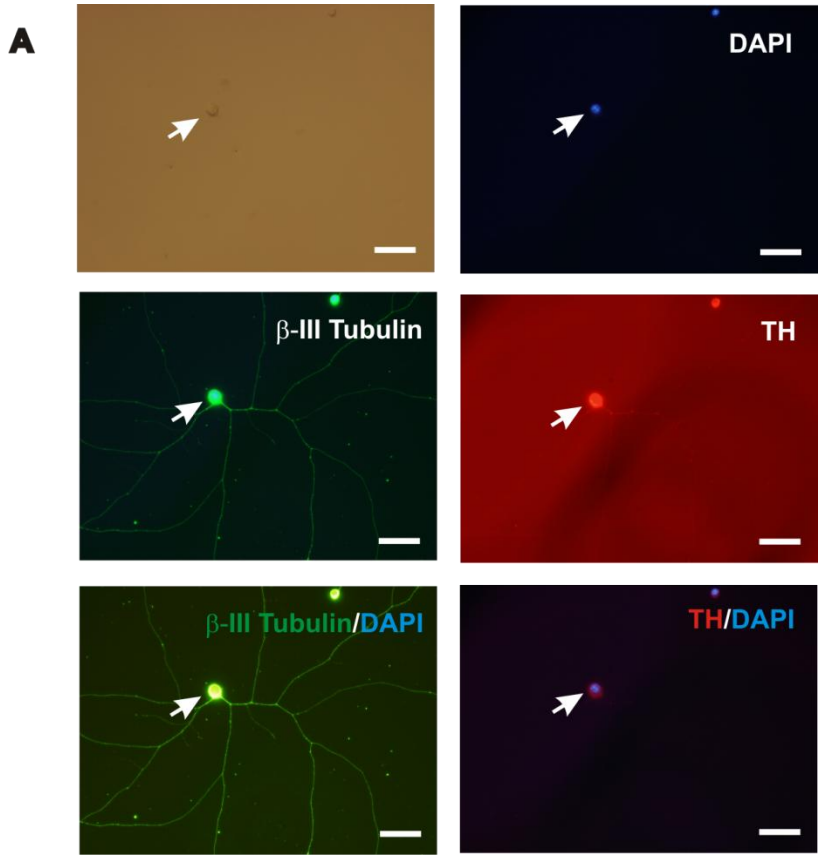


Figure 7.2: Expression of TH in cultured P1 neonatal SCG neurons. P1 SCG neurons were grown for 24h in 10ng/NGF. Cells identified by brightfield images (upper left). Cells were fixed and immunocytochemically stained for (A) neuronal marker DAPI (blue), β-III Tubulin (green), TH (red) and counterstained with DAPI (blue). Scale bar 50µm.

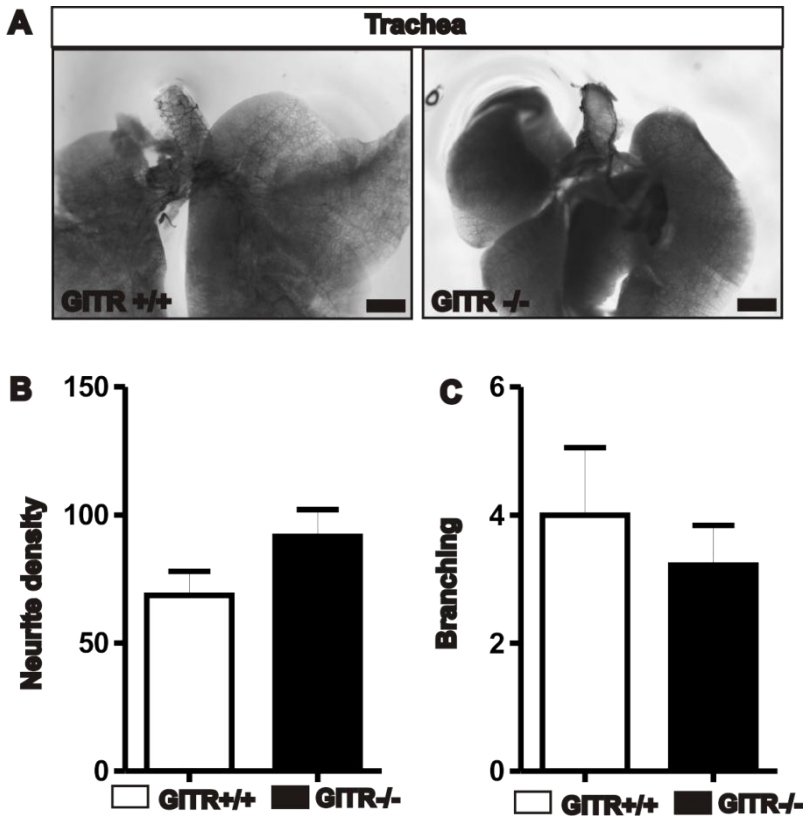


Figure 7.3: Sympathetic innervation of the trachea is not affected in P1 GITR-/- mouse pups. (A) Representative images of P1 mouse trachea which was whole-mount DAB-TH immunostained showing the extent of innervation in GITR-/- compared to control GITR+/+ P1 mouse pups. (B) Quantification of nerve density using a modified line incept method to compare sympathetic innervation between GITR+/+ and GITR-/- P1 mouse pups. (C) Branching, where the number of bifurcations was measured in three randomly placed boxes of set size over the trachea micrographs, in GITR+/+ and GITR-/- P1 mouse pups. N = 3. Statistical comparisons: No statistical significant difference compared with controls was found using an unpaired student t-test Scale bar = 1mm.

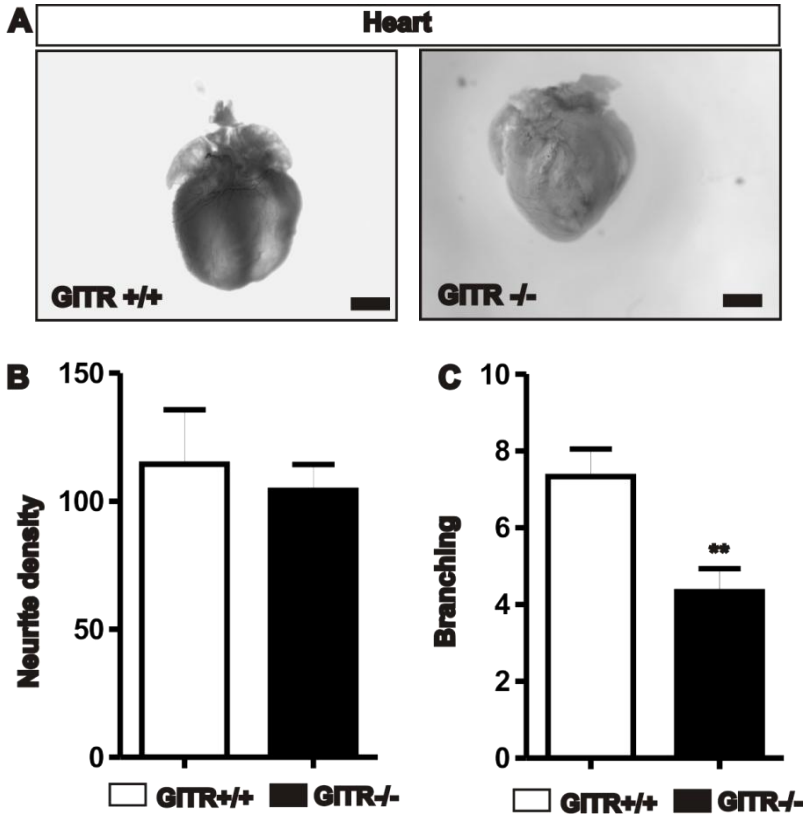


Figure 7.4: Sympathetic branching within the heart is reduced in P1 GITR-/- mouse pups. (A) Representative images of P1 mouse heart which was whole-mount DAB-TH immunostained showing the extent of innervation of the heart in GITR-/- compared to control GITR+/+ P1 mouse pups. (B) Quantification of nerve density using a modified line incept method to compare sympathetic innervation of the heart between GITR+/+ and GITR-/- P1 mouse pups. (C) Branching, where the number of bifurcations was measured in three randomly placed boxes of set size over the heart micrographs, in GITR+/+ and GITR-/- P1 mouse pups. N = 3. Statistical comparisons: ** P<0.01 compared with controls was found using an unpaired student t-test. Scale bar = 1mm.

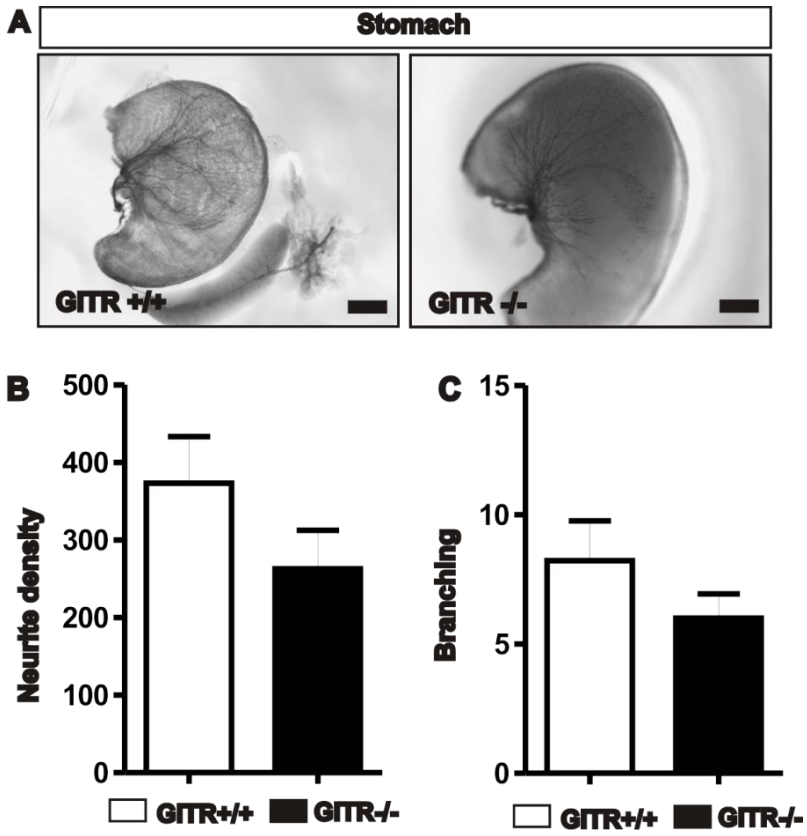


Figure 7.5: Sympathetic innervation of the stomach is not affected in P1 GITR-/- mouse pups. (A) Representative images of P1 mouse stomach which was whole-mount DAB-TH immunostained showing the extent of innervation of the stomach in GITR-/- compared to control GITR+/+ P1 mouse pups. (B) Quantification of nerve density using a modified line incept method to compare sympathetic innervation of the stomach between GITR+/+ and GITR-/- P1 mouse pups. (C) Branching, where the number of bifurcations was measured in three randomly placed boxes of set size over the stomach micrographs of GITR+/+ and GITR-/- P1 mouse pups. N = 3. Statistical comparisons: No statistical significant difference compared with controls was found using an unpaired student t-test. Scale bar = 1mm.

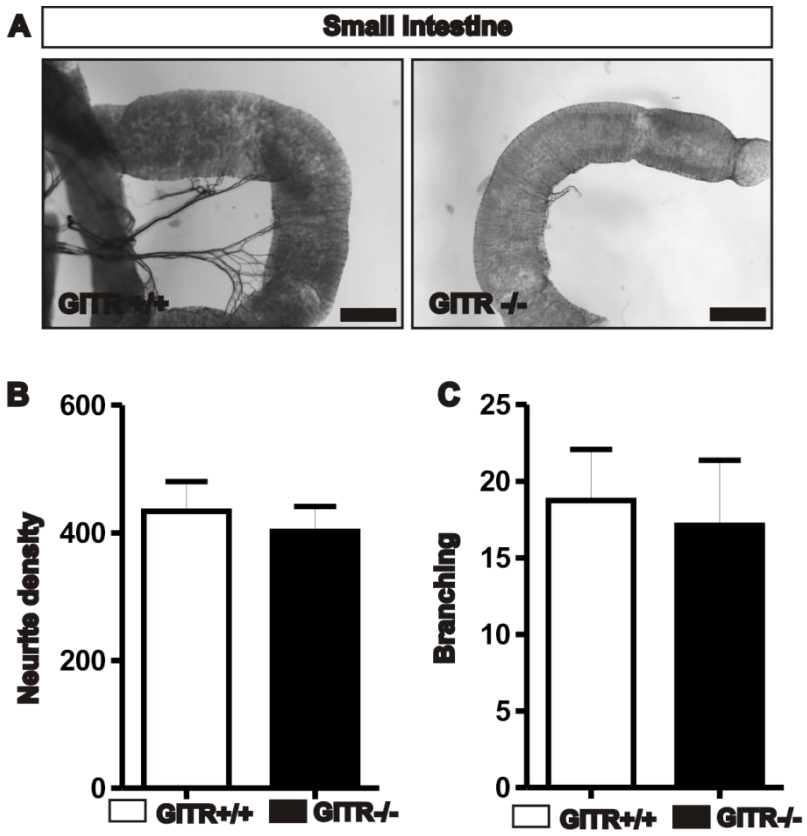


Figure 7.6: Sympathetic innervation of the small intestine is not affected in P1 GITR-/- mouse pups. (A) Representative images of P1 mouse small intestine which was whole-mount DAB-TH immunostained showing the extent of innervation of the small intestine in GITR-/- compared to control GITR+/+ P1 mouse pups. (B) Quantification of nerve density using a modified line incept method to compare sympathetic innervation of the small intestine between GITR+/+ and GITR-/- P1 mouse pups. (C) Branching, where the number of bifurcations was measured in three randomly placed boxes of set size over the small intestine micrographs of GITR+/+ and GITR-/- P1 mouse pups. N = 3. Statistical comparisons: No statistical significant difference compared with controls was found using an unpaired student t-test. Scale bar = 1mm.

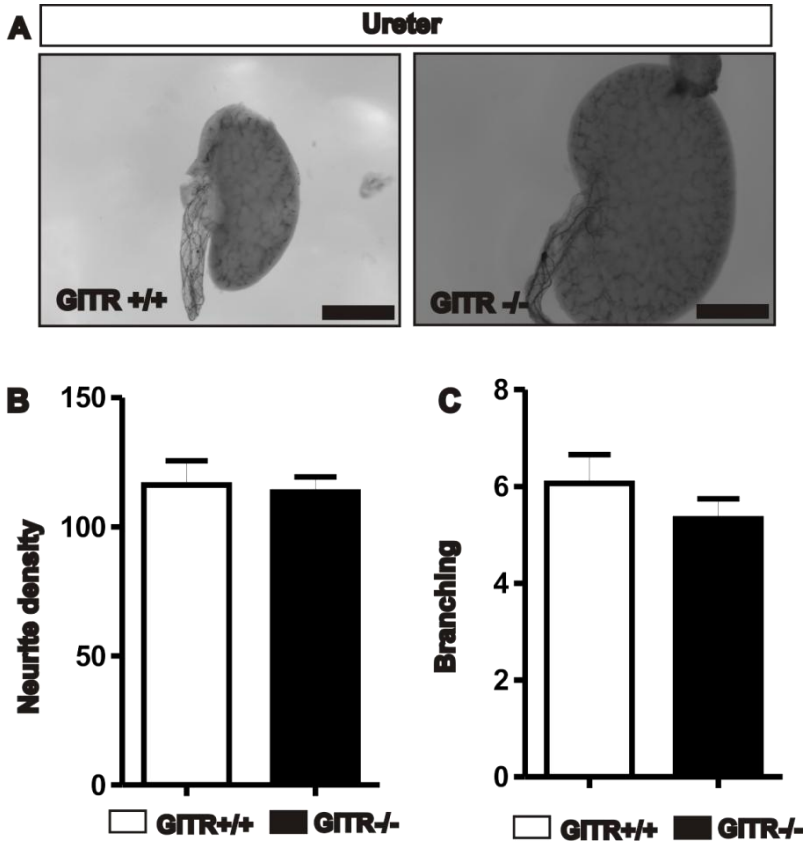


Figure 7.7: Sympathetic innervation of the ureter is not affected in P1 GITR-/- mouse pups. (A) Representative images of P1 mouse ureter which was whole-mount DAB-TH immunostained showing the extent of innervation of the ureter in GITR-/- compared to control GITR+/+ P1 mouse pups. (B) Quantification of nerve density using a modified line incept method to compare sympathetic innervation of the small intestine between GITR+/+ and GITR-/- P1 mouse pups. (C) Branching, where the number of bifurcations was measured in three randomly placed boxes of set size over the ureter micrographs of GITR+/+ and GITR-/- P1 mouse pups. N = 3. Statistical comparisons: No statistical significant difference compared with controls was found using an unpaired student t-test. Scale bar = 1mm.

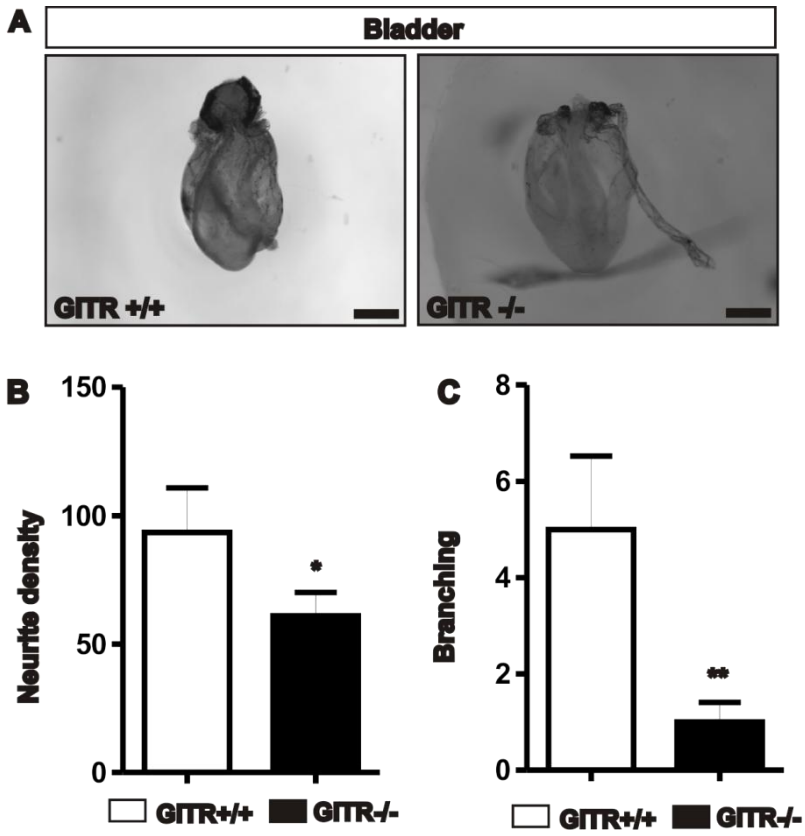


Figure 7.8: Sympathetic innervation density and branching within the bladder is reduced P1 GITR-/- mouse pups. (A) Representative images of P1 mouse bladder which was whole-mount DAB-TH immunostained showing the extent of innervation of the bladder in GITR-/- compared to control GITR+/+ P1 mouse pups. (B) Quantification of nerve density using a modified line incept method to compare sympathetic innervation of the bladder between GITR+/+ and GITR-/- P1 mouse pups. (C) Branching, where the number of bifurcations was measured in three randomly placed boxes of set size over the bladder micrographs, in GITR+/+ and GITR-/- P1 mouse pups. N = 3. Statistical comparisons: ** $P<0.01$, * $P<0.05$, compared with controls was found by using an unpaired student t-test. Scale bar = 1mm.

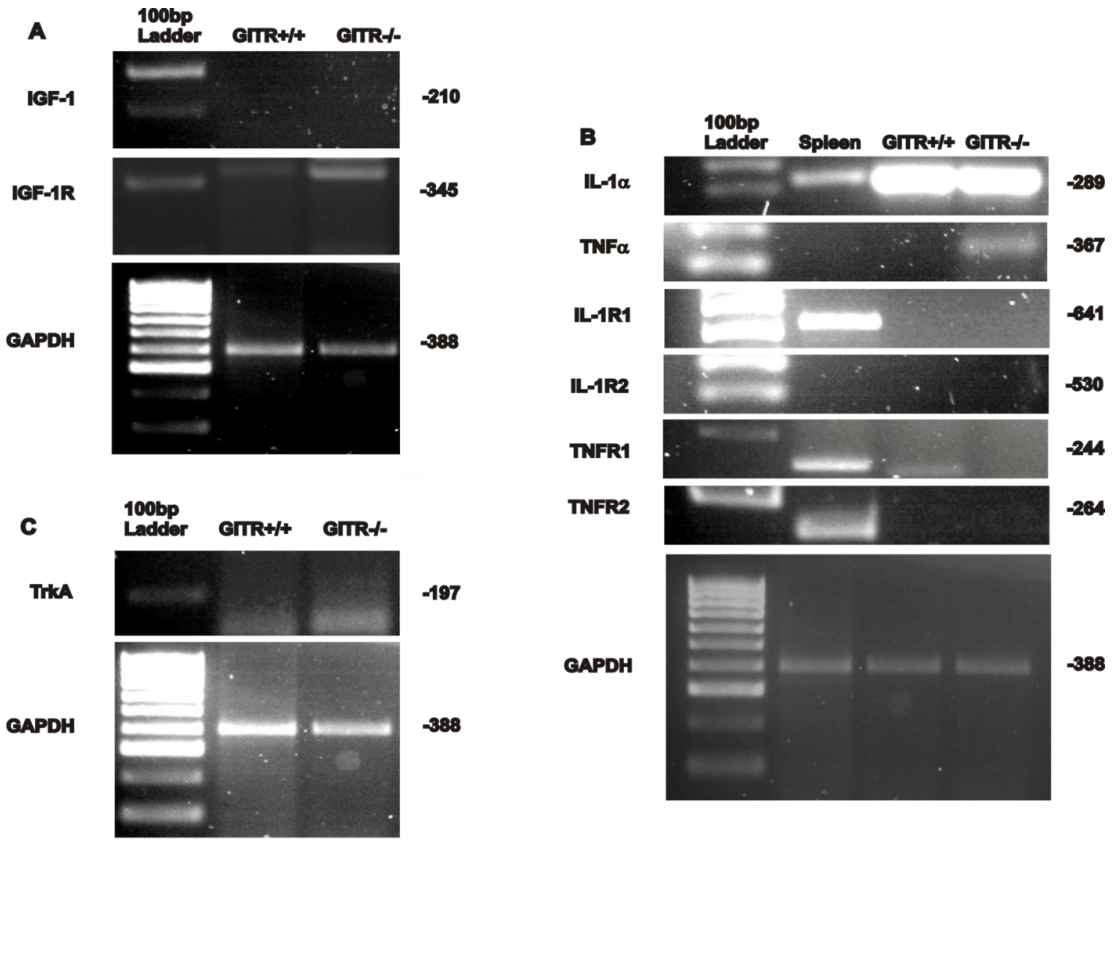


Figure 7.9: IGF-1R and TNFα mRNAs are up-regulated in the absence of GITR in neonatal SCG neurons. (A, B, C) Expression of (A) IGF-1, IGF-1R, GAPDH (B) IL-1α, TNFα, IL-1R1, IL1R2, TNFR1, TNFR2, GAPDH and (C) TrkA, GAPDH mRNAs in GITR+/+ and GITR-/- P1 mouse SCG. Upregulation of IGF-1R (A) and TNFα (B) mRNA was evident following RT-PCR in GITR-/- P1 SCG neurons when compared to GITR+/+ P1 SCG neurons. PCR products of 210bp, 345bp, 289bp, 367bp, 641bp, 530bp, 244bp, 264bp, 197bp, 388bp indicate IGF-1, IGF-R1, IL-1α, TNF-α, IL-1R1, IL-1R2, TNFR1, TNFR2 and GAPDH expression, respectively.

Organs	GITR-/-	
	Neurite density	**Branching**
Trachea	-	-
Heart	-	⇩ ** P<0.01
Stomach	-	-
Small Intestine	-	-
Ureter	-	-
Bladder	⇩ * P<0.05	⇩ ** P<0.01

Table 7.1: Sympathetic neurite density and branching in GITR-/- organs. Table 7.1 summarises the extent of neurite density and branching in organs from P1 GITR-/- SV-129 neonates compared to GITR+/+ neonates. Organs include trachea, heart, stomach, small intestine, ureter and bladder. There was a significant reduction in branching in GITR-/- heart compared to GITR+/+ (** P<0.01), while neurite density and branching was significantly reduced in GITR-/- bladder compared to GITR+/+ (* P<0.05; ** P<0.01). (-) refers to no change compared to control or GITR+/+ neonates.

7.6 Discussion

There is a heterogeneous *in vivo* requirement for NGF in peripheral target organ innervation of the PNS (*Glebova and Ginty, 2004*). GITR is required for NGF-promoted growth and target innervation of developing sympathetic neurons (*O'Keeffe, et al., 2008*). However the requirement for GITR in regulating NGF-dependent target innervation has only been established in target organs of the SCG, including the nasal mucosa and iris (*O'Keeffe, et al., 2008*). The requirement of GITR for NGF-promoted axonal growth and target innervation in target organs from other sympathetic ganglia has not been investigated.

TH is expressed by sympathetic neurons and functions as a rate-limiting enzyme involved in catalyzing the biosynthesis of catecholamines such as dopamine, epinephrine and norepinephine (*Levitt, et al., 1965*). The growth promoting effects of NGF are accompanied by selective induction of TH, whereby NGF produces a 15-20 fold increase in TH activity in SCG neurons from neonatal rats (*Thoenen, et al., 1971*). In this chapter, TH has been selected as a marker of sympathetic neurite density and branching in neonatal sympathetic neurons. The expression of TH was confirmed in P1 mouse SCG and dissociated cultured SCG. As a confirmed marker of sympathetic neurons, TH staining was used in subsequent experiments examining the extent of sympathetic innervation in GITR-/- mice. Organs examined included the heart, in which target innervation is greatly reduced in the absence of NGF (*Glebova and Ginty, 2004*); the stomach, small intestine, ureter and bladder in which target innervation is diminished in the absence of NGF (*Glebova and Ginty, 2004*); and the trachea in which target innervation is unaffected in the absence of NGF (*Glebova and Ginty, 2004*). Here, we found that there was a significant decrease in innervation in terms of branching in the heart (Figure 7.3), in addition to a reduction in neurite density and branching in the bladder (Figure 7.8) of GITR-/- mice when compared to controls. These results suggest that sympathetic neurons requirements for GITRL-GITR signalling in target organ innervation corresponds to that of NGF in the trachea (Figure 7.3), heart and bladder (Figure 7.4 and 7.8). However this is not the case for the stomach, small intestine and ureters (Figure 7.5, 7.6 and 7.7). Glebova and Ginty report a pattern in which targets of paravertebral ganglia display

a greater reduction in sympathetic innervation than targets of prevertebral ganglia in the absence of NGF and suggest that targets of prevertebral ganglia may produce neurotrophic factors other than NGF, and as a result depend on these factors for full target innervation (*Glebova and Ginty, 2004*). This is supported by a study that found postganglionic neurons arising from prevertebral ganglia express TrkB to a greater extent than neurons from paravertebral ganglia (*Dixon and McKinnon, 1994*) implying that targets from prevertebral ganglia require neurotrophins BDNF and/or NT-4 for correct innervation. It could be argued that the reduction of innervation density in some targets and not others may be due to a down regulation of TH in innervating neurons. This was addressed by O'Keeffe et al in which levels of TH mRNA and TH immunofluorescence were quantified in the SCG of GITR+/+ and GITR-/- mice. There was no significant difference in the levels of TH mRNA or TH immunofluorescence in SCG of GITR-/- mice compared to controls indicating that the reduction in TH staining in the sympathetic targets of GITR-null mice is the result of a reduction in the number of sympathetic axons and not down regulation of TH in these targets (*O'Keeffe, et al., 2008*). On this basis, it was presumed that the reduction in target innervation in the heart and bladder of GITR-/- mice is due only to the decrease in number of axons innervating sympathetic targets.

A number of additional factors have recently been implicated in sympathetic target innervation. Egr3 is a NGF-induced transcriptional regulator expressed by sympathetic neurons and is required for normal sympathetic target innervation as demonstrated by target tissue innervation abnormalities and physiologic sympathetic dysfunction, similar to humans with dysautonomia in mice lacking Egr3 (*Eldredge, et al., 2008; Li, et al., 2011; Quach, et al., 2013*). Like NGF and GITR, Egr3 affects target tissue innervation heterogeneously. In some tissues, such as salivary glands, heart, spleen, bowel, kidney, pineal gland and the eye, Egr3 is essential for normal innervation, whereas in other tissues such as lung, stomach, pancreas and liver, Egr3 appears to have little role in innervation (*Li, et al., 2011*). NGF is expressed normally in the submandibular gland and the heart in the absence of Egr3 (*Li, et al., 2011*) indicating that abnormal target tissue innervation is not due to dysregulation of NGF in these target tissues. Glebova and Ginty found that NGF is required for target innervation of these organs (*Glebova and Ginty, 2004*). Combined studies

suggest Egr3 is just one of a number of effectors of NGF signalling and therefore could have a relatively restricted function in a sub-population of NGF-dependent neurons. Previous studies show that Egr3 is regulated by NGF signalling in sympathetic neurons; therefore it is possible Egr3 modulates gene expression required for at least some aspects of NGF-mediated sympathetic terminal axon extension and target tissue innervation (*Eldredge, et al., 2008*). Similiarly, GITRL-GITR signalling appears to modulate NGF-dependant sympathetic target innervation in a non uniform manner. This is demonstrated by a requirement for NGF for the innervation of salivary glands, iris, heart, stomach, small intestine, ureters and bladder (*Glebova and Ginty, 2004*), whereas GITR is required for NGF-promoted innervation of iris (*O'Keeffe, et al., 2008*), heart and bladder (shown in the present study).

Using RT-PCR, we found that knocking out GITR resulted in an increase in TNFα mRNA expression in SCG neurons. Treatment of neonatal SCG neurons with TNFα also results in the inhibition of neurite growth in these neurons (*Gutierrez, et al., 2008*). Increased production of pro-inflammatory cytokines including TNFα can be due to increased immune activation such as in maternal inflammation (*Cai, et al., 2000; Liverman, et al., 2006*) and may contribute to the development of neurological diseases such as cerebral palsy (*Nelson and Willoughby, 2000*). Exposure to pro-inflammatory cytokine IL-1β impairs neural progenitor cell proliferation and alters their differentiation. In addition, IL-1β inhibits developing sympathetic neuron axonal growth (*Nolan, et al., 2011*). TNF-α is considered a potent cytotoxic agent in neuronal tissue (*Botchkina, et al., 1999*) and its application results in a significant inhibition of sympathetic neuronal growth in the developing PNS (*Gutierrez, et al., 2008*). Given that inhibition of GITR increased TNFα levels as shown in the present study and both inhibition of GITR and increased levels of TNFα result in the inhibition of neurite growth in addition to effects of maternal inflammation, it is possible that GITR knock null mutants could be a possible future model of inflammation in neonatal mice. However TNFα is only one cytokine and to establish the possibility of GITR knock down as a model of maternal inflammation, the effect of GITR on other cytokines including IL-1β and receptors needs to be undertaken.

The specific target genes regulated by GITRL-GITR signalling during NGF-induced axonal growth and target tissue innervation in sympathetic tissue are currently unknown. To investigate specific target genes regulated by GITR we used an alternative approach. Inhibition of GITRL-GITR signalling results in the inhibition of neurite growth in P1 SCG neurons that mirrors the inhibition of neurite growth in P1 SCG neurons treated with TNFα (*Gutierrez, et al., 2008*). It could be postulated that the inhibition of GITR results in an inhibition of neurite growth by and increase in TNFα. This could be investigated by transfecting neurons with GITRW plasmid (where the GPD is deleted) and examining the effect on growth by sholl analysis and expression of TNFa by IHC and densitometric analysis.

Using mRNA extracted from TNFα treated SCG cells; a microarray analysis was performed to identify changes in gene expression in TNFα-treated compared with control-treated tissue. Microarray analysis identified two genes that were upregulated in response to treatment, Insulin-like growth factor 1 (IGF-1) and receptor IGF-1R. RT-PCR, performed to examine the expression of these genes in GITR-/- SCG, demonstrated an increase in IGF-1R expression in GITR-/- SCG compared with control. IGF-1 and IGF-1R are members of the IGF family of proteins and play an important role in the regulation of systemic growth (*Liu, et al., 1993*). Interestingly, disruption to IGF1-R gene has more severe consequences than that of IGF-1 gene, resulting in invariable death at birth due to respiratory failure, more severe growth deficiency, muscle hypoplasia, developmental delays in ossification and CNS abnormalities (*Liu, et al., 1993*). This is similar to disruption of NGF versus receptor TrkA, where consequences of TrkA gene disruption are of greater severity that those resulting from NGF gene disruption and is highlighted by symptoms of HSAN IV versus HSAN V neuropathies (*Indo, et al., 1996*). Both IGF-1 and IGF-1R are expressed in SCG neurons of rat (*Bitar, et al., 1997*) and has IGF-1 been shown to enhance neurite outgrowth in cultured sympathetic neuroblasts but not postnatal sympathetic neurons (*DiCicco-Bloom and Black, 1988*). In the present study, there is an increase in the expression of IGF-1R mRNA when GITR is inhibited. GITR inhibition results in a reduction in neurite growth, therefore the question stands, given the role of IGF-1R in the enhancement of growth why would its expression be increased in a model of growth inhibition (i.e. GITR-/-)? In a recent

model of maternal diabetes, there is a significant upregulation of IGF-1R, as seen by real time RT-PCR, in the cerebellum of rat pups born to diabetic mothers at P0 compared to controls (*Haghir, et al., 2013*). If we imagine maternal diabetes and GITR inhibition as the insult and inhibition of growth as the effect, then perhaps IGF-1R is responding to the insult in an effort to control the negative growth inhibitory effect and therefore the consequences of changes in IGF-1R levels in GITR knock down SCG tissue may be compensatory for growth inhibition. In the same study, there was a marked reduction in cerebellar expression of IGF-1R mRNA in the diabetic group of neonates by P7. Given that levels of GITR mRNA peak in the SCG between P1-3, it is plausible that there would be reduction in IGF-1R levels in SCG from P7 GITR-/- mice also. However, further work is required to investigate the relationship between GITR and IGF-1R further.

In summary, this chapter reveals a heterogenous requirement for GITR in NGF-promoted sympathetic target innervation in the PNS. In addition, GITR inhibition results in an upregulation of TNFα, providing food for thought regarding GITR as a novel model of inflammation while IGF-1R may act as a regulatory molecule in the control of neonatal neuronal growth.

8.0 Final Discussion

The correct development of the SNS is crucial for optimal functioning of body organs. Abnormal development of the SNS and its manifestations is highlighted by HSAN IV (*Indo, et al., 1996*). An autosomal recessive disorder, HSAN IV is predominantly characterised by congenital insensitivity to pain with anhidrosis and results from mutations in the TrkA gene, which encodes for TrkA, the high affinity receptor for NGF (*Indo, et al., 1996*). NGF binds two receptors TrkA of the Trk family and p75NTR of the TNFRSF, of which p75NTR increases the sensitivity of sympathetic neurons to NGF (*Lee, et al., 1994b*) and can do so by modulating NGF-TrkA binding (*Matusica, et al., 2013*). NGF-TrkA binding is essential for the survival, axonal growth and target innervation of developing sympathetic neurons (*Glebova and Ginty, 2004; Kuruvilla, et al., 2004; Levi-Montalcini, 1987*).

GITR is a member of the TNFRSF and has an established role in the immune system where it regulates innate and acquired immune responses (*Nocentini, et al., 1997*). However, it is now known that GITR plays an important role in SNS development in which it is required for NGF-induced ERK1/2 activation resulting in the promotion of growth and target innervation of developing sympathetic neurons (*O'Keeffe, et al., 2008*). This is a novel finding and little is known regarding the molecular mechanism behind GITR-promotion of growth in developing sympathetic neurons. Postganglionic sympathetic neurons of the SCG, are an extensively used, experimentally tractable model to study axonal growth and target innervation of sympathetic neurons (*Gutierrez, et al., 2008; Nolan, et al., 2011; O'Keeffe, et al., 2008; Vizard, et al., 2008*). This project uses postganglionic sympathetic neurons of P1 mouse SCG to study the molecular basis of GITR in axonal growth and target innervation of sympathetic neurons.

Prior to this project, it was not known how GITR promoted the growth and target innervation of NGF-dependant sympathetic neurons. One hypothesis was that it did so by increasing neurons sensitivity to NGF, similar to its TNFRSF member p75NTR (*Lee, et al., 1994b*). Chapter 5.0 results indicate that GITR signalling may affects the sensitivity of SCG neurons to NGF at concentrations of 1ng/ml NGF. Recently, a mechanism by which p75NTR increases sympathetic neuron's sensitivity

was put forward. By interaction of the intracellular domain of p75NTR (p75ICD) with TrkA, the binding of NGF to TrkA was modulated, significantly increasing the amount of NGF bound to TrkA-expressing cells (*Matusica, et al., 2013*). Indeed it may be possible that GITR interacts with p75NTR directly where p75NTR subsequently increases sympathetic neurons sensitivity to TrkA. This study went on to examine the effect of GITR, and specifically the intracellular region of GITR, on TrkA expression in sympathetic neurons. In Chapter 6.0, the effect on TrkA expression in P1 SCG neurons transfected with a mutant plasmid in which almost the entire intracellular region was missing (GITRδW) was examined. There was no significant reduction in TrkA expression in these neurons. A supporting result is found in chapter 7.0, in which there is no difference in mRNA expression for TrkA in GITR-/- compared to GITR+/+. However, when TrkA expression was examined in neurons transfected with GITRδ5, in which sites of the juxtamembrane intracellular region, Tyr190 and Ser199 (amino acids 12 and 21), were constitutively phosphorylated, there was a significant reduction in TrkA expression. Indeed, in chapter 5.0, there was a reduction in neurite length and branching in cells transfected with GITRδ5. Given these results and previous findings mentioned, it may be possibly that constitutive phosphorylation at these sites in the GPD of GITR affects TrkA, possible by reducing cell-TrkA expression, resulting in fewer available binding sites for NGF and subsequently reducing NGF binding to TrkA, thereby decreasing the TrkA expressing cells' sensitivity to NGF. It would be interesting to see the effect of inhibiting phosphorylation at these same sites, Tyr190 and Ser199, on TrkA expression using mutant plasmid GITRδ4. This was not indicated earlier as cells transfected with GITRδ4 showed no significant reduction in sympathetic neuronal growth. Given antagonist GITRL treatment was effective reducing sympathetic neuronal growth at concentration of 1ng/ml NGF as seen in chapter 5.0, it would be interesting to look the effects of these discussed plasmids on TrkA expression in media containing 1ng/ml NGF. In addition, it would be very interesting to investigate the interaction of GITR and p75NTR by first assessing for co-expression of both receptors and subsequently the effect of GITRδW and GITRδ5 on the expression of p75NTR by means of transfection, immunocytochemistry and densitometry. These experiments may provide answers to the question of why

constitutive phosphorylation of sites in the GPD of GITR reduces TrkA expression. Perhaps GITR regulates TrkA expression indirectly, via p75NTR.

Although, it was previously known that GITR is crucial for NGF-promoted growth in SCG neurons, the region of GITR responsible for these effects was unknown. Chapter 5.0 results indicates that GITRL-GITR signalling may be via the GITR receptor and not the ligand. This direction of signalling is in contrast to that of 'reversed' signalling reported in the immune system (*Grohmann, et al., 2007*). To confirm GITRL-GITR signalling is forward and not reversed as is the case in the immune system, one could examine the the effect of a Fc-chimera reversed signalling molecule, similar to that used by Kisiswa et al (*Kisiswa, et al., 2013*) on the growth of sympathetic neurons. Next it was found that the GITR receptor exerts growth promoting effects via the juxtamembrane intracellular region, the GPD, of GITR. These data were accomplished by transfection experiments using mutant plasmids containing deletions of the ligand and receptor's intracellular domains. In further analysis of the intracellular region and subsequent intracellular signalling, it was demonstrated that the GPD of GITR activates ERK1/2 and inhibits NF-κB signalling in an inverse fashion to allow for optimal growth of neurons. While GITR has previously been found to facilitate NGF-induced ERK1/2 activation in sympathetic neurons (*O'Keeffe, et al., 2008*), it was unknown as to the effects of GITR on NF-κB in sympathetic neurons. In the immune system, GITR inhibition of NF-κB has been previously shown to involve the engagement of TRAF 2 (*Esparza and Arch, 2005b*) and TRAF 3 (*Hauer, et al., 2005*). However, the location of the TRAF binding site in the GITR receptor is outside the GPD suggesting GITR inhibition of NF-κB is TRAF independent. Given that it has been previously shown that members of the TNFRSF can activate intracellular signalling pathways, such as NF-kB and ERK (Leo, et al., 1999), via adapter proteins, perhaps it is possible that GITR similiarly inhibits and activates these pathways via adapter proteins. Further work to ascertain the precise mechanism for GITR-mediated inhibition of NF-κB may involve screening for known adapter proteins that interact with members of the TNFRSF; investigate the expression of these proteins in P1 SCG neurons; examine the effect of transfecting plasmid GITRδW on the expression of proteins in P1 SCG

neurons and if indicated the effect of transfecting mutant plasmids of adapter proteins (affected by GITRδW) on NF-κB and ERK signalling by IHC.

It has been reported that TNFα treatment of sympathetic neurons results in the inhibition of NF-κB signalling (*Gutierrez, et al., 2008*) and subsequent reduction in sympathetic neurite growth (*Gutierrez, et al., 2008*). The reduction in neurite growth displayed in cells treated with TNFα is comparable to the reduction in growth exhibited by cells where GITRL-GITR signalling is inhibited as shown in the present results. In chapter 7.0, TNFα mRNA levels were higher in GITR-/- compared with GITR+/+ SCG tissue as shown by RT-PCR. Given, that increased production of pro-inflammatory cytokines including TNFα can be due to increased immune activation such as in maternal inflammation (*Cai, et al., 2000; Liverman, et al., 2006*), there may be a role for GITR knock out as a model for maternal inflammation. In addition, there is an upregulation in IGF-1R mRNA in GITR-/- SCG tissue compared to controls in chapter 7.0. Levels of IGF-1R have recently been found to be upregulated in cerebellar tissue of neonatal rat pups born to diabetic mothers (*Haghir, et al., 2013*). As diabetes is an inflammatory disease (*Xie and Du, 2011*), these studies provide support for the potential use of GITR knock out as a model of inflammation.

Previously, GITR requirement for NGF-promotion of target innervation had only been established in target organs of the SCG, including the nasal mucosa and iris (*O'Keeffe, et al., 2008*). To address how extensively GITR is involved in the establishment of sympathetic innervation, target innervation in various organs of the GITR-/- P1 mice was examined. Organs included the trachea, heart, stomach, small intestine, ureters and bladder. NGF is heterogeneously required for sympathetic innervation, and specifically required for sympathetic innervation of the salivary glands, iris, heart, stomach, small intestine, ureters and bladder (*Glebova and Ginty, 2004*). Here, we found GITR is required for NGF-target innervation of the heart and bladder but not the stomach, small intestines and ureters. This discrepancy in the requirement for NGF and GITR for sympathetic target innervation is similar to that of NGF and Egr3. Egr3 is regulated by NGF signaling in sympathetic neurons, however tissues that require NGF for target innervation do not homogeneously require Egr3 (*Li, et al., 2011*). It is possible Egr3 modulates gene expression required

for at least some aspects of NGF-mediated sympathetic terminal axon extension and target tissue innervation (*Eldredge, et al., 2008*) and similarly, GITR appears to play a role in NGF-sympathetic target innervation in a non uniform manner.

In conclusion, the aim of this thesis was to answer basic biological questions pertaining to the role of GITR in the promotion of growth and target innervation of sympathetic neurons. These biological questions included (i) whether GITR increased the sensitivity of sympathetic neurons to NGF similar to that of p75NTR; (ii) what region of GITR is responsible for its growth promoting effects; (ii) the effect of GITR on downstream pathways including ERK1/2 and NF-κB and (iv) how extensively is GITR involved in the target innervation of the developing sympathetic nervous system. This thesis has added to a large body of knowledge regarding factors involved in the development of the sympathetic nervous system. GITR and its specific ligand GITRL is expressed by neonatal sympathetic neurons of which binding occurs through the extracellular tail of GITRL which activates GITR and specifically the juxtamembrane region of GITR to promote the growth of sympathetic neurons. The GPD of GITR activates ERK1/2 and inhibits NF-κB activity in an inverse fashion to induce the growth promoting effects of GITR while the phosphorylation sites Tyr190 and Ser199 of the same region regulate TrkA expression and possible TrkA – NGF binding in these neurons, in a manner that may increase sympathetic neuron's sensitivity to NGF. GITR is required for NGF-target innervation of developing sympathetic neurons; however its requirement is heterogenous. Inhibition of GITR signalling results in the reduction of sympathetic neurite growth to the same extent as treatment with pro-inflammatory cytokine TNFα. TNFα is upregulated in GITR-/- SCG tissue along with IGF-1R. As IGF-1R is upregulated in neural tissue post maternal inflammation, it is therefore possible that GITR knock out could be considered as a model of inflammation in future studies.

9.0 Bibliography

Adams RH, Betz H, Puschel AW (1996). A novel class of murine semaphorins with homology to thrombospondin is differentially expressed during early embryogenesis. Mech Dev 57: 33-45.

Anderson DJ, Groves A, Lo L, Ma Q, Rao M, Shah NM, Sommer L (1997). Cell lineage determination and the control of neuronal identity in the neural crest. Cold Spring Harb Symp Quant Biol 62: 493-504.

Angeletti PU, Levi-Montalcini R (1971). Growth regulation of the sympathetic nervous system: immunosympathectomy and chemical sympathectomy. Rev Eur Etud Clin Biol 16: 866-874.

Arch RH, Gedrich RW, Thompson CB (1998). Tumor necrosis factor receptor-associated factors (TRAFs)--a family of adapter proteins that regulates life and death. Genes Dev 12: 2821-2830.

Atwal JK, Massie B, Miller FD, Kaplan DR (2000). The TrkB-Shc site signals neuronal survival and local axon growth via MEK and P13-kinase. Neuron 27: 265-277.

Axelrod FB, Gold-von Simson G (2007). Hereditary sensory and autonomic neuropathies: types II, III, and IV. Orphanet J Rare Dis 2: 39.

Bae EM, Kim WJ, Suk K, Kang YM, Park JE, Kim WY, Choi EM, Choi BK, Kwon BS, Lee WH (2008). Reverse signaling initiated from GITRL induces NF-kappaB activation through ERK in the inflammatory activation of macrophages. Mol Immunol 45: 523-533.

Baldwin AS, Jr. (1996). The NF-kappa B and I kappa B proteins: new discoveries and insights. Annu Rev Immunol 14: 649-683.

Baloh RH, Tansey MG, Lampe PA, Fahrner TJ, Enomoto H, Simburger KS, Leitner ML, Araki T, Johnson EM, Jr., Milbrandt J (1998). Artemin, a novel member of the GDNF ligand family, supports peripheral and central neurons and signals through the GFRalpha3-RET receptor complex. Neuron 21: 1291-1302.

Bamji SX, Majdan M, Pozniak CD, Belliveau DJ, Aloyz R, Kohn J, Causing CG, Miller FD (1998). The p75 neurotrophin receptor mediates neuronal apoptosis and is essential for naturally occurring sympathetic neuron death. J Cell Biol 140: 911-923.

Banks WA, Kastin AJ (1991). Blood to brain transport of interleukin links the immune and central nervous systems. Life Sci 48: PL117-121.

Bar-On E, Floman Y, Sagiv S, Katz K, Pollak RD, Maayan C (2000). Orthopaedic manifestations of familial dysautonomia. A review of one hundred and thirty-six patients. J Bone Joint Surg Am 82-A: 1563-1570.

Barao I (2012). The TNF receptor-ligands 4-1BB-4-1BBL and GITR-GITRL in NK cell responses. Front Immunol 3: 402.

Barker PA, Shooter EM (1994). Disruption of NGF binding to the low affinity neurotrophin receptor p75LNTR reduces NGF binding to TrkA on PC12 cells. Neuron 13: 203-215.

Beigelman A, Levy J, Hadad N, Pinsk V, Haim A, Fruchtman Y, Levy R (2009). Abnormal neutrophil chemotactic activity in children with congenital insensitivity to pain with anhidrosis (CIPA): the role of nerve growth factor. Clinical immunology (Orlando, Fla) 130: 365-372.

Beissert S, Schwarz A, Schwarz T (2006). Regulatory T cells. J Invest Dermatol 126: 15-24.

Bellinger DL, Brouxhon SM, Lubahn C, Tran L, Kang JI, Felten DL, Lorton D (2001). Strain differences in the expression of corticotropin-releasing hormone immunoreactivity in nerves that supply the spleen and thymus. Neuroimmunomodulation 9: 78-87.

Berkemeier LR, Winslow JW, Kaplan DR, Nikolics K, Goeddel DV, Rosenthal A (1991). Neurotrophin-5: a novel neurotrophic factor that activates trk and trkB. Neuron 7: 857-866.

Besedovsky HO, del Rey A (1992). Immune-neuroendocrine circuits: integrative role of cytokines. Front Neuroendocrinol 13: 61-94.

Besedovsky HO, del Rey A (1996). Immune-neuro-endocrine interactions: facts and hypotheses. Endocr Rev 17: 64-102.

Birchmeier C, Gherardi E (1998). Developmental roles of HGF/SF and its receptor, the c-Met tyrosine kinase. Trends Cell Biol 8: 404-410.

Bitar MS, Pilcher CW, Khan I, Waldbillig RJ (1997). Diabetes-induced suppression of IGF-1 and its receptor mRNA levels in rat superior cervical ganglia. Diabetes Res Clin Pract 38: 73-80.

Blume-Jensen P, Hunter T (2001). Oncogenic kinase signalling. Nature 411: 355-365.

Bodmer D, Ascano M, Kuruvilla R (2011). Isoform-specific dephosphorylation of dynamin1 by calcineurin couples neurotrophin receptor endocytosis to axonal growth. Neuron 70: 1085-1099.

Bogoyevitch MA, Court NW (2004). Counting on mitogen-activated protein kinases--ERKs 3, 4, 5, 6, 7 and 8. Cell Signal 16: 1345-1354.

Bonizzi G, Karin M (2004). The two NF-kappaB activation pathways and their role in innate and adaptive immunity. Trends Immunol 25: 280-288.

Bossen C, Ingold K, Tardivel A, Bodmer JL, Gaide O, Hertig S, Ambrose C, Tschopp J, Schneider P (2006). Interactions of tumor necrosis factor (TNF) and TNF receptor family members in the mouse and human. J Biol Chem 281: 13964-13971.

Botchkina GI, Geimonen E, Bilof ML, Villarreal O, Tracey KJ (1999). Loss of NF-kappaB activity during cerebral ischemia and TNF cytotoxicity. Mol Med 5: 372-381.

Boulton TG, Gregory JS, Cobb MH (1991). Purification and properties of extracellular signal-regulated kinase 1, an insulin-stimulated microtubule-associated protein 2 kinase. Biochemistry 30: 278-286.

Britsch S, Li L, Kirchhoff S, Theuring F, Brinkmann V, Birchmeier C, Riethmacher D (1998). The ErbB2 and ErbB3 receptors and their ligand, neuregulin-1, are essential for development of the sympathetic nervous system. Genes Dev 12: 1825-1836.

Cai Z, Pan ZL, Pang Y, Evans OB, Rhodes PG (2000). Cytokine induction in fetal rat brains and brain injury in neonatal rats after maternal lipopolysaccharide administration. Pediatr Res 47: 64-72.

Campenot RB (1994). NGF and the local control of nerve terminal growth. J Neurobiol 25: 599-611.

Campenot RB, Draker DD, Senger DL (1994). Evidence that protein kinase C activities involved in regulating neurite growth are localized to distal neurites. J Neurochem 63: 868-878.

Cano G, Sved AF, Rinaman L, Rabin BS, Card JP (2001). Characterization of the central nervous system innervation of the rat spleen using viral transneuronal tracing. J Comp Neurol 439: 1-18.

Canossa M, Twiss JL, Verity AN, Shooter EM (1996). p75(NGFR) and TrkA receptors collaborate to rapidly activate a p75(NGFR)-associated protein kinase. The EMBO journal 15: 3369-3376.

Cardona ID, Goleva E, Ou LS, Leung DY (2006). Staphylococcal enterotoxin B inhibits regulatory T cells by inducing glucocorticoid-induced TNF receptor-related protein ligand on monocytes. J Allergy Clin Immunol 117: 688-695.

Casademunt E, Carter BD, Benzel I, Frade JM, Dechant G, Barde YA (1999). The zinc finger protein NRIF interacts with the neurotrophin receptor p75(NTR) and participates in programmed cell death. The EMBO journal 18: 6050-6061.

Caunt CJKSM (2012). Dual-specificity MAP kinase phosphatases (MKPs): shaping the outcome of MAP kinase signalling. FEBS J 280: 489-504.

Centner CM, Bateman KJ, Heckmann JM (2013). Manifestations of HIV infection in the peripheral nervous system. Lancet Neurol 12: 295-309.

Chang L, Karin M (2001). Mammalian MAP kinase signalling cascades. Nature 410: 37-40.

Chao MV, Hempstead BL (1995). p75 and Trk: a two-receptor system. Trends Neurosci 18: 321-326.
Chen FE, Huang DB, Chen YQ, Ghosh G (1998). Crystal structure of p50/p65 heterodimer of transcription factor NF-kappaB bound to DNA. Nature 391: 410-413.

Chen LF, Greene WC (2004). Shaping the nuclear action of NF-kappaB. Nat Rev Mol Cell Biol 5: 392-401.

Chun LL, Patterson PH (1977). Role of nerve growth factor in the development of rat sympathetic neurons in vitro. I. Survival, growth, and differentiation of catecholamine production. J Cell Biol 75: 694-704.

Cohen AD, Schaer DA, Liu C, Li Y, Hirschhorn-Cymmerman D, Kim SC, Diab A, Rizzuto G, Duan F, Perales MA, Merghoub T, Houghton AN, Wolchok JD (2010). Agonist anti-GITR monoclonal antibody induces melanoma tumor immunity in mice by altering regulatory T cell stability and intra-tumor accumulation. PloS one 5: e10436.

Cohen S, Levi-Montalcini R, Hamburger V (1954). A NERVE GROWTH-STIMULATING FACTOR ISOLATED FROM SARCOM AS 37 AND 180. Proc Natl Acad Sci U S A 40: 1014-1018.

Cole SW, Jamieson BD, Zack JA (1999). cAMP up-regulates cell surface expression of lymphocyte CXCR4: implications for chemotaxis and HIV-1 infection. J Immunol 162: 1392-1400.

Cole SW, Korin YD, Fahey JL, Zack JA (1998). Norepinephrine accelerates HIV replication via protein kinase A-dependent effects on cytokine production. J Immunol 161: 610-616.

Cosmi L, Liotta F, Lazzeri E, Francalanci M, Angeli R, Mazzinghi B, Santarlasci V, Manetti R, Vanini V, Romagnani P, Maggi E, Romagnani S, Annunziato F (2003). Human CD8+CD25+ thymocytes share phenotypic and functional features with CD4+CD25+ regulatory thymocytes. Blood 102: 4107-4114.

Crowley C, Spencer SD, Nishimura MC, Chen KS, Pitts-Meek S, Armanini MP, Ling LH, McMahon SB, Shelton DL, Levinson AD, et al. (1994). Mice lacking nerve growth factor display perinatal loss of sensory and
sympathetic neurons yet develop basal forebrain cholinergic neurons. Cell 76: 1001-1011.

Cuzzocrea S, Nocentini G, Di Paola R, Agostini M, Mazzon E, Ronchetti S, Crisafulli C, Esposito E, Caputi AP, Riccardi C (2006). Proinflammatory role of glucocorticoid-induced TNF receptor-related gene in acute lung inflammation. J Immunol 177: 631-641.

Davies AM, Bandtlow C, Heumann R, Korsching S, Rohrer H, Thoenen H (1987). Timing and site of nerve growth factor synthesis in developing skin in relation to innervation and expression of the receptor. Nature 326: 353-358.

Davies AM, Lee KF, Jaenisch R (1993). p75-deficient trigeminal sensory neurons have an altered response to NGF but not to other neurotrophins. Neuron 11: 565-574.

Debby-Brafman A, Burstyn-Cohen T, Klar A, Kalcheim C (1999). F-Spondin, expressed in somite regions avoided by neural crest cells, mediates inhibition of distinct somite domains to neural crest migration. Neuron 22: 475-488.

Deckwerth TL, Elliott JL, Knudson CM, Johnson EM, Jr., Snider WD, Korsmeyer SJ (1996). BAX is required for neuronal death after trophic factor deprivation and during development. Neuron 17: 401-411.

Dempsey PW, Doyle SE, He JQ, Cheng G (2003). The signaling adaptors and pathways activated by TNF superfamily. Cytokine Growth Factor Rev 14: 193-209.

Denes A, Boldogkoi Z, Uhereczky G, Hornyak A, Rusvai M, Palkovits M, Kovacs KJ (2005). Central autonomic control of the bone marrow: multisynaptic tract tracing by recombinant pseudorabies virus. Neuroscience 134: 947-963.

Deppmann CD, Mihalas S, Sharma N, Lonze BE, Niebur E, Ginty DD (2008). A model for neuronal competition during development. Science 320: 369-373.

Deshmukh M, Johnson EM, Jr. (1997). Programmed cell death in neurons: focus on the pathway of nerve growth factor deprivation-induced death of sympathetic neurons. Mol Pharmacol 51: 897-906.

DiCicco-Bloom E, Black IB (1988). Insulin growth factors regulate the mitotic cycle in cultured rat sympathetic neuroblasts. Proc Natl Acad Sci U S A 85: 4066-4070.

Dixon JE, McKinnon D (1994). Expression of the trk gene family of neurotrophin receptors in prevertebral sympathetic ganglia. Brain Res Dev Brain Res 77: 177-182.

Doherty GJ, McMahon HT (2009). Mechanisms of endocytosis. Annu Rev Biochem 78: 857-902.

Dong C, Waters SB, Holt KH, Pessin JE (1996). SOS phosphorylation and disassociation of the Grb2-SOS complex by the ERK and JNK signaling pathways. J Biol Chem 271: 6328-6332.

Durbec PL, Larsson-Blomberg LB, Schuchardt A, Costantini F, Pachnis V (1996). Common origin and developmental dependence on c-ret of subsets of enteric and sympathetic neuroblasts. Development 122: 349-358.

Edwards RH, Rutter WJ, Hanahan D (1989). Directed expression of NGF to pancreatic beta cells in transgenic mice leads to selective hyperinnervation of the islets. Cell 58: 161-170.

Eickholt BJ, Mackenzie SL, Graham A, Walsh FS, Doherty P (1999). Evidence for collapsin-1 functioning in the control of neural crest migration in both trunk and hindbrain regions. Development 126: 2181-2189.

Eldredge LC, Gao XM, Quach DH, Li L, Han X, Lomasney J, Tourtellotte WG (2008). Abnormal sympathetic nervous system development and physiological dysautonomia in Egr3-deficient mice. Development 135: 2949-2957.

ElShamy WM, Linnarsson S, Lee KF, Jaenisch R, Ernfors P (1996). Prenatal and postnatal requirements of NT-3 for sympathetic neuroblast survival and innervation of specific targets. Development 122: 491-500.

Enomoto H, Crawford PA, Gorodinsky A, Heuckeroth RO, Johnson EM, Jr., Milbrandt J (2001). RET signaling is essential for migration, axonal growth and axon guidance of developing sympathetic neurons. Development 128: 3963-3974.

Erickson CA, Loring JF, Lester SM (1989). Migratory pathways of HNK-1-immunoreactive neural crest cells in the rat embryo. Dev Biol 134: 112-118.

Esler MD, Hasking GJ, Willett IR, Leonard PW, Jennings GL (1985). Noradrenaline release and sympathetic nervous system activity. J Hypertens 3: 117-129.

Esparza EM, Arch RH (2004). TRAF4 functions as an intermediate of GITR-induced NF-kappaB activation. Cell Mol Life Sci 61: 3087-3092.

Esparza EM, Arch RH (2005a). Glucocorticoid-induced TNF receptor functions as a costimulatory receptor that promotes survival in early phases of T cell activation. J Immunol 174: 7869-7874.

Esparza EM, Arch RH (2005b). Glucocorticoid-induced TNF receptor, a costimulatory receptor on naive and activated T cells, uses TNF receptor-associated factor 2 in a novel fashion as an inhibitor of NF-kappa B activation. J Immunol 174: 7875-7882.

Esparza EM, Lindsten T, Stockhausen JM, Arch RH (2006). Tumor necrosis factor receptor (TNFR)-associated factor 5 is a critical intermediate of costimulatory signaling pathways triggered by glucocorticoid-induced TNFR in T cells. J Biol Chem 281: 8559-8564.

Esposito D, Patel P, Stephens RM, Perez P, Chao MV, Kaplan DR, Hempstead BL (2001). The cytoplasmic and transmembrane domains of the p75 and Trk A receptors regulate high affinity binding to nerve growth factor. J Biol Chem 276: 32687-32695.

Falls DL (2003). Neuregulins: functions, forms, and signaling strategies. Exp Cell Res 284: 14-30.

Felten DL, Felten SY, Carlson SL, Olschowka JA, Livnat S (1985). Noradrenergic and peptidergic innervation of lymphoid tissue. J Immunol 135: 755s-765s.

Ferrell JE, Jr., Bhatt RR (1997). Mechanistic studies of the dual phosphorylation of mitogen-activated protein kinase. J Biol Chem 272: 19008-19016.

Finch AR, Caunt CJ, Perrett RM, Tsaneva-Atanasova K, McArdle CA (2012). Dual specificity phosphatases 10 and 16 are positive regulators of EGF-stimulated ERK activity: indirect regulation of ERK signals by JNK/p38 selective MAPK phosphatases. Cell Signal 24: 1002-1011.

Frade JM, Barde YA (1998). Nerve growth factor: two receptors, multiple functions. Bioessays 20: 137-145.

Gallagher D, Gutierrez H, Gavalda N, O'Keeffe G, Hay R, Davies AM (2007). Nuclear factor-kappaB activation via tyrosine phosphorylation of inhibitor kappaB-alpha is crucial for ciliary neurotrophic factor-promoted neurite growth from developing neurons. The Journal of neuroscience : the official journal of the Society for Neuroscience 27: 9664-9669.

Gavalda N, Gutierrez H, Davies AM (2009a). Developmental regulation of sensory neurite growth by the tumor necrosis factor superfamily member LIGHT. The Journal of neuroscience : the official journal of the Society for Neuroscience 29: 1599-1607.

Gavalda N, Gutierrez H, Davies AM (2009b). Developmental switch in NF-kappaB signalling required for neurite growth. Development 136: 3405-3412.

Ghali J, Murugasu A, Day T, Nicholls K (2012). Carpal tunnel syndrome in fabry disease. JIMD Rep 2: 17-23.

Giger RJ, Wolfer DP, De Wit GM, Verhaagen J (1996). Anatomy of rat semaphorin III/collapsin-1 mRNA expression and relationship to developing nerve tracts during neuroembryogenesis. J Comp Neurol 375: 378-392.

Gilmore TD (2006). Introduction to NF-kappaB: players, pathways, perspectives. Oncogene 25: 6680-6684.

Glebova NO, Ginty DD (2004). Heterogeneous requirement of NGF for sympathetic target innervation in vivo. The Journal of neuroscience : the official journal of the Society for Neuroscience 24: 743-751.

Glebova NO, Ginty DD (2005). Growth and survival signals controlling sympathetic nervous system development. Annu Rev Neurosci 28: 191-222.

Goldstein DS (1987). Stress-induced activation of the sympathetic nervous system. Baillieres Clin Endocrinol Metab 1: 253-278.

Gondek DC, Lu LF, Quezada SA, Sakaguchi S, Noelle RJ (2005). Cutting edge: contact-mediated suppression by CD4+CD25+ regulatory cells involves a granzyme B-dependent, perforin-independent mechanism. J Immunol 174: 1783-1786.

Goold RG, Gordon-Weeks PR (2005). The MAP kinase pathway is upstream of the activation of GSK3beta that enables it to phosphorylate MAP1B and contributes to the stimulation of axon growth. Mol Cell Neurosci 28: 524-534.

Goridis C, Rohrer H (2002). Specification of catecholaminergic and serotonergic neurons. Nat Rev Neurosci 3: 531-541.

Graef IA, Wang F, Charron F, Chen L, Neilson J, Tessier-Lavigne M, Crabtree GR (2003). Neurotrophins and netrins require calcineurin/NFAT signaling to stimulate outgrowth of embryonic axons. Cell 113: 657-670.

Greene LA (1977). Quantitative in vitro studies on the nerve growth factor (NGF) requirement of neurons. I. Sympathetic neurons. Dev Biol 58: 96-105.

Grohmann U, Volpi C, Fallarino F, Bozza S, Bianchi R, Vacca C, Orabona C, Belladonna ML, Ayroldi E,
Nocentini G, Boon L, Bistoni F, Fioretti MC, Romani L, Riccardi C, Puccetti P (2007). Reverse signaling through GITR ligand enables dexamethasone to activate IDO in allergy. Nat Med 13: 579-586.

Gurney AL, Marsters SA, Huang RM, Pitti RM, Mark DT, Baldwin DT, Gray AM, Dowd AD, Brush AD,
Heldens AD, Schow AD, Goddard AD, Wood WI, Baker KP, Godowski PJ, Ashkenazi A (1999). Identification of a new member of the tumor necrosis factor family and its receptor, a human ortholog of mouse GITR. Curr Biol 9: 215-218.

Gutierrez H, Davies AM (2011). Regulation of neural process growth, elaboration and structural plasticity by NF-kappaB. Trends Neurosci 34: 316-325.

Gutierrez H, Hale VA, Dolcet X, Davies A (2005). NF-kappaB signalling regulates the growth of neural processes in the developing PNS and CNS. Development 132: 1713-1726.

Gutierrez H, Kisiswa L, O'Keeffe GW, Smithen MJ, Wyatt S, Davies AM (2013). Regulation of neurite growth by tumour necrosis superfamily member RANKL. Open Biol 3: 120150.

Gutierrez H, O'Keeffe GW, Gavalda N, Gallagher D, Davies AM (2008). Nuclear factor kappa B signaling either stimulates or inhibits neurite growth depending on the phosphorylation status of p65/RelA. J Neurosci 28: 8246-8256.

Hacker H, Karin M (2006). Regulation and function of IKK and IKK-related kinases. Sci STKE 2006: re13.

Haghir H, Rezaee AA, Sankian M, Kheradmand H, Hami J (2013). The effects of induced type-I diabetes on developmental regulation of insulin & insulin like growth factor-1 (IGF-1) receptors in the cerebellum of rat neonates. Metab Brain Dis.

Hall DM, Suo JL, Weber RJ (1998). Opioid mediated effects on the immune system: sympathetic nervous system involvement. J Neuroimmunol 83: 29-35.

Hallbook F, Ibanez CF, Persson H (1991). Evolutionary studies of the nerve growth factor family reveal a novel member abundantly expressed in Xenopus ovary. Neuron 6: 845-858.

Hamanoue M, Middleton G, Wyatt S, Jaffray E, Hay RT, Davies AM (1999). p75-mediated NF-kappaB activation enhances the survival response of developing sensory neurons to nerve growth factor. Mol Cell Neurosci 14: 28-40.

Hanabuchi S, Watanabe N, Wang YH, Ito T, Shaw J, Cao W, Qin FX, Liu YJ (2006). Human plasmacytoid predendritic cells activate NK cells through glucocorticoid-induced tumor necrosis factor receptor-ligand (GITRL). Blood 107: 3617-3623.

Harrington AW, Ginty DD (2013). Long-distance retrograde neurotrophic factor signalling in neurons. Nat Rev Neurosci 14: 177-187.

Hauer J, Puschner S, Ramakrishnan P, Simon U, Bongers M, Federle C, Engelmann H (2005). TNF receptor (TNFR)-associated factor (TRAF) 3 serves as an inhibitor of TRAF2/5-mediated activation of the noncanonical NF-kappaB pathway by TRAF-binding TNFRs. Proc Natl Acad Sci U S A 102: 2874-2879.

Hayden MS, Ghosh S (2004). Signaling to NF-kappaB. Genes Dev 18: 2195-2224.

Hayden MS, West AP, Ghosh S (2006). NF-kappaB and the immune response. Oncogene 25: 6758-6780.

Heumann R, Korsching S, Scott J, Thoenen H (1984). Relationship between levels of nerve growth factor (NGF) and its messenger RNA in sympathetic ganglia and peripheral target tissues. The EMBO journal 3: 3183-3189.

Hoffmann A, Natoli G, Ghosh G (2006). Transcriptional regulation via the NF-kappaB signaling module. Oncogene 25: 6706-6716.

Honma Y, Araki T, Gianino S, Bruce A, Heuckeroth R, Johnson E, Milbrandt J (2002). Artemin is a vascular-derived neurotropic factor for developing sympathetic neurons. Neuron 35: 267-282.

Horton A, Laramee G, Wyatt S, Shih A, Winslow J, Davies AM (1997). NGF binding to p75 enhances the sensitivity of sensory and sympathetic neurons to NGF at different stages of development. Mol Cell Neurosci 10: 162-172.

Huang EJ, Reichardt LF (2003). Trk receptors: roles in neuronal signal transduction. Annu Rev Biochem 72: 609-642.

Indo Y, Tsuruta M, Hayashida Y, Karim MA, Ohta K, Kawano T, Mitsubuchi H, Tonoki H, Awaya Y, Matsuda I (1996). Mutations in the TRKA/NGF receptor gene in patients with congenital insensitivity to pain with anhidrosis. Nature genetics 13: 485-488.

Jelinek T, Dent P, Sturgill TW, Weber MJ (1996). Ras-induced activation of Raf-1 is dependent on tyrosine phosphorylation. Mol Cell Biol 16: 1027-1034.

Johnson GL, Lapadat R (2002). Mitogen-activated protein kinase pathways mediated by ERK, JNK, and p38 protein kinases. Science 298: 1911-1912.

Kamenov ZA, Traykov LD (2012). Diabetic autonomic neuropathy. Adv Exp Med Biol 771: 176-193.

Kammer GM (1988). The adenylate cyclase-cAMP-protein kinase A pathway and regulation of the immune response. Immunol Today 9: 222-229.

Kanamaru F, Youngnak P, Hashiguchi M, Nishioka T, Takahashi T, Sakaguchi S, Ishikawa I, Azuma M (2004). Costimulation via glucocorticoid-induced TNF receptor in both conventional and CD25+ regulatory CD4+ T cells. J Immunol 172: 7306-7314.

Kaplan DR, Miller FD (1997). Signal transduction by the neurotrophin receptors. Curr Opin Cell Biol 9: 213-221.

Kaplan DR, Miller FD (2000). Neurotrophin signal transduction in the nervous system. Curr Opin Neurobiol 10: 381-391.

Karin M (1999). How NF-kappaB is activated: the role of the IkappaB kinase (IKK) complex. Oncogene 18: 6867-6874.

Karin M, Ben-Neriah Y (2000). Phosphorylation meets ubiquitination: the control of NF-[kappa]B activity. Annu Rev Immunol 18: 621-663.

Kawakami A, Kitsukawa T, Takagi S, Fujisawa H (1996). Developmentally regulated expression of a cell surface protein, neuropilin, in the mouse nervous system. J Neurobiol 29: 1-17.

Kawasaki T, Bekku Y, Suto F, Kitsukawa T, Taniguchi M, Nagatsu I, Nagatsu T, Itoh K, Yagi T, Fujisawa H (2002). Requirement of neuropilin 1-mediated Sema3A signals in patterning of the sympathetic nervous system. Development 129: 671-680.

Kenchappa RS, Tep C, Korade Z, Urra S, Bronfman FC, Yoon SO, Carter BD (2010). p75 neurotrophin receptor-mediated apoptosis in sympathetic neurons involves a biphasic activation of JNK and up-regulation of tumor necrosis factor-alpha-converting enzyme/ADAM17. J Biol Chem 285: 20358-20368.

Kim BJ, Li Z, Fariss RN, Shen DF, Mahesh SP, Egwuagu C, Yu CR, Nagineni CN, Chan CC, Nussenblatt RB (2004). Constitutive and cytokine-induced GITR ligand expression on human retinal pigment epithelium and photoreceptors. Invest Ophthalmol Vis Sci 45: 3170-3176.

Kim HJ, Kim HY, Kim BK, Kim S, Chung DH (2006). Engagement of glucocorticoid-induced TNF receptor costimulates NKT cell activation in vitro and in vivo. J Immunol 176: 3507-3515.

Kim JD, Choi BK, Bae JS, Lee UH, Han IS, Lee HW, Youn BS, Vinay DS, Kwon BS (2003a). Cloning and characterization of GITR ligand. Genes Immun 4: 564-569.

Kim JY, Sun Q, Oglesbee M, Yoon SO (2003b). The role of ErbB2 signaling in the onset of terminal differentiation of oligodendrocytes in vivo. The Journal of neuroscience : the official journal of the Society for Neuroscience 23: 5561-5571.

Kisiswa L, Osorio C, Erice C, Vizard T, Wyatt S, Davies AM (2013). TNFalpha reverse signaling promotes sympathetic axon growth and target innervation. Nat Neurosci 16: 865-873.

Koblar SA, Krull CE, Pasquale EB, McLennan R, Peale FD, Cerretti DP, Bothwell M (2000). Spinal motor axons and neural crest cells use different molecular guides for segmental migration through the rostral half-somite. J Neurobiol 42: 437-447.

Kohm AP, Sanders VM (2001). Norepinephrine and beta 2-adrenergic receptor stimulation regulate CD4+ T and B lymphocyte function in vitro and in vivo. Pharmacol Rev 53: 487-525.

Kohm AP, Williams JS, Miller SD (2004). Cutting edge: ligation of the glucocorticoid-induced TNF receptor enhances autoreactive CD4+ T cell activation and experimental autoimmune encephalomyelitis. J Immunol 172: 4686-4690.

Korsching S, Thoenen H (1983). Nerve growth factor in sympathetic ganglia and corresponding target organs of the rat: correlation with density of sympathetic innervation. Proc Natl Acad Sci U S A 80: 3513-3516.

Korsching S, Thoenen H (1985). Treatment with 6-hydroxydopamine and colchicine decreases nerve growth factor levels in sympathetic ganglia and increases them in the corresponding target tissues. The Journal of neuroscience : the official journal of the Society for Neuroscience 5: 1058-1061.

Korsmeyer SJ (1999). BCL-2 gene family and the regulation of programmed cell death. Cancer Res 59: 1693s-1700s.

Krausz LT, Bianchini R, Ronchetti S, Fettucciari K, Nocentini G, Riccardi C (2007). GITR-GITRL system, a novel player in shock and inflammation. ScientificWorldJournal 7: 533-566.

Krull CE (2001). Segmental organization of neural crest migration. Mech Dev 105: 37-45.

Krull CE, Lansford R, Gale NW, Collazo A, Marcelle C, Yancopoulos GD, Fraser SE, Bronner-Fraser M (1997). Interactions of Eph-related receptors and ligands confer rostrocaudal pattern to trunk neural crest migration. Curr Biol 7: 571-580.

Kuruvilla R, Zweifel LS, Glebova NO, Lonze BE, Valdez G, Ye H, Ginty DD (2004). A neurotrophin signaling cascade coordinates sympathetic neuron development through differential control of TrkA trafficking and retrograde signaling. Cell 118: 243-255.

Kwon B, Yu KY, Ni J, Yu GL, Jang IK, Kim YJ, Xing L, Liu D, Wang SX, Kwon BS (1999). Identification of a novel activation-inducible protein of the tumor necrosis factor receptor superfamily and its ligand. J Biol Chem 274: 6056-6061.

Lafreniere RG, MacDonald ML, Dube MP, MacFarlane J, O'Driscoll M, Brais B, Meilleur S, Brinkman RR, Dadivas O, Pape T, Platon C, Radomski C, Risler J, Thompson J, Guerra-Escobio AM, Davar G, Breakefield XO, Pimstone SN, Green R, Pryse-Phillips W, Goldberg YP, Younghusband HB, Hayden MR, Sherrington R, Rouleau GA, Samuels ME (2004). Identification of a novel gene (HSN2) causing hereditary sensory and autonomic neuropathy type II through the Study of Canadian Genetic Isolates. American journal of human genetics 74: 1064-1073.

Langer J, Goebel HH, Veit S (1981). Eccrine sweat glands are not innervated in hereditary sensory neuropathy type IV. An electron-microscopic study. Acta Neuropathol 54: 199-202.

Langley JN (1898). On the Union of Cranial Autonomic (Visceral) Fibres with the Nerve Cells of the Superior Cervical Ganglion. J Physiol 23: 240-270.

Lanier LL (2005). NK cell recognition. Annu Rev Immunol 23: 225-274.

Lee KF, Bachman K, Landis S, Jaenisch R (1994a). Dependence on p75 for innervation of some sympathetic targets. Science 263: 1447-1449.

Lee KF, Davies AM, Jaenisch R (1994b). p75-deficient embryonic dorsal root sensory and neonatal sympathetic neurons display a decreased sensitivity to NGF. Development 120: 1027-1033.

Lee SJ, Chun MH, Kim BR, Kang Y, Kim DY, Park JY (2013). Measurements of anteroposterior and intersidal asymmetry in patients with diabetic peripheral neuropathy. Am J Phys Med Rehabil 92: 118-126.

Leibrock J, Lottspeich F, Hohn A, Hofer M, Hengerer B, Masiakowski P, Thoenen H, Barde YA (1989). Molecular cloning and expression of brain-derived neurotrophic factor. Nature 341: 149-152.

Levi-Montalcini R (1987). The nerve growth factor 35 years later. Science 237: 1154-1162.

Levi-Montalcini R, Angeletti PU (1968). Nerve growth factor. Physiol Rev 48: 534-569.

Levi-Montalcini R, Booker B (1960). DESTRUCTION OF THE SYMPATHETIC GANGLIA IN MAMMALS BY AN ANTISERUM TO A NERVE-GROWTH PROTEIN. Proc Natl Acad Sci U S A 46: 384-391.

Levi-Montalcini R, Hamburger V (1951). Selective growth stimulating effects of mouse sarcoma on the sensory and sympathetic nervous system of the chick embryo. J Exp Zool 116: 321-361.

Levitt M, Spector S, Sjoerdsma A, Udenfriend S (1965). ELUCIDATION OF THE RATE-LIMITING STEP IN NOREPINEPHRINE BIOSYNTHESIS IN THE PERFUSED GUINEA-PIG HEART. J Pharmacol Exp Ther 148: 1-8.

Lewin GR, Barde YA (1996). Physiology of the neurotrophins. Annu Rev Neurosci 19: 289-317.

Li L, Eldredge LC, Quach DH, Honasoge A, Gruner K, Tourtellotte WG (2011). Egr3 dependent sympathetic target tissue innervation in the absence of neuron death. PloS one 6: e25696.

Li N, Batzer A, Daly R, Yajnik V, Skolnik E, Chardin P, Bar-Sagi D, Margolis B, Schlessinger J (1993). Guanine-nucleotide-releasing factor hSos1 binds to Grb2 and links receptor tyrosine kinases to Ras signalling. Nature 363: 85-88.

Liang Y, Zhou Y, Shen P (2004). NF-kappaB and its regulation on the immune system. Cell Mol Immunol 1: 343-350.

Liepinsh E, Ilag LL, Otting G, Ibanez CF (1997). NMR structure of the death domain of the p75 neurotrophin receptor. The EMBO journal 16: 4999-5005.

Liu H, Margiotta JF, Howard MJ (2005). BMP4 supports noradrenergic differentiation by a PKA-dependent mechanism. Dev Biol 286: 521-536.

Liu JP, Baker J, Perkins AS, Robertson EJ, Efstratiadis A (1993). Mice carrying null mutations of the genes encoding insulin-like growth factor I (Igf-1) and type 1 IGF receptor (Igf1r). Cell 75: 59-72.

Liverman CS, Kaftan HA, Cui L, Hersperger SG, Taboada E, Klein RM, Berman NE (2006). Altered expression of pro-inflammatory and developmental genes in the fetal brain in a mouse model of maternal infection. Neuroscience letters 399: 220-225.

Lockhart ST, Turrigiano GG, Birren SJ (1997). Nerve growth factor modulates synaptic transmission between sympathetic neurons and cardiac myocytes. The Journal of neuroscience : the official journal of the Society for Neuroscience 17: 9573-9582.

Lonze BE, Riccio A, Cohen S, Ginty DD (2002). Apoptosis, axonal growth defects, and degeneration of peripheral neurons in mice lacking CREB. Neuron 34: 371-385.

Madden KS, Sanders VM, Felten DL (1995). Catecholamine influences and sympathetic neural modulation of immune responsiveness. Annu Rev Pharmacol Toxicol 35: 417-448.

Maden CH, Gomes J, Schwarz Q, Davidson K, Tinker A, Ruhrberg C (2012). NRP1 and NRP2 cooperate to regulate gangliogenesis, axon guidance and target innervation in the sympathetic nervous system. Dev Biol 369: 277-285.

Mahadeo D, Kaplan L, Chao MV, Hempstead BL (1994). High affinity nerve growth factor binding displays a faster rate of association than p140trk binding. Implications for multi-subunit polypeptide receptors. J Biol Chem 269: 6884-6891.

Maina F, Hilton MC, Andres R, Wyatt S, Klein R, Davies AM (1998). Multiple roles for hepatocyte growth factor in sympathetic neuron development. Neuron 20: 835-846.

Mains RE, Patterson PH (1973). Primary cultures of dissociated sympathetic neurons. I. Establishment of long-term growth in culture and studies of differentiated properties. J Cell Biol 59: 329-345.

Maisonpierre PC, Belluscio L, Friedman B, Alderson RF, Wiegand SJ, Furth ME, Lindsay RM, Yancopoulos GD (1990). NT-3, BDNF, and NGF in the developing rat nervous system: parallel as well as reciprocal patterns of expression. Neuron 5: 501-509.

Makol A, Grover M (2008). Adalimumab induced mononeuritis multiplex in a patient with refractory rheumatoid arthritis: a case report. Cases J 1: 287.

Marais R, Wynne J, Treisman R (1993). The SRF accessory protein Elk-1 contains a growth factor-regulated transcriptional activation domain. Cell 73: 381-393.

Mardy S, Miura Y, Endo F, Matsuda I, Sztriha L, Frossard P, Moosa A, Ismail EA, Macaya A, Andria G,
Toscano E, Gibson W, Graham GE, Indo Y (1999). Congenital insensitivity to pain with anhidrosis: novel mutations in the TRKA (NTRK1) gene encoding a high-affinity receptor for nerve growth factor. American journal of human genetics 64: 1570-1579.

Markus A, Patel TD, Snider WD (2002). Neurotrophic factors and axonal growth. Curr Opin Neurobiol 12: 523-531.

Marshall JS, Stead RH, McSharry C, Nielsen L, Bienenstock J (1990). The role of mast cell degranulation products in mast cell hyperplasia. I. Mechanism of action of nerve growth factor. J Immunol 144: 1886-1892.

Martin DP, Schmidt RE, DiStefano PS, Lowry OH, Carter JG, Johnson EM, Jr. (1988). Inhibitors of protein synthesis and RNA synthesis prevent neuronal death caused by nerve growth factor deprivation. J Cell Biol 106: 829-844.

Martini FH (2004). **Fundamentals of Anatomy and Physiology**. Pearson Education Inc, 1301 Sansome Street, San Francisco, CA 94111.

Matusica D, Skeldal S, Sykes AM, Palstra N, Sharma A, Coulson EJ (2013). An intracellular domain fragment of the p75 neurotrophin receptor (p75NTR) enhances TrkA receptor function. J Biol Chem.

Mayhew T (1991). The new stereological methods for interpreting functional morphology from slices of cells and organs.

McHugh RS, Whitters MJ, Piccirillo CA, Young DA, Shevach EM, Collins M, Byrne MC (2002). CD4(+)CD25(+) immunoregulatory T cells: gene expression analysis reveals a functional role for the glucocorticoid-induced TNF receptor. Immunity 16: 311-323.

Melamed I, Kelleher CA, Franklin RA, Brodie C, Hempstead B, Kaplan D, Gelfand EW (1996). Nerve growth factor signal transduction in human B lymphocytes is mediated by gp140trk. Eur J Immunol 26: 1985-1992.

Melamed I, Levy J, Parvari R, Gelfand EW (2004). A novel lymphocyte signaling defect: trk A mutation in the syndrome of congenital insensitivity to pain and anhidrosis (CIPA). Journal of clinical immunology 24: 441-448.

Melero I, Hirschhorn-Cymerman D, Morales-Kastresana A, Sanmamed MF, Wolchok JD (2013). Agonist Antibodies to TNFR Molecules That Costimulate T and NK Cells. Clin Cancer Res 19: 1044-1053.

Meloche S, Pouyssegur J (2007). The ERK1/2 mitogen-activated protein kinase pathway as a master regulator of the G1- to S-phase transition. Oncogene 26: 3227-3239.

Meltzer JC, Grimm PC, Greenberg AH, Nance DM (1997). Enhanced immunohistochemical detection of autonomic nerve fibers, cytokines and inducible nitric oxide synthase by light and fluorescent microscopy in rat spleen. J Histochem Cytochem 45: 599-610.

Minde J, Toolanen G, Andersson T, Nennesmo I, Remahl IN, Svensson O, Solders G (2004). Familial insensitivity to pain (HSAN V) and a mutation in the NGFB gene. A neurophysiological and pathological study. Muscle Nerve 30: 752-760.

Moberg G (2000). **The Biology of Animal Stress: Basic Principles and Implications for Animal Welfare** CABI Publishing, Cambridge, MA.

Nakae S, Suto H, Iikura M, Kakurai M, Sedgwick JD, Tsai M, Galli SJ (2006). Mast cells enhance T cell activation: importance of mast cell costimulatory molecules and secreted TNF. J Immunol 176: 2238-2248.

Nam J, Onitsuka I, Hatch J, Uchida Y, Ray S, Huang S, Li W, Zang H, Ruiz-Lozano P, Mukouyama YS (2013). Coronary veins determine the pattern of sympathetic innervation in the developing heart. Development 140: 1475-1485.

Nance DM, Burns J (1989). Innervation of the spleen in the rat: evidence for absence of afferent innervation. Brain Behav Immun 3: 281-290.

Nance DM, Hopkins DA, Bieger D (1987). Re-investigation of the innervation of the thymus gland in mice and rats. Brain Behav Immun 1: 134-147.

Nance DM, Sanders VM (2007). Autonomic innervation and regulation of the immune system (1987-2007). Brain Behav Immun 21: 736-745.

Nardelli B, Zaritskaya L, McAuliffe W, Ni Y, Lincoln C, Cho YH, Birse CE, Halpern W, Ullrich S, Moore PA (2006). Osteostat/tumor necrosis factor superfamily 18 inhibits osteoclastogenesis and is selectively expressed by vascular endothelial cells. Endocrinology 147: 70-78.

Nelson KB, Willoughby RE (2000). Infection, inflammation and the risk of cerebral palsy. Curr Opin Neurol 13: 133-139.

Neumann H, Schweigreiter R, Yamashita T, Rosenkranz K, Wekerle H, Barde YA (2002). Tumor necrosis factor inhibits neurite outgrowth and branching of hippocampal neurons by a rho-dependent mechanism. The Journal of neuroscience : the official journal of the Society for Neuroscience 22: 854-862.

Nishino J, Mochida K, Ohfuji Y, Shimazaki T, Meno C, Ohishi S, Matsuda Y, Fujii H, Saijoh Y, Hamada H (1999). GFR alpha3, a component of the artemin receptor, is required for migration and survival of the superior cervical ganglion. Neuron 23: 725-736.

Nobes CD, Tolkovsky AM (1995). Neutralizing anti-p21ras Fabs suppress rat sympathetic neuron survival induced by NGF, LIF, CNTF and cAMP. Eur J Neurosci 7: 344-350.

Nocentini G, Bartoli A, Ronchetti S, Giunchi L, Cupelli A, Delfino D, Migliorati G, Riccardi C (2000). Gene structure and chromosomal assignment of mouse GITR, a member of the tumor necrosis factor/nerve growth factor receptor family. DNA Cell Biol 19: 205-217.

Nocentini G, Giunchi L, Ronchetti S, Krausz LT, Bartoli A, Moraca R, Migliorati G, Riccardi C (1997). A new member of the tumor necrosis factor/nerve growth factor receptor family inhibits T cell receptor-induced apoptosis. Proc Natl Acad Sci U S A 94: 6216-6221.

Nocentini G, Riccardi C (2005). GITR: a multifaceted regulator of immunity belonging to the tumor necrosis factor receptor superfamily. Eur J Immunol 35: 1016-1022.

Nocentini G, Ronchetti S, Petrillo MG, Riccardi C (2012). Pharmacological modulation of GITRL/GITR system: therapeutic perspectives. Br J Pharmacol 165: 2089-2099.

Nolan AM, Nolan YM, O'Keeffe GW (2011). IL-1beta inhibits axonal growth of developing sympathetic neurons. Mol Cell Neurosci 48: 142-150.

O'Keeffe GW, Gutierrez H, Pandolfi PP, Riccardi C, Davies AM (2008). NGF-promoted axon growth and target innervation requires GITRL-GITR signaling. Nat Neurosci 11: 135-142.

Omerovic J, Prior IA (2009). Compartmentalized signalling: Ras proteins and signalling nanoclusters. FEBS J 276: 1817-1825.

Oppenheim RW (1989). The neurotrophic theory and naturally occurring motoneuron death. Trends Neurosci 12: 252-255.

Osborn SL, Sohn SJ, Winoto A (2007). Constitutive phosphorylation mutation in Fas-associated death domain (FADD) results in early cell cycle defects. J Biol Chem 282: 22786-22792.

Ottaway CA, Husband AJ (1994). The influence of neuroendocrine pathways on lymphocyte migration. Immunol Today 15: 511-517.

Otten U, Ehrhard P, Peck R (1989). Nerve growth factor induces growth and differentiation of human B lymphocytes. Proc Natl Acad Sci U S A 86: 10059-10063.

Panuncio AL, De La Pena S, Gualco G, Reissenweber N (1999). Adrenergic innervation in reactive human lymph nodes. J Anat 194 (Pt 1): 143-146.

Park YC, Burkitt V, Villa AR, Tong L, Wu H (1999). Structural basis for self-association and receptor recognition of human TRAF2. Nature 398: 533-538.

Patel TD, Jackman A, Rice FL, Kucera J, Snider WD (2000). Development of sensory neurons in the absence of NGF/TrkA signaling in vivo. Neuron 25: 345-357.

Pazyra-Murphy MF, Hans A, Courchesne SL, Karch C, Cosker KE, Heerssen HM, Watson FL, Kim T, Greenberg ME, Segal RA (2009). A retrograde neuronal survival response: target-derived neurotrophins regulate MEF2D and bcl-w. The Journal of neuroscience : the official journal of the Society for Neuroscience 29: 6700-6709.

Pearson G, Robinson F, Beers Gibson T, Xu BE, Karandikar M, Berman K, Cobb MH (2001). Mitogen-activated protein (MAP) kinase pathways: regulation and physiological functions. Endocr Rev 22: 153-183.

Pelicci G, Lanfrancone L, Grignani F, McGlade J, Cavallo F, Forni G, Nicoletti I, Pawson T, Pelicci PG (1992). A novel transforming protein (SHC) with an SH2 domain is implicated in mitogenic signal transduction. Cell 70: 93-104.

Perkins ND (2007). Integrating cell-signalling pathways with NF-kappaB and IKK function. Nat Rev Mol Cell Biol 8: 49-62.

Plante-Bordeneuve V, Said G (2011). Familial amyloid polyneuropathy. Lancet Neurol 10: 1086-1097.

Quach DH, Oliveira-Fernandes M, Gruner KA, Tourtellotte WG (2013). A sympathetic neuron autonomous role for egr3-mediated gene regulation in dendrite morphogenesis and target tissue innervation. The Journal of neuroscience : the official journal of the Society for Neuroscience 33: 4570-4583.

Rapp UR, Goldsborough MD, Mark GE, Bonner TI, Groffen J, Reynolds FH, Jr., Stephenson JR (1983). Structure and biological activity of v-raf, a unique oncogene transduced by a retrovirus. Proc Natl Acad Sci U S A 80: 4218-4222.

Reichardt LF (2006). Neurotrophin-regulated signalling pathways. Philos Trans R Soc Lond B Biol Sci 361: 1545-1564.

Reissmann E, Ernsberger U, Francis-West PH, Rueger D, Brickell PM, Rohrer H (1996). Involvement of bone morphogenetic protein-4 and bone morphogenetic protein-7 in the differentiation of the adrenergic phenotype in developing sympathetic neurons. Development 122: 2079-2088.

Rickmann M, Fawcett JW, Keynes RJ (1985). The migration of neural crest cells and the growth of motor axons through the rostral half of the chick somite. J Embryol Exp Morphol 90: 437-455.

Rio C, Rieff HI, Qi P, Khurana TS, Corfas G (1997). Neuregulin and erbB receptors play a critical role in neuronal migration. Neuron 19: 39-50.

Rodriguez-Tebar A, Dechant G, Barde YA (1990). Binding of brain-derived neurotrophic factor to the nerve growth factor receptor. Neuron 4: 487-492.

Roff M, Thompson J, Rodriguez MS, Jacque JM, Baleux F, Arenzana-Seisdedos F, Hay RT (1996). Role of IkappaBalpha ubiquitination in signal-induced activation of NFkappaB in vivo. J Biol Chem 271: 7844-7850.

Rojas M, Yao S, Lin YZ (1996). Controlling epidermal growth factor (EGF)-stimulated Ras activation in intact cells by a cell-permeable peptide mimicking phosphorylated EGF receptor. J Biol Chem 271: 27456-27461.

Ronchetti S, Zollo O, Bruscoli S, Agostini M, Bianchini R, Nocentini G, Ayroldi E, Riccardi C (2004). GITR, a member of the TNF receptor superfamily, is costimulatory to mouse T lymphocyte subpopulations. Eur J Immunol 34: 613-622.

Rothwarf DM, Karin M (1999). The NF-kappa B activation pathway: a paradigm in information transfer from membrane to nucleus. Sci STKE 1999: RE1.

Rotthier A, Baets J, Timmerman V, Janssens K (2012). Mechanisms of disease in hereditary sensory and autonomic neuropathies. Nat Rev Neurol 8: 73-85.

Roux PP, Blenis J (2004). ERK and p38 MAPK-activated protein kinases: a family of protein kinases with diverse biological functions. Microbiol Mol Biol Rev 68: 320-344.

Rubin E (1985a). Development of the rat superior cervical ganglion: ganglion cell maturation. The Journal of neuroscience : the official journal of the Society for Neuroscience 5: 673-684.

Rubin E (1985b). Development of the rat superior cervical ganglion: ingrowth of preganglionic axons. The Journal of neuroscience : the official journal of the Society for Neuroscience 5: 685-696.

Rubin E (1985c). Development of the rat superior cervical ganglion: initial stages of synapse formation. The Journal of neuroscience : the official journal of the Society for Neuroscience 5: 697-704.

Ruohonen ST, Abe K, Kero M, Toukola L, Ruohonen S, Roytta M, Koulu M, Pesonen U, Zukowska Z, Savontaus E (2009). Sympathetic nervous system-targeted neuropeptide Y overexpression in mice enhances
neointimal formation in response to vascular injury. Peptides 30: 715-720.

Ryu YK, Collins SE, Ho HY, Zhao H, Kuruvilla R (2013). An autocrine Wnt5a-Ror signaling loop mediates sympathetic target innervation. Dev Biol.

Sakaguchi S, Sakaguchi N, Asano M, Itoh M, Toda M (1995). Immunologic self-tolerance maintained by activated T cells expressing IL-2 receptor alpha-chains (CD25). Breakdown of a single mechanism of self-tolerance causes various autoimmune diseases. J Immunol 155: 1151-1164.

Sanders VM, Straub RH (2002). Norepinephrine, the beta-adrenergic receptor, and immunity. Brain Behav Immun 16: 290-332.

Santucci L, Agostini M, Bruscoli S, Mencarelli A, Ronchetti S, Ayroldi E, Morelli A, Baldoni M, Riccardi C (2007). GITR modulates innate and adaptive mucosal immunity during the development of experimental colitis
in mice. Gut 56: 52-60.

Sarasola E, Rodriguez JA, Garrote E, Aristegui J, Garcia-Barcina MJ (2011). A short in-frame deletion in NTRK1 tyrosine kinase domain caused by a novel splice site mutation in a patient with congenital insensitivity to pain with anhidrosis. BMC medical genetics 12: 86.

Schaer DA, Murphy JT, Wolchok JD (2012). Modulation of GITR for cancer immunotherapy. Curr Opin Immunol 24: 217-224.

Scheidereit C (2006). IkappaB kinase complexes: gateways to NF-kappaB activation and transcription. Oncogene 25: 6685-6705.

Schneider C, Wicht H, Enderich J, Wegner M, Rohrer H (1999). Bone morphogenetic proteins are required in vivo for the generation of sympathetic neurons. Neuron 24: 861-870.

Scotto L, Naiyer AJ, Galluzzo S, Rossi P, Manavalan JS, Kim-Schulze S, Fang J, Favera RD, Cortesini R,
Suciu-Foca N (2004). Overlap between molecular markers expressed by naturally occurring CD4+CD25+ regulatory T cells and antigen specific CD4+CD25+ and CD8+CD28- T suppressor cells. Hum Immunol 65: 1297-1306.

Sears R, Nuckolls F, Haura E, Taya Y, Tamai K, Nevins JR (2000). Multiple Ras-dependent phosphorylation pathways regulate Myc protein stability. Genes Dev 14: 2501-2514.

Senftleben U, Cao Y, Xiao G, Greten FR, Krahn G, Bonizzi G, Chen Y, Hu Y, Fong A, Sun SC, Karin M (2001). Activation by IKKalpha of a second, evolutionary conserved, NF-kappa B signaling pathway. Science 293: 1495-1499.

Shao Y, Akmentin W, Toledo-Aral JJ, Rosenbaum J, Valdez G, Cabot JB, Hilbush BS, Halegoua S (2002). Pincher, a pinocytic chaperone for nerve growth factor/TrkA signaling endosomes. J Cell Biol 157: 679-691.

Sharma N, Deppmann CD, Harrington AW, St Hillaire C, Chen ZY, Lee FS, Ginty DD (2010). Long-distance control of synapse assembly by target-derived NGF. Neuron 67: 422-434.

Shatzky S, Moses S, Levy J, Pinsk V, Hershkovitz E, Herzog L, Shorer Z, Luder A, Parvari R (2000). Congenital insensitivity to pain with anhidrosis (CIPA) in Israeli-Bedouins: genetic heterogeneity, novel mutations in the TRKA/NGF receptor gene, clinical findings, and results of nerve conduction studies. American journal of medical genetics 92: 353-360.

Shevach EM, Stephens GL (2006). The GITR-GITRL interaction: co-stimulation or contrasuppression of regulatory activity? Nat Rev Immunol 6: 613-618.

Shimizu J, Yamazaki S, Takahashi T, Ishida Y, Sakaguchi S (2002). Stimulation of CD25(+)CD4(+) regulatory T cells through GITR breaks immunological self-tolerance. Nat Immunol 3: 135-142.

Shimizu N, Hori T, Nakane H (1994). An interleukin-1 beta-induced noradrenaline release in the spleen is mediated by brain corticotropin-releasing factor: an in vivo microdialysis study in conscious rats. Brain Behav
Immun 8: 14-23.

Shin HH, Kim SG, Lee MH, Suh JH, Kwon BS, Choi HS (2003). Soluble glucocorticoid-induced TNF receptor (sGITR) induces inflammation in mice. Exp Mol Med 35: 358-364.

Shin HH, Kim SJ, Kang SY, Lee DS, Choi HS (2006). Soluble glucocorticoid-induced tumor necrosis factor receptor stimulates osteoclastogenesis by down-regulation of osteoprotegerin in bone marrow stromal cells. Bone 39: 716-723.

Shin HH, Kim SJ, Lee DS, Choi HS (2005). Soluble glucocorticoid-induced tumor necrosis factor receptor (sGITR) stimulates osteoclast differentiation in response to receptor activator of NF-kappaB ligand (RANKL) in osteoclast cells. Bone 36: 832-839.

Sofroniew MV, Howe CL, Mobley WC (2001). Nerve growth factor signaling, neuroprotection, and neural repair. Annu Rev Neurosci 24: 1217-1281.

Stephens GL, McHugh RS, Whitters MJ, Young DA, Luxenberg D, Carreno BM, Collins M, Shevach EM (2004). Engagement of glucocorticoid-induced TNFR family-related receptor on effector T cells by its ligand mediates resistance to suppression by CD4+CD25+ T cells. J Immunol 173: 5008-5020.

Strakova J, Demizieux L, Campenot RB, Vance DE, Vance JE (2011). Involvement of CTP:phosphocholine cytidylyltransferase-beta2 in axonal phosphatidylcholine synthesis and branching of neurons. Biochim Biophys Acta 1811: 617-625.

Straub RH (2004). Complexity of the bi-directional neuroimmune junction in the spleen. Trends Pharmacol Sci 25: 640-646.

Suvas S, Kim B, Sarangi PP, Tone M, Waldmann H, Rouse BT (2005). In vivo kinetics of GITR and GITR ligand expression and their functional significance in regulating viral immunopathology. J Virol 79: 11935-11942.

Swanson AG (1963). Congenital insensitivity to pain with anhydrosis. A unique syndrome in two male siblings. Arch Neurol 8: 299-306.

Swanson AG, Buchan GC, Alvord EC, Jr. (1965). ANATOMIC CHANGES IN CONGENITAL INSENSITIVITY TO PAIN. ABSENCE OF SMALL PRIMARY SENSORY NEURONS IN GANGLIA, ROOTS, AND LISSAUER'S TRACT. Arch Neurol 12: 12-18.

Tergaonkar V (2006). NFkappaB pathway: a good signaling paradigm and therapeutic target. Int J Biochem Cell Biol 38: 1647-1653.

Thoenen H, Angeletti PU, Levi-Montalcini R, Kettler R (1971). Selective induction by nerve growth factor of tyrosine hydroxylase and dopamine- -hydroxylase in the rat superior cervical ganglia. Proc Natl Acad Sci U S A 68: 1598-1602.

Thompson J, Dolcet X, Hilton M, Tolcos M, Davies AM (2004). HGF promotes survival and growth of maturing sympathetic neurons by PI-3 kinase- and MAP kinase-dependent mechanisms. Mol Cell Neurosci 27: 441-452.

ThyagaRajan S, Madden KS, Teruya B, Stevens SY, Felten DL, Bellinger DL (2011). Age-associated alterations in sympathetic noradrenergic innervation of primary and secondary lymphoid organs in female Fischer 344 rats. J Neuroimmunol 233: 54-64.

Tone M, Tone Y, Adams E, Yates SF, Frewin MR, Cobbold SP, Waldmann H (2003). Mouse glucocorticoid-induced tumor necrosis factor receptor ligand is costimulatory for T cells. Proc Natl Acad Sci U S A 100: 15059-15064.

Toscano E, Andria G (2001). Congenital insensitivity to pain with anhidrosis: an NGF/TrkA-related disorder. American journal of medical genetics 99: 164-165.

Trier H, Krishnasamy VP, Kasi PM (2013). Clinical manifestations and diagnostic challenges in acute porphyrias. Case Rep Hematol 2013: 628602.

Tuttolomondo A, Simonetta I, Miceli S, Pinto A, Licata G (2013). Anderson-Fabry disease: a multiorgan disease. Curr Pharm Des.

Uraushihara K, Kanai T, Ko K, Totsuka T, Makita S, Iiyama R, Nakamura T, Watanabe M (2003). Regulation of murine inflammatory bowel disease by CD25+ and CD25- CD4+ glucocorticoid-induced TNF receptor family-related gene+ regulatory T cells. J Immunol 171: 708-716.

Verdi JM, Anderson DJ (1994). Neurotrophins regulate sequential changes in neurotrophin receptor expression by sympathetic neuroblasts. Neuron 13: 1359-1372.

Vizard TN, O'Keeffe GW, Gutierrez H, Kos CH, Riccardi D, Davies AM (2008). Regulation of axonal and dendritic growth by the extracellular calcium-sensing receptor. Nat Neurosci 11: 285-291.

Wan F, Anderson DE, Barnitz RA, Snow A, Bidere N, Zheng L, Hegde V, Lam LT, Staudt LM, Levens D, Deutsch WA, Lenardo MJ (2007). Ribosomal protein S3: a KH domain subunit in NF-kappaB complexes that mediates selective gene regulation. Cell 131: 927-939.

Wang HU, Anderson DJ (1997). Eph family transmembrane ligands can mediate repulsive guidance of trunk neural crest migration and motor axon outgrowth. Neuron 18: 383-396.

Wang J, Devgan V, Corrado M, Prabhu NS, El-Deiry WS, Riccardi C, Pandolfi PP, Missero C, Dotto GP (2005). Glucocorticoid-induced tumor necrosis factor receptor is a p21Cip1/WAF1 transcriptional target conferring resistance of keratinocytes to UV light-induced apoptosis. J Biol Chem 280: 37725-37731.

Watkins LR, Goehler LE, Relton JK, Tartaglia N, Silbert L, Martin D, Maier SF (1995). Blockade of interleukin-1 induced hyperthermia by subdiaphragmatic vagotomy: evidence for vagal mediation of immune-brain communication. Neuroscience letters 183: 27-31.

Webster JI, Tonelli L, Sternberg EM (2002). Neuroendocrine regulation of immunity. Annu Rev Immunol 20: 125-163.

Wickramasinghe SR, Alvania RS, Ramanan N, Wood JN, Mandai K, Ginty DD (2008). Serum response factor mediates NGF-dependent target innervation by embryonic DRG sensory neurons. Neuron 58: 532-545.

Wingerd KL, Goodman NL, Tresser JW, Smail MM, Leu ST, Rohan SJ, Pring JL, Jackson DY, Clegg DO (2002). Alpha 4 integrins and vascular cell adhesion molecule-1 play a role in sympathetic innervation of the heart. The Journal of neuroscience : the official journal of the Society for Neuroscience 22: 10772-10780.

Wright EM, Vogel KS, Davies AM (1992). Neurotrophic factors promote the maturation of developing sensory neurons before they become dependent on these factors for survival. Neuron 9: 139-150.

Wright LL, Cunningham TJ, Smolen AJ (1983). Developmental neuron death in the rat superior cervical sympathetic ganglion: cell counts and ultrastructure. J Neurocytol 12: 727-738.

Wyatt S, Davies AM (1995). Regulation of nerve growth factor receptor gene expression in sympathetic neurons during development. J Cell Biol 130: 1435-1446.

Wyatt S, Pinon LG, Ernfors P, Davies AM (1997). Sympathetic neuron survival and TrkA expression in NT3-deficient mouse embryos. The EMBO journal 16: 3115-3123.

Xiao G, Harhaj EW, Sun SC (2001). NF-kappaB-inducing kinase regulates the processing of NF-kappaB2 p100. Mol Cell 7: 401-409.

Xie W, Du L (2011). Diabetes is an inflammatory disease: evidence from traditional Chinese medicines. Diabetes Obes Metab 13: 289-301.

Xing J, Ginty DD, Greenberg ME (1996). Coupling of the RAS-MAPK pathway to gene activation by RSK2, a growth factor-regulated CREB kinase. Science 273: 959-963.

Yan H, Newgreen DF, Young HM (2003). Developmental changes in neurite outgrowth responses of dorsal root and sympathetic ganglia to GDNF, neurturin, and artemin. Dev Dyn 227: 395-401.

Yang XM, Toma JG, Bamji SX, Belliveau DJ, Kohn J, Park M, Miller FD (1998). Autocrine hepatocyte growth factor provides a local mechanism for promoting axonal growth. The Journal of neuroscience : the official journal of the Society for Neuroscience 18: 8369-8381.

Yu KY, Kim HS, Song SY, Min SS, Jeong JJ, Youn BS (2003). Identification of a ligand for glucocorticoid-induced tumor necrosis factor receptor constitutively expressed in dendritic cells. Biochemical and biophysical research communications 310: 433-438.

Zelenika D, Adams E, Humm S, Graca L, Thompson S, Cobbold SP, Waldmann H (2002). Regulatory T cells overexpress a subset of Th2 gene transcripts. J Immunol 168: 1069-1079.

Zerial M, McBride H (2001). Rab proteins as membrane organizers. Nat Rev Mol Cell Biol 2: 107-117.

Zheng CF, Guan KL (1993). Cloning and characterization of two distinct human extracellular signal-regulated kinase activator kinases, MEK1 and MEK2. J Biol Chem 268: 11435-11439.

Zhou Z, Tone Y, Song X, Furuuchi K, Lear JD, Waldmann H, Tone M, Greene MI, Murali R (2008). Structural basis for ligand-mediated mouse GITR activation. Proc Natl Acad Sci U S A 105: 641-645.

Zhu Y, Yao S, Chen L (2011). Cell surface signaling molecules in the control of immune responses: a tide model. Immunity 34: 466-478.

10.0 Acknowledgements

Firstly, to my supervisor Dr. Gerard O'Keeffe, I can't thank you enough for the opportunity to work with you, your invaluable time, advice and patience, the door was always open for questions big and small. I am very grateful.

To the whole department of Anatomy and Neuroscience, you know who you all are, it's been interesting ☺. Thanks for all you've done for me, everyone one of you in your own way.

To all the minions, what can I say, you're the best! From silliness to seriousness, from laughs to cries, you were there!

To my amazing family and friends, I swear this is the end of college! (I hope) Thanks so much for everything.

Last but far from least, to Tom, my best friend, my person. Thanks for always being there x